POLITECNICO DI TORINO

Master of Science in Electronics Engineering

Master Thesis

Readout system for molecular field-coupled nanocomputing based on a molecular junction

Supervisors
Prof. Gianluca Piccinini
Prof. Mariagrazia Graziano
Dr. Yuri Ardesi
M.Sc Giuliana Beretta
M.Sc Federico Ravera

Candidate
Gabriele Farchetti

27/10/2023

Compiled with LaTeX on October 15, 2023.

Abstract

The field-coupled nanocomputing (FCN) is one of the most interesting beyond-CMOS technologies, in particular, its molecular implementation (molFCN) takes advantage of its intrinsic features: nanometric dimensions and low power requirement. With each passing year, it becomes increasingly important in electronics due to the slowdown in the scaling of traditional electronics. Until today, in the scientific literature, no integrated systems with molFCN and CMOS have been proposed. This thesis investigates the possibility of interfacing the CMOS technology with the FCN one.

Three solutions have been thought of, which exploit different physical phenomena: capacitive coupling, photons scattering, and energy levels alteration. The system designed in this thesis is the molecular junction-based one. It is based on a nanogap made of gold (1,1,1) and Sulphur atoms were employed as anchoring groups. The molecules have been analyzed through the ORCA software to obtain the optimized geometry, the dipole moment parameter, and the polarizability values (the 3x3 tensor and the isotropic one). The results, in terms of polarizability and polarity, have been delivered on the QuantumATK environment, for building the molecular junction. The simulations performed through ORCA and QuantumATK are achieved with DFT accuracy. An ad hoc driver molecule has been designed to mimic the charge localization of molFCN in the ATK software, it is formed by a carbons chain with nitrogen at one side to provide the positive pole and oxygens on the other side to provide the negative pole. The goodness of the junction molecule is determined by the transmission spectrum and IV plot, but, for a deeper overview of the system quality, the orbitals and the conduction path in terms of angle and weight have been simulated. The IV plot is the most important result because it shows clearly the detection possibility of the binary value encoded in the molFCN; if the current difference between the two configurations is large enough, the system could distinguish the logic value. Orbital change provides direct proof of the driver's influence on the molecular junction, while conduction pathways contain the effective interaction between the atoms that compose the molecular junction and the traveling electrons.

The results reveal the possibility of performing the readout using molecular junctions, in particular, the most conductive molecules exhibit a larger current difference between the two logic configurations. Two main molecule characteristics have been identified as crucial parameters, polarity and polarizability. The first one represents how much the dipoles inside the molecule orient themselves when an electric field is applied; while the second one provides asymmetry to the structure, therefore a different behavior depending on the configurations. The polar behavior is highlighted by the not-odd function represented in the IV plot, while the molecular junction based on the molecule with the

highest polarizability values shows an odd graph in the trans-characteristic. For some molecules, additional analysis has been performed: the driver has been moved away from the initial position until double the initial distance and a smaller driver has been used; the simulations aimed to discover the robustness of the system to the fabrication tolerances and the not-perfect molecules positioning in realistic devices.

This thesis places the basis for the research of readout systems able to adapt MolFCN structures to the standard CMOS technology.

Sommario

Il field-coupled nanocomputing (FCN) è una delle più interessanti tecnologie chiamate beyond-CMOS, in particolare la sua implementazione molecolare, chiamata molecular FCN (molFCN), presenta due vantaggi intrinesci, ovvero le sue dimensioni nanometriche e la bassa richiesta di potenza. Con il passare degli anni, il molFCN è diventato sempre più importante nell'elettronica grazie al rallentamento nello scaling dell'elettronica tradizionale. Fino ad ora non sono stati presentati sistemi volti ad integrare il molFCN con la tecnologia CMOS. Questa tesi si pone l'obiettivo di investigare un possibile sistema di interfacciamento tra le due tecnologie citate in precedenza.

Sono state pensate tre diverse soluzioni al problema sopra esposto, ciascuna sfrutta differenti fenomeni fisici: accoppiamento capacitivo, disperisone fotonica e alterazione dei livelli energetici. In questa tesi è stato sviluppato il sistema basato sulla giunzione molecolare. Essa è basata su nanogap di oro (1,1,1) e come gruppi di ancoraggio sono stati usati degli atomi di zolfo. Le molecole sono state analizzate tramite il software ORCA per ricavare la geometria ottimizzata, il momento di dipolo e il valore di polarizzabilità (il tensore 3x3 e il valore isotropico). I risultati di polarità e polarizzabilità sono stati trasmessi al programma QuantumATK, al fine di montare la giunzione molecolare. Le simulazioni svolte con ORCA e QuantumAtk sono svolte con precisione DFT. Una molecola driver ad hoc è stata progettata per riprodurre la localizzazione della carica del molFCN in QuantumATK, essa è formata da una catena di carboni con un azoto da un'estremità per fornire il comportamento polare positivo ed ossigeni dall'altro lato per fornire il comportamento polare negativo. La bontà della molecola nella giunzione è determinata dallo spettro di trasmissione e dalla caratterisitca IV, ma, per una migliore panoramica del sistema, si sono simulati anche gli orbitali e i percorsi della conduzione. La caratteristica IV è la più significativa, perché mostra chiaramente la possibilità (o non possibilità) del corretto rilevamento del valore logico codificato nel molFCN; se la differenza in corrente tra le due configurazioni è abbastanza grande, il sistema è capace di distingure il valore logico. La modifica degli orbitali fornisce una prova diretta dell'influenza del driver sulla molecola nella giunzione, mentre i percorsi di conduzione contengono le effettive interazioni tra gli atomi che formano la giunzione e gli elettroni.

I risultati mostrano l'effettiva possibilità di eseguire il readout usando una giunzione molecolare, in particolare le molecole con alta conduttività esibiscono una differenza sostanziale tra le correnti associate ai due valori logici. Polarità e polarizzabilità sono due caratteristiche delle molecole che sono state idenficati come cruciali nel sistema. La polarizzabilità rappresenta quanto i dipoli all'interno della molecola si orientano quando sono soggetti ad un campo elettrico; mentre la polarità fornisce asimmetria alla struttura,

perciò un comporamento differente è atteso per le due configurazioni. Il comportamento polare è sottolineato dalla funzione non dispari nella caratteristica IV, mentre le molecole contraddistinte da un elevato valore di polarizzabilità mostrano una trans-caratteristica dispari. Per alcune molecole sono state svolte analisi supplementari: il driver è stato allontanato dalla giunzione fino a raddoppiarne la distanza e un driver più corto è stato utilizzato; queste simulazioni sono volte a scoprire la robustezza del sistema alle tolleranze di fabbricazione e al non perfetto posizionamento delle molecole nei dispositivi reali.

Questa tesi pone le basi per la ricerca volta a sistemi di readout che adattino le strutture basate su molFCN alla tecnologia CMOS.

Ringraziamenti

Ci tengo a rigraziare il professor Piccinini e la professoressa Graziano per avermi introdotto questi argomenti, per avermi affidato questa ricerca innovativa e per avermi seguito nel percorso. I vostri insegnamenti di natura scolastica e umana mi hanno aiutato a maturare.

Un sentito ringraziamento lo rivolgo a Yuri, Giuliana e Federico per il loro impareggiabile contributo quotidiano, per avermi seguito, guidato e consigliato con passione in questo magnifico percorso. Farò tesoro di tutti i consigli che mi avete dato. Ringrazio anche Fabrizio e Chiara che, anche da remoto, sono riusciti a condividere con me risultati e a fornirmi alcune dritte sull'argomento.

Un doveroso ringraziamento va alla mia famiglia, che mi ha sostenuto nel mio intero percorso universitario e che mi è sempre stata vicina. Mi avete sopportato in tutti questi anni (e viceversa) e mi avete aiutato a cresecere senza farmi mai mancare nulla.

Grazie ai miei zii, ai miei cugini ed ai miei nonni per il loro affetto, la loro felicità e la loro comprensione.

Un pensiero lo rivolgo sicuramente ai miei amici, con cui condivido gioie e dolori. Non vi citerò uno ad uno perché sicuramente qualcuno me lo dimentico, ma sappiate che il vostro contributo è stato fondametale in questo percorso universitario. Grazie di ogni singolo momento trascorso insieme.

Un ringraziamento lo rivolgo a tutte quelle persone che ho incotrato durante questi anni, professori, colleghi e tutti gli altri, grazie perché parlando con voi ho imparato molto. Anche voi avete forgiato una parte di me con consigli ed insegnamenti.

Ultima, ma non per importanza, vorrei ringraziare di cuore Sofi, non ho parole per descrivere quanto tu sia fondamentale ed indispensabile nella mia vita. Posso semplicemente affermare che il mondo visto con la tua mano stretta alla mia è un posto migliore.

Per chiunque legga queste poche righe sappia che Gabriele ha scritto la tesi, ma Gabriele senza l'aiuto e i consigli delle persone citate precedentemente non sarebbe mai riuscito a fare tutto ciò.

Contents

List of Tables

List of Figures

List of acronyms and abbreviations

ITRS	International Technology Roadmap for Semiconductors
MtM	More than Moore
BC	Beyond CMOS
CMOS	Complementary Metal-Oxide Semiconductor
MEMS	Micro Electro-Mechanical System
IC	Integrated Circuit
FET	Field-Effect Transistor
MolFET	Molecular Field-Effect Transistor
FCN	Field-Coupled Nanocomputing
MolFCN	Molecular Field-Coupled Nanocomputing
QCA	Quantum-dot Cellular Automata
MV	Majority Voter
SET	Single Electron transistor
RS	Raman Scattering
TERS	Tip-enhanced Raman Spectroscopy
LED	Light-Emitting Diode
NW	Nanowire
QD	Quantum-dot
MT	Molecular transistor
SCF	Self Consisting Field
RT	Room Temperature
LT	Low Temperature
SNR	Signal-to-Noise Ratio
CP-SCF	Coupled-Perturbed equations for SCF
TS	Transmission Spectrum
IV	Current-Voltage characteristic
HOMO	Highest Occupied Molecular Orbital
LUMO	Lowest Unoccupied Molecular Orbital
OPV	Oligo(Phenylene Vinylene)
OPE	Oligo(Phenylene Ethynylene)
TT	Thiophene
Pc	Phthalocyanine
ZnPc	Zinc Phthalocyanine
OPAMP	OPerational AMPlifier

Chapter 1

Introduction

1.1 Moore's laws limits

Moore's laws are a milestone of the electronic, they have ruled its development for 50 years. In 1965 Moore predicted the trend of important parameters for electronic devices, in particular the scaling of the dimensions, the number of transistors per die and the clock frequency [1]. The first Moore's law can be described as "the number of transistors per die doubles each one year and a half", the sentence can be synthesized in the equation 1.1.

$$\#TR(t) = \#TR\,(t_0)\,2^{\frac{t-t_0}{1.5}} \tag{1.1}$$

Moore's law concerning the minimum dimension is related to the channel length, in particular, "the channel length decreases of 30 % every 3 years"; the mathematical expression is written in the equation 1.2.

$$L_{CH}(t) = L_{CH}(t_0)0.7^{\frac{t-t_0}{3}} \tag{1.2}$$

A wider decrease in channel length leads to effects that are not appreciable for transistors with large channel lengths, those effects are called *short channel effects* [2, 3].

The operational frequency is very important in electronic devices, not only for the speed of the system but also for the power consumption. The dynamic power plays a significant role in the modern electronic; it can be defined as in the equation 1.3, where V_{DD} is the supply voltage, F_{CK} is the clock frequency, C is the load capacitance and α is the switching activities factor. Increasing the frequency increases the power consumption, consequentially the heat dissipation is more relevant; for this reason, the operational frequency has seen a stalemate at a few GHZ in recent years.

$$P_{dynamic} = \frac{1}{2}\alpha C F_{CK} V_{DD}^2 \tag{1.3}$$

The already presented problems are not the only ones that a scale device suffers, at the nanoscale classical physics leaves the reins in favor of quantum mechanics, and the consequences are discrete and quantized energy levels instead of continuous ones.

In order to keep pace with Moore's Laws new technologies and ideas have been proposed; in the ITRS two main approaches have been investigated [4]:

- *More than Moore*: it consists in a heterogeneous integration, typically it allows the coexistence of analog and digital signals and of different chips (such as MEMSs, ICs, electronic actuators,..) [5]. The underlying concept is to assemble different systems like in a System-on-Chip.
- *Beyond CMOS*: it refers to new paradigms, it abandons the CMOS technology to exploit different ideas for overcoming the analyzed limitations. The field-coupled nanocomputing concept is one of the more interesting theories proposed.

1.2 Field-Coupled Nanocomputing

The FCN theory is based on fields (magnetic, electric or both), the information are encoded in the field orientation. The key feature of the FCN is that no conduction is needed, the coupling between the nanometric devices allows the passage of information. The benefit in terms of conduction is very important, the power dissipated is theoretically zero (not completely true because a clock system must be implemented to mark the correct passage of data in terms of time).

There are different implementations of FCN [6]:

- *Metallic*: the main advantage is the technology, we can reproduce metal dot systems to test prototypes; the disadvantages are linked to the signal integrity, small errors pile up, therefore the final result is wrong [7];
- *Semiconductor*: the semiconductor technologies are well known due to the standard microelectronic processes, but it works at low temperature in order to maintain the coulomb blockade [8].
- *Magnetic*: the nanomagnets evince a specific polarity when subjected to a magnetic field, the key features are the practically zero standby power (magnetic properties in ferromagnetic materials are not volatile) and the low switching energy; the main drawbacks related to this technology are the occupied area, the clock generation, the low operational frequency and the thermal noise [9, 10, 11].
- *Molecular*: it is the most flexible and promising, it will be investigated in detail in the following sections.

They exploit different materials, technologies and physical phenomena, but the key concept remains the same. The MolFCN is one of the most promising implementations of the FCN paradigm, because:

- it works at room temperature;
- it is very small;
- it is self-assembly;
- the power consumption is very low;
- its switching time is very high (frequency $>$ 10 THz).

1.3 QCA & MolFCN

The MolFCN relies to the QCA paradigm, therefore, for a better knowledge of the task, it is important to introduce the QCA model.

1.3.1 QCA: principle

The QCA can be introduced considering 4 dots (figure 1.1a) with 2 electrons (the circles are the dots, the colored parts represent the electrons). The coulombic force between the two electrons allows only two possible stable states (figures 1.1b and 1.1c), in these configurations are encoded the '0' logic and the '1' logic, which are the bricks of the binary logic.

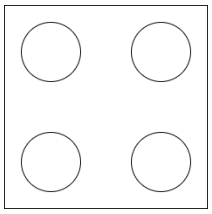

(a) Scheme of a QCA base cell.

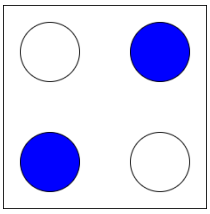

(b) Scheme of a QCA logic '0' configuration.

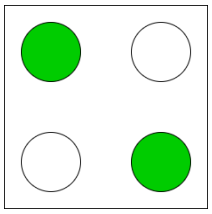

(c) Scheme of a QCA logic '1' configuration.

A key feature of the electronic components is the information propagation, the transport of data must be performed without a high error rate. The base cells of QCA can be placed next to each other (figure 1.2), the repulsive force between electrons makes possible the propagation of the information due to the correct arrangement of each base cell [12].

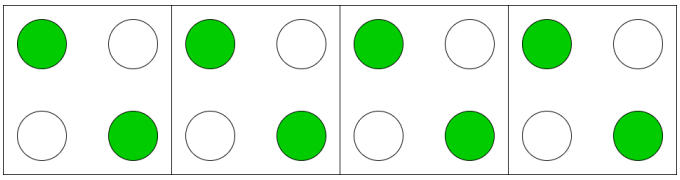

Figure 1.2: Scheme of a wire made of QCA base cells.

Each dot influences all the others, not only the nearest, but the electric field decreases with the distance according to the equation 1.4. The consequence is that the nearest dots (the previous and the following one) "confirm" the configuration of the selected ones, which leads to greater robustness to noise.

$$\vec{E} = \frac{1}{4\pi\epsilon_0}\frac{Q}{r^2}\frac{\vec{r}}{r} \tag{1.4}$$

1.3.2 QCA: logic

One of the most used operators is the inverter (logic not), in which the output is the complementary value of the input. The most stable and efficient geometry is drawn in

figure 1.3. The problem related to the inverter is the effective area, it is bigger than the MV [13]. There are some other geometries for the inversion, but they are more subjected to the noise and the consequence is the lower reliability of the data.

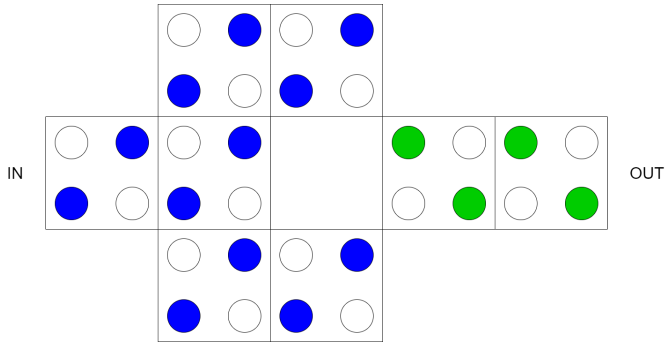

Figure 1.3: Scheme of an inverter made of QCA base cells.

The logic functions of the QCA are based on the majority voter; it is a device with 3 inputs, the output value is the most present input; a scheme of the logic gate is shown in figure 1.4. The MV truth table is reported in figure 1.5, where the IN_X are the inputs of the system and the OUT is the result of the logic function.

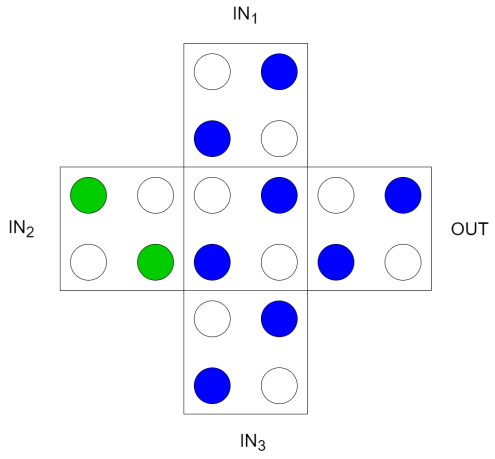

Figure 1.4: Scheme of the MV implemented by QCA paradigm.

IN_1	IN_2	IN_3	OUT
0	0	0	0
0	0	1	0
0	1	0	0
0	1	1	1
1	0	0	0
1	0	1	1
1	1	0	1
1	1	1	1

Figure 1.5: Truth table of the MV logic function.

Startung from the MV it is possible to design the foundamental logic functions, in particular looking at the figure 1.5 fixing IN_1 and considering IN_2 and IN_3 as inputs [14]:

- $IN_1 =$ '0' $\rightarrow OUT = IN_2 * IN_2$;
- $IN_1 =$ '1' $\rightarrow OUT = IN_2 + IN_2$.

The circuits of the two logic gates are reported in the figures 1.6 and 1.7, in which the black parts are the fixed constrains of the designed system.

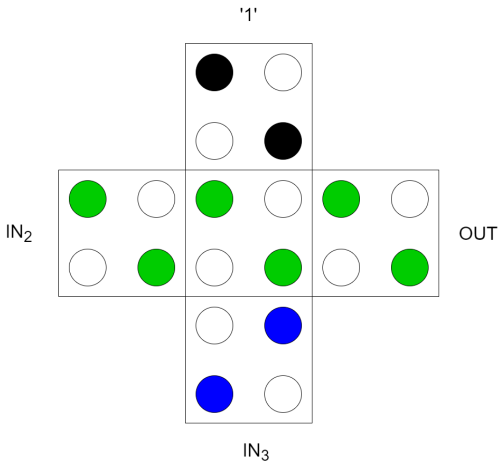

Figure 1.6: Scheme of the OR gate implemented through the MV base cell.

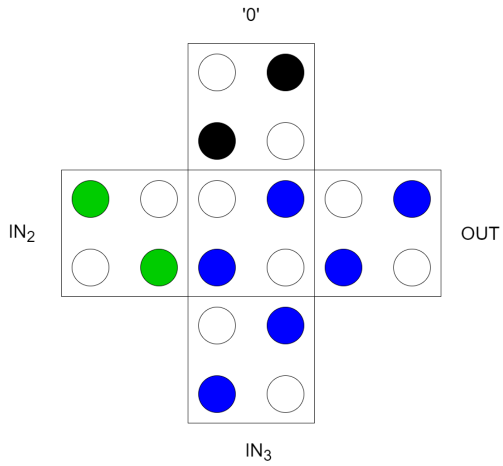

Figure 1.7: Scheme of the AND gate implemented through the MV base cell.

1.3.3 QCA: clock

In digital systems, the schedule of the data is fundamental for obtaining the correct results. As in microprocessors, the QCA paradigm involves a clock signal that sets the time flow of information. The 4 dots model cannot be applied in this case, because, in addition to the binary values, a reset condition is required, which means that a 6 dots model should be exploited. In figure 1.8a is shown the null state, in figures 1.8b and 1.8c are drawn the general binary values.

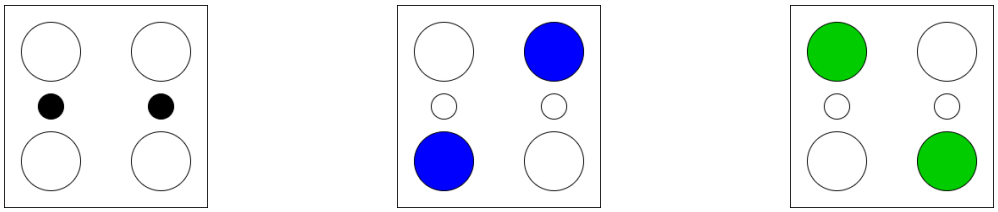

(a) null configuration. (b) logic '0' configuration. (c) logic '1' configuration.

Figure 1.8: Scheme of QCA configurations with 6 dots cell.

A clock signal is applied at the structure, it can be divided in 4 phases: *switch, hold, release and reset*, in figure 1.9 is shown the clock signal for one phase. Alternating these phases it is possible to design a device in which information flow with the right timing, usually four different zones are considered, the difference in the clock signals is only the initial phase of the signals [15].

In MolFCN the clock signal is an electric field, it is applied through electrodes on top and bottom of the molecules. The results uphold the correct switch at the different clock phases, even in more complex structures like the logical gates as long as the zones are well designed [16, 17].

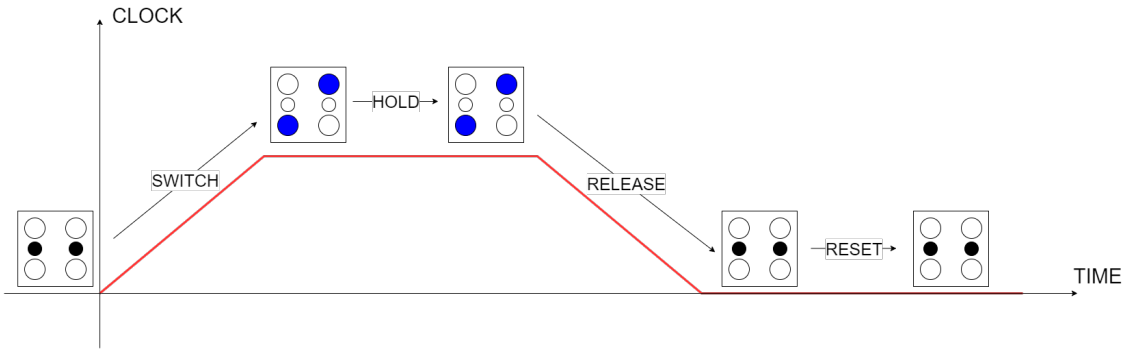

Figure 1.9: QCA clock signal representation, highlighting the 4 phases: switch, hold, release and reset.

1.3.4 MolFCN: Molecules

The selection of the molecule for MolFCN is still being researched today, one of the best candidates (at the moment) to fill the role is bis-ferrocene. It is formed by two ferrocenes and a carbazone molecule, as an anchoring group to the gold a thiol chain is adopted. The bis-ferrocene molecule can be seen as three aggregates of charge that simulate the 3 dots requested by the QCA paradigm [18]. Figure 1.10 shows the bis-ferrocene molecule, highlighting the three groups of charges which are composed of the dots representing the two logical values and the null state.

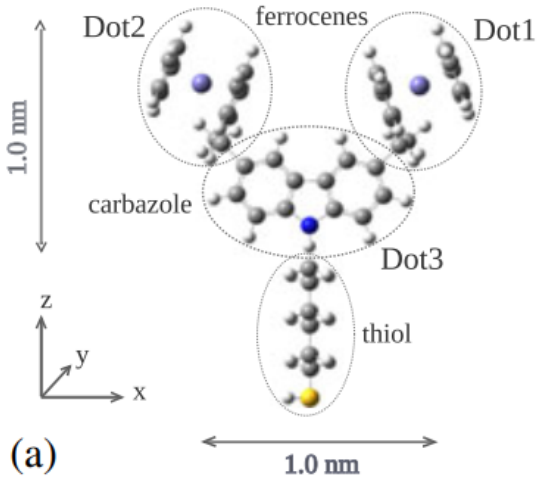

Figure 1.10: Positionig of the three dots in a Bis-ferrocene molecule [12].

1.4 Readout problem

The aim of the thesis is to find a readout system for the MolFCN, therefore device sensible to the charge at the nanoscale should be designed. A key feature of the system should be the integration with the standard CMOS process, so the device must translate the MolFCN information in data compatible with the standard electronic. The interaction between the standard CMOS and the beyond-CMOS technologies could greatly increase the performance of devices, it will allow us to explore increasingly complex and fast systems, keeping the power consumption low.

A representation is shown in figure 1.11.

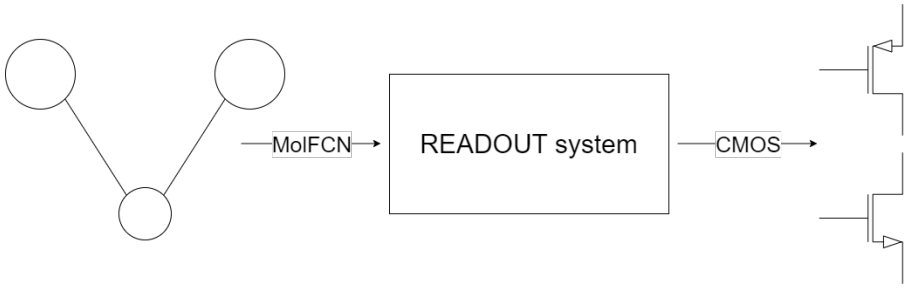

Figure 1.11: Readout system, black-box representation.

An important issue to take into consideration is the possible interaction between clock generation (the electric field that times the passage of information) and the potential of the readout system, in order to not compromise the two independent systems.

Chapter 2

Possible solutions

Three different methods have been devised to solve the readout problem, they explore different physical principles, in particular:

- **Single Electron Transistor**: capacitive coupling between QCA and island;
- **Raman Scattering**: different scattering in terms of wavelength considering asymmetric QCA;
- **Molecular Transistor**: interaction between the electric field generated by the QCA and the junction molecule.

2.1 Single Electron Transistor

The SET is a device in which is possible to control the flow of one electron through the channel with a proper applied voltage. The device is composed by the island (it represents the channel) and two electrodes, the source and the drain. The island is formed by a quantum dot, it is coupled with the electrodes through tunnel junctions, which allow the passage of electrons thanks to the tunneling effect, this is the main difference concerning the field effect transistor. Due to the nanometric scale of a quantum dot, the SET is based intrinsically on quantum phenomenons [19]. One or more gate electrodes could be added to the structure, their purpose is to change the potential in the device. A scheme of a SET is reported in the figure 2.1.

The SET working principle is based on the Coulomb blockade. The Coulomb blockade can be defined through three factors [20] :

- Coulomb energy: the coulombic blockade energy is defined as in the equation 2.1, it is the amount of energy needed for repelling the upcoming electron by the one already present in the island.
- Tunnel resistance: the tunnel junction is an important part of the structure, it has to be well designed to assure a specific resistance and capacitance. These two parameters are defined by the conductive part and the dielectric medium.

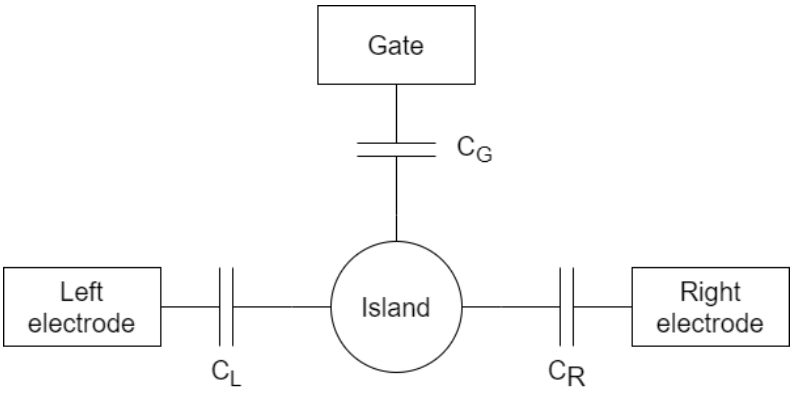

Figure 2.1: Capacitive model of a SET

- Excess electrons: an electron provides a repulsive force to another one. The addition or subtraction of electrons in the island changes the electrostatic energy.

$$E_c = \frac{e^2}{2C} \tag{2.1}$$

where e is the electron charge and C is the effective capacitance of the island. For small islands the corresponding capacitance is very low, the consequence is a high value of E_c therefore electrons can pass one-by-one through the tunnel junction.

The charging energy of the system [21] can be expressed as in the equation 2.2.

$$E_{ch} = \frac{1}{2}\frac{Q_{isld}^2}{C_\Sigma} = \frac{1}{2}\frac{n^2e^2}{C_\Sigma} \tag{2.2}$$

where Q_{isld} is the island charge, n is the number of excess electrons and C_Σ is the total capacitance of the island (reported in equation 2.3).

$$C_\Sigma = C_L + C_R + C_G \tag{2.3}$$

The effect of an applied gate voltage is the change of the charging energy, in particular, the relation is written in the equation 2.4.

$$E_{ch} = \frac{1}{2}\frac{Q^2}{C_\Sigma} = \frac{1}{2}\frac{(ne - V_G C_G)^2}{C_\Sigma} = \frac{1}{2}\frac{(ne - Q_G)^2}{C_\Sigma} \tag{2.4}$$

For achieving the coulomb blockade some important relations must be respected, otherwise, the blockade is overstepped [19]:

- the bias voltage must be lower than the electron charge divided by the capacitance (equation 2.5).

$$V_{bias} < \frac{e}{C} \tag{2.5}$$

- The thermal energy must be lower than the charging energy otherwise the electron overcomes the blockade (equation 2.6).

$$K_B T < \frac{e^2}{C} \tag{2.6}$$

  where K_B is the Boltzmann's constant and T is the temperature in K.

- From Heisenberg's uncertainty principle is possible to derive the minimum tunnel resistance, the result is reported in the equation 2.7.

$$R_T > \frac{h}{2\pi e^2} = 25813\Omega \tag{2.7}$$

The threshold voltage of a SET is the minimum voltage that allows to overcome the coulomb blockade, the expression for no gate voltage applied [21] is reported in the equation 2.8.

$$V_{th} = \frac{e}{2C_\Sigma} \tag{2.8}$$

If a gate voltage is applied the threshold voltage changes because the capacitive coupling influences the potential. The effect of a V_G on V_{DS} is analyzed in the equation 2.9, solving the capacitive circuit.

$$V_{DS}\left(V_G\right) = \frac{C_G}{C_\Sigma} V_G \tag{2.9}$$

The condition of threshold voltage equal to 0 for $V_{DS} = 0$ is met when the relation in the equation 2.10 is verified.

$$V_{th}\left(V_{DS} = 0\right) = \frac{e}{2C_G} \tag{2.10}$$

The SET is well suited for charge sensing, the coupling between a charge and the island changes deeply the charging energy and the result is a variation in the electrons flow [21, 22, 23, 24, 25]. This result is supported by the equations 2.4 and 2.10, in which a charge (Q_G) modifies the charging energy of the system and the threshold voltage.

2.2 Raman Scattering

The Raman scattering is a physical property of the matter; considering a sample illuminated by a monochromatic source it is possible to see that some photons pass through the sample (the sample is transparent to them), some of them could be absorbed, these phenomenons depend on the material and on the source. The two scenarios presented before are not the only ones that could happen, a small amount of photons is scattered by the sample atoms. The scattering can be divided into two types, regarding the emission frequency [26]:

- if the emission frequency is the same as the incident radiation the photons are elastically scattered (Rayleigh scattering);

- if the emission frequency is different than the incident one the photons are inelastically scattered (Raman scattering), it can be subdivided into two cases:

- emission frequency lower than excitation frequency (Stokes scattering)
- emission frequency higher than excitation frequency (anti-Stokes scattering)

The energy of a photon can be express as in the equation 2.11.

$$E_{photon} = h\nu = h\frac{c}{\lambda} \tag{2.11}$$

Considering the energy difference of the excitation photon and emitted photon is possible to find the relation in the equation 2.12.

$$\Delta E = E_{ex} - E_{em} = h\nu_{ex} - h\nu_{em} = hc\left(\frac{1}{\lambda_{ex}} - \frac{1}{\lambda_{em}}\right) \tag{2.12}$$

where λ_{ex} is the excitation wavelength and λ_{em} is the emitted wavelength. The parameter that describes the Raman scattering is the wavenumber, it is defined in the equation 2.13.

$$\tilde{\nu} = \frac{1}{\lambda_{ex}} - \frac{1}{\lambda_{em}} \tag{2.13}$$

The Raman scattering is well suited for the identification of molecules [27], the technique that takes advantage of this physical phenomenon is called Raman spectroscopy. Nowadays there are a lot of different types of Raman spectroscopy: Surface-enhanced hyper Raman Scattering (HR) scattering, Tip-enhanced Raman Spectroscopy (TERS), Coherent anti-Stokes Raman Spectroscopy (CARS), Stimulated Raman Scattering (SRS), Resonance Raman Spectroscopy (RRS), Confocal Raman microscopy and Raman imaging microscopy [28]. The technique that fits well for the molFCN readout problem is the TERS, in which a sharp metal tip (10-50 nm) enhances the field of the incident radiation on the sample. Diffraction limits the spatial resolution in ordinary optical microscopy, which follows the Abbe formula [29] (reported in the equation 2.14).

$$\Delta x = \frac{0.61\lambda}{NA} \tag{2.14}$$

where λ is the wavelength of the incident radiation and NA is the numerical aperture. The best resolution in optical microscopy is approximately 200 nm in the visible range, instead in TERS it is possible to reach a spatial resolution of 1-10 nm [30].

It has been demonstrated that an asymmetrich molecule used as molFCN can show different Raman spectra accordingly of the molecule charge distribution [31].

In order to distinguish the logical '0' from the logical '1' a system was designed as shown in the figure 2.2.

The working principle of the designed solution can be summarized as below:

- the excitation source provides the excitation radiation at a specific wavelength (excitation wavelength), it could be a laser or an LED;
- the excitation wavelength (λ_0 in the equation 2.13) strikes the molecule;
- a part of the incident radiation remains at the same wavelength, while the other part shifts up or down (Raman scattering);

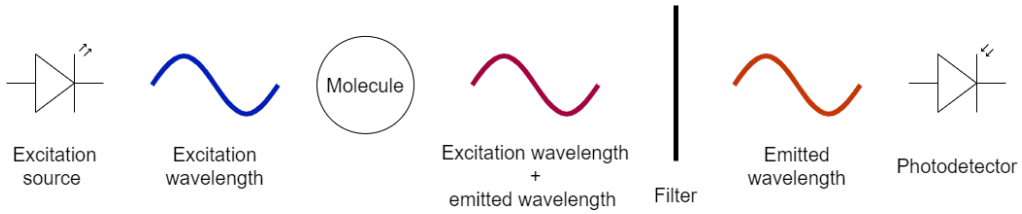

Figure 2.2: System designed to distinguish the bit logic values using the Raman scattering.

- the filter has to be:
  - transparent to the emitted wavelength;
  - dark to the excitation radiation (reflect it);
- a photodetector must convert the incident radiation in a measurable current.

The difference in the Raman spectrum can be detected through the different currents generated by the photodetector.

2.2.1 Excitation source

The excitation source plays a relevant role in the designed system. The discriminating parameters for the choice of the device can be summarized in the list below:

- as close as possible to an ideal monochromatic source;
- the emitted wavelength.

It is very hard to obtain a monochromatic source, it is more realistic to design a narrow-band laser. Fiber-based lasers can reach narrow spectral response, close to a monochromatic one[32]; in particular, a random distributed feedback laser can provide an emission of spectral width of about 0.05 nm [33]. Another manner to obtain monochromatic radiation is to consider a general source and then filter the emitted radiation, the Fabry-Perot cavity can be a good choice as a filter, the finesse parameter describes how much narrower is the output radiation [34, 35].

2.2.2 Photodetector

Two of the main issues related to photodetectors for this application are the responsivity and the response speed. The first parameter determines the current generated per each Watt of incident photon power; the second one tells us the time between the arrival of the incident power and the generation of the current. They are important for different reasons: the molFCN can reach about hundreds of MHz of frequency, if the photodetector is too slow it becomes the system bottleneck; the photons scattered are an insignificant part with respect to the photons generated by the excitation source, low power means lower current generated.

In the table 2.1 are reported some photodetectors whose features fit well the design constraints, they are in the nanometric scale and they work at room temperature. We can

subdivide them into three main groups accordingly to the shape and confined dimensions: nanowires [36], quantum-dots and field effect transistor.

Table 2.1: Features of the selected photodetectors for the Raman scattering method.

Type	**Material**	**Incident wavelength**	**Responsivity [A/W]**	**Response speed**	**Ref.**
Single horizontal NW	GaAs core AlGaAs shell	800 nm	10^{-4}	5 ps	[37]
Single standing vertical NW	GaAs on GaAs substrate	808 nm	5x10^{-7}	$\sim$ 1 ps	[38]
Sandwich QD	Pb-Se	800 nm	0.36	70 ps	[39]
Graphene FET	graphene	1.55 μm	6.1x10^{-3}	<11 ps	[40]

2.3 Molecular Transistor

The MT is a transistor in which the channel is a molecule. It is composed of the source, the drain, the gate and the channel (the molecule), in the case of a molecular junction the gate electrode is missing and the channel is driven by the source-drain voltage. The key concept of the device is related to the molecule, it can be modelized as a quantum dot, for this reason, the physics that rules the device is not classical physics but is the quantum mechanical one. The behavior in terms of conduction in a quantum dot is described by Landauer's equation, it is reported in the equation 2.15.

$$I_{DS} = \frac{2q}{h} \int T(E) \left[f(E, E_{FS}) - f(E, E_{FD}) \right] dE \tag{2.15}$$

where:

- q is the elementary charge, its value is roughly 1.602 x 10^{-19} C;
- h is the Planck's constant, its value is roughly 6.626 x 10^{-34} $\frac{m^2 kg}{s}$;
- $T(E)$ is the transmission spectrum;
- $f(E)$ is the Fermi's function, reported in the equation 2.16;
- E_{FS} and E_{FD} are the Fermi level of source and drain.

$$f(E) = \frac{1}{e^{\frac{E}{k_B T}} + 1} \tag{2.16}$$

where:

- k_B is the Boltzmann's constant, its value is 1.380648 x 10^{-23} $\frac{m^2 kg}{s^2 K}$;

- T is the temperature in Kelvin.

Depending on the interaction between electrodes and dot it is possible to diversify two different conditions:

- *weak coupling*: it is charcaterized by sequential tunnelings, so the tunnel process source-dot is independent respect to the dot-drain one;
- *strong coupling*: the electrons can continuously be transferred from source to drain, they are not independent processes, the transport is coherent.

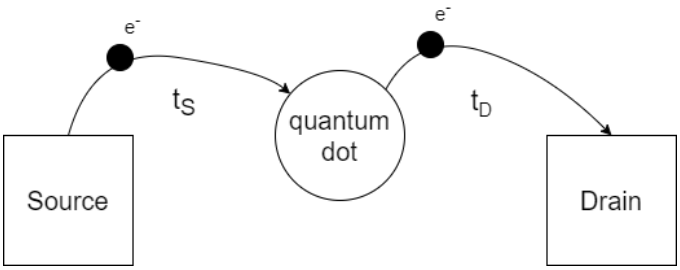

Figure 2.3: Time model of the interaction between electrodes and dot.

The coupling factor is the parameter that describes the interaction between electrode and dot, it can be express as in the equation 2.17.

$$\gamma = \frac{\hbar}{\tau} \tag{2.17}$$

where:

- $\hbar$ is the normalized Planck's constant;
- τ is the time that an electron takes to go from the dot to the electrode or vice versa (described in figure 2.3).

Equation 2.18 is the transmission spectrum for the weak coupling condition. The energy levels considered in the $T(E)$ are the ones which fall in the bias window, the latter is the gap that derives from the voltage applied between source and drain.

$$T_{Discr}(E) = \sum_{i=1}^{n} \frac{\pi \gamma_{iS} \gamma_{iD}}{\gamma_{iS} + \gamma_{iD}} N_{0D_{Discr}}(E) \tag{2.18}$$

$N_{0D_{Discr}}(E)$ is the density of state for the 0 dimension structrure (quantum dot) for a single level in case of weak coupling and therefore of discrete levels. Its expression is shown in the equation 2.19.

$$N_{0D_{Discr}} = 2\delta(E - E_{Li}) \tag{2.19}$$

The transmission spectrum in strong coupling conditions is described by the equation 2.20, in which the energy levels are not discrete but broader.

$$T_{BR}(E) = \sum_{i=1}^{n} \frac{\pi \gamma_{iS} \gamma_{iD}}{\gamma_{iS} + \gamma_{iD}} N_{0D_{BR}}(E) \tag{2.20}$$

The density of state in this case ($N_{0D_{BR}}(E)$) is a Lorentzian distribution, it is reported in the equation 2.21 the function for a single level.

$$N_{0D_{BR}}(E) = 2 \frac{\frac{\gamma_i}{2\pi}}{\left(\frac{\gamma_i}{2}\right)^2 + (E - E_{Li})^2} \tag{2.21}$$

where

$$\gamma_i = \gamma_{iS} + \gamma_{iD} \tag{2.22}$$

It is necessary to refer the energy levels position of the dot in function of the applied voltage. In order to complete this task a capacitive model has been considered, the model is shown in figure 2.4.

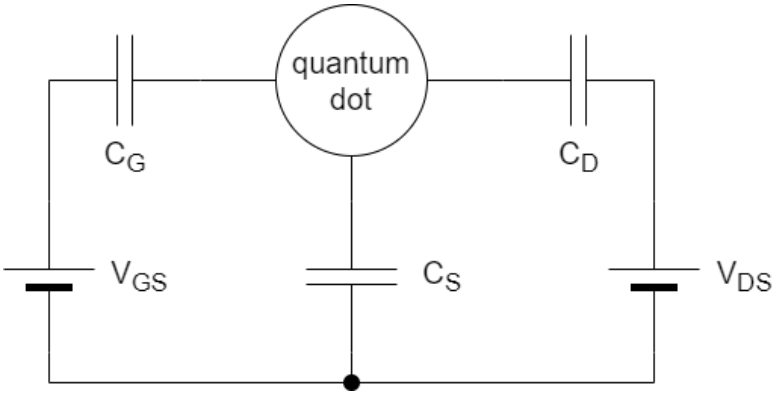

Figure 2.4: Capacitive model of the MT.

Solving the capacitive circuit it is possible to find the relation in equation 2.23.

$$V_{dot} = \frac{C_D}{C_{ES}} V_{DS} + \frac{C_G}{C_{ES}} V_{GS} \tag{2.23}$$

where

$$C_{ES} = C_D + C_S + C_G \tag{2.24}$$

From the V_{dot} it can be estimated the energy of the dot (U_{dot}), the expression is written in the equation 2.25.

$$U_{dot}\left(V_{GS}, V_{DS}\right) = -q \frac{C_D}{C_{ES}} V_{DS} - q \frac{C_G}{C_{ES}} V_{GS} \tag{2.25}$$

The energy levels of the quantum dot don't depend only on the applied voltages, but also on the number of electrons in the dot. An electron that goes or leaves the dot couses

a change of the energy levels in the spectrum, this phenomena is called charging effect. From the capacitive model it can be found the equation 2.26, it represents the potential variation due to an electron that jumps into the dot from the electrode.

$$\Delta V_{dot} = \frac{\Delta Q}{C_{ES}} = \frac{-q}{C_{ES}} \tag{2.26}$$

The final expression of the quantum dot energy is reported in the equation 2.27.

$$U_{dot}\left(V_{GS}, V_{DS}, N\right) = -q\frac{C_D}{C_{ES}}V_{DS} - q\frac{C_G}{C_{ES}}V_{GS} + \frac{q^2}{C_{ES}}\left(N - N_0\right) \tag{2.27}$$

where N is the number of electrons in the dot, while N_0 is the number of electrons in the dot at the equilibrium.

Considering all the contributions analyzed before, the current expression is written in the equation 2.28.

$$I_{DS}\left(V_{DS}, V_{GS}, N\right) = \frac{2q}{h}\int T_{BR}\left(E - U_{dot}\right)\left[f\left(E, E_{FS}\right) - f\left(E, E_{FD}\right)\right]dE \tag{2.28}$$

The solution at the equation 2.28 can be found using a SCF algorithm, so through an iterative process.

Chapter 3

Chosen solution and necessary features

3.1 Comparison of the possible solutions

In the previous chapter have been presented the three possible solutions projected for solving the Readout problem. Each method has its strengths and weaknesses, in this section, it has been tried to analyze them in a deep way.

In literature it is possible to find some examples of nanoelectrometers based on SET, its high sensitivity to the charge and high speed make it an ideal candidate. The deep knowledge of semiconductor technology and the nanoscopic dimensions of the device fit well for the readout task. The main limitations are related to the Coulomb Blockade, it requires low temperature and precise design of resistance and capacitance values.

The solution involving the Raman Scattering is the most interesting one, it could work at room temperature (it depends on the photodetector), it can be integrated with the MolFCN but it is also possible to use a tip (with the photodetector) in order to acquire the emission wavelength. Unfortunately, there are many disadvantages related to the radiation, in particular it is needed a very selective filtering to separate the emission and excitation radiations. A precise focus of the excitation source is a difficult task to perform and the molFCN must be covered around in order to mask the environment matter because it has a different scattering and so it affects the measurements. Last, but not least, the photodetectors are very slow or the responsibility is very low, therefore a large amount of incident power is requested.

The MTs are very flexible because by changing the junction molecule the characteristics of the device can change even in a deep way. The molecule is placed in a nanometric gap [41], hence the device is intrinsically nanoscopic. The MT works at room temperature, thus no cooling systems are needed. An unknown is linked to the nanogap technology, it is recent therefore it is not as developed as the semiconductor one. The main limitation is related to the not availability of data in research because it is the first time that such an application is performed through an MT.

Analyzing all the pros and cons *the MT solution is the one chosen for the readout system*, in the table 3.1 are summarized the advantages and disadvantages of each proposed

solution.

Table 3.1: Table in which are summarized the advantages and the disadvantages of each possible solution.

	Pros	**Cons**
SET	- Theoretical study in literature; - High speed; - High sensitivity to charge; - Intrinsically nanoscopic; - Well known technology.	- Works at LT; - Design of tunneling resistance; - Precise capacitance design.
RS	- Could work at RT; - Can be integrated with MolFCN; - It is possible to use a tip.	- Filtering design; - Slow (due to photodetectors); - Focus the excitation source; - More devices than others metodhs; - Low SNR; - Large amount of incident power; - Reflective surface around the molFCN.
MT	- Changing the molecule changes the system properties; - Works at RT; - Intrinsically nanoscopic.	- No data available in literature; - Choice of the molecule; - More recent technology.

3.2 Polarizability

The polarizability could be a key parameter to consider for the junction molecule. The molecular polarizability measures the capability of the electronic system of a molecule to align when an electric field is applied [42]; the mathematical relation is written in the equation 3.1. The higher its value, the higher the probability that the orbitals' shape changes when subjected to an external field.

$$\mu = \alpha E \tag{3.1}$$

where μ is the dipole moment, α is the polarizability tensor and E is the applied electric field. The polarizability is indicated through a 3x3 tensor, the polarizability tensor (equation 3.2). The tensor could be diagonalized in order to obtain only three values placed in the matrix diagonal. This is not the only mathematical trick used, because also the isotropic polarizability can be estimated: its value is the mean value of the components of the diagonalized tensor.

$$\alpha = \begin{bmatrix} \alpha_{11} & \alpha_{12} & \alpha_{13} \\ \alpha_{21} & \alpha_{22} & \alpha_{23} \\ \alpha_{31} & \alpha_{32} & \alpha_{33} \end{bmatrix} \tag{3.2}$$

The calculation of the polarizability tensor is complex for molecules because it is the result of the interactions of each atom. Simulators usually ask for an electric field value

for which the polarizability is computed. A brief explanation of one possible solution adopted in some programs is reported below.

Considering all the atoms in the molecule, the moment of the dipole of each atom can be expressed as in the equation 3.3 [43]:

$$\mu_i = \alpha_i \left[E_i - \sum_{j(\neq i)} T_{ij}\mu_j \right] \tag{3.3}$$

where T is the dipole tensor connecting atoms. By expressing the electric field as a function of the dipole moment, the equation 3.4 can be obtained.

$$\alpha_i^{-1}\mu_i + \sum_{j(\neq i)} T_{ij}\mu_j = E_i \tag{3.4}$$

Writing the equation 3.4 in terms of vectors and matrix it is possible to obtain the equation 3.5:

$$A\mu = E \tag{3.5}$$

where A is a LxL matrix, where L is the number of atoms in the molecule (reported in the equation 3.6).

$$A\mu = \begin{bmatrix} \alpha_1^{-1} & T_{12} & ... & T_{1L} \\ T_{21} & \alpha_2^{-1} & ... & T_{2L} \\ ... & ... & ... & ... \\ ... & ... & ... & ... \\ T_{L1} & T_{L2} & ... & \alpha_L^{-1} \end{bmatrix} \begin{bmatrix} \mu_1 \\ \mu_2 \\ . \\ . \\ \mu_L \end{bmatrix} \tag{3.6}$$

By inverting the expression we get the equation 3.7, where B is the inverse of A.

$$\mu = BE \tag{3.7}$$

The equation 3.7 contains L equations (i goes from 1 to L) as reported in the equation 3.8.

$$\mu_i = \sum_j B_{ij}E_j \tag{3.8}$$

If the external field is constant all the components in the E vector are the same, therefore the polarizability tensor can be computed as reported in the equation 3.9.

$$\alpha_{mol} = D \left[\sum_j B_{ij} \right] D^t = \begin{bmatrix} \alpha_{1mol} & . & . \\ . & \alpha_{2mol} & . \\ . & . & \alpha_{3mol} \end{bmatrix} \tag{3.9}$$

The isotropic polarizability can be estimate as in the equation 3.10.

$$\alpha_{mol} = \frac{\alpha_{1mol} + \alpha_{2mol} + \alpha_{3mol}}{3} \tag{3.10}$$

3.3 Polarity

A polar molecule is a molecule that exhibits a partial positive charge on one side and a negative one on another side. The dipoles formed arrange themselves in accordance with the electronegativity of the atoms that make up the molecule. The electronegativity is the capability of an atom to attract electrons; this parameter influences many characteristics of molecules composed of specific atoms [44].

The computation of the electronegativity is not a simple task, many different methods have been proposed [45]. The electronegativity increases from bottom to top and from left to right in the periodic table, in fact, fluorine has the highest value (≈ 4), followed by oxygen and chlorine.

The polarity of a molecule could be an interesting property for this task because it could break the symmetry and enhance the difference between the two logic values.

Chapter 4

Methodology

As described in the chapter before, the necessary features to know about the selected molecules are the polarizability and dipole moment values. After the choice of the molecule, a transmission spectrum and conduction analysis must be performed in order to see the current difference between the two possible configurations.

4.1 Polarizability & Dipole Moment

The simulations of the polarizability and dipole moment were performed through the software *ORCA*. They are not the only simulations done with this software, in fact, the main function of ORCA is the geometrical optimization of the molecule. This last task calculates the more probable configuration of the molecule, solving the equations necessary to define it, it gives a XYZ file in which is contained the final geometrical optimization. The software receives in input a file generated by the Avogadro program, in which are specificated the starting position of the atoms; it gives as output a text file in which are contained all the steps performed for the geometric optimization, a table for the dipole moment and the polarizability tensor.

The input part (over the atoms' position) is reported below:

```
! UKS OPT CAM-B3LYP D3 def2-TZVP
%scf
  SCFMode Direct
  MaxIter 200
end
%elprop
  Dipole true
  Polar 2
  EField 1e-3
end
%pal
  nprocs 6
end
```

in which:

- *UKS*: it selects the spin unresctricted SCF.
- *CAM-B3LYP*: it is related to the range-separated hybrid functionals, in particular, it considers the Handy's fit.
- *def2-TZVP*: it means Valence triple-zeta basis set.
- *scf*: self consistent field loop, those are the code lines for the optimization of the geometry; they were performed in the mode direct and the maximum number of iterations allowed was 200.
- *elprop*: electronic properties, those lines serve to the calculation of dipole moment and polarizability. In particular, the *Dipole true* is the command that tells the software to estimate the dipole moment, instead, *Polar 2* is a method used to compute the polarizability values and the *EField 1e-3* is the value of the electric field used to calculate the polarizability tensor. Near Polar is reported as a number because there are three ways to calculate it:
  - 1: analytical method, it solves the CP-SCF;
  - 2: analytical-numerical method, the calculations are solved analytically but the orbitals are considered frozen;
  - 3: fully numerical approach.
- *pal*: it specifies the number of processors used to compute the simulation.

All the information are taken on the software manual [46].

4.2 Conduction

The conduction analysis was performed through the QuantumATK program. The software can make a lot of different types of simulations, in this work only a few of them were considered. The simulations are structured as follows:

- *Calculators*: first you have to choose it because his task is to solve all the equations needed to compute the requested analysis;
- *Analysis blocks*: they have a specific purpose, the user sets the blocks of what he wants to calculate.

QuantumATK provides different calculators, each of them has its own advantages and disadvantages; for the characterization of the system, the *Semi-Empirical Calculator* was used. From the default condition, some parameters have been modified, in particular:

- Hamiltonian: the parametrization used was Extended Huckel Theory, with the SCF loop;

- Numerical Accuracy: it has been set the k-points preset densities to [4.0, 4.0, 150.0] Å;
- Poisson Solver: it has been chosen the [Parallel] Conjugate gradient as the solver type, with Dirichlet boundary conditions in the conduction direction and Periodic boundary conditions in the other directions.

4.2.1 TS & IV

The transmission spectrum is foundamental for the correct understanding of the IV plot. They are the most important parameters of the system because the current is the means by which it is possible to define the logical value corresponding to the MolFCN.

There are two analysis blocks that compute the two tasks, for the transmission spectrum block the key feature is the energy range. It is the range in which the TS is calculated; in the simulation, the interval considered was [-3, 3] eV, divided by 151 points. For the IV block there are more parameters to set, the most important are:

- Energy Range: it is the range in which the TS spectrum is calculated, the difference with respect to the TS block is that in this case for each voltage point, the TS is calculated. In the analysis, the interval considered was [-3, 3] eV, divided into 151 points.
- Voltage Range: it is the range in which the IV plot is plotted, in the simulation the value used was [-1, 1] V, divided by 41 points.

4.2.2 Orbitals & Pathways

Orbitals and Pathways are two interesting plots to see. The orbitals tell us if the electric field influences the molecule conduction because the orbitals are directly related to the conduction. There is not a specific block for the orbitals with respect to TS and IV, but there are two steps to follow to obtain the orbitals picture:

1. find the numbers of the junction atoms, otherwise all the atoms are considered and it is not useful to see the orbitals in the driver or in the electrodes;
2. select the molecular energy block, insert the numbers previously found;
3. the output of the molecular energy analysis is a set of quantic numbers, at each number is associated an energy value and a probability one;
4. search the first positive value of energy, it is the LUMO level;
5. select the eigenstate block, inserting the numbers of the junction atoms and the quantum number of the energy level that you want to see the orbitals.

The orbitals are the eigenstates of the Hamiltonian operator in the Schrodinger equation, for this reason, the simulation, in this case, is fast because the equation is already solved in the SCF loop.

The pathway is a plot in which is possible to see the electrons' path. The simulation is performed using just one block, the only parameter to insert is the energy of the transmission spectrum in which we want to observe the pathways.

4.2.3 Drivers

In the QuantumATK software is impossible to set the bisferrocene molecule with the charge localization, for this reason, two driver molecules have been projected. Their aim is to generate the electric field which is mimicking the charge localization in the molecule of MolFCN. The drivers are composed of:

- carbons chain: its purpose is to fit the length constrain;
- NH_3^+: it gives the positive pole of the molecule;
- O^-: it provides the negative pole of the molecule.

The difference between the drivers is related only to the length of the molecule, this implies also a different dipole moment because it is a direct consequence of the distance between the poles. In the table 4.1 are reported the cited features for the two drivers.

Table 4.1: Drivers comparison table, in which are reported the length in Angstrom (it is the difference between the nitrogen atom and the single bonded oxygen atom) and the magnitude of the total dipole moment.

	Length [Å]	Dipole moment [a.u.]	Dipole Moment [Debye]
Long driver	9.904	15.36010	39.04227
Small driver	7.367	10.80334	27.45992

Long driver

Figure 4.1 is a picture of the long driver molecule after the geometrical optimization made by the ORCA program.

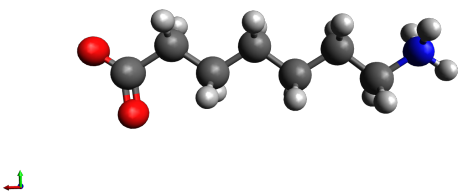

Figure 4.1: Picture of the long driver molecule used in the conduction simulations; the white atoms are hydrogens, the grey ones are carbons, the reds are oxygens and the blue one is nitrogen.

The long driver is the projected driver that shows the highest dipole moment. In the table 4.2 are reported the complete dipole moment data, differentiated in the various Cartesian components. The negative sign is due to the direction of the field, in this case, it is along the -x direction.

Table 4.2: Long driver dipole moment table, where X, Y and Z are the cartesian coordinates.

	X	Y	Z
Electronic contribution	10.97506	-1.52857	-0.32080
Nuclear contribution	-26.29729	2.58832	0.51783
Total dipole moment	**-15.32223**	**1.05975**	**0.19703**

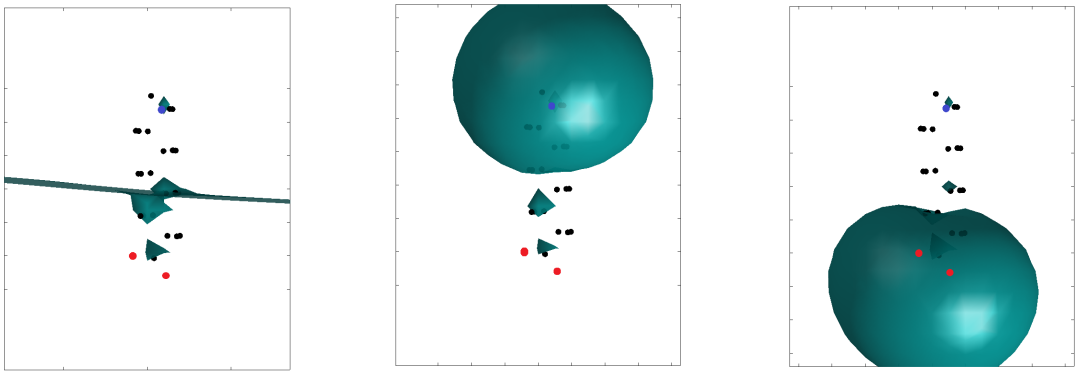

(a) potential 0 V. (b) potential 1 V. (c) potential -1 V.

Figure 4.2: Picture of the potential isosurfaces for the long driver, the red atoms in the figure's bottom are the oxygen atoms, while the blue one on the top is the nitrogen.

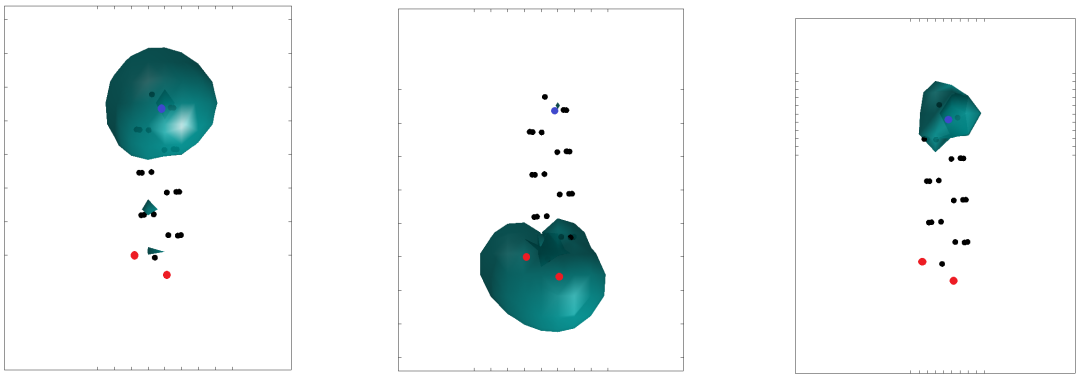

(a) potential 2.5 V. (b) potential -2.5 V. (c) potential 5 V.

Figure 4.3: Picture of the potential isosurfaces for the long driver, the red atoms in the figure's bottom are the oxygen atoms, while the blue one on the top is the nitrogen.

The dipole moment parameter is not the only simulation considered for deriving the driver molecule polarity. A deeper analysis has been performed to observe the potential isosurfaces for a determined potential, the simulation consists of a previous analysis through the keyword *chelpg*, and then the results are processed with a Matlab code to obtain a clear image of the potential isosurfaces. The figures 4.2, 4.3, 4.4 and 4.5 show the obtained results, in which is possible to notice the goodness of the long driver molecule because in the 0 V potential (figure 4.2a) the main part of the surface is place in the middle of the driver. The positive isosurfaces are close to the nitrogen atom, while the negative ones are near the oxygens, as expected. The higher the potential, the lower the area of the isosurface, which is a coherent behavior.

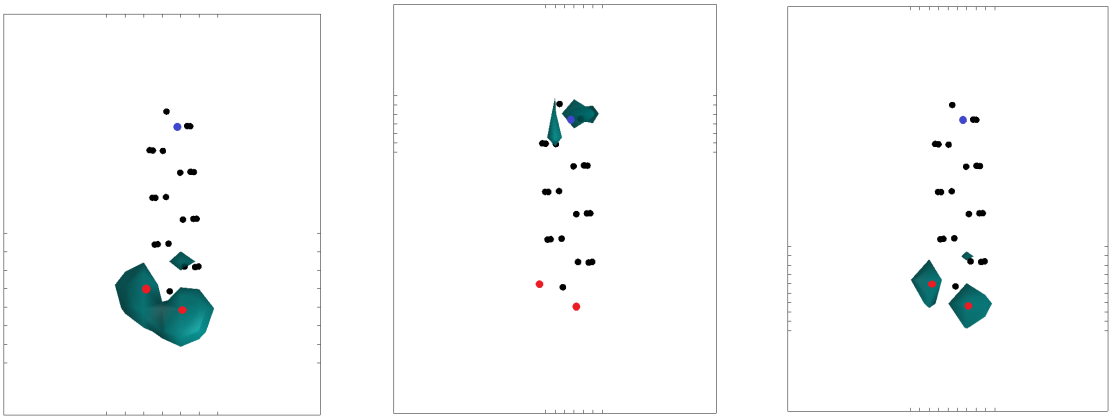

(a) potential -5 V. (b) potential 7.5 V. (c) potential -7.5 V.

Figure 4.4: Picture of the potential isosurfaces for the long driver, the red atoms in the figure's bottom are the oxygen atoms, while the blue one on the top is the nitrogen.

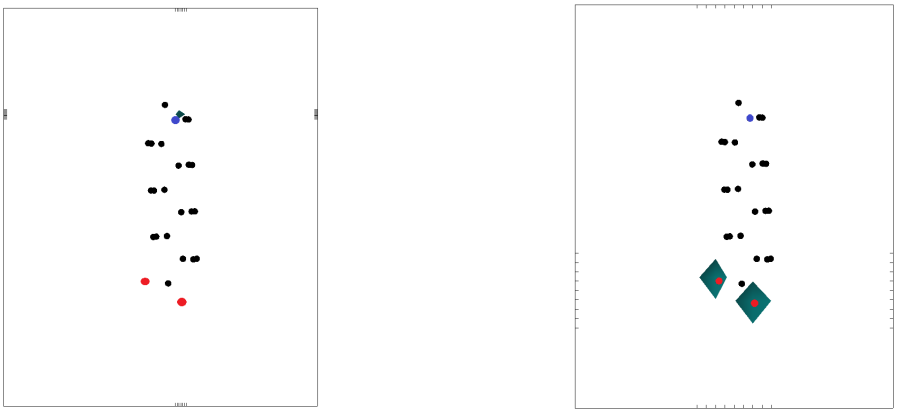

(a) potential 10 V. (b) potential -10 V.

Figure 4.5: Picture of the potential isosurfaces for the long driver, the red atoms in the figure's bottom are the oxygen atoms, while the blue one on the top is the nitrogen.

Small driver

The same consideration (as the long driver) can be done for the small driver molecule. In the table 4.3 are written the dipole moment data and in the figure 4.6 is reported a picture of the molecule.

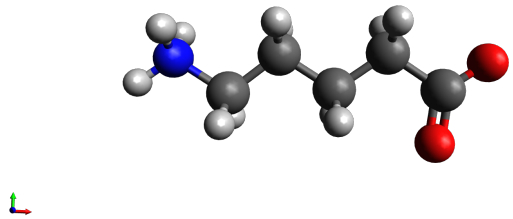

Figure 4.6: Picture of the small driver molecule used in the conduction simulations; the white atoms are hydrogens, the grey ones are carbons, the reds are oxygens and the blue one is nitrogen.

Table 4.3: Small driver dipole moment table, where X, Y and Z are the cartesian coordinates.

	X	Y	Z
Electronic contribution	7.73223	-1.49454	-0.20947
Nuclear contribution	-18.46196	2.74244	0.37638
Total dipole moment	**-10.72973**	**1.24790**	**0.16691**

Also in the small driver case, the potential isosurfaces have been calculated and the results are shown in figures 4.7, 4.8, 4.9 and 4.10.

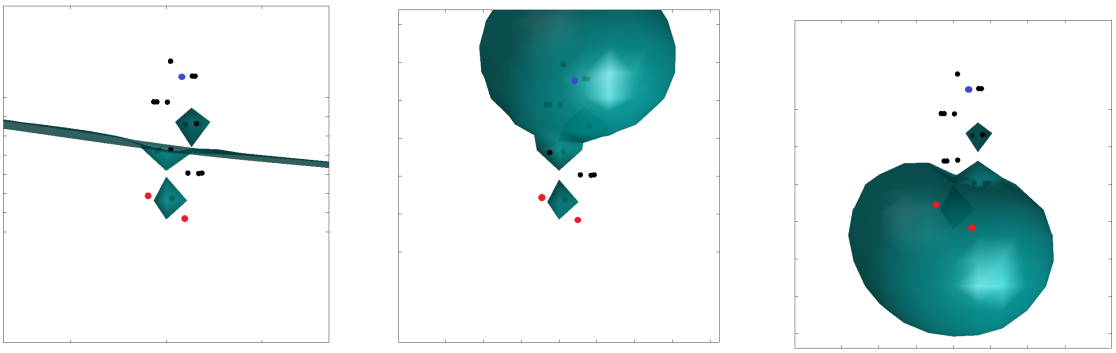

(a) potential 0 V. (b) potential 1 V. (c) potential -1 V.

Figure 4.7: Picture of the potential isosurfaces for the small driver, the red atoms in the figure's bottom are the oxygen atoms, while the blue one on the top is the nitrogen.

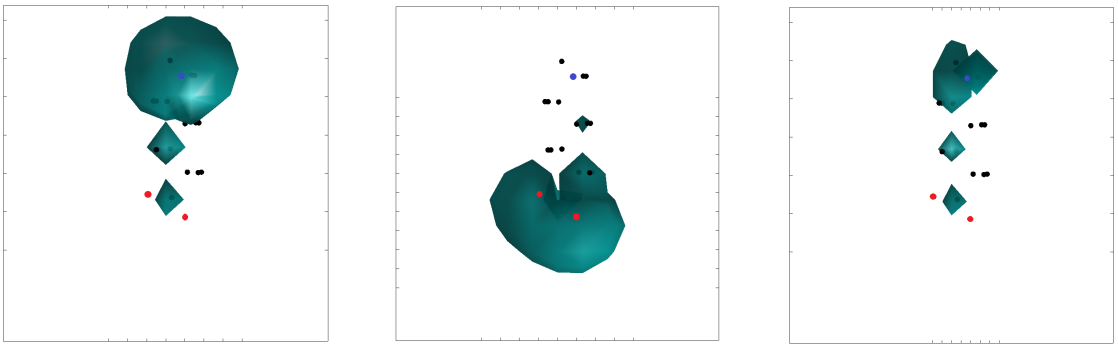

(a) potential 2.5 V. (b) potential -2.5 V. (c) potential 5 V.

Figure 4.8: Picture of the potential isosurfaces for the small driver, the red atoms in the figure's bottom are the oxygen atoms, while the blue one on the top is the nitrogen.

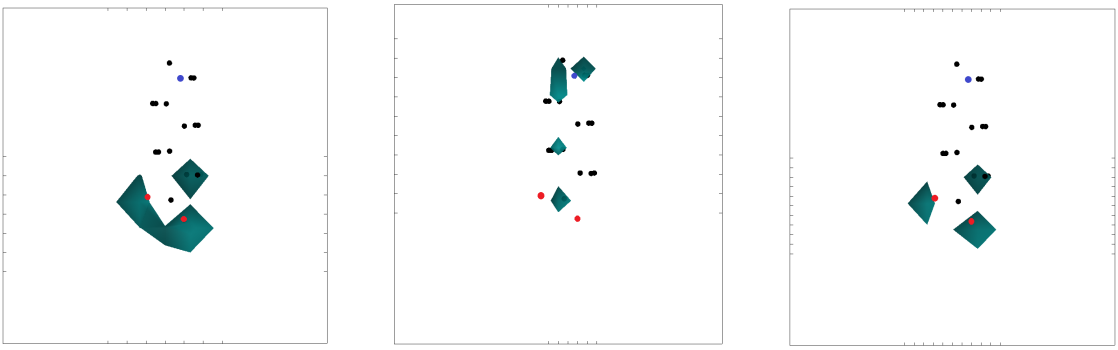

(a) potential -5 V. (b) potential 7.5 V. (c) potential -7.5 V.

Figure 4.9: Picture of the potential isosurfaces for the small driver, the red atoms in the figure's bottom are the oxygen atoms, while the blue one on the top is the nitrogen.

(a) potential 10 V. (b) potential -10 V.

Figure 4.10: Picture of the potential isosurfaces for the small driver, the red atoms in the figure's bottom are the oxygen atoms, while the blue one on the top is the nitrogen.

In general, the small driver molecule presents a lower dipole moment due to its shorter length, for this reason, for the same potential, the long driver exhibits a larger isopotential surface.

4.3 Procedure

The following procedure can be summarized as in figure 4.11. The bold writings are the software used to perform the simulation. The procedure in the figure refers only to the molecular junctions, the driver simulation was performed before.

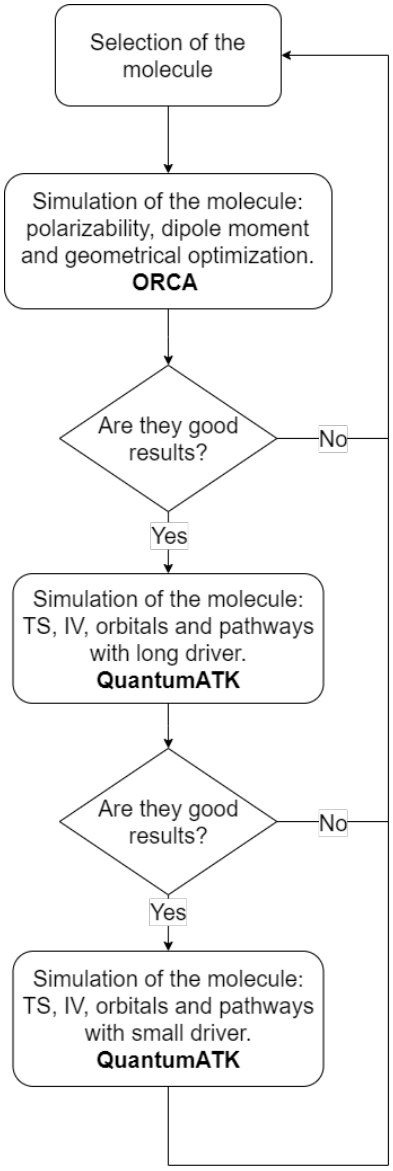

Figure 4.11: Flow chart of the steps followed during the design of the system.

Chapter 5

Results: Polarizability & Polarity

In this chapter are described the two main criteria for the choice of the junction molecule, then the selected molecules are presented highlighting the obtained results. All of the simulations performed for this chapter are made through the ORCA software.

The tables regarding the polarizability, polarity and channel length are reported at the end of the chapter in order to provide a better readability to the section.

5.1 Polarizability

The polarizability is higher in the molecules that have more atoms (therefore more electrons) because the influence of the nuclei is lower on the electrons and in the molecules with a large distance between nuclei and electrons (less control on them).

These hints are perfectly respected in the data reported in table 5.9 which summarize the polarizability results obtained with the selected molecules.

The Zn Pt molecule shows the highest value of polarizability, the OPV3, OPE5 and OPE3 molecules present a high value and they are also currently employed in MT; all of these molecules have a lot of atoms. The selected molecules for the polarizability features are the three cited before.

Below are reported the complete polarizability tensor and the diagonalized one for the selected molecules.

5.2 Polarity

The polarity value depends on the electronegativity of the atoms, in the table 5.10 are reported the dipole moment of the simulated molecules.

The molecules selected for the polarity parameter are 4aminobenzoic acid, Ethyl4-(benzyl-methylamino) benzoate, polar molecule 2 and polar molecule 7 because they have a high value of dipole moment and a shape that could allow good conduction.

For the selected molecules a more precise analysis is reported below, the polarity value is the sum of the electronic and nuclear contribution in each cartesian direction.

5.3 Channel length

The channel length is an important parameter because it influences the conduction properties and the dipole moment of the molecules. The channel length of the selected molecule is summarized in the table 5.11.

5.4 OPV3

The OPV molecules are widely used for molecular junctions because they show good conductance and they can be connected at the gold electrodes through thiol groups [47]. For the readout system has been chosen the OPV3, because it is the best trade-off between conductance and polarizability. The OPV3 is formed by three benzene rings, which are linked together by double-bond carbon atoms. A picture of the optimized geometry is shown in figure 5.1.

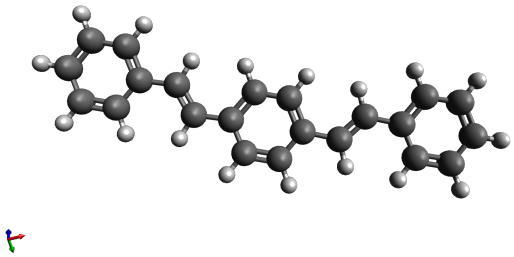

Figure 5.1: Picture of the optimized geometry of the OPV3 molecule. The grey atoms are the carbons, and the white ones are the hydrogens.

The isotropic polarizability of OPV3 is quite high, its value is 321.34993; in the equation 5.1 is reported the complete polarizability tensor, while in the equation 5.2 is written the diagonalized one. It is possible to note that the value in the z-direction (the channel length direction) is very high with respect to the other two directions.

$$\begin{bmatrix} 531.32953 & 139.19253 & -14.70177 \\ 139.19253 & 264.18557 & -67.31812 \\ -14.70177 & -67.31812 & 168.53469 \end{bmatrix} \tag{5.1}$$

$$\begin{bmatrix} 125.40586 & 244.15713 & 594.48680 \end{bmatrix} \tag{5.2}$$

The OPV3 molecule was not selected for its polar behavior, but the parameters related to the dipole moment are given below in the table 5.1.

5.5 OPE3

The OPE molecule differs from the OPV one for the triple bond instead of the double one for the carbon atoms that connect the benzene rings. Also, the OPE conduction

Table 5.1: OPV3 dipole moment table, where X, Y and Z are the cartesian coordinates.

	X	Y	Z
Electronic contribution	-0.17614	0.33993	-0.24174
Nuclear contribution	0.17679	-0.34173	0.24116
Total dipole moment	**0.00064**	**-0.00180**	**-0.00058**

properties are very interesting, hence it is widely studied in the molecular junctions [48]. In the performed analysis the OPE3 molecule is considered; a picture of the optimized geometry is shown in figure 5.2.

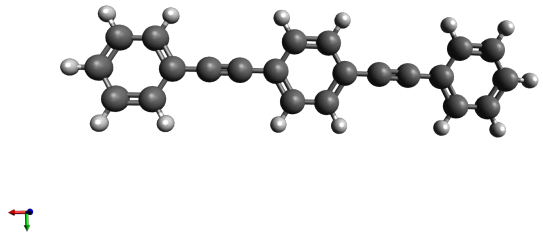

Figure 5.2: Picture of the optimized geometry of the OPE3 molecule. The grey atoms are the carbons, the white ones are the hydrogens.

The OPE3 molecule was selected for its high polarizability parameter, in the equation 5.3 is written the complete polarizability tensor, while in the equation 5.4 is reported the diagonalized one. As before (for the OPV) the direction of the conduction presents the highest value of polarizability in the diagonalized tensor.

$$\begin{bmatrix} 581.36259 & -19.06739 & -82.03654 \\ -19.06739 & 225.80413 & 1.45529 \\ -82.03654 & 1.45529 & 137.62186 \end{bmatrix} \tag{5.3}$$

$$\begin{bmatrix} 122.90473 & 224.86534 & 597.01852 \end{bmatrix} \tag{5.4}$$

In the table 5.2 are reported the electronic contribution, nuclear contribution and the total dipole moment of the considered molecule.

Table 5.2: OPE3 dipole moment table, where X, Y and Z are the cartesian coordinates.

	X	Y	Z
Electronic contribution	-0.00452	-0.11975	0.02180
Nuclear contribution	0.00357	0.13236	-0.02461
Total dipole moment	**-0.00095**	**0.01261**	**-0.00281**

5.6 OPE5

The OPE5 molecule has been selected for its high polarizability value. I thank Chiara for providing me with the optimized geometry shown in figure 5.3.

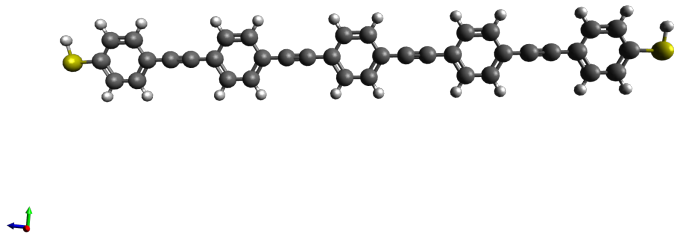

Figure 5.3: Picture of the optimized geometry of the OPE5 molecule. The grey atoms are the carbons, the white ones are the hydrogens and the yellow ones are sulfurs.

As said before, the polarizability value of the OPE5 is very high, in the equation 5.5 is reported the polarizability 3x3 tensor, while in the eqution 5.6 the diagonalized one.

$$\begin{bmatrix} 225.90477 & -2.30643 & 32.16278 \\ -2.30643 & 410.46452 & -127.83587 \\ 32.16278 & -127.83587 & 1558.42985 \end{bmatrix} \tag{5.5}$$

$$\begin{bmatrix} 225.12543 & 396.40992 & 1573.26379 \end{bmatrix} \tag{5.6}$$

In the table 5.3 are reported the electronic contribution, nuclear contribution and the total dipole moment of the considered molecule.

Table 5.3: OPE5 dipole moment table, where X, Y and Z are the cartesian coordinates.

	X	Y	Z
Electronic contribution	-0.03447	-1.80204	-0.20353
Nuclear contribution	0.04418	2.42292	0.27258
Total dipole moment	**0.00971**	**0.62089**	**0.06905**

5.7 Zinc Phthalocyanine with thiols chains

The Pc molecules have attracted the curiosity of researchers for their unique conduction properties [49]. The Pc can host in its center different metals, for our task it has been selected the ZnPc, because it has a very high polarizability value (the highest of the simulated molecules) and a good conduction. The ZnPc can be bonded to the gold electrodes through thiols chains [50]. A picture of the optimized geometry is shown in figure 5.4.

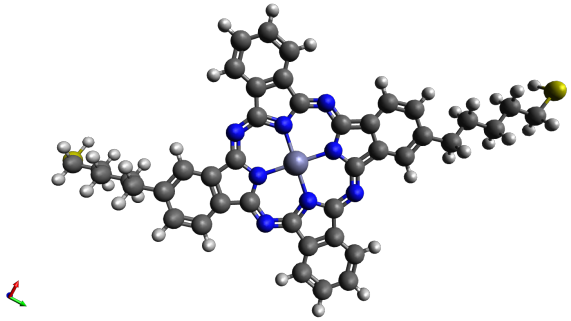

Figure 5.4: Picture of the optimized geometry of the ZnPc molecule. The grey atoms are the carbons, the white ones are the hydrogens, the blue atoms are the nitrogens, the yellow ones are sulfurs and the light grey one (in the middle) is the zinc atom.

The complete polarizability tensor is reported in the equation 5.7, while in the equation 5.8 is written the diagonalized one.

$$\begin{bmatrix} 1052.82440 & 110.87819 & 84.90770 \\ 110.87819 & 1154.49575 & 0.60511 \\ 84.90770 & 0.60511 & 336.69448 \end{bmatrix} \tag{5.7}$$

$$\begin{bmatrix} 326.57933 & 989.33084 & 1228.10447 \end{bmatrix} \tag{5.8}$$

In the table 5.4 are reported the polarity data of the ZnPc.

Table 5.4: Zinc Phthalocyanine with thiols chains dipole moment table, where X, Y and Z are the cartesian coordinates.

	X	Y	Z
Electronic contribution	-7.67886	1.78035	-12.97492
Nuclear contribution	7.58317	-1.66861	12.69459
Total dipole moment	**-0.09569**	**0.11174**	**-0.28033**

5.8 Phthalocyanine & Zinc Phthalocyanine

These data are taken from Alessio Cassella's thesis, I thank him for sharing with me his results. The optimized geometries are reported in figure 5.5.

5.9 4-Aminobenzoic acid

The 4-Aminobenzoic acid is not a common molecule used for molecular junctions, in literature there are no studies about it. It was selected for its important features: the starting block is the benzene, to which nitrogen is added on one side and oxygens on the other. This specific geometry allows us to obtain a good polarity (nitrogen provides

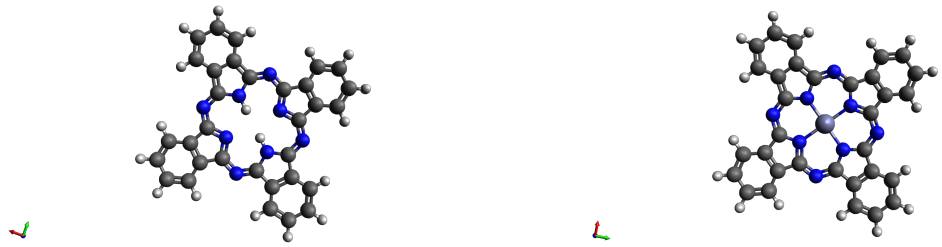

(a) Phthalocyanine molecule. (b) Zinc Phthalocyanine molecule.

Figure 5.5: Picture of the optimized geometry of the Pc and ZnPc molecules. The grey atoms are the carbons, the white ones are the hydrogens, the red atoms are the oxygens, the blue one is the nitrogen and the light grey atom is the zinc.

the positive pole, while oxygens the negative one) and the benzene is deeply studied in molecular junctions [51]. Figure 5.6 is the result of the optimized geometry obtained through the ORCA program.

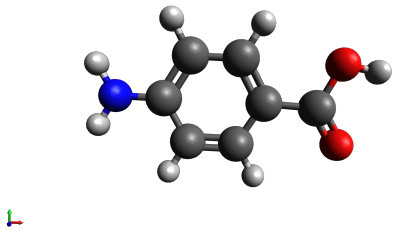

Figure 5.6: Picture of the optimized geometry of the 4-Aminobenzoic acid molecule. The grey atoms are the carbons, the white ones are the hydrogens, the red atoms are the oxygens and the blue one is the nitrogen.

The selected molecule is not chosen for its polarizability value, but in any case in the equation 5.9 is reported the complete polarizability tensor and in the equation 5.10 the diagonalized one.

$$\begin{bmatrix} 143.42545 & -2.74613 & -0.00093 \\ -2.74613 & 95.42753 & -0.00067 \\ -0.00093 & -0.00067 & 50.94163 \end{bmatrix} \tag{5.9}$$

$$\begin{bmatrix} 50.94163 & 95.27092 & 143.582057 \end{bmatrix} \tag{5.10}$$

In the table 5.5 is possible to notice the electronic and nuclear contribution to the dipole moment for the 4-Aminobenzoic acid. In the x-direction, the dipole moment is high, as expected, because the x-direction is the red arrow in the figure 5.6 (it is the conduction direction). The nitrogen and the oxygens provide the two poles which are responsible for the polarity of the molecule. The sign of the dipole moment is due to the orientation of the dipole, in this case, the positive pole is closer to the beginning of the x-axis, for this reason, the overall value is negative (the arrow concerning the electric field generated by the dipole is in the opposite direction with respect the x-axis).

Table 5.5: 4-Aminobenzoic acid dipole moment table, where X, Y and Z are the cartesian coordinates.

	X	Y	Z
Electronic contribution	5.35138	-0.49855	-0.00033
Nuclear contribution	-6.94100	1.10748	0.00031
Total dipole moment	**-1.58962**	**0.60893**	**-0.00002**

5.10 Ethyl4-(benzyl-methylamino)benzoate

The Ethyl4-(benzyl-methylamino)benzoate was considered thanks to the similarity with OPV and OPE molecules but it has also nitrogen and oxygens in the chain which could provide the polarity to the molecule. There are no studies in literature in which this molecule is used as the junction channel.

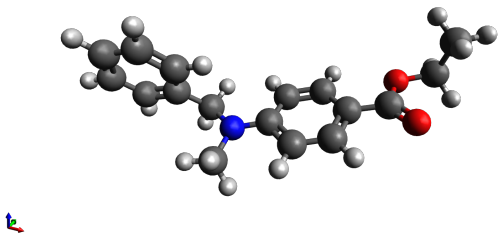

Figure 5.7: Picture of the optimized geometry of the Ethyl4-(benzyl-methylamino) benzoate molecule. The grey atoms are the carbons, the white ones are the hydrogens, the red atoms are the oxygens and the blue one is the nitrogen.

In the equation 5.11 is written the complete polarizability tensor, while in the equation 5.12 the diagonalized one. Due to the long dimension of the channel, its isotropic polarizability is one of the highest of the simulated molecules.

$$\begin{bmatrix} 299.56308 & 57.54605 & 8.37999 \\ 57.54605 & 196.67547 & 2.78950 \\ 8.37999 & 2.78950 & 164.88877 \end{bmatrix} \tag{5.11}$$

$$\begin{bmatrix} 164.29351 & 171.04631 & 325.78750 \end{bmatrix} \tag{5.12}$$

The long channel, the oxygens and the nitrogen cause the polarity value to be the third of the selected molecules, behind only to L-serine and 4-Aminobenzoic acid. In the table 5.6 are reported the contributions of the dipole moment, it is possible to see that the highest contribution is in the x-direction, so the considerations are the same as before. In this case, the nuclear contribution is more relevant with respect to the electronic one.

Table 5.6: Ethyl4-(benzyl-methylamino)benzoate dipole moment table, where X, Y and Z are the cartesian coordinates.

	X	Y	Z
Electronic contribution	-0.01017	-0.48755	-2.20393
Nuclear contribution	-1.55378	0.44457	2.16073
Total dipole moment	**-1.56395**	**-0.04298**	**-0.04320**

5.11 Polar molecule 2

The polar molecule 2 is not present in nature, it has been designed specifically for this purpose. The body of the molecule is a benzene chain, made with 4 benzenes bound together. From this body, OH and NH_2 groups were added to provide respectively the negative and positive poles.

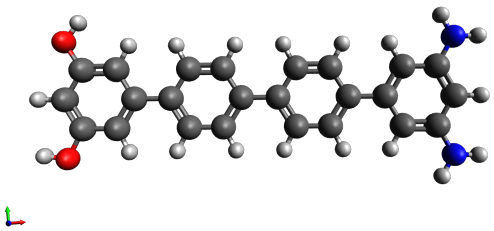

Figure 5.8: Picture of the optimized geometry of the polar molecule 2. The grey atoms are the carbons, the white ones are the hydrogens, the red atoms are the oxygens and the blue one is the nitrogen.

The body of the molecule is similar to the OPV3 and OPE3 molecules, therefore high polarizability is also expected. The results are reported in the equations 5.13 (polarizability tensor) and 5.14 (diagonalized tensor).

$$\begin{bmatrix} 602.83776 & -17.11357 & -0.00063 \\ -17.11357 & 305.06889 & -0.01674 \\ -0.00063 & -0.01674 & 144.53408 \end{bmatrix} \tag{5.13}$$

$$\begin{bmatrix} 144.53408 & 304.08856 & 603.81809 \end{bmatrix} \tag{5.14}$$

The table 5.7 is very important because it highlights the polar behavior of the molecule, thus the goodness of the molecule design.

5.12 Polar molecule 7

The polar molecule 7 is not present in nature, it has been designed specifically for this purpose. The body of the molecule is an OPE3 molecule, at which OH and NH_2 groups

Table 5.7: Polar molecule 2 dipole moment table, where X, Y and Z are the cartesian coordinates.

	X	Y	Z
Electronic contribution	-14.98708	0.61688	0.00066
Nuclear contribution	15.96325	-0.21784	-0.00110
Total dipole moment	**1.06617**	**0.39904**	**-0.00044**

were added to provide respectively the negative and positive poles. In figure 5.9 is shown the optimized geometry of the molecule.

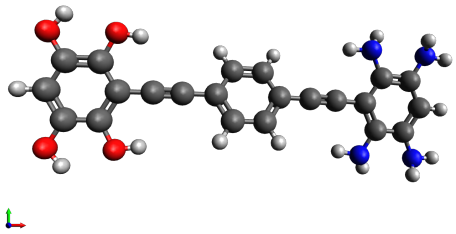

Figure 5.9: Picture of the optimized geometry of the polar molecule 7. The grey atoms are the carbons, the white ones are the hydrogens, the red atoms are the oxygens and the blue one is the nitrogen.

Since it is similar to the OPE3 molecule, a high polarizability value is expected. The results in the equations 5.15 5.16 confirm the expectations.

$$\begin{bmatrix} 645.85234 & -16.38106 & -85.78338 \\ -16.38106 & 313.50418 & -1.15200 \\ -85.78338 & -1.15200 & 169.78504 \end{bmatrix} \tag{5.15}$$

$$\begin{bmatrix} 154.70056 & 312.87301 & 661.56799 \end{bmatrix} \tag{5.16}$$

Table 5.8 highlights the polar properties of the molecule with the highest dipole moment value between the simulated ones. The molecule design has been performed in a good way because the polar molecule 7 exhibits the more relevant polar behavior.

Table 5.8: Polar molecule 7 dipole moment table, where X, Y and Z are the cartesian coordinates.

	X	Y	Z
Electronic contribution	-26.43883	1.47961	4.87276
Nuclear contribution	29.08194	-1.59202	-5.24742
Total dipole moment	**2.64310**	**-0.11240**	**-0.37466**

Table 5.9: Polarizability results of the selected molecules.

Pos	**Molecule**	**Isotropic polarizability**
1	Zinc Phthalocyanine with thiols chains	848.00488
2	OPE5	731.59971
3	Zinc Phthalocyanine	647.900
4	Phthalocyanine	645.606
5	Polar molecule 7	376.38052
6	Polar molecule 2	350.81358
7	Polar molecule 6	348.89216
8	Polar molecule 4	348.07290
9	Polar molecule 1	334.52060
10	Polar molecule 3	324.61291
11	Polar molecule 5	324.27997
12	OPV3	321.34993
13	OPE3	314.92953
14	Ethyl4-(benzyl-methylamino) benzoate	220.37577
15	Ethyl4-[(benzylamino)methyl] benzoate	211.68717
16	1,2-dimethyl-1H-indol-3-yl benzoate	184.37797
17	3TT	138.85508
18	Methyl anthranilate	107.62820
19	5methyl-3heptanone	97.12313
20	4aminobenzoic acid	96.59820
21	Methyl benzoate	96.04181
22	L-glutamine	81.90181
23	L-asparagine	69.96155
24	L-proline	68.67093
25	L-cysteine	67.18006
26	L-threonine	65.61772
27	Benzene	64.05507
28	Trimethyl-aluminium	61.92885
29	L-serine	53.30319
30	Acetaldehyde	27.71692

Table 5.10: Polarity results of the selected molecules.

Pos	**Molecule**	**Dipole moment (a.u.)**	**Dipole moment (Debye)**
1	Polar molecule 7	2.67189	6.79141
2	L-serine	1.93994	4.93094
3	Polar molecule 6	1.84579	4.69161
4	4aminobenzoic-acid	1.70226	4.32680
5	Ethyl4-(benzyl-methylamino) benzoate	1.56395	3.97827
6	L-asparagine	1.46974	3.73577
7	L-glutamine	1.26720	3.22098
8	Polar molecule 2	1.13840	2.89359
9	Acetaldehyde	1.12697	2.86452
10	L-threonine	1.07481	2.73196
11	L-proline	1.03592	2.63311
12	5methyl-3heptanone	1.00792	2.56192
13	Methyl benzoate	0.77581	1.97195
14	Ethyl4-[(benzylamino)methyl] benzoate	0.74985	1.90598
15	OPE5	0.62479	1.58809
16	Polar molecule 5	0.62000	1.57591
17	Polar molecule 4	0.50164	1.27507
18	Polar molecule 3	0.49402	1.25570
19	Polar molecule 1	0.35028	0.89035
20	Zinc Phthalocyanine with thiol chains	0.31659	0.80470
21	L-cysteine	0.26470	0.67282
21	3TT	0.16500	0.41940
23	Methyl anthranilate	0.15497	0.39390
24	1,2-dimethyl-1H-indol-3-yl benzoate	0.09476	0.24086
25	OPE3	0.01295	0.03292
26	OPV3	0.00200	0.00508
27	Trimethyl-Aluminum	0.00131	0.00333
28	Benzene	0.00000	0.00001

Table 5.11: Channel length of the selected molecules.

Pos	**Molecule**	**Channel length (Å)**
1	OPE5	33.772
2	Zinc Phthalocyanine with thiols chains	27.135
3	OPE3	18.626
4	Polar molecule 6	18.608
5	Polar molecule 7	18.538
6	Polar molecule 2	18.175
7	OPV3	18.108
8	Polar molecule 1	17.940
9	Polar molecule 5	17.887
10	Polar molecule 3	17.803
11	Polar molecule 4	17.784
12	Zinc Phthalocyanine	15.513
13	Phthalocyanine	15.113
14	Ehyl4-[(benzylamino)methyl] benzoate	14.100
15	Ethyl4-(benzyl-methylamino) benzoate	13.926
16	1,2-dimethyl-1H-indol-3-yl benzoate	11.651
17	3TT	8.410
18	L-glutamine	8.168
19	4aminobenzoic acid	7.902
20	5methyl-3heptanone	7.833
21	Methyl benzoate	7.791
22	Methyl anthralinate	7.776
23	L-asparagine	6.099
24	L-threonine	5.845
25	L-proline	5.664
26	L-cysteine	5.035
27	Benzene	4.935
28	Trimethyl-aluminium	4.846
29	L-serine	4.173
30	Acetaldehyde	3.101

Chapter 6

Results: Conduction

In this chapter all the simulations are performed at 300 K and all the TS plots shown are obtained at equilibrium, hence no voltage is applied. All the electrodes are made of gold with Miller index (1,1,1) and the anchoring groups are always sulfur atoms. The default distance between the driver and the junction molecule is 7 Å, in some cases, the distance is greater, but in these particular analyses, the distance is explicitly written.

6.1 OPV3

The OPV3 molecule has been selected for its high polarizability value and it is also well known in molecular junction literature. In figure 6.1 are shown the QuantumATK builders related to the long driver, figure 6.1a stands for the logic '0' configuration, while figure 6.1b for the logic '1' one.

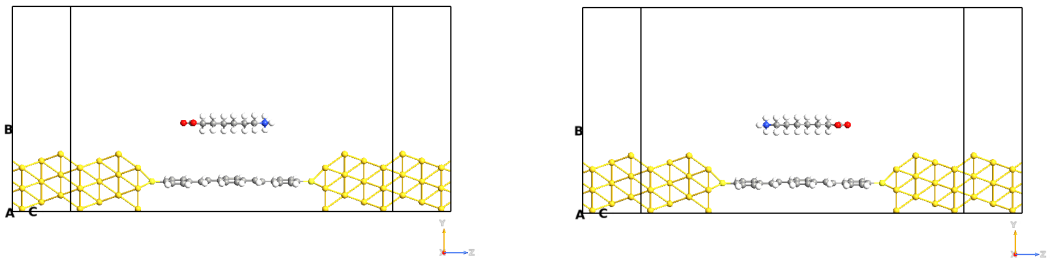

(a) logic '0' configuration.

(b) logic '1' configuration.

Figure 6.1: Picture of the QuantumATK builder for the OPV3 molecule with the long driver. The white atoms are the hydrogens, the yellow ones are gold atoms, the lighter yellow ones are the sulfurs, the blue ones are nitrogens, the reds are the oxygens and the grey atoms are carbons.

In figure 6.2 are reported the builders related to the small driver. This analysis was performed only for two molecules (OPV3 and OPE3) because they are the only ones that

are currently employed in MTs. It is possible to notice the two different configurations thanks to the driver molecule orientation.

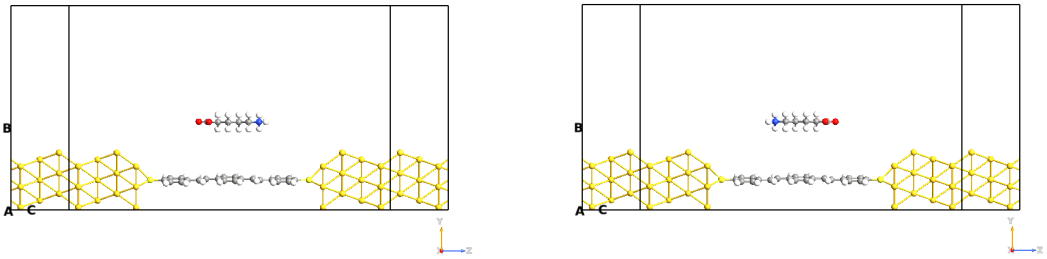

(a) logic '0' configuration. (b) logic '1' configuration.

Figure 6.2: Picture of the QuantumATK builder for the OPV3 molecule with the small driver. The white atoms are the hydrogens, the yellow ones are gold atoms, the lighter yellow ones are the sulfurs, the blue ones are nitrogens, the reds are the oxygens and the grey atoms are carbons.

6.1.1 Long driver: TS

The figure 6.3a shows the TS for the OPV3 molecule considering the long driver, it is possible to notice that the shape of the two configurations is roughly the same, but the differences are related to the wideness and the amplitude of the peaks. Seeing the figure 6.3a is observable that the conduction is LUMO type because the LUMO peaks are closer to the 0 eV than the HOMO ones.

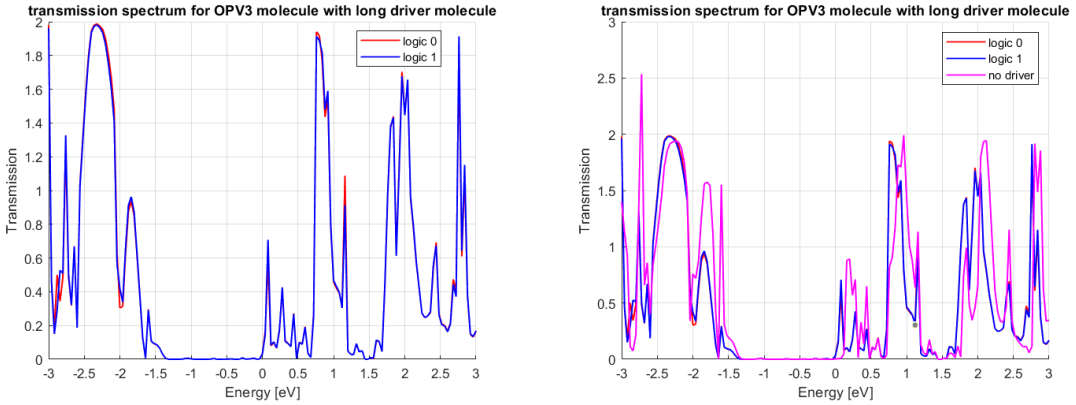

(a) without no driver configurations. (b) with no driver configurations.

Figure 6.3: Picture of the TS for the OPV3 molecule considering the long driver; the red curve is the one for the logic '0' configuration, the blue one is for the logic '1' and the magenta one for the no driver configuration.

An interesting characteristic to notice is the difference between the two configurations

and the no driver one, in which is possible to appreciate the influence of the electric field generated by the driver on the junction. In figure 6.3b the driver seems to push electrons away from the nucleus therefore a lower force of attraction is applied to the electrons and the consequence is a higher current for the two driver configurations with respect to the no driver one.

6.1.2 Small driver: TS

The figure 6.4a represents the TS considering the small driver. The lower dipole moment (with respect to the long driver) influences them in a different way the molecular junction, the peaks have higher amplitude but they are narrower. As before the differences between the two configurations are not related to the shape but only to the amplitude and wideness.

In the figure 6.4b is reported the TS for the two configurations and the no driver one. It is possible to notice that the shape is changed for the no driver configuration to the other two configurations; a higher current is expected in the two configurations because the LUMO peak is closer to the 0 eV with respect to the no driver one.

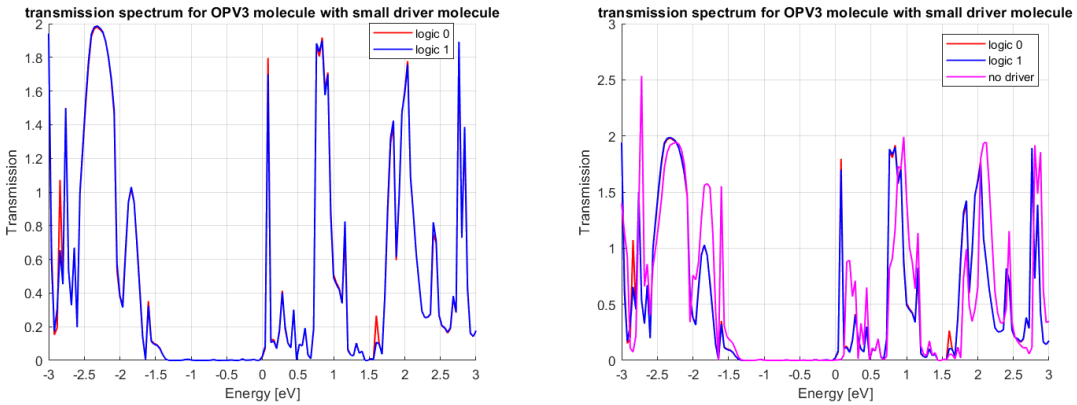

(a) without no driver configurations.

(b) with no driver configurations.

Figure 6.4: Picture of the TS for the OPV3 molecule considering the small driver; the red curve is the one for the logic '0' configuration, the blue one is for the logic '1' and the magenta one for the no driver configuration.

6.1.3 Long vs Small driver: TS

In this section are analyzed the results for the two different logic values considering the two drivers. The aim of this comparison is to study the effect of different applied electric fields. This analysis can rely upon the not-perfect QCA in the molecular FCN, thus when the charge is not perfectly localized in the logic dot.

In the figure 6.5 are reported the two plots for the logic '0' (figure 6.5a) and logic '1' (figure 6.5b). The influence is not changing significantly the trend of the curves, but it

changes the wideness and amplitude of the TS. The small driver peaks are narrower and higher than the long driver ones.

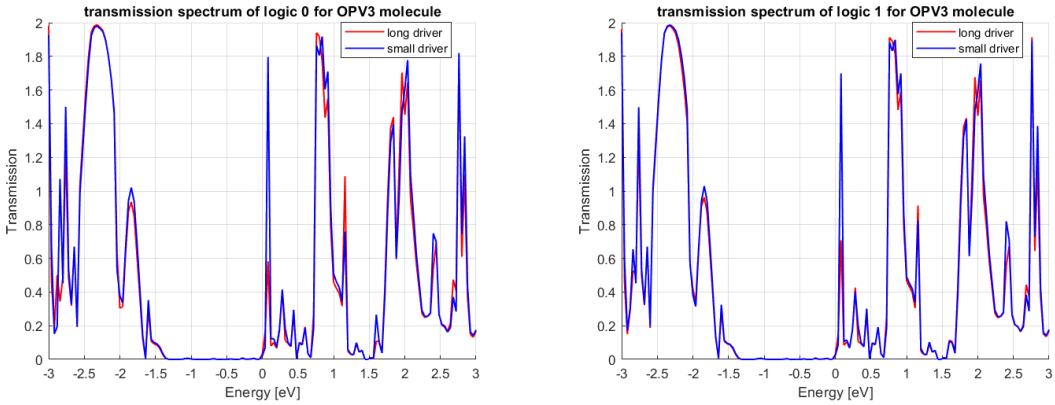

(a) Logic '0' configuration.

(b) Logic '1' configuration.

Figure 6.5: Pictures of the TS curve of the logic '0' and logic '1' for the OPV3 molecule considering the long driver - 9.9 Å (red line) and the small driver - 7.3 Å (blue line).

6.1.4 Long driver: IV

The IV plot is the most relevant one because the current is the physical quantity that can be read by the CMOS world. In the figure 6.6a are shown the two IV curves for the OPV3 molecule considering the long driver. It is possible to appreciate that the current values are quite high (thousands of nA, so few μA) and the difference around the 0.35 V of applied voltage is large enough to sense it.

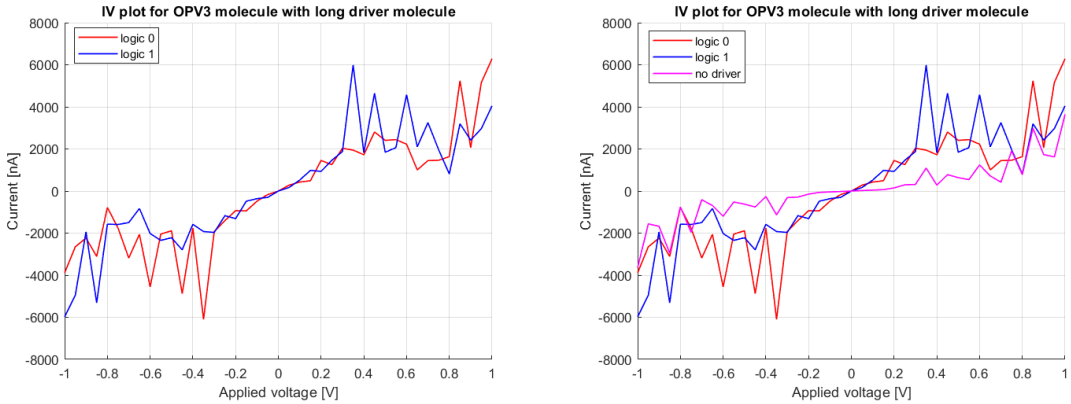

(a) Without the no driver configuration.

(b) With the no driver configuration.

Figure 6.6: Picture of the IV for the OPV3 molecule considering the long driver; the red curve is the one for the logic '0' configuration, the blue one is for the logic '1' and the magenta one for the no driver configuration.

Figure 6.6b shows the influence of the drivers on the junction because the magenta curve is the one without drivers. As expected, the current in the no driver condition is lower than the other ones. The electric field generated by the driver helps the applied voltage to increase the current.

From the figure 6.7 we can easily say that the readout system made by the molecular junction works, the current difference is enough to distinguish the two logic values. In particular, the picture shows the modules' current difference between the two configurations under the influence of the long driver. It is possible to observe that the graph shows an odd function behavior, it is expected in the high polarizability molecule because they are more symmetrical than the ones with a high dipole moment.

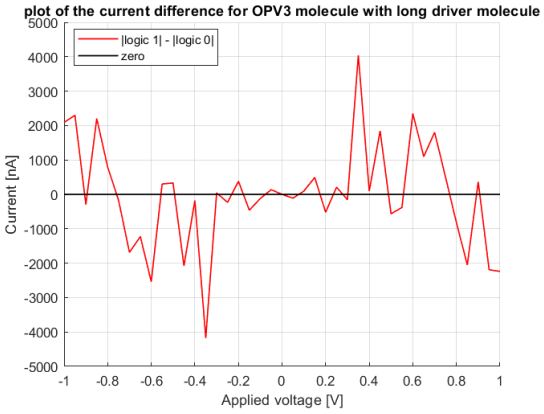

Figure 6.7: Picture of the current difference between |logic '1'| and |logic '0'| for the OPV3 molecule considering the long driver, the black line is the zero line.

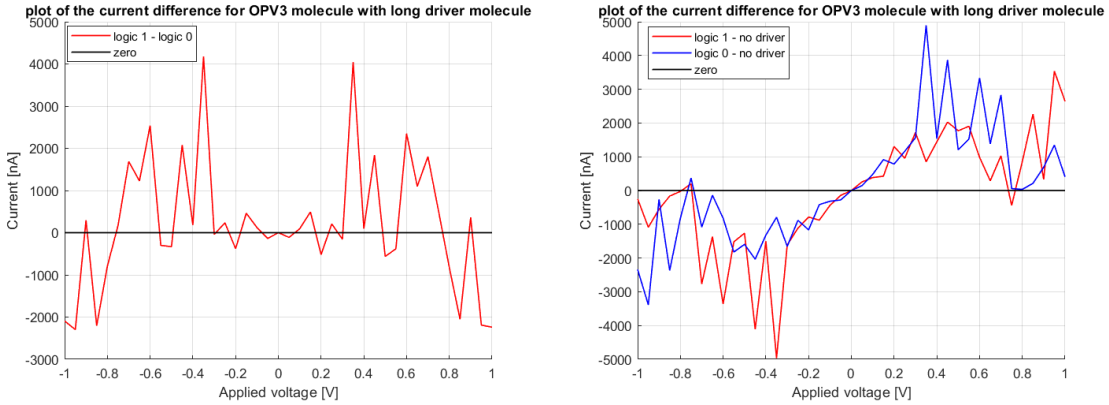

(a) logic '1' - logic '0'.

(b) logic '1' or logic '0' - no driver.

Figure 6.8: Picture of the current difference for the OPV3 molecule considering the long driver.

In the figure 6.8 are reported two graphs which represent different conditions. Figure 6.8a is the same as figure 6.7 but instead of absolute values of current are taken the values

with sign (the flow direction); while the figure 6.8b is obtained through the subtraction of the current corresponding to the two logic values and the no driver condition for highlighting the effect of the electric field generated by the driver on the junction. As expected, the current of the logic configuration is higher than the no driver configuration one.

6.1.5 Small driver: IV

The current trend follows the same course also in the case of small driver. It is possible to observe that the bigger current difference is placed at 0.35 V of applied voltage (the same as the long driver case). In the figure 6.9 are reported the two IV plot, one with the no driver configuration (figure 6.9b) and the other without the no driver configuration (figure 6.9a).

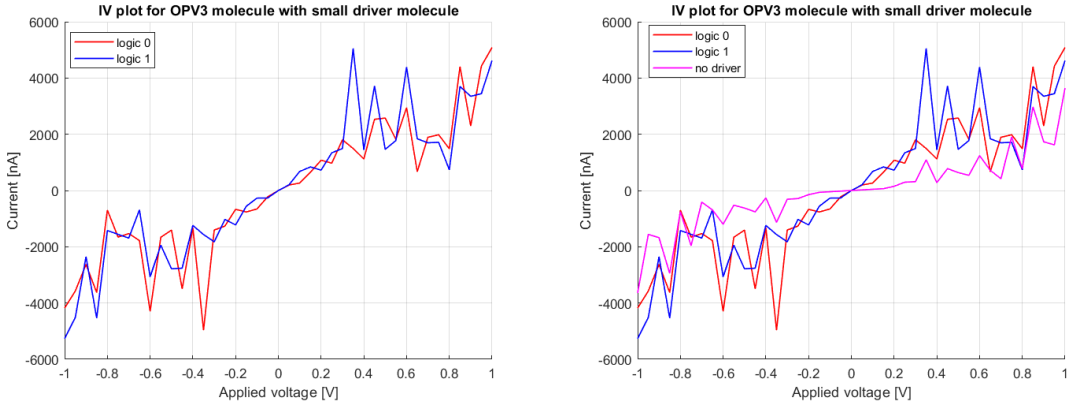

(a) Without the no driver configuration.

(b) With the no driver configuration.

Figure 6.9: Picture of the IV for the OPV3 molecule considering the small driver; the red curve is the one for the logic '0' configuration, the blue one is for the logic '1' and the magenta one for the no driver configuration.

Figure 6.10 shows the feasibility of a molecular junction for the readout system, because the highest peak corresponds to a difference of about 3.5 μA between the two configurations. As expected, this value is lower than the long driver one (about 4 μA) because the dipole moment of the small driver is lower than the long driver one. The function appears to be an odd function in the range (-0.8 V, 0.8 V).

The figure 6.11 shows two plots: figure 6.11a represents the current difference between the two logic values while figure 6.11b is the current difference between the logic values and the no driver condition. Each of the figures highlights the importance and the influence of the driver, it is a good result to sense the logic values difference.

6.1.6 Long vs Small driver: IV

In this section will be deeply analyzed the influence of the drivers on the molecular junction, comparing the different results due to the different drivers on the same logic

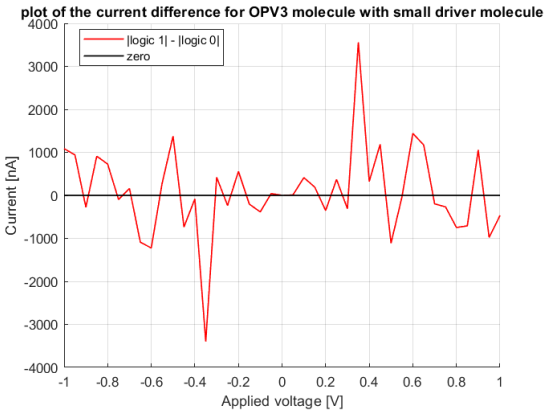

Figure 6.10: Picture of the current difference between |logic '1'| and |logic '0'| for the OPV3 molecule considering the small driver, the black line is the zero line.

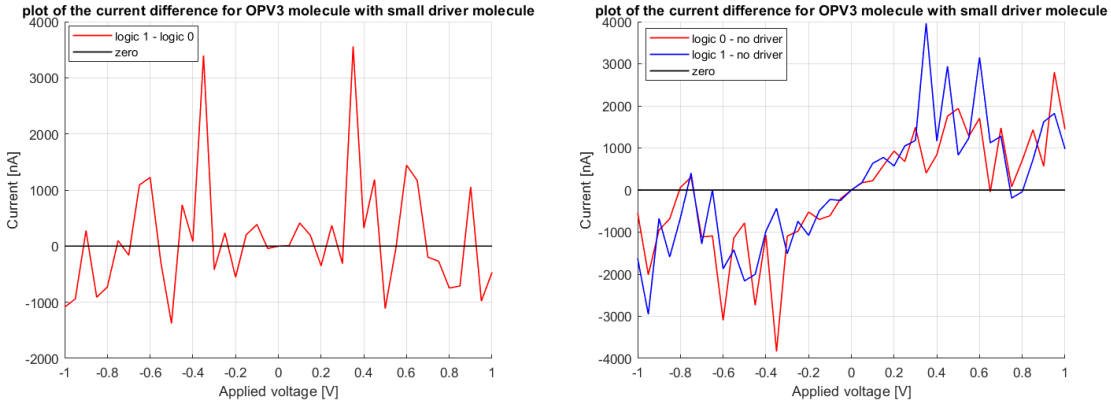

(a) logic '1' - logic '0'.

(b) logic '1' or logic '0' - no driver.

Figure 6.11: Picture of the current difference for the OPV3 molecule considering the small driver.

value configuration.

In figure 6.12 is plotted the IV curves for the different configurations. The figure 6.12a shows the logic '0' value for the two different drivers, it is possible to notice that the long driver current is higher (in absolute value) almost everywhere in the bias range than the small driver one. The same conclusions can be deduced from the figure 6.12b which exhibits the logic '1' value.

In the figure 6.13 are reported the current differences for the different logic values. In figure 6.13a is displayed the difference with the sign of the long driver case minus the small driver one, while figure 6.13b shows the difference considering the absolute value of the current; of course, for positive voltages, the plots are the same in the two cases.

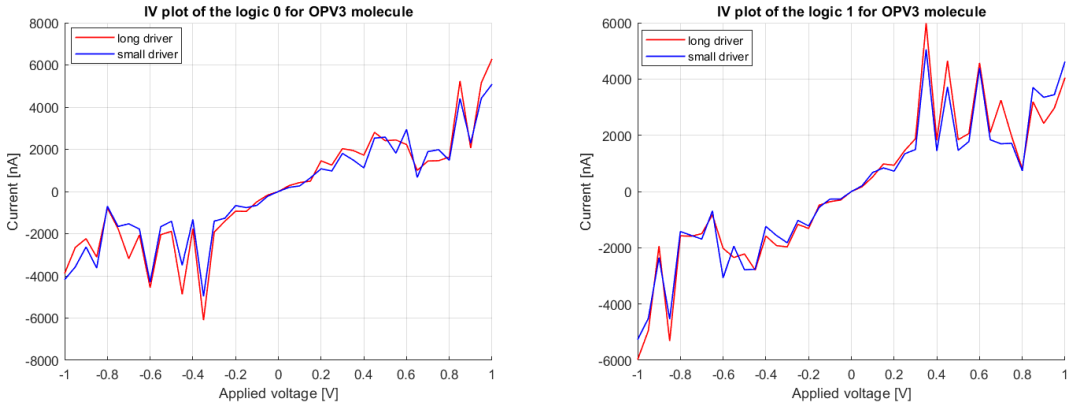

(a) logic '0' configuration.

(b) logic '1' configuration.

Figure 6.12: Picture of the IV curve of the logic '0' and logic '1' for the OPV3 molecule considering the long driver - 9.9 Å (red line) and the small driver - 7.3 Å (blue line).

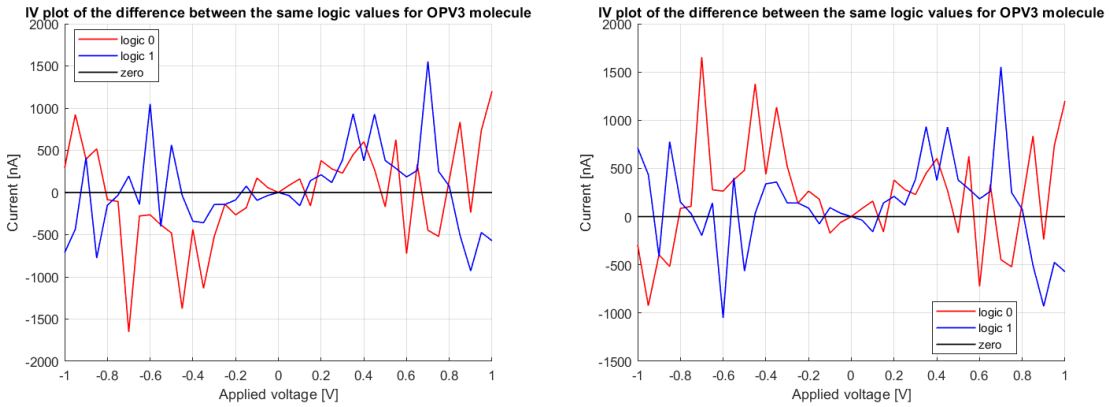

(a) long driver - small driver.

(b) |long driver| - |small driver|.

Figure 6.13: Picture of the current difference between long and small driver (I long driver - I small driver) of the logic '1' (blue curve) and logic '0' (red curve) for the OPV3 molecule.

6.1.7 Long driver: Orbitals

The orbital view could highlight the influence of the driver on the junction molecule. As we can notice in figures 6.14, 6.15 and 6.16 the orbitals shape of HOMO-1 level are very different between the two configurations. The logic '0' plot (6.14a is more spread along the molecule, while the logic '1' one (6.14b) is more concentrated on the electrode close to the negative pole of the driver.

For all the other energy levels, the orbitals are the same or are complementary, this result can be interpreted in the same way because the orbitals are the eigenstate of the solution of Schrödinger's equation. This means that they have the same shape but different phases.

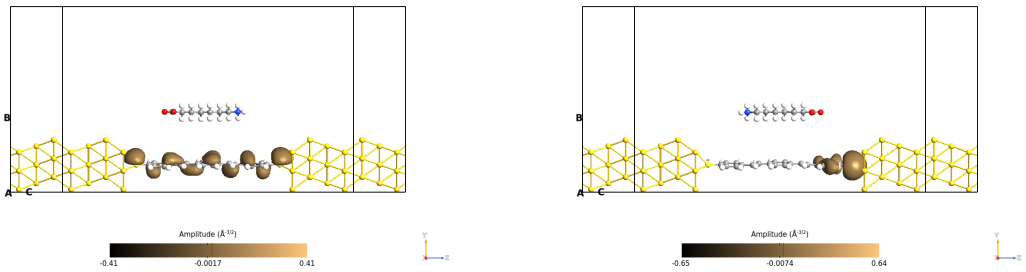

(a) logic '0'. (b) logic '1'.

Figure 6.14: Picture of the orbitals corresponding to the HOMO-1 level for the OPV3 molecule with long driver on the yz plane. The orbitals are taken with an isosurface value equal to 0.015.

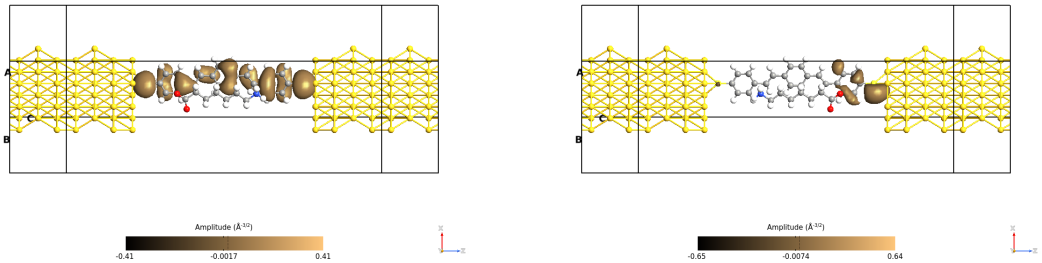

(a) logic '0'. (b) logic '1'.

Figure 6.15: Picture of the orbitals corresponding to the HOMO-1 level for the OPV3 molecule with long driver on the xz plane with the driver. The orbitals are taken with an isosurface value equal to 0.015.

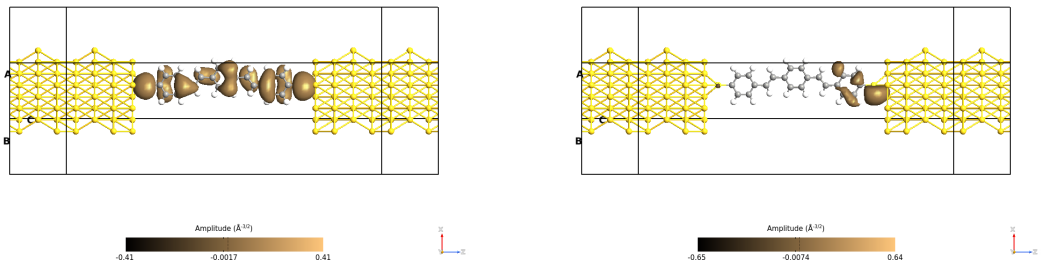

(a) logic '0'. (b) logic '1'.

Figure 6.16: Picture of the orbitals corresponding to the HOMO-1 level for the OPV3 molecule with long driver on the xz plane without the driver. The orbitals are taken with an isosurface value equal to 0.015.

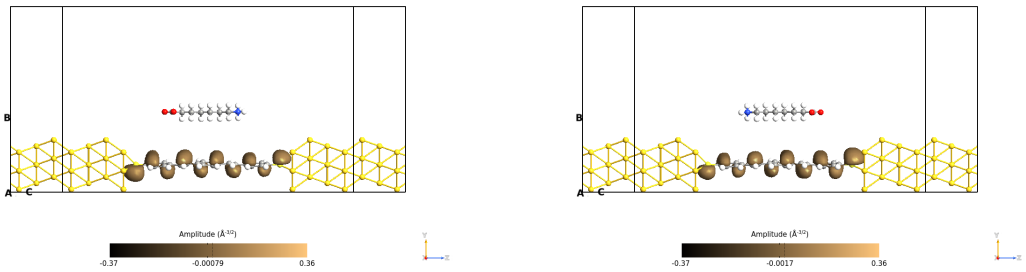

(a) logic '0'. (b) logic '1'.

Figure 6.17: Picture of the orbitals corresponding to the HOMO level for the OPV3 molecule with long driver on the yz plane. The orbitals are taken with an isosurface value equal to 0.015.

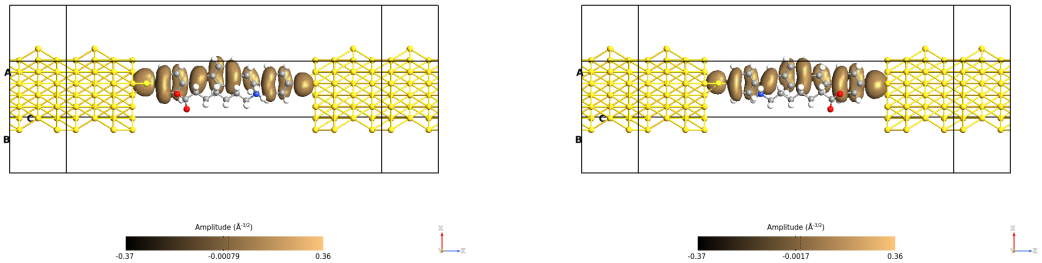

(a) logic '0'. (b) logic '1'.

Figure 6.18: Picture of the orbitals corresponding to the HOMO level for the OPV3 molecule with long driver on the xz plane with the driver. The orbitals are taken with an isosurface value equal to 0.015.

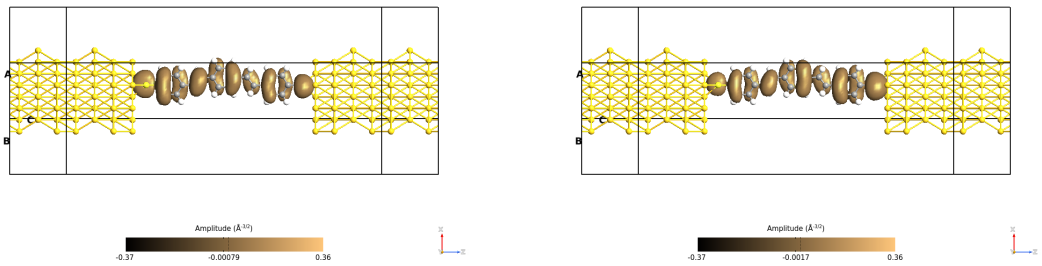

(a) logic '0'. (b) logic '1'.

Figure 6.19: Picture of the orbitals corresponding to the HOMO level for the OPV3 molecule with long driver on the xz plane without the driver. The orbitals are taken with an isosurface value equal to 0.015.

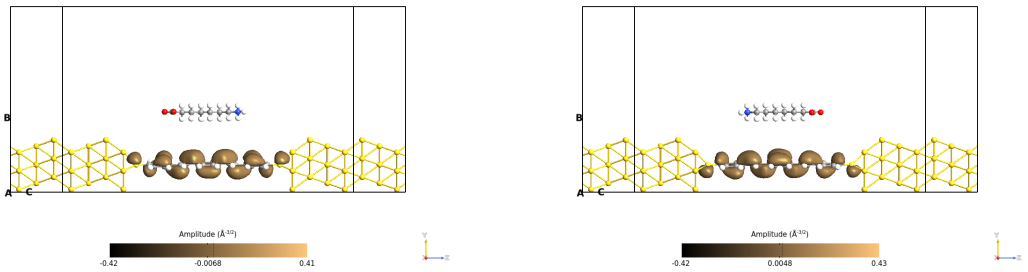

(a) logic '0'. (b) logic '1'.

Figure 6.20: Picture of the orbitals corresponding to the LUMO level for the OPV3 molecule with long driver on the yz plane. The orbitals are taken with an isosurface value equal to 0.015.

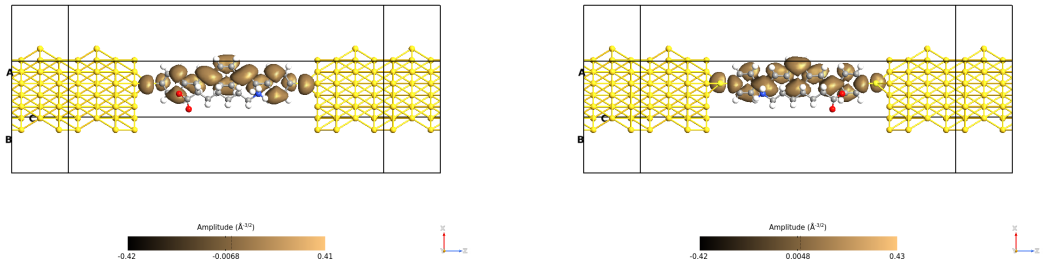

(a) logic '0'. (b) logic '1'.

Figure 6.21: Picture of the orbitals corresponding to the LUMO level for the OPV3 molecule with long driver on the xz plane with the driver. The orbitals are taken with an isosurface value equal to 0.015.

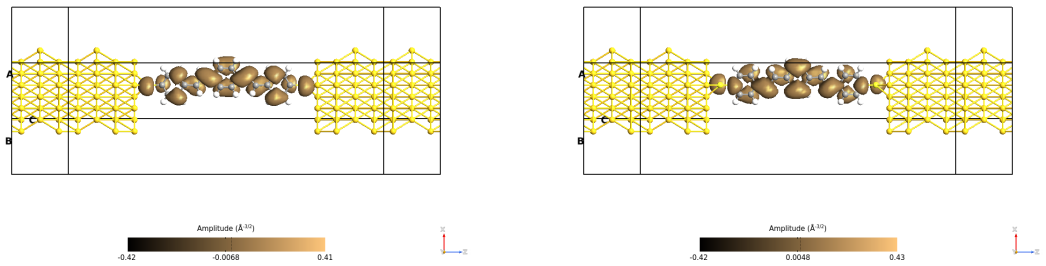

(a) logic '0'. (b) logic '1'.

Figure 6.22: Picture of the orbitals corresponding to the LUMO level for the OPV3 molecule with long driver on the xz plane without the driver. The orbitals are taken with an isosurface value equal to 0.015.

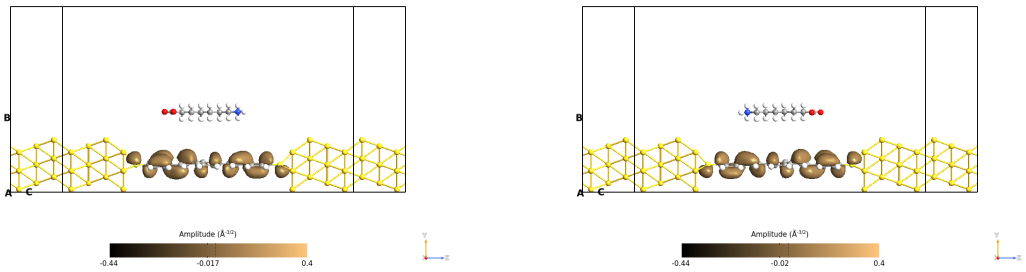

(a) logic '0'. (b) logic '1'.

Figure 6.23: Picture of the orbitals corresponding to the LUMO+1 level for the OPV3 molecule with long driver on the yz plane. The orbitals are taken with an isosurface value equal to 0.015.

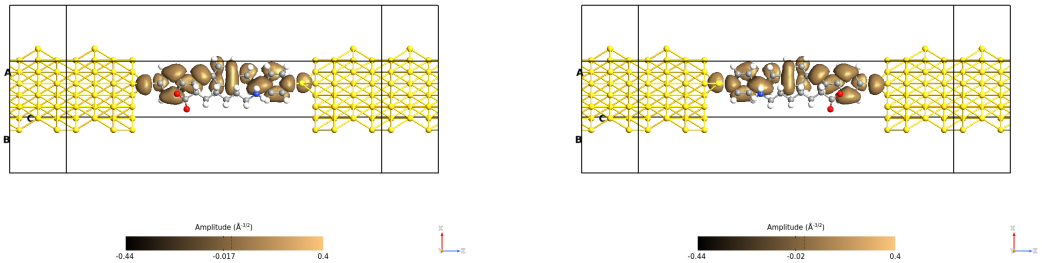

(a) logic '0'. (b) logic '1'.

Figure 6.24: Picture of the orbitals corresponding to the LUMO+1 level for the OPV3 molecule with long driver on the xz plane with the driver. The orbitals are taken with an isosurface value equal to 0.015.

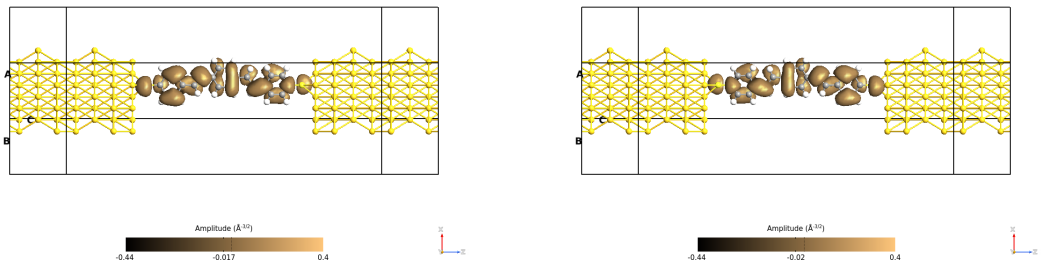

(a) logic '0'. (b) logic '1'.

Figure 6.25: Picture of the orbitals corresponding to the LUMO+1 level for the OPV3 molecule with long driver on the xz plane without the driver. The orbitals are taken with an isosurface value equal to 0.015.

6.1.8 Small driver: Orbitals

In this section are shown the orbitals of OPV3 considering the small driver. The HOMO-1 level (figures 6.26b, 6.26b and 6.26b) exhibits a mirrored behavior, which means that the orbital shape remains the same according to the rotation of the driver molecule. It is possible to notice it thanks to the triangular shape orbital which is on the carbons that bond the two benzenes, it is always close to the driver negative pole.

For the other levels, the orbitals show complementary behavior. It is difficult to appreciate differences, it is possible to say that the shape is practically the same.

Comparing the small and long driver orbitals is possible to observe that the LUMO level is the one more similar between the two drivers, while the HOMO-1 is the most different one. The LUMO+1 energy level traces the same plot in the central part (the benzene in the middle). The HOMO one is completely different, the small driver orbitals are thin and high while the long driver ones are larger and shorter.

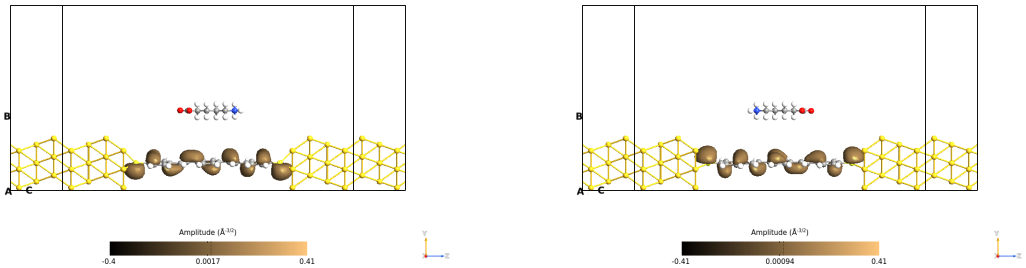

(a) logic '0'. (b) logic '1'.

Figure 6.26: Picture of the orbitals corresponding to the HOMO-1 level for the OPV3 molecule with small driver on the yz plane. The orbitals are taken with an isosurface value equal to 0.015.

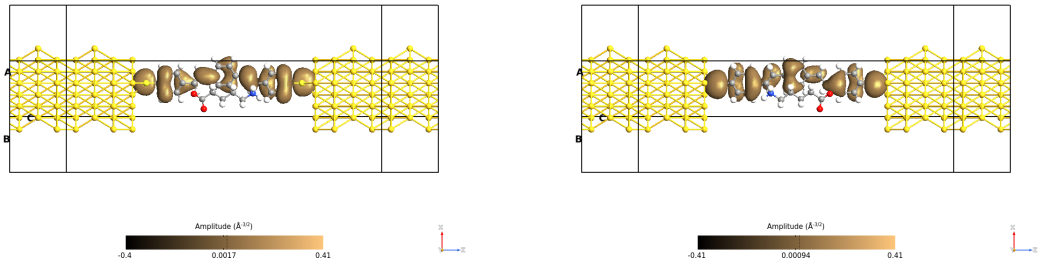

(a) logic '0'. (b) logic '1'.

Figure 6.27: Picture of the orbitals corresponding to the HOMO-1 level for the OPV3 molecule with small driver on the xz plane with the driver. The orbitals are taken with an isosurface value equal to 0.015.

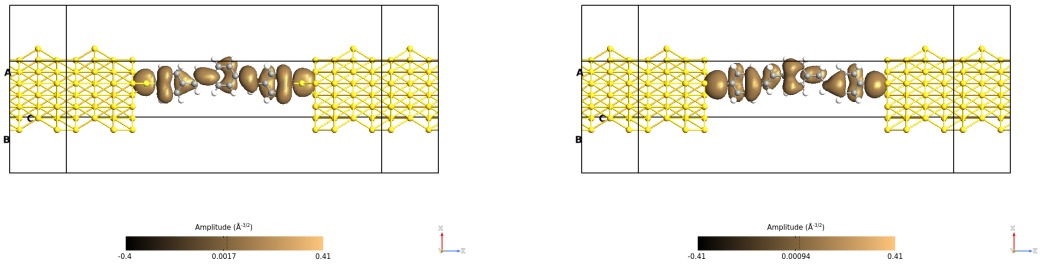

(a) logic '0'. (b) logic '1'.

Figure 6.28: Picture of the orbitals corresponding to the HOMO-1 level for the OPV3 molecule with small driver on the xz plane without the driver. The orbitals are taken with an isosurface value equal to 0.015.

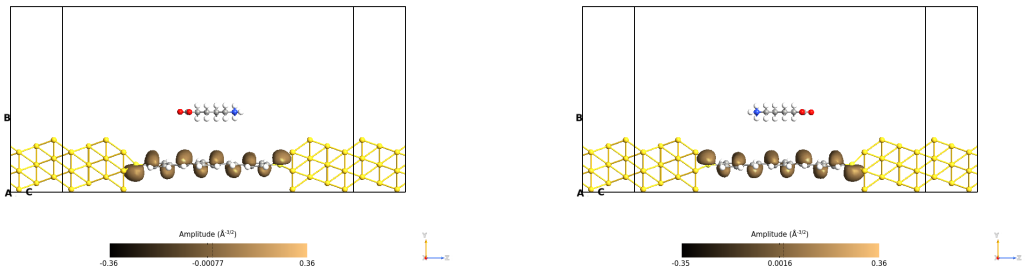

(a) logic '0'. (b) logic '1'.

Figure 6.29: Picture of the orbitals corresponding to the HOMO level for the OPV3 molecule with small driver on the yz plane. The orbitals are taken with an isosurface value equal to 0.015.

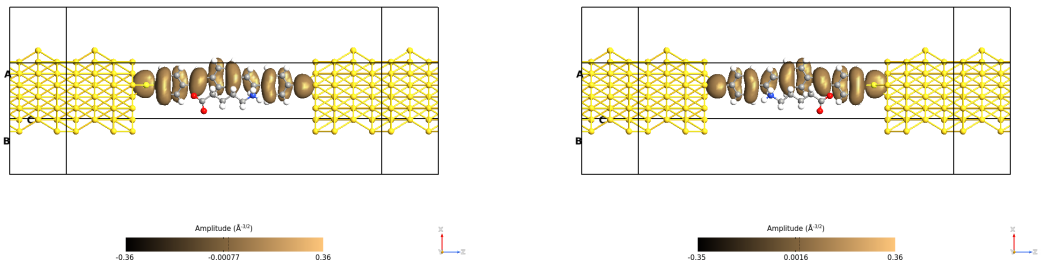

(a) logic '0'. (b) logic '1'.

Figure 6.30: Picture of the orbitals corresponding to the HOMO level for the OPV3 molecule with small driver on the xz plane with the driver. The orbitals are taken with an isosurface value equal to 0.015.

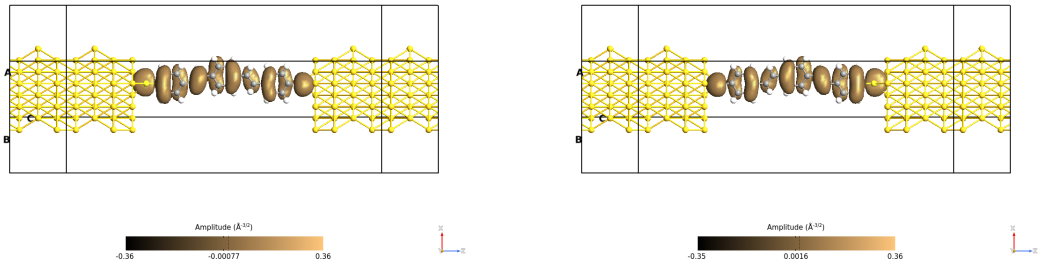

(a) logic '0'. (b) logic '1'.

Figure 6.31: Picture of the orbitals corresponding to the HOMO level for the OPV3 molecule with small driver on the xz plane without the driver. The orbitals are taken with an isosurface value equal to 0.015.

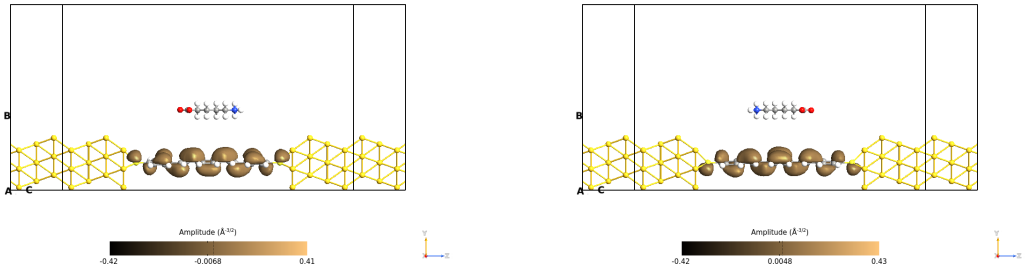

(a) logic '0'. (b) logic '1'.

Figure 6.32: Picture of the orbitals corresponding to the LUMO level for the OPV3 molecule with the small driver on the yz plane. The orbitals are taken with an isosurface value equal to 0.015.

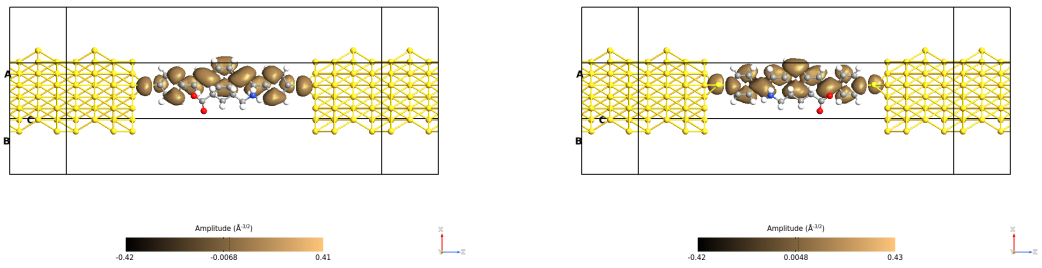

(a) logic '0'. (b) logic '1'.

Figure 6.33: Picture of the orbitals corresponding to the LUMO level for the OPV3 molecule with the small driver on the xz plane with the driver. The orbitals are taken with an isosurface value equal to 0.015.

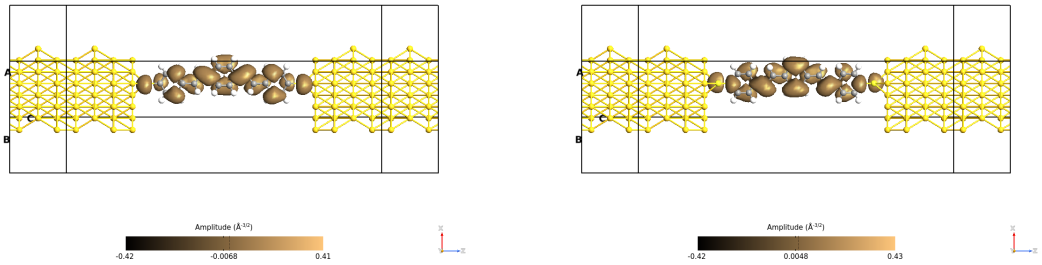

(a) logic '0'. (b) logic '1'.

Figure 6.34: Picture of the orbitals corresponding to the LUMO level for the OPV3 molecule with the small driver on the xz plane without the driver. The orbitals are taken with an isosurface value equal to 0.015.

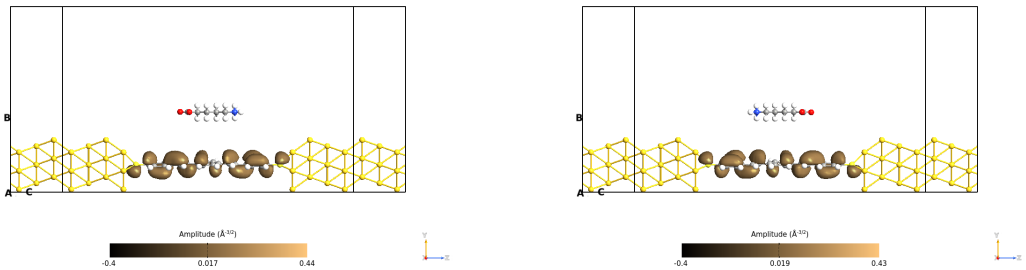

(a) logic '0'. (b) logic '1'.

Figure 6.35: Picture of the orbitals corresponding to the LUMO+1 level for the OPV3 molecule with small driver on the yz plane. The orbitals are taken with an isosurface value equal to 0.015.

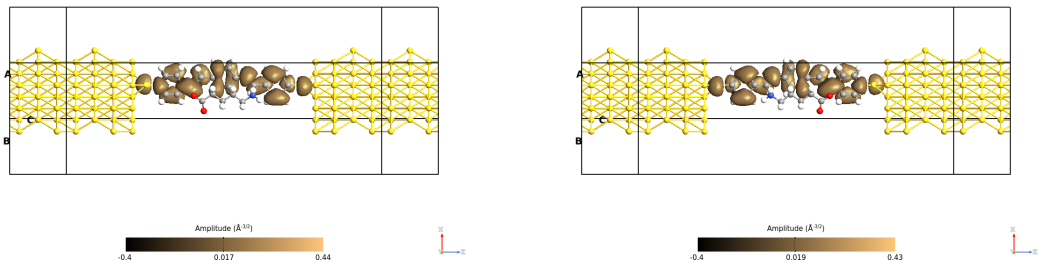

(a) logic '0'. (b) logic '1'.

Figure 6.36: Picture of the orbitals corresponding to the LUMO+1 level for the OPV3 molecule with small driver on the xz plane with the driver. The orbitals are taken with an isosurface value equal to 0.015.

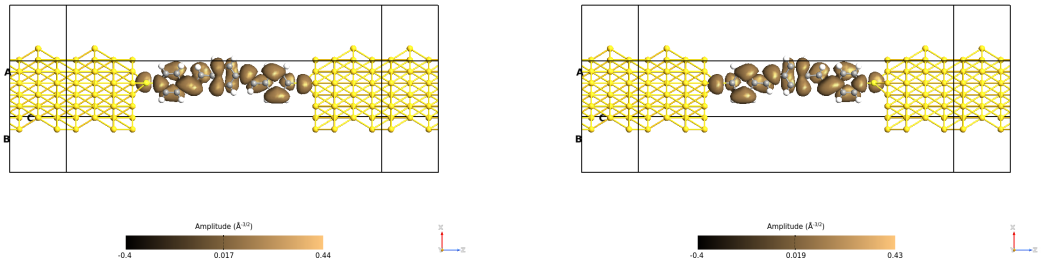

(a) logic '0'. (b) logic '1'.

Figure 6.37: Picture of the orbitals corresponding to the LUMO+1 level for the OPV3 molecule with small driver on the xz plane without the driver. The orbitals are taken with an isosurface value equal to 0.015.

6.1.9 Long driver: Pathways

The pathways are very interesting pictures because they tell us where and how many electrons passed. They are taken considering the TS at equilibrium, therefore the conditions are not the same as when an external voltage is applied, but they give an important idea of the conduction path.

When the energy is higher is possible to notice that the conduction path (figures 6.38, 6.39 and 6.40) shows some red arrows, which are electrons that travel in the opposite direction with respect to the z-axis (conduction direction). The magnitude is more predictable, because, looking at the TS, it is easily identifiable which peaks could possess the highest values. As expected, the peaks at 0.08 eV show the highest magnitude, while the others exhibit lower values. It is important to pay attention a the scale, otherwise, the conclusions made after looking at the pictures are completely wrong. For example the transmission pathways at 0.08 eV (figure 6.41) seem to be worse than the one at 0.28 eV (6.42) because the red is more intense in this last, but if we look better at the scale it is possible to notice that the 0.08 eV magnitude is higher than the other one.

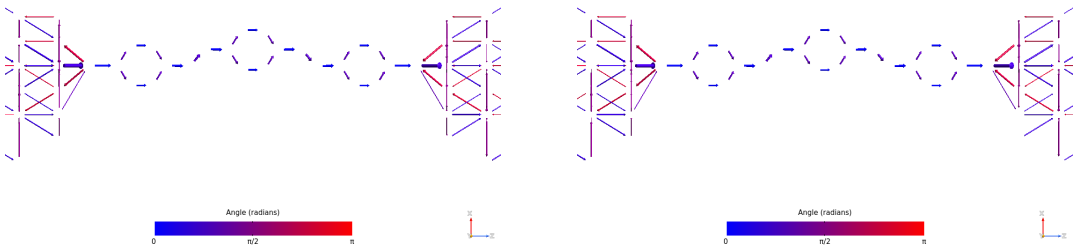

(a) logic '0'. (b) logic '1'.

Figure 6.38: Picture of the pathways corresponding to the energy 0.08 eV for the OPV3 molecule with long driver on the xz plane. The blue arrows are in the same direction as the z-axis, while the red ones are in the opposite direction.

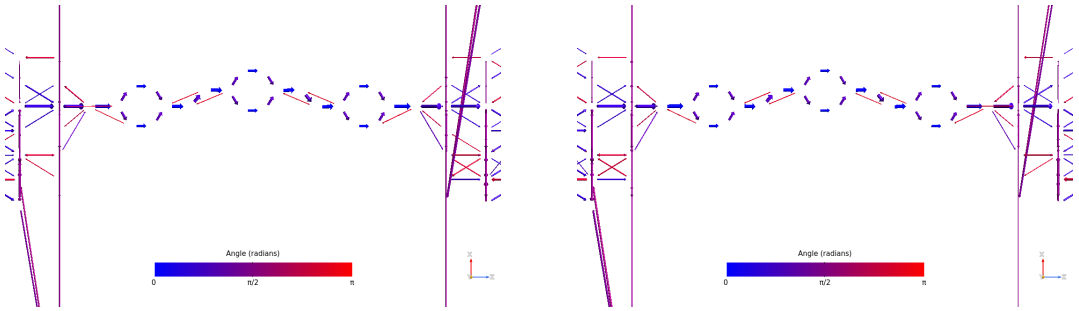

(a) logic '0'. (b) logic '1'.

Figure 6.39: Picture of the pathways corresponding to the energy 0.28 eV for the OPV3 molecule with long driver on the xz plane. The blue arrows are in the same direction as the z-axis, while the red ones are in the opposite direction.

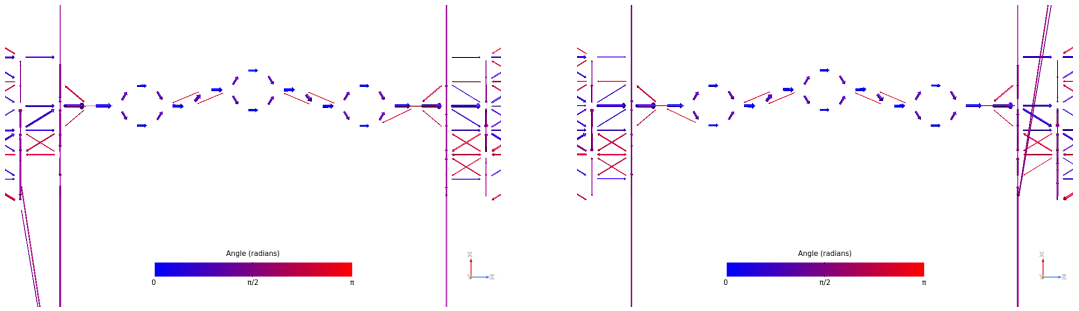

(a) logic '0'. (b) logic '1'.

Figure 6.40: Picture of the pathways corresponding to the energy 0.44 eV for the OPV3 molecule with long driver on the xz plane. The blue arrows are in the same direction as the z-axis, while the red ones are in the opposite direction.

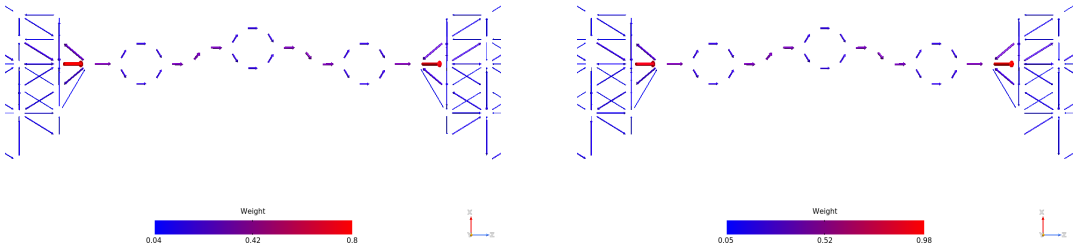

(a) logic '0'. (b) logic '1'.

Figure 6.41: Picture of the pathways corresponding to the energy 0.08 eV for the OPV3 molecule with long driver on the xz plane. The plots show the arrows' magnitude.

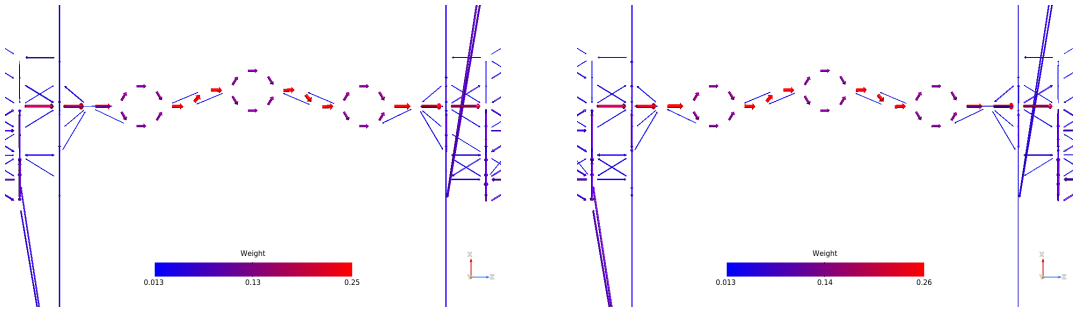

(a) logic '0'. (b) logic '1'.

Figure 6.42: Picture of the pathways corresponding to the energy 0.28 eV for the OPV3 molecule with long driver on the xz plane. The plots show the arrows' magnitude.

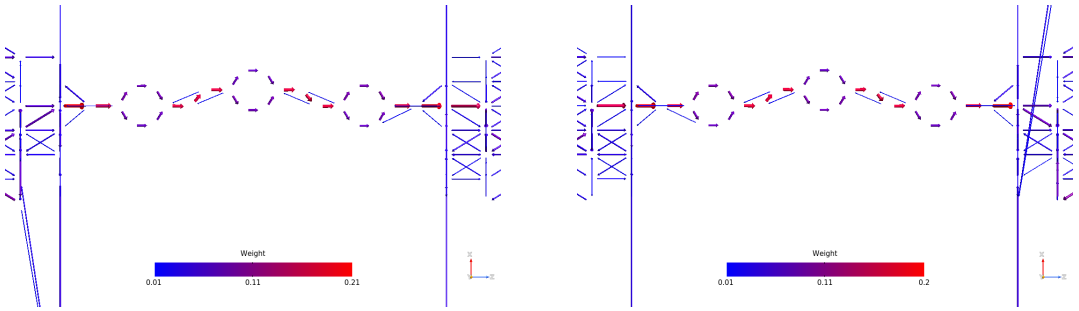

(a) logic '0'. (b) logic '1'.

Figure 6.43: Picture of the pathways corresponding to the energy 0.44 eV for the OPV3 molecule with long driver on the xz plane. The plots show the arrows' magnitude.

6.1.10 Small driver: Pathways

The transmission pathways related to the small driver are close to the long driver ones. The pictures 6.44, 6.45 and 6.46 are very similar to the long driver ones.

The magnitude pathways (figures 6.47, 6.49 and 6.49) trace the same behavior as the long driver, except for the 0.08 eV one. It has a very high weight value (higher than 1) with respect to the other driver. This result is coherent with the TS, in particular, looking at the figure 6.5, it is possible to observe the difference in terms of transmission between the two drivers. In both configurations, the small driver exceeded the long one widely.

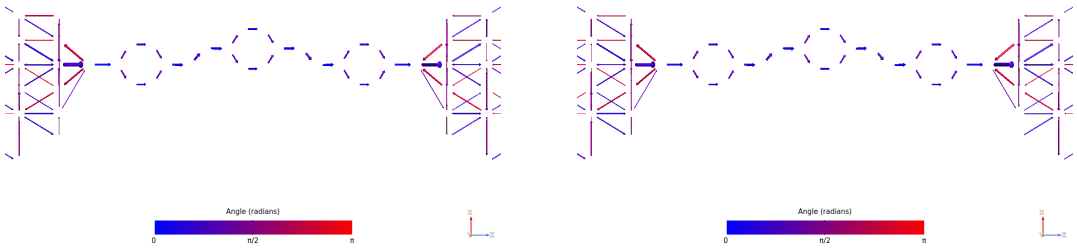

(a) logic '0'. (b) logic '1'.

Figure 6.44: Picture of the pathways corresponding to the energy 0.08 eV for the OPV3 molecule with small driver on the xz plane. The blue arrows are in the same direction as the z-axis, while the red ones are in the opposite direction.

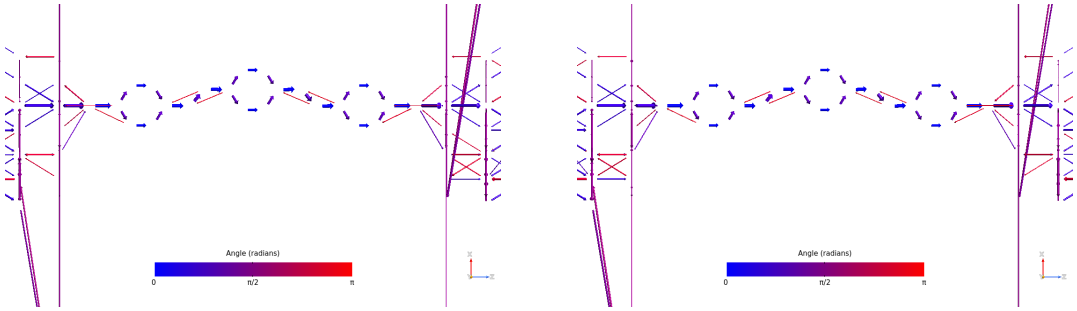

(a) logic '0'. (b) logic '1'.

Figure 6.45: Picture of the pathways corresponding to the energy 0.28 eV for the OPV3 molecule with small driver on the xz plane. The blue arrows are in the same direction as the z-axis, while the red ones are in the opposite direction.

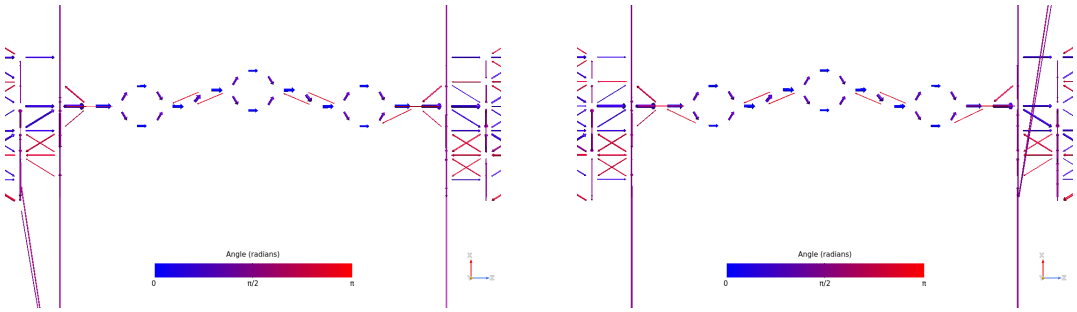

(a) logic '0'. (b) logic '1'.

Figure 6.46: Picture of the pathways corresponding to the energy 0.44 eV for the OPV3 molecule with small driver on the xz plane. The blue arrows are in the same direction as the z-axis, while the red ones are in the opposite direction.

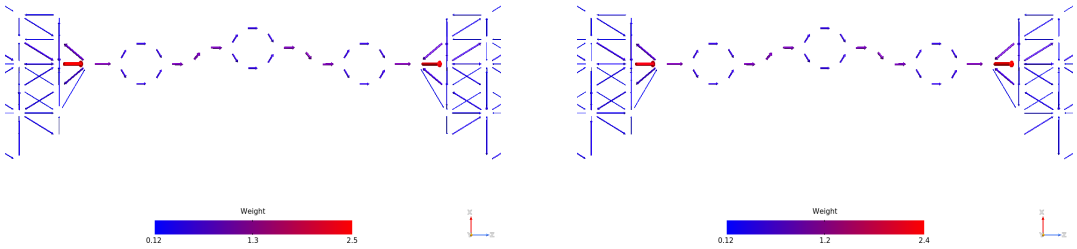

(a) logic '0'. (b) logic '1'.

Figure 6.47: Picture of the pathways corresponding to the energy 0.08 eV for the OPV3 molecule with small driver on the xz plane. The plots show the arrows' magnitude.

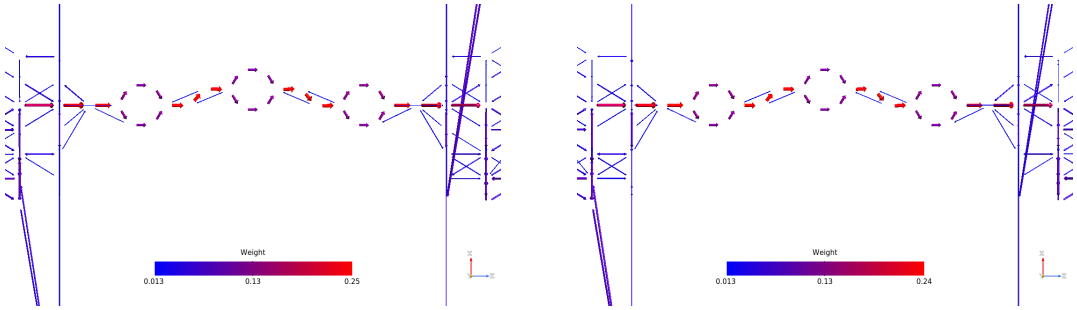

(a) logic '0'. (b) logic '1'.

Figure 6.48: Picture of the pathways corresponding to the energy 0.28 eV for the OPV3 molecule with small driver on the xz plane. The plots show the arrows' magnitude.

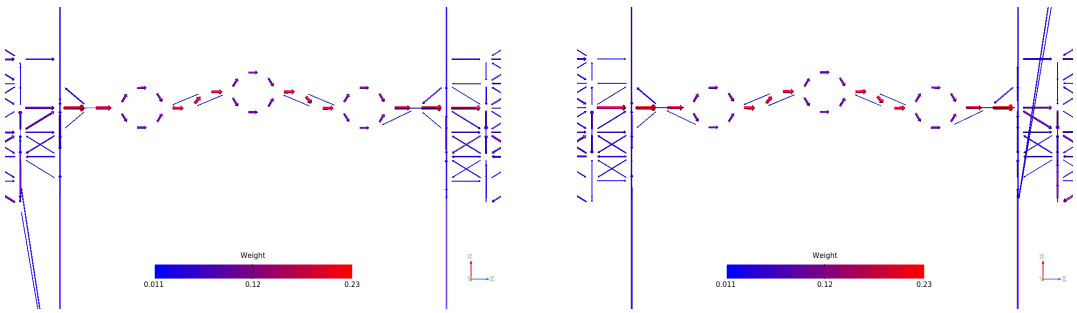

(a) logic '0'. (b) logic '1'.

Figure 6.49: Picture of the pathways corresponding to the energy 0.44 eV for the OPV3 molecule with small driver on the xz plane. The plots show the arrows' magnitude.

6.2 OPE3

The OPE3 molecule is widely studied in molecular junctions. It has been selected for its high polarizability value.

Figure 6.50 shows the builder screen of two different logic configurations considering the long driver, while figure 6.51 contains the builder with the small driver.

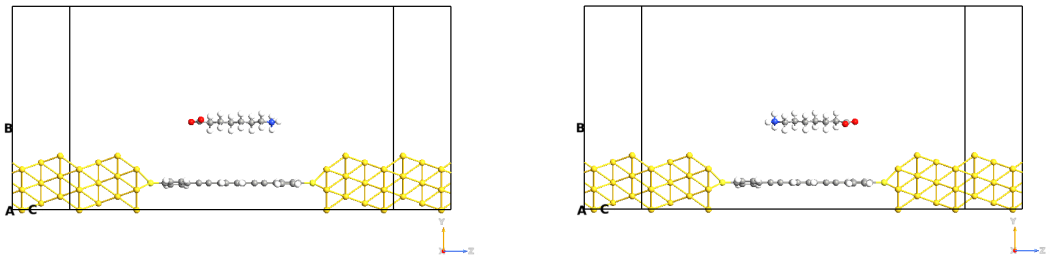

(a) logic '0' configuration. (b) logic '1' configuration.

Figure 6.50: Picture of the QuantumATK builder for the OPE3 molecule with the long driver. The white atoms are the hydrogens, the yellow ones are gold atoms, the lighter yellow ones are the sulfurs, the blue ones are nitrogens, the reds are the oxygens and the grey atoms are carbons.

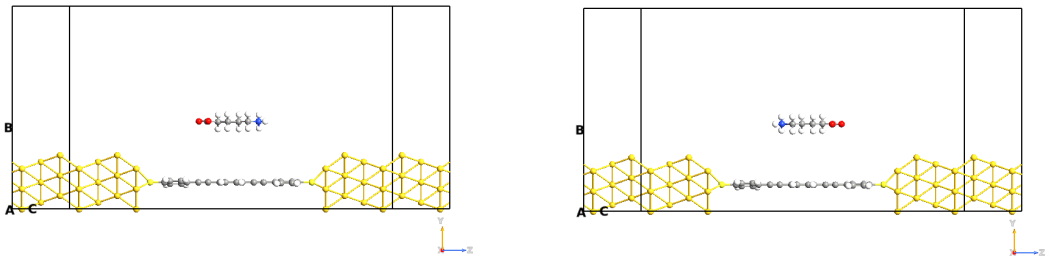

(a) logic '0' configuration. (b) logic '1' configuration.

Figure 6.51: Picture of the QuantumATK builder for the OPE3 molecule with the small driver. The white atoms are the hydrogens, the yellow ones are gold atoms, the lighter yellow ones are the sulfurs, the blue ones are nitrogens, the reds are the oxygens and the grey atoms are carbons.

6.2.1 Long driver: TS

Figure 6.52a shows the TS for a molecular junction with the OPE3 molecule placed in the junction. It is possible to notice that the conduction properties of the MT are good also at low energy because the LUMO peaks are close to the 0 eV of the energy axis.

The HOMO peaks, on the contrary, are quite distant from the origin of the energy axis, therefore the conduction is LUMO type. The trend of the curves is the same for the two configurations, the differences are related to the amplitude and the width of the peaks in the TS. Thanks to this behavior the OPE3 is a good candidate to play the role of readout system.

As for the OPV3 molecule, the influence of the driver in the OPE3 causes a change in the shape of the TS, it is possible to observe it in the figure 6.52b.

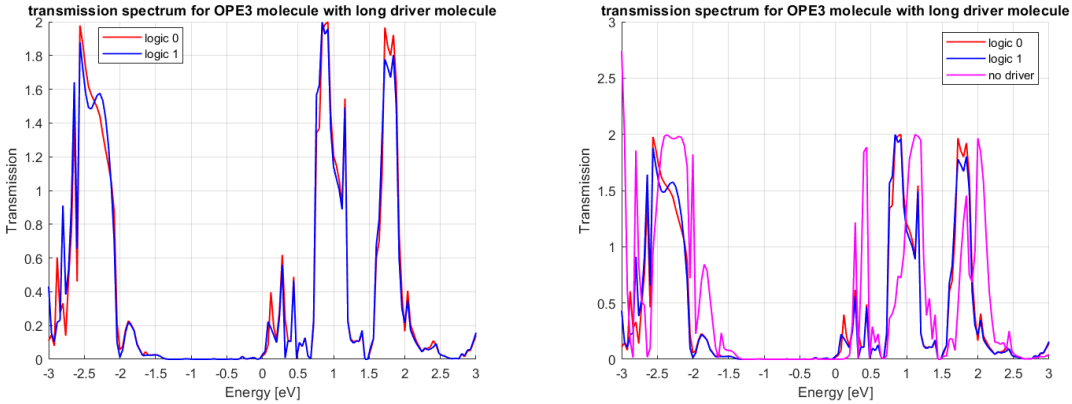

(a) without no driver configurations.

(b) with no driver configurations.

Figure 6.52: Picture of the TS for the OPE3 molecule considering the long driver; the red curve is the one for the logic '0' configuration, the blue one is for the logic '1' and the magenta one for the no driver configuration.

6.2.2 Small driver: TS

The OPE3 molecule seems to work well as a readout system, for this reason also small driver simulations have been performed.

In the figure 6.53a is reported the TS, it is possible to notice the variations between the two configurations. The same comment done for the long driver can be written in this case. In figure 6.53b is possible to observe the change in the curve for the no driver conditions, this phenomenon is important for our task because it is a mark of the driver influence.

6.2.3 Long vs Small driver: TS

After the comparison of the different configurations can be interesting to see the effect of the driver dipole moment. In figure 6.54 are reported the TS for the different drivers and configurations. Figure 6.54a compares the driver effect on the logic '0' configuration, in the small driver curve the peaks are narrower but higher than the long one. The figure 6.54b, instead, is related to the logic '1' configuration.

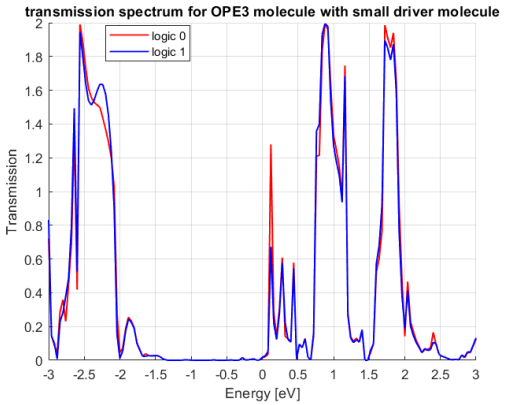

(a) without no driver configurations.

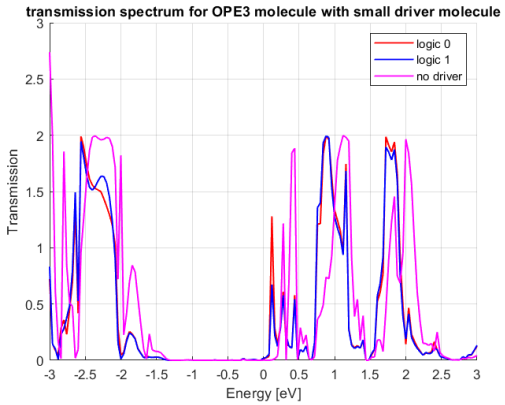

(b) with no driver configurations.

Figure 6.53: Picture of the TS for the OPE3 molecule considering the small driver; the red curve is the one for the logic '0' configuration, the blue one is for the logic '1' and the magenta one for the no driver configuration.

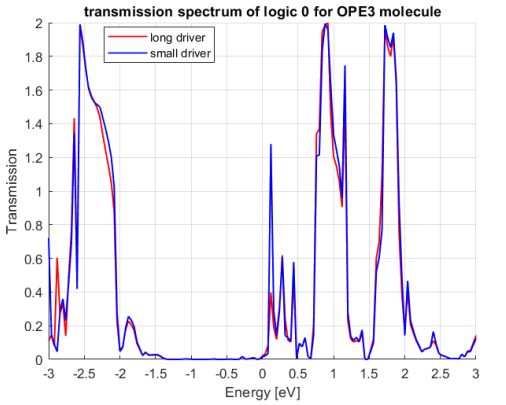

(a) Logic '0' configuration.

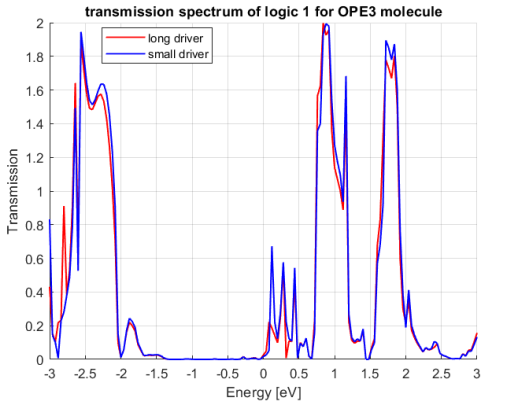

(b) Logic '1' configuration.

Figure 6.54: Pictures of the TS curve of the logic '0' and logic '1' for the OPE3 molecule considering the long driver - 9.9 Å (red line) and the small driver - 7.3 Å (blue line).

6.2.4 Long driver: IV

As expected, the OPE3 molecule can drive a high amount of current (few μA) and the difference between the two configurations is large enough to sense them, it is evident looking at the figure 6.55a. The influence of the driver causes an increase of the current (figure 6.55b), as for the OPV3 molecule.

The feasibility of the readout system based on an OPE3 molecular junction is evinced by looking at the figure 6.56, which represents the current difference between the two configurations in absolute value. As for the OPV3 molecule, the peak around 0.35 V is well suited for our application because it has a high value (beyond 3 μA) and its corresponding potential is low, hence should not overcome the clock signal.

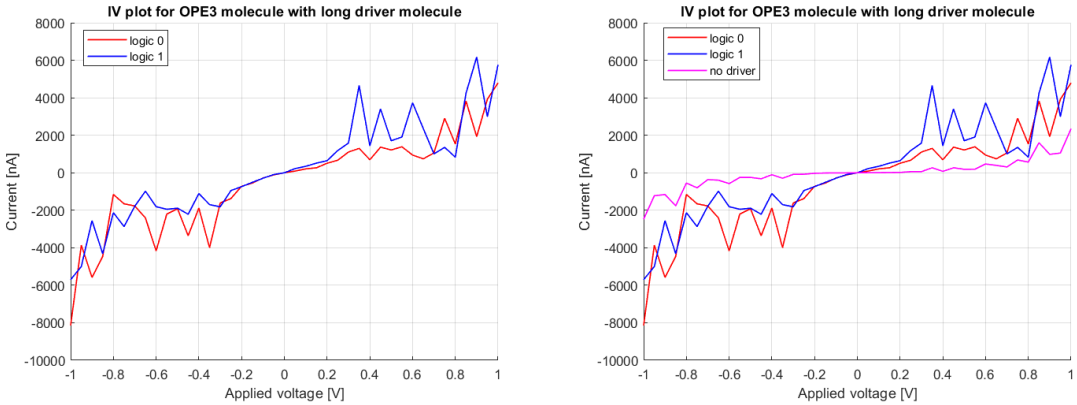

(a) Without the no driver configuration.

(b) With the no driver configuration.

Figure 6.55: Picture of the IV for the OPE3 molecule considering the long driver; the red curve is the one for the logic '0' configuration, the blue one is for the logic '1' and the magenta one for the no driver configuration.

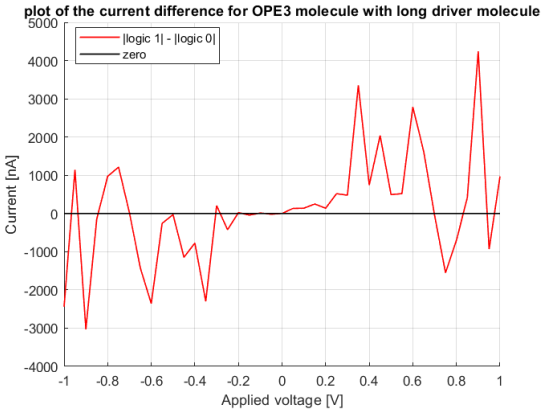

Figure 6.56: Picture of the current difference between |logic '1'| and |logic '0'| for the OPE3 molecule considering the long driver, the black line is the zero line.

Figure 6.57 enhances the probabilities of the feasibility of the readout system, it shows a deep influence related to the driver. The figure 6.57a is the current difference between the logic '1' and logic '0' configuration considering also the direction of the current flow (the current sign), while the figure 6.57b takes into account the driver consequences with respect the no driver configuration.

6.2.5 Small driver: IV

The small driver IV plot (figure 6.58) confirms the goodness of the OPE3 molecule for the readout system. In the figure 6.58a is possible to observe the large difference corresponding to the 0.35 V, which allows us to distinguish the different logic configurations. Figure 6.58b, instead, indicates the effective influence of the driver on the junction.

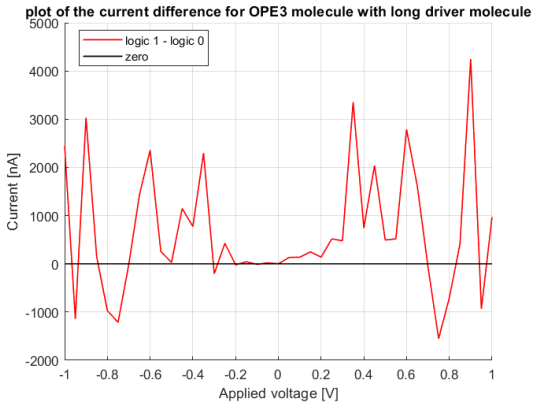

(a) logic '1' - logic '0'.

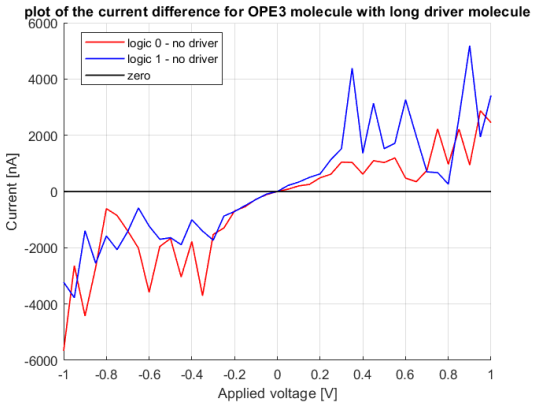

(b) logic '1' or logic '0' - no driver.

Figure 6.57: Picture of the current difference for the OPE3 molecule considering the long driver.

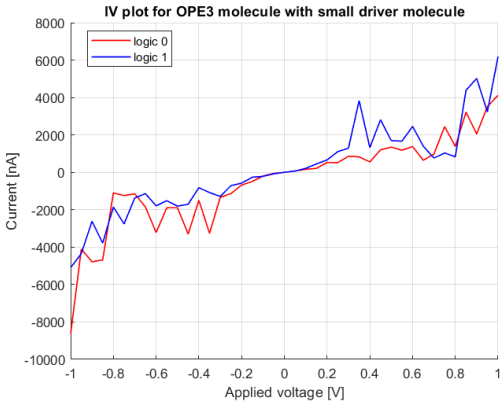

(a) Without the no driver configuration.

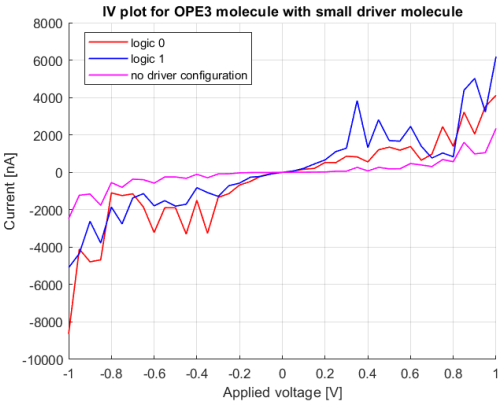

(b) With the no driver configuration.

Figure 6.58: Picture of the IV for the OPE3 molecule considering the small driver; the red curve is the one for the logic '0' configuration, the blue one is for the logic '1' and the magenta one for the no driver configuration.

Figure 6.59 shows the current difference in absolute values for the two logic configurations. The curve is very important because it provides us the actual proof of the readout system feasibility. As expected, the peak around 0.35 V is lower than the long driver one (3 μA for the small driver, beyond 3 μA for the long driver).

The figures 6.60a and 6.60b prove the driver influence, in terms of presence and orientation.

6.2.6 Long vs Small driver: IV

The comparison between small and long drivers is important for two main reasons: the effective influence of the dipole moment generated by the driver on the junction and the

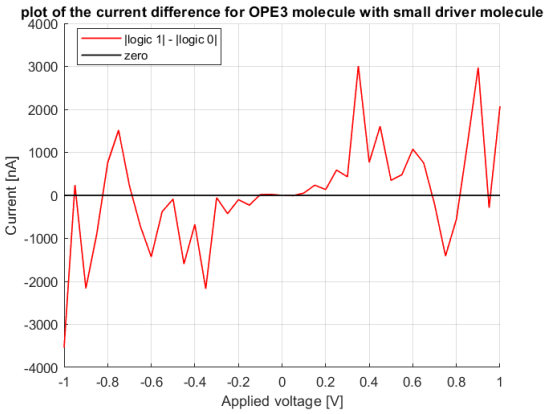

Figure 6.59: Picture of the current difference between |logic '1'| and |logic '0'| for the OPE3 molecule considering the small driver, the black line is the zero line.

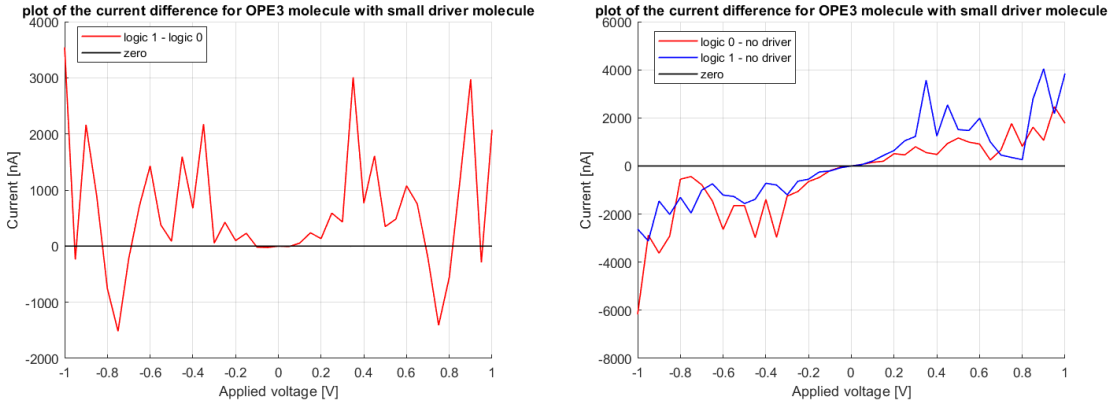

(a) logic '1' - logic '0'.

(b) logic '1' or logic '0' - no driver.

Figure 6.60: Picture of the current difference for the OPE3 molecule considering the small driver.

robustness of the system to the non-idealities of the molFCN.

In figure 6.61 are reported the two IV plots, one for the logic '0' configuration (figure 6.61a) and the other for the logic '1' one (figure 6.61b).

The readout system based on the OPE3 molecule is robust, we can deduce it from figure 6.62 in which the difference between the long driver and small driver at the 0.35 V is about 800 nA for the logic '1' configuration and 500 nA for the logic '0' one. These differences are much lower than the current difference between logic '1' and logic '0' configurations for the same applied voltage.

The interval in which the logic '1' configuration is higher than the logic '0' one is more wide with respect to the OPV3 molecule. In particular, in this case, the range is roughly 0 - 0.7 V while for the OPV3 molecule is 0.3 V - 0.6 V.

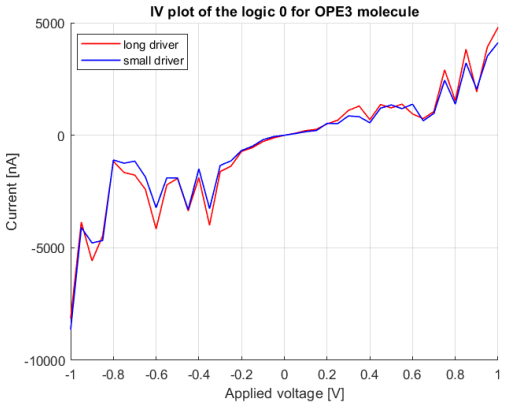

(a) logic '0' configuration.

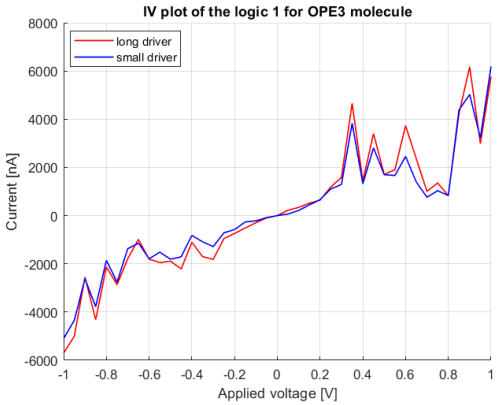

(b) logic '1' configuration.

Figure 6.61: Picture of the IV curve of the logic '0' and logic '1' for the OPE3 molecule considering the long driver - 9.9 Å (red line) and the small driver - 7.3 Å (blue line).

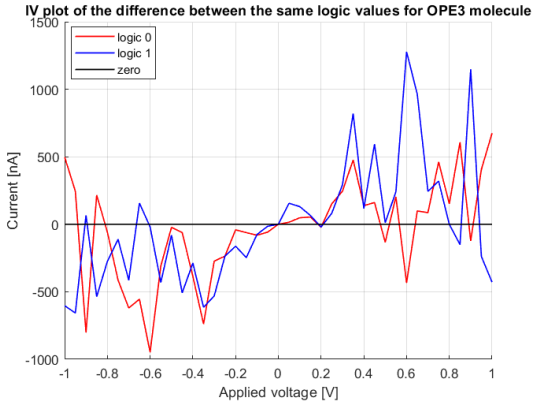

(a) long driver - small driver.

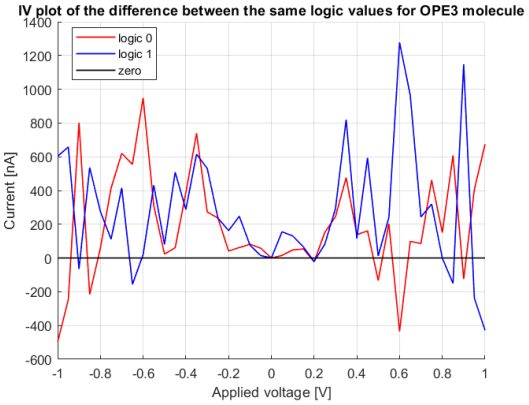

(b) |long driver| - |small driver|.

Figure 6.62: Picture of the current difference between long and small driver (I long driver - I small driver) of the logic '1' (blue curve) and logic '0' (red curve) for the OPE3 molecule.

6.2.7 Long driver: Orbitals

Below are reported the orbitals for the OPE3 molecule considering the long driver. It is possible to notice that the shapes are complementary for all the energy levels between the two configurations.

The HOMO and LUMO orbitals are speeded along all the molecules. The HOMO orbitals (figures 6.66, 6.67 and 6.68) are thinner and higher with respect to the LUMO ones (figures 6.69, 6.70 and 6.71), these last are large and short. The HOMO-1 (figures 6.63, 6.64 and 6.65) and LUMO+1 (figures 6.72, 6.73 and 6.74) are more confined to one side of the molecular junction, in particular, in the HOMO-1 levels they are close to the negative pole, while in the LUMO+1 near the positive pole.

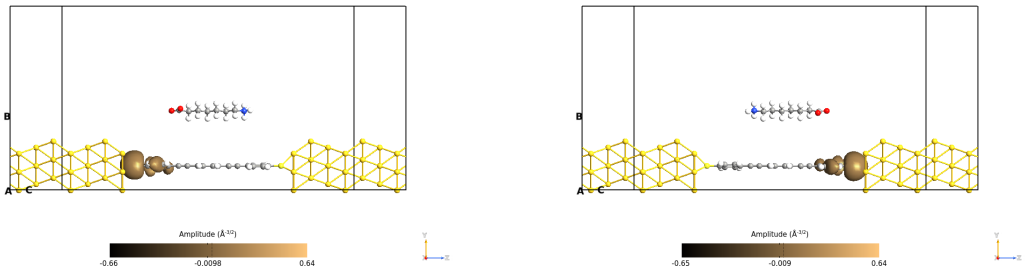

(a) logic '0'. (b) logic '1'.

Figure 6.63: Picture of the orbitals corresponding to the HOMO-1 level for the OPE3 molecule with long driver on the yz plane. The orbitals are taken with an isosurface value equal to 0.015.

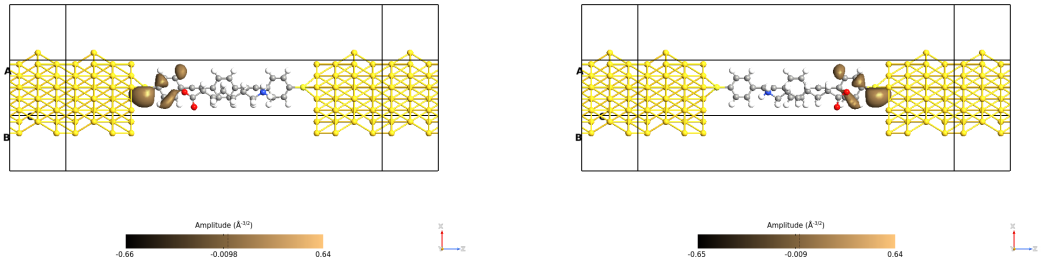

(a) logic '0'. (b) logic '1'.

Figure 6.64: Picture of the orbitals corresponding to the HOMO-1 level for the OPE3 molecule with long driver on the xz plane with the driver. The orbitals are taken with an isosurface value equal to 0.015.

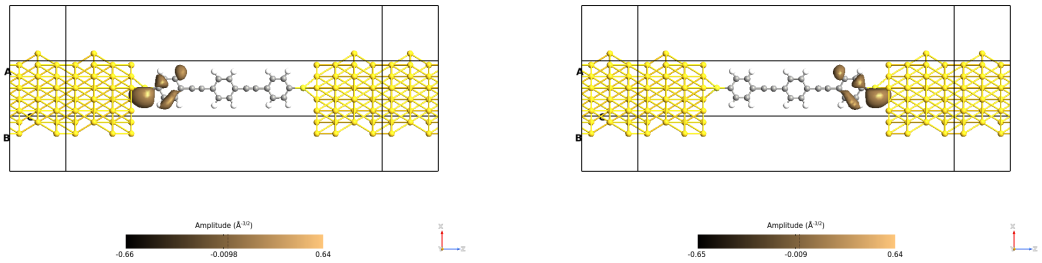

(a) logic '0'. (b) logic '1'.

Figure 6.65: Picture of the orbitals corresponding to the HOMO-1 level for the OPE3 molecule with long driver on the xz plane without the driver. The orbitals are taken with an isosurface value equal to 0.015.

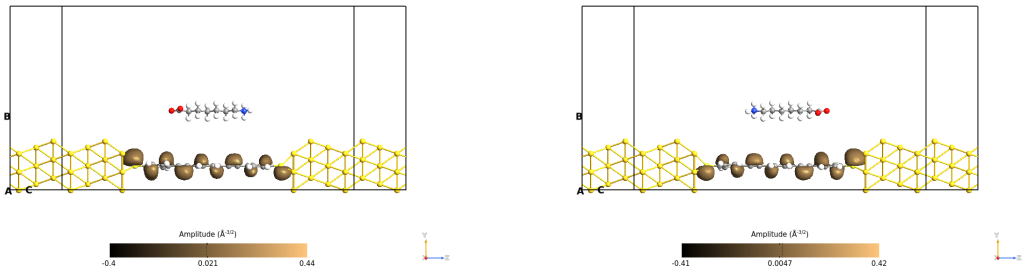

(a) logic '0'. (b) logic '1'.

Figure 6.66: Picture of the orbitals corresponding to the HOMO level for the OPE3 molecule with long driver on the yz plane. The orbitals are taken with an isosurface value equal to 0.015.

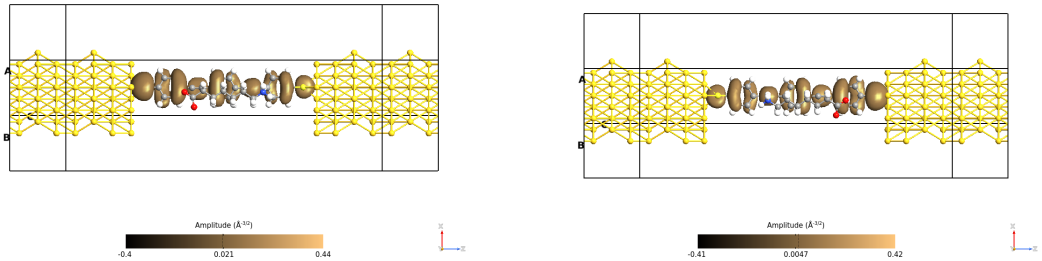

(a) logic '0'. (b) logic '1'.

Figure 6.67: Picture of the orbitals corresponding to the HOMO level for the OPE3 molecule with long driver on the xz plane with the driver. The orbitals are taken with an isosurface value equal to 0.015.

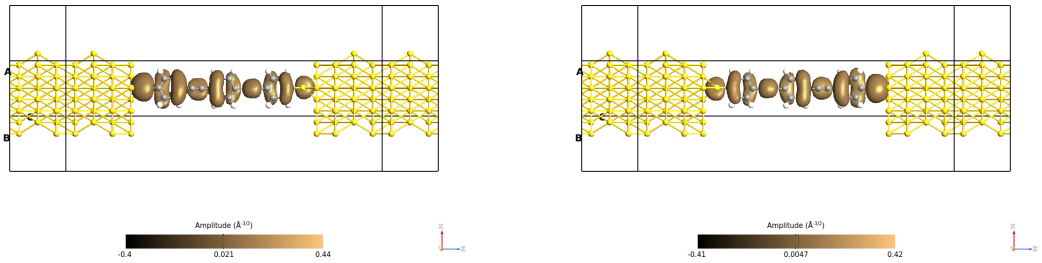

(a) logic '0'. (b) logic '1'.

Figure 6.68: Picture of the orbitals corresponding to the HOMO level for the OPE3 molecule with long driver on the xz plane without the driver. The orbitals are taken with an isosurface value equal to 0.015.

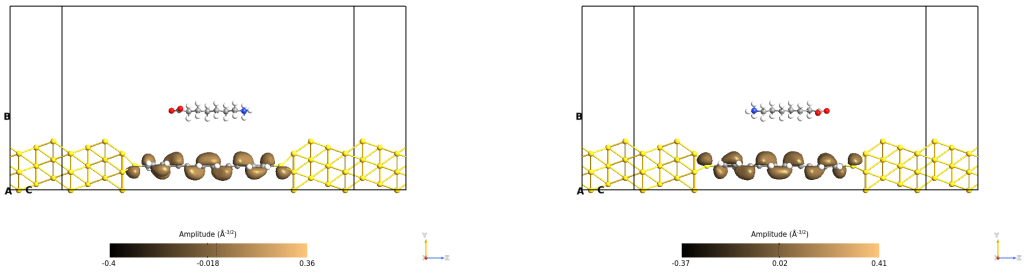

(a) logic '0'. (b) logic '1'.

Figure 6.69: Picture of the orbitals corresponding to the LUMO level for the OPE3 molecule with long driver on the yz plane. The orbitals are taken with an isosurface value equal to 0.015.

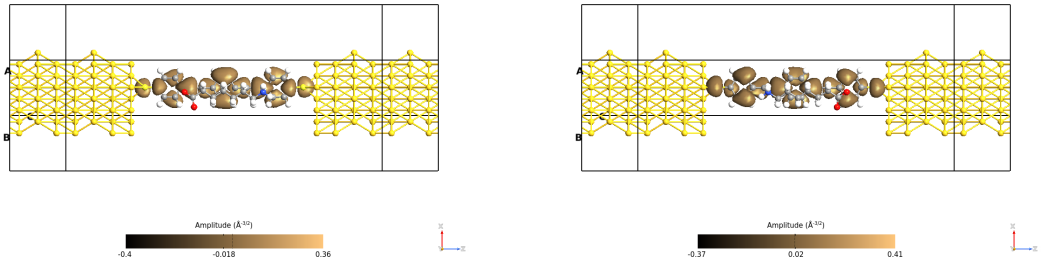

(a) logic '0'. (b) logic '1'.

Figure 6.70: Picture of the orbitals corresponding to the LUMO level for the OPE3 molecule with long driver on the xz plane with the driver. The orbitals are taken with an isosurface value equal to 0.015.

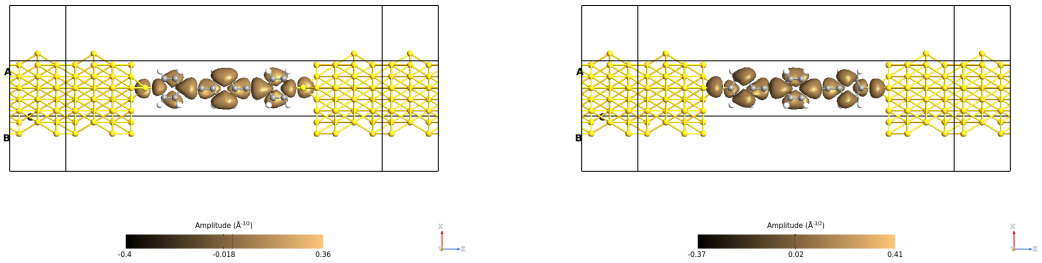

(a) logic '0'. (b) logic '1'.

Figure 6.71: Picture of the orbitals corresponding to the LUMO level for the OPE3 molecule with long driver on the xz plane without the driver. The orbitals are taken with an isosurface value equal to 0.015.

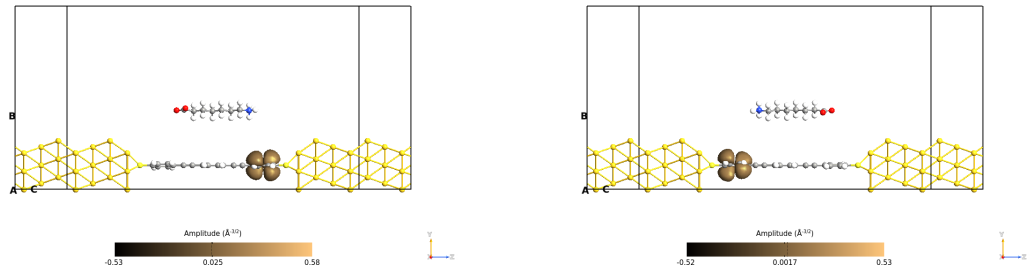

(a) logic '0'. (b) logic '1'.

Figure 6.72: Picture of the orbitals corresponding to the LUMO+1 level for the OPE3 molecule with long driver on the yz plane. The orbitals are taken with an isosurface value equal to 0.015.

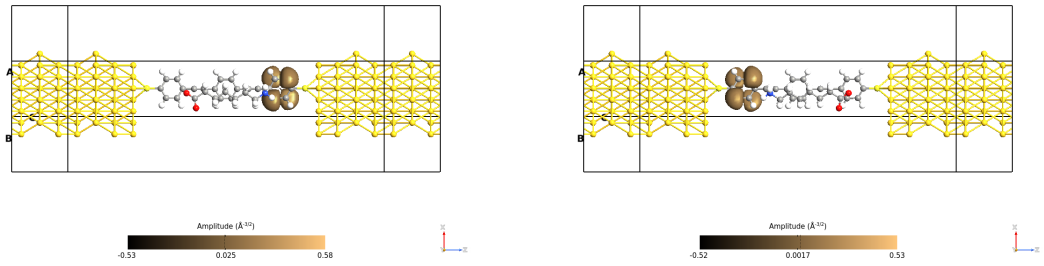

(a) logic '0'. (b) logic '1'.

Figure 6.73: Picture of the orbitals corresponding to the LUMO+1 level for the OPE3 molecule with long driver on the xz plane with the driver. The orbitals are taken with an isosurface value equal to 0.015.

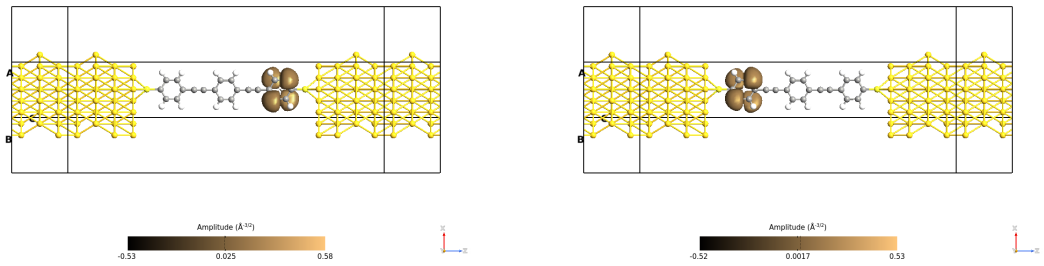

(a) logic '0'. (b) logic '1'.

Figure 6.74: Picture of the orbitals corresponding to the LUMO+1 level for the OPE3 molecule with long driver on the xz plane without the driver. The orbitals are taken with an isosurface value equal to 0.015.

6.2.8 Small driver: Orbitals

The small driver orbitals are completely different for each energy level, except for the LUMO ones (figures 6.81, 6.82 and 6.83) which show complementary trend.

The most relevant difference can be seen in the LUMO+1 energy level (figures 6.84, 6.85 and 6.86) and HOMO level (figures 6.78, 6.79 and 6.80), in which the logic '0' orbitals are spread along the molecule, while the logic '1' ones are close to the sulfur close to the positive pole of the driver.

In the HOMO-1 level (figures 6.75, 6.76 and 6.77) is possible to notice that the orbitals are close to right electrode in both configuration, but the shape is significantly different. In the logic '1' configuration the orbital shapes are narrower than the logic '0' ones.

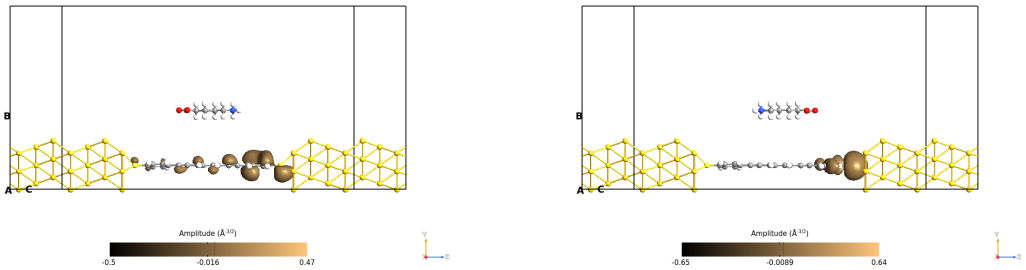

(a) logic '0'.

(b) logic '1'.

Figure 6.75: Picture of the orbitals corresponding to the HOMO-1 level for the OPE3 molecule with small driver on the yz plane. The orbitals are taken with an isosurface value equal to 0.015.

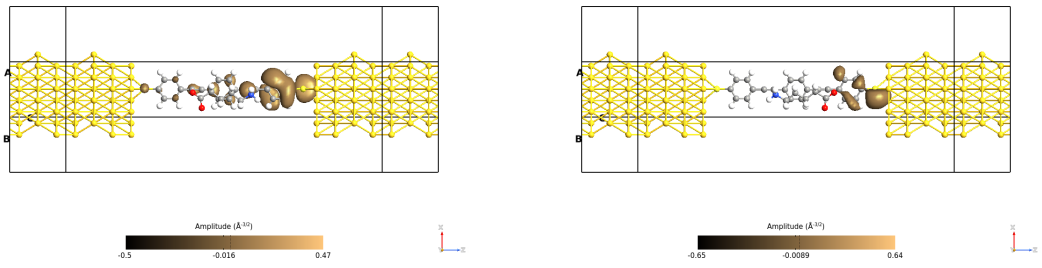

(a) logic '0'.

(b) logic '1'.

Figure 6.76: Picture of the orbitals corresponding to the HOMO-1 level for the OPE3 molecule with small driver on the xz plane with the driver. The orbitals are taken with an isosurface value equal to 0.015.

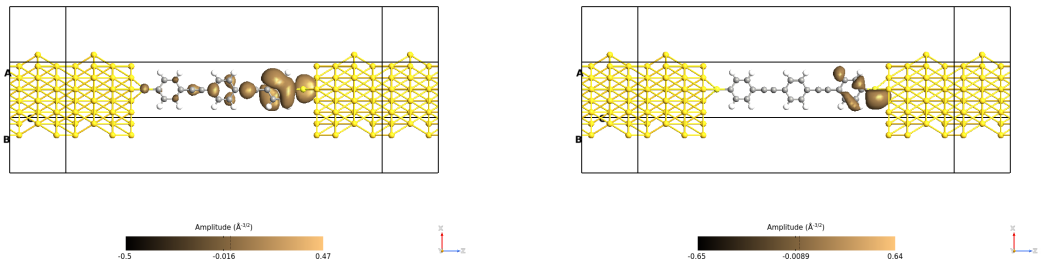

(a) logic '0'. (b) logic '1'.

Figure 6.77: Picture of the orbitals corresponding to the HOMO-1 level for the OPE3 molecule with small driver on the xz plane without the driver. The orbitals are taken with an isosurface value equal to 0.015.

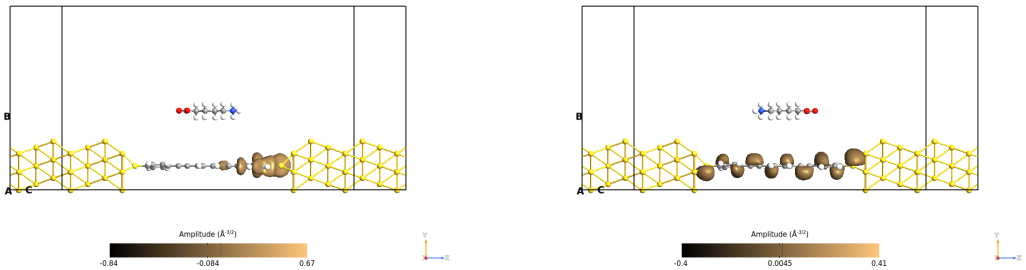

(a) logic '0'. (b) logic '1'.

Figure 6.78: Picture of the orbitals corresponding to the HOMO level for the OPE3 molecule with small driver on the yz plane. The orbitals are taken with an isosurface value equal to 0.015.

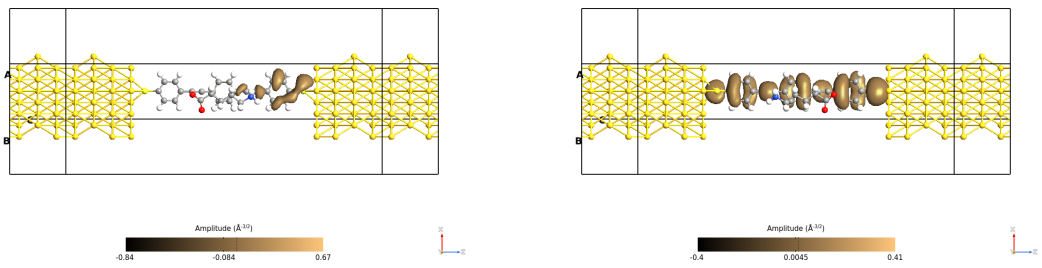

(a) logic '0'. (b) logic '1'.

Figure 6.79: Picture of the orbitals corresponding to the HOMO level for the OPE3 molecule with small driver on the xz plane with the driver. The orbitals are taken with an isosurface value equal to 0.015.

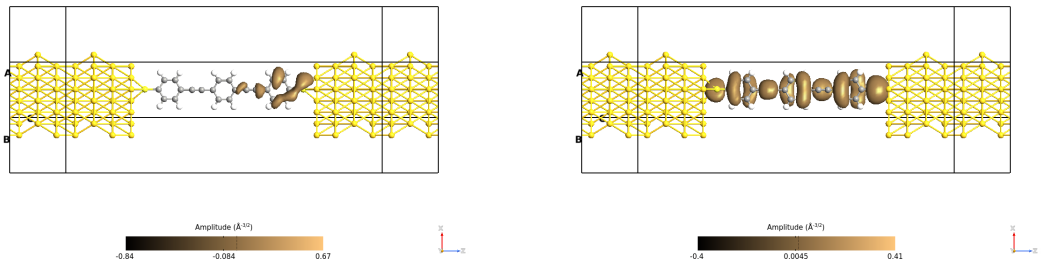

(a) logic '0'. (b) logic '1'.

Figure 6.80: Picture of the orbitals corresponding to the HOMO level for the OPE3 molecule with small driver on the xz plane without the driver. The orbitals are taken with an isosurface value equal to 0.015.

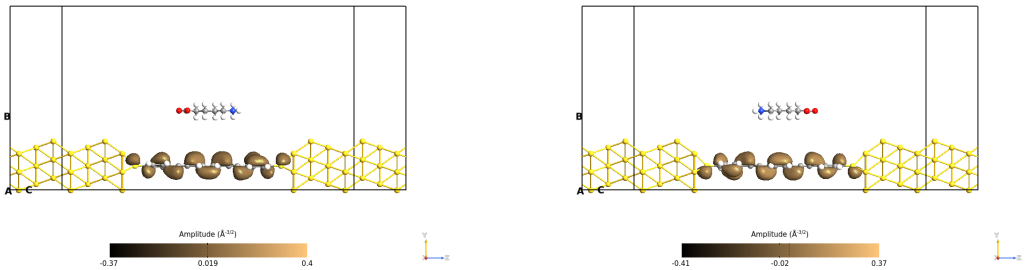

(a) logic '0'. (b) logic '1'.

Figure 6.81: Picture of the orbitals corresponding to the LUMO level for the OPE3 molecule with small driver on the yz plane. The orbitals are taken with an isosurface value equal to 0.015.

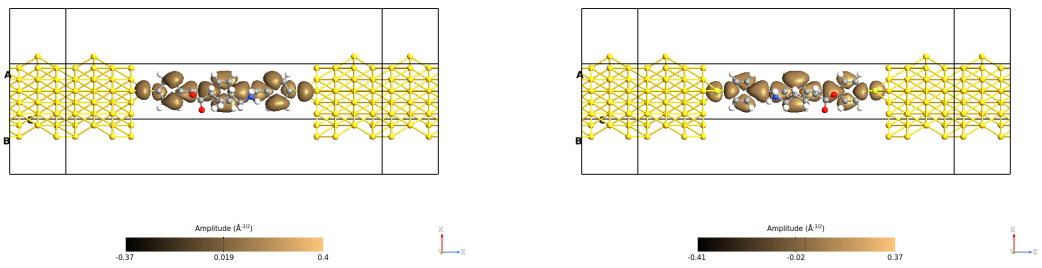

(a) logic '0'. (b) logic '1'.

Figure 6.82: Picture of the orbitals corresponding to the LUMO level for the OPE3 molecule with small driver on the xz plane with the driver. The orbitals are taken with an isosurface value equal to 0.015.

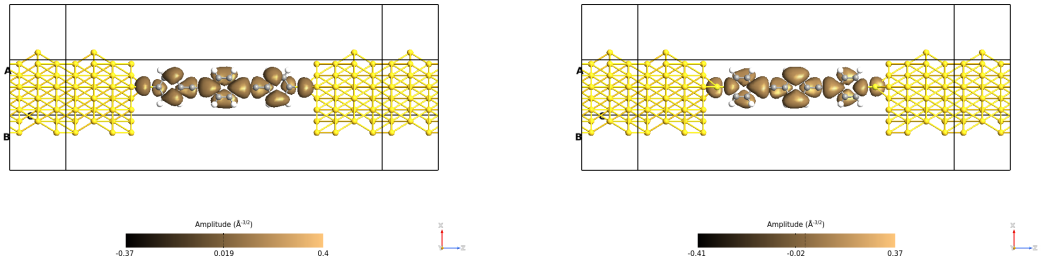

(a) logic '0'. (b) logic '1'.

Figure 6.83: Picture of the orbitals corresponding to the LUMO level for the OPE3 molecule with small driver on the xz plane without the driver. The orbitals are taken with an isosurface value equal to 0.015.

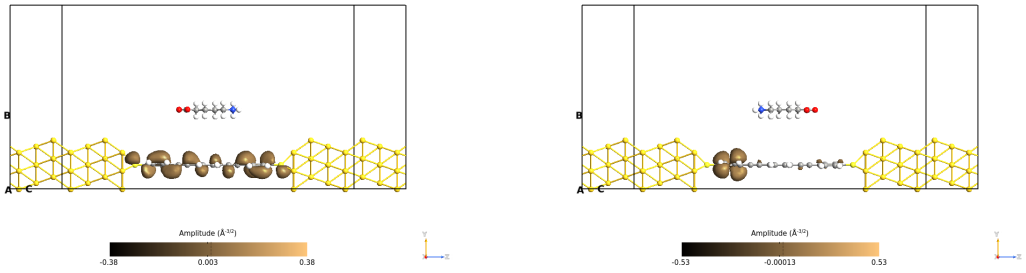

(a) logic '0'. (b) logic '1'.

Figure 6.84: Picture of the orbitals corresponding to the LUMO+1 level for the OPE3 molecule with small driver on the yz plane. The orbitals are taken with an isosurface value equal to 0.015.

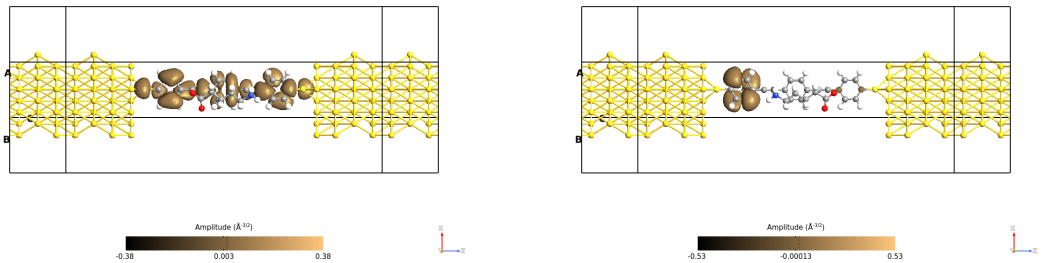

(a) logic '0'. (b) logic '1'.

Figure 6.85: Picture of the orbitals corresponding to the LUMO+1 level for the OPE3 molecule with the small driver on the xz plane with the driver. The orbitals are taken with an isosurface value equal to 0.015.

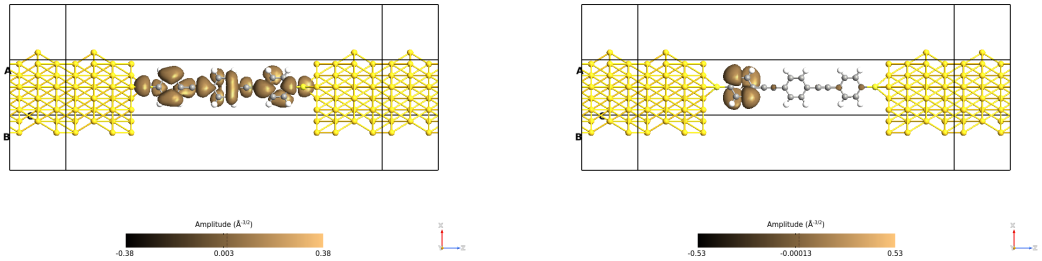

(a) logic '0'. (b) logic '1'.

Figure 6.86: Picture of the orbitals corresponding to the LUMO+1 level for the OPE3 molecule with small driver on the xz plane without the driver. The orbitals are taken with an isosurface value equal to 0.015.

6.2.9 Long driver: Pathways

The OPE3 transmission pathways regarding the angle (figures 6.87, 6.88 and 6.89) hold no surprises, the electrons follow the expected path, and when they reach the benzene the path splits in two different branches, which rejoin when the benzene is finished.

The weight transmission pathways (figures 6.90, 6.91 and 6.92) are coherent with the TS. The plot for the 0.28 eV shows the highest value in terms of magnitude because it has the highest transmission value on the TS (figure 6.52). As expected, the wider difference is detectable in the 0.08 eV pictures, it is easy to notice because the scales are the same but the color of the arrows that bond the benzenes are different, for the logic '0' (figure 6.90a) the arrows are red, while for the logic '1' (figure 6.90b) they are blue. The 0.44 eV plots are practically the same, they are very similar, as expected looking at the TS.

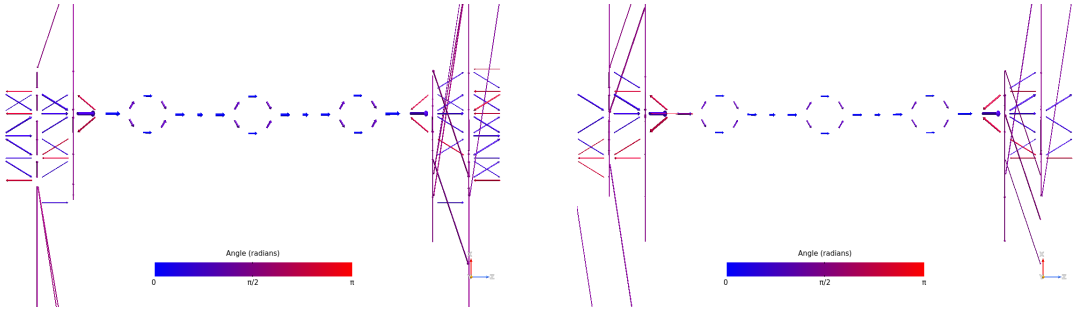

(a) logic '0'. (b) logic '1'.

Figure 6.87: Picture of the pathways corresponding to the energy 0.08 eV for the OPE3 molecule with long driver on the xz plane. The blue arrows are in the same direction as the z-axis, while the red ones are in the opposite direction.

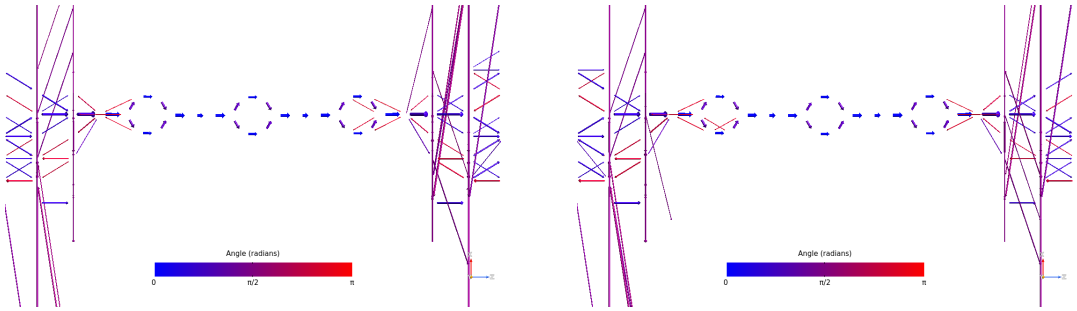

(a) logic '0'. (b) logic '1'.

Figure 6.88: Picture of the pathways corresponding to the energy 0.28 eV for the OPE3 molecule with long driver on the xz plane. The blue arrows are in the same direction as the z-axis, while the red ones are in the opposite direction.

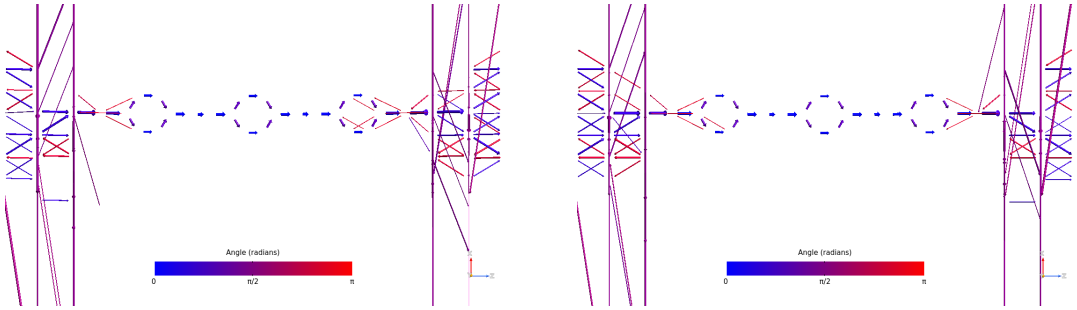

(a) logic '0'. (b) logic '1'.

Figure 6.89: Picture of the pathways corresponding to the energy 0.44 eV for the OPE3 molecule with long driver on the xz plane. The blue arrows are in the same direction as the z-axis, while the red ones are in the opposite direction.

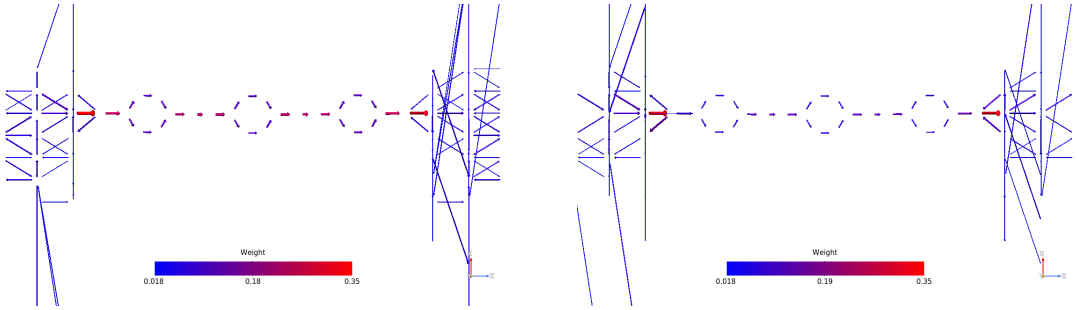

(a) logic '0'. (b) logic '1'.

Figure 6.90: Picture of the pathways corresponding to the energy 0.08 eV for the OPE3 molecule with long driver on the xz plane. The plots show the arrows' magnitude.

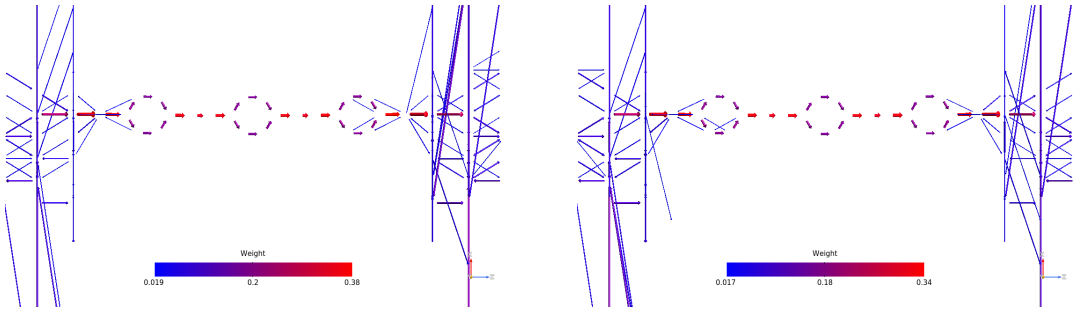

(a) logic '0'. (b) logic '1'.

Figure 6.91: Picture of the pathways corresponding to the energy 0.28 eV for the OPE3 molecule with long driver on the xz plane. The plots show the arrows' magnitude.

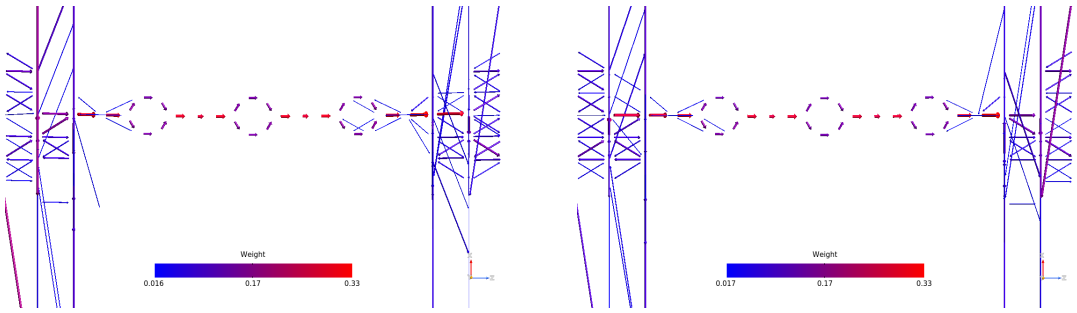

(a) logic '0'. (b) logic '1'.

Figure 6.92: Picture of the pathways corresponding to the energy 0.44 eV for the OPE3 molecule with long driver on the xz plane. The plots show the arrows' magnitude.

6.2.10 Small driver: Pathways

The transmission pathways that represent the conduction direction (figures 6.93, 6.94 and 6.95) show that for lower energies no electrons flow in the opposite direction of the conduction direction, while for higher energy values some carriers go against the conduction direction. This phenomenon is appreciable in the benzenes close to the anchoring group, the middle benzene in each case doesn't exhibit this behavior.

Concerning the weight transmission pathways, the most important difference is expected for the 0.12 eV, because, looking at the TS (figure 6.53), it is possible to notice the wide difference between the two peak amplitudes. As expected, the 0.12 eV plots (figure 6.93) show that the logic '0' configuration has a higher magnitude value with respect to the other configuration, in particular, it is possible to appreciate that the arrows colors are the same but the two highest value of the scale are 1.1 for the logic '0' and 0.61 for the logic '1', which is roughly the half. For the other two energy values (figures 6.94 and 6.95) there are no significant differences, in fact, the TS tells us that the amplitude peaks corresponding to these energies are roughly the same.

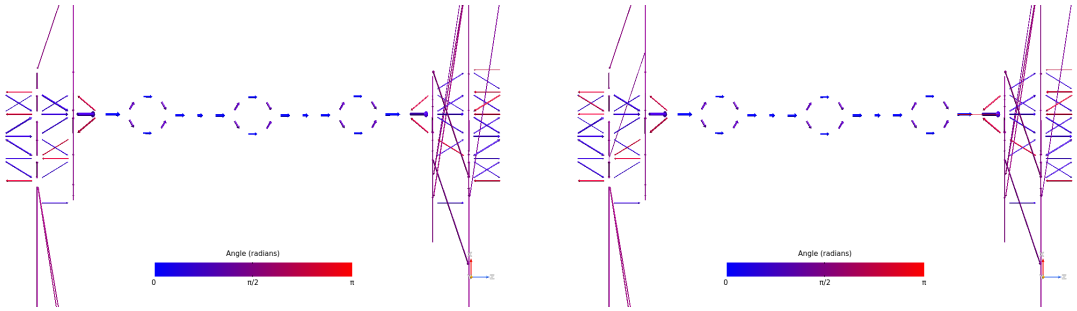

(a) logic '0'. (b) logic '1'.

Figure 6.93: Picture of the pathways corresponding to the energy 0.12 eV for the OPE3 molecule with small driver on the xz plane. The blue arrows are in the same direction as the z-axis, while the red ones are in the opposite direction.

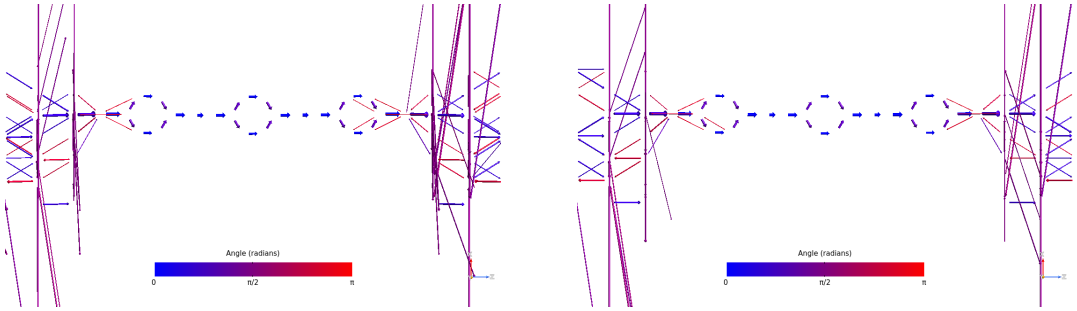

(a) logic '0'. (b) logic '1'.

Figure 6.94: Picture of the pathways corresponding to the energy 0.28 eV for the OPE3 molecule with small driver on the xz plane. The blue arrows are in the same direction as the z-axis, while the red ones are in the opposite direction.

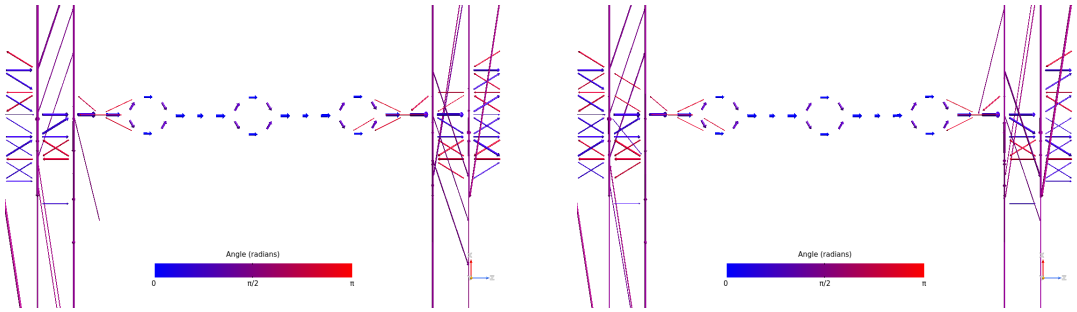

(a) logic '0'. (b) logic '1'.

Figure 6.95: Picture of the pathways corresponding to the energy 0.44 eV for the OPE3 molecule with small driver on the xz plane. The blue arrows are in the same direction as the z-axis, while the red ones are in the opposite direction.

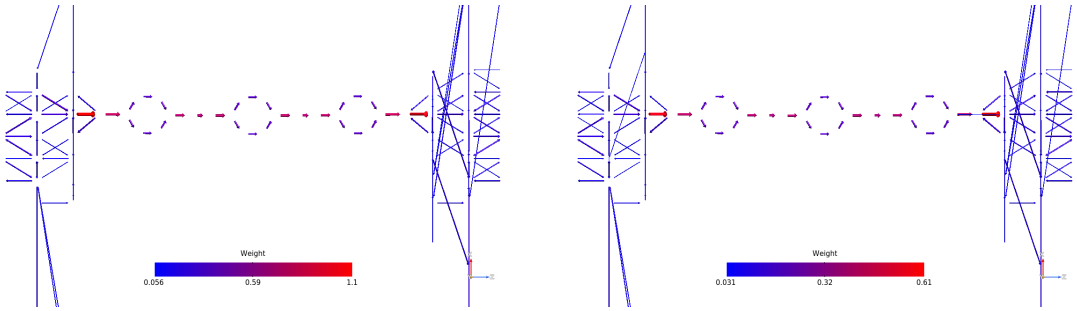

(a) logic '0'. (b) logic '1'.

Figure 6.96: Picture of the pathways corresponding to the energy 0.12 eV for the OPE3 molecule with small driver on the xz plane. The plots show the arrows' magnitude.

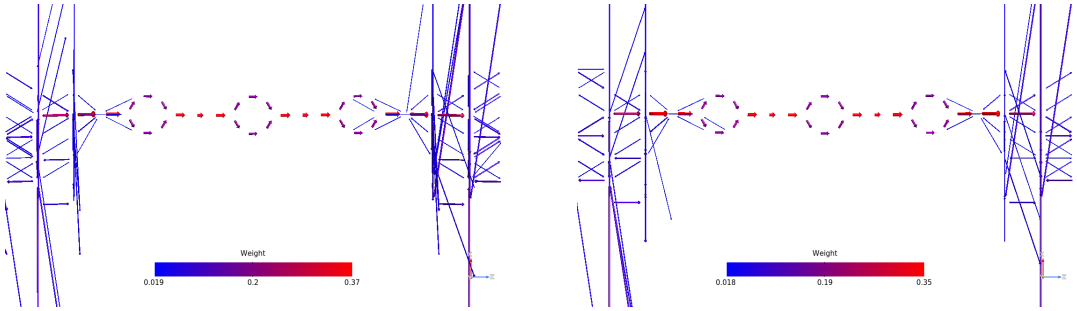

(a) logic '0'. (b) logic '1'.

Figure 6.97: Picture of the pathways corresponding to the energy 0.28 eV for the OPE3 molecule with small driver on the xz plane. The plots show the arrows' magnitude.

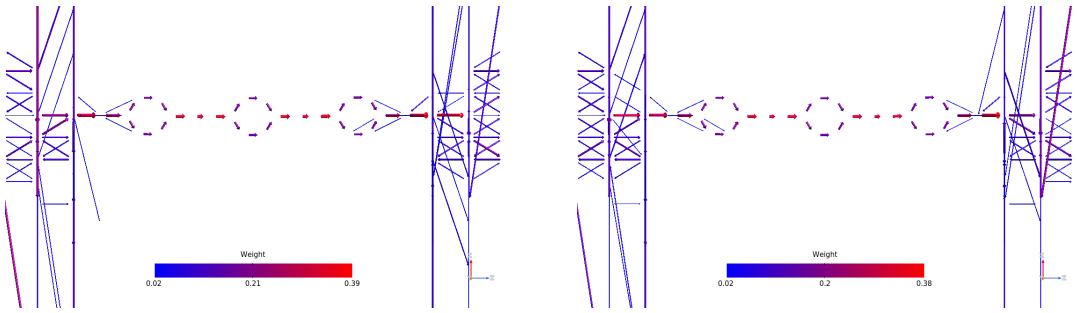

(a) logic '0'. (b) logic '1'.

Figure 6.98: Picture of the pathways corresponding to the energy 0.44 eV for the OPE3 molecule with small driver on the xz plane. The plots show the arrows' magnitude.

6.3 OPE5

The OPE5 molecule is formed by five benzenes connected together by carbons with triple bounds. The builder views are reported in figure 6.99, in which is possible to see the

driver rotation to emulate the two logic values.

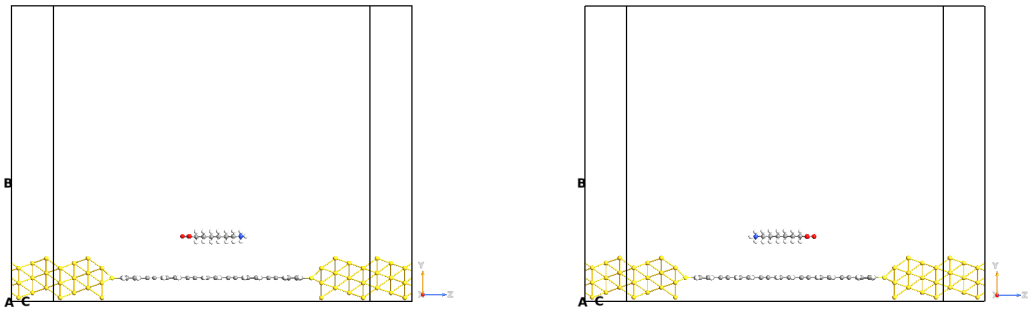

(a) logic '0' configuration.

(b) logic '1' configuration.

Figure 6.99: Picture of the QuantumATK builder for the OPE5 molecule. The white atoms are the hydrogens, the yellow ones are gold atoms, the lighter yellow ones are the sulfurs, the blue ones are nitrogens, the reds are the oxygens and the grey atoms are carbons.

6.3.1 TS

The TS trends for the two logic configurations are practically the same. The main differences are related to the amplitude of the transmission peaks.

The plot in figure 6.100 reveals good conduction properties for the OPE5 molecule. The LUMO peaks are close to the energy axis' origin, this means that the conduction is LUMO-type. The expected current is lower than the OPE3 and OPV3 ones, but it shuld be high enough to provide good conduction properties to the molecular junction.

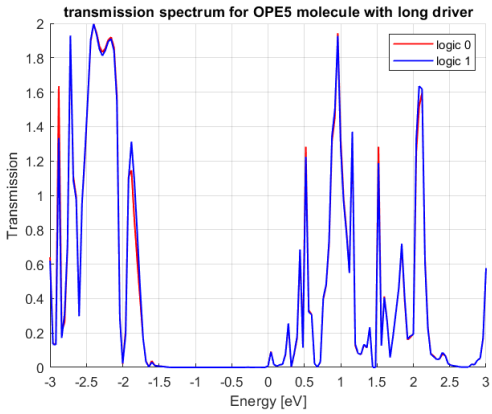

Figure 6.100: Picture of TS for the OPE5 molecule considering the long driver, the red curve represents the logic '0' configuration while the blue one the logic '1' configuration.

6.3.2 IV

The IV plot (figure 6.101) reveals good conduction properties for the OPE5 molecule. The current is always higher than 1 μA, with a maximum value higher than 4 μA for voltages of about 1 V.

The IV picture shows differences between the two logic configurations, they can be detected with today's technologies.

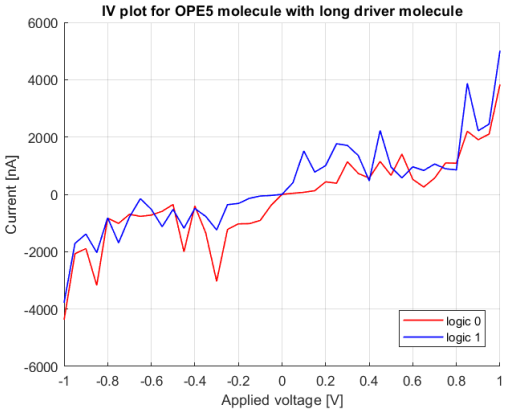

Figure 6.101: Picture of IV for the OPE5 molecule considering the long driver, the red curve represents the logic '0' configuration while the blue one the logic '1' configuration.

The current difference plots (figure 6.102) tell us the feasibility of the readout system based on an OPE5 molecular junction. The wider difference is placed at -0.35 V (higher than 1.5 μA), but the interesting interval could be the one from 0 V to 0.4 V in which the current difference is always positive and the values are similar. The OPE5 presents worse results than the OPE3 and OPV3, nevertheless, they are very interesting.

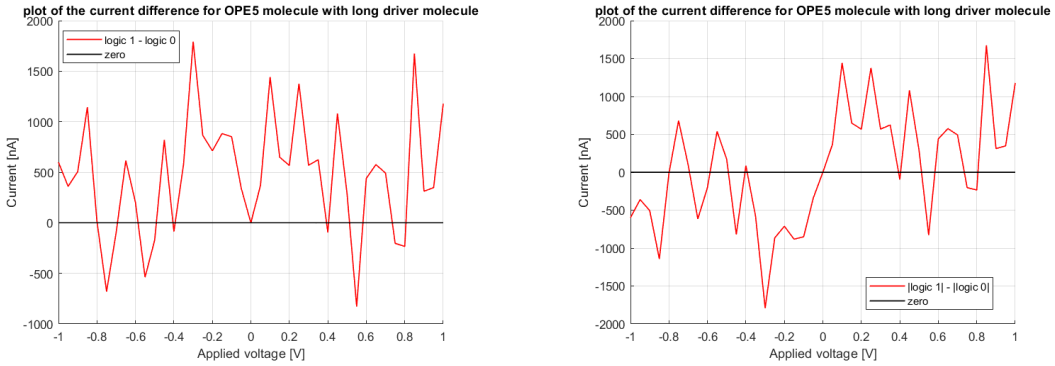

(a) logic '1' - logic '0'.

(b) |logic '1'| - |logic '0'|.

Figure 6.102: Picture of the current difference for the OPE5 molecule considering the long driver.

6.3.3 Orbitals

As for the OPV3 and OPE3 molecules, it is difficult to derive some information through the orbitals view, because they present mainly two different behaviors, the first one is the same trend between the two configurations, and the other one is the complementary shape between them.

The HOMO and LUMO+1 orbitals (figures 6.106, 6.107, 6.108, 6.112, 6.113 and 6.114) are the ones that show a complementary behavior between logic '0' and logic '1'.

The other two energy levels (figures 6.103, 6.104, 6.105, 6.109, 6.110 and 6.111) present the same orbital shape for the two logic configurations.

In some cases, it is also possible to notice the different wideness of the orbital shape close to the electrodes between the two configurations.

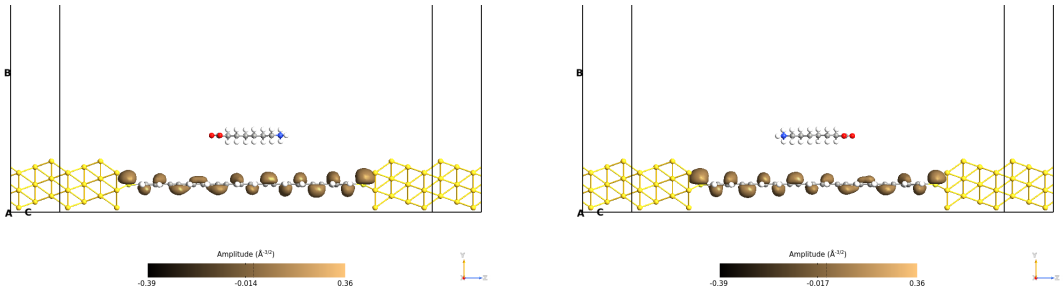

(a) logic '0'. (b) logic '1'.

Figure 6.103: Picture of the orbitals corresponding to the HOMO-1 level for the OPE5 molecule with long driver on the yz plane. The orbitals are taken with an isosurface value equal to 0.015.

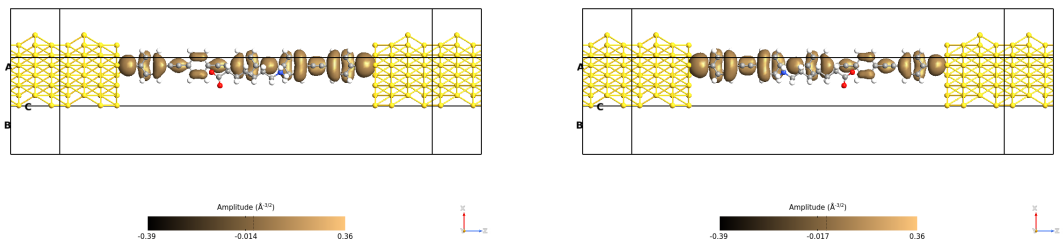

(a) logic '0'. (b) logic '1'.

Figure 6.104: Picture of the orbitals corresponding to the HOMO-1 level for the OPE5 molecule with long driver on the xz plane with the driver. The orbitals are taken with an isosurface value equal to 0.015.

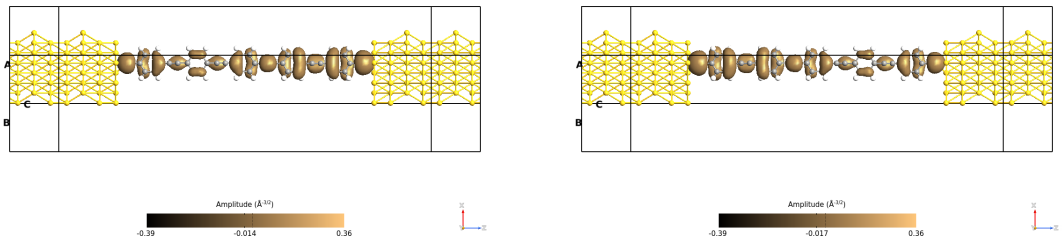

(a) logic '0'. (b) logic '1'.

Figure 6.105: Picture of the orbitals corresponding to the HOMO-1 level for the OPE5 molecule with long driver on the xz plane without the driver. The orbitals are taken with an isosurface value equal to 0.015.

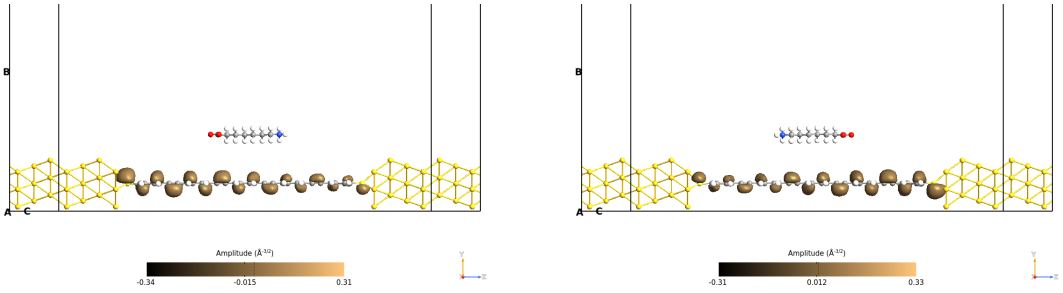

(a) logic '0'. (b) logic '1'.

Figure 6.106: Picture of the orbitals corresponding to the HOMO level for the OPE5 molecule with long driver on the yz plane. The orbitals are taken with an isosurface value equal to 0.015.

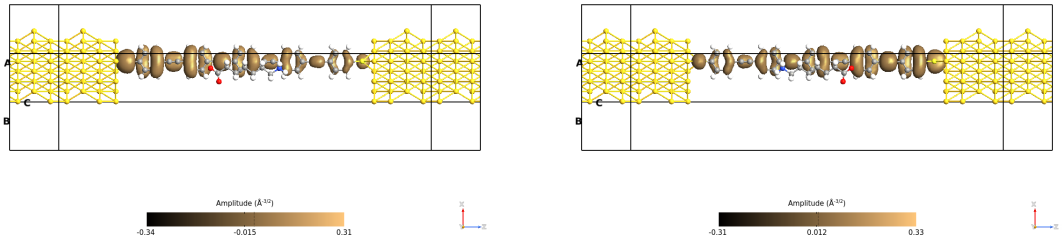

(a) logic '0'. (b) logic '1'.

Figure 6.107: Picture of the orbitals corresponding to the HOMO level for the OPE5 molecule with long driver on the xz plane with the driver. The orbitals are taken with an isosurface value equal to 0.015.

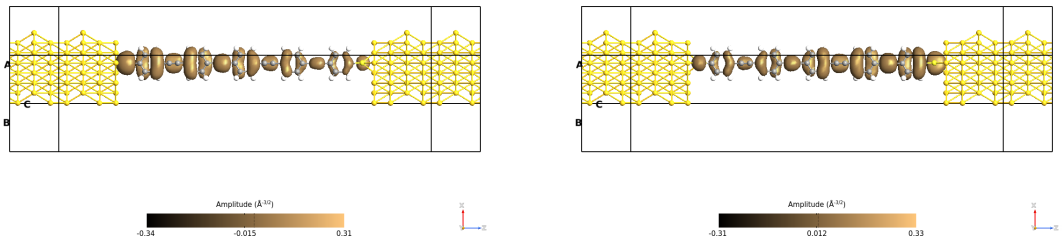

(a) logic '0'. (b) logic '1'.

Figure 6.108: Picture of the orbitals corresponding to the HOMO level for the OPE5 molecule with long driver on the xz plane without the driver. The orbitals are taken with an isosurface value equal to 0.015.

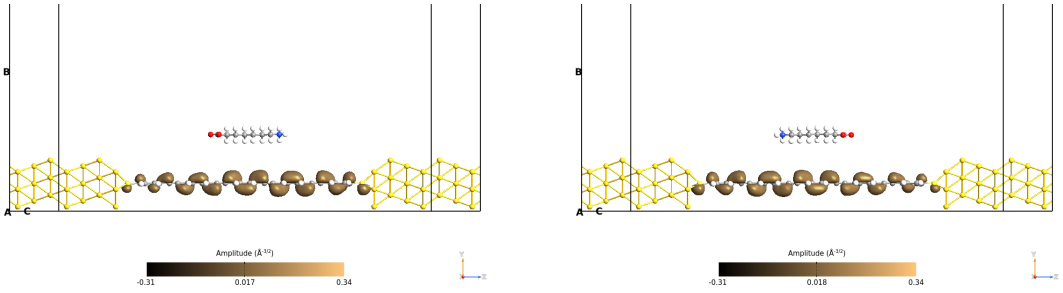

(a) logic '0'. (b) logic '1'.

Figure 6.109: Picture of the orbitals corresponding to the LUMO level for the OPE5 molecule with long driver on the yz plane. The orbitals are taken with an isosurface value equal to 0.015.

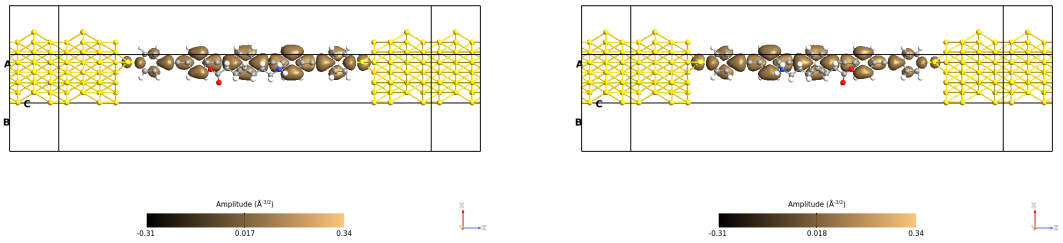

(a) logic '0'. (b) logic '1'.

Figure 6.110: Picture of the orbitals corresponding to the LUMO level for the OPE5 molecule with long driver on the xz plane with the driver. The orbitals are taken with an isosurface value equal to 0.015.

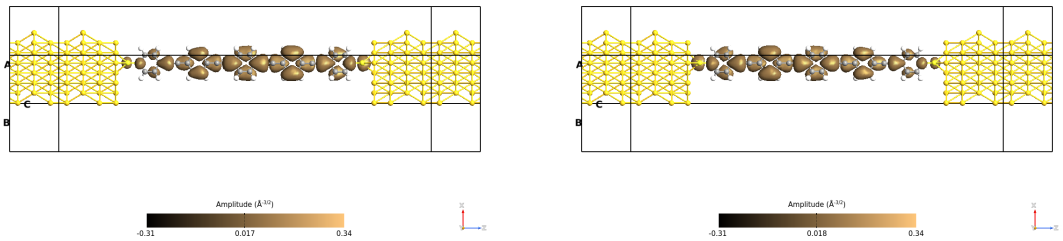

(a) logic '0'. (b) logic '1'.

Figure 6.111: Picture of the orbitals corresponding to the LUMO level for the OPE5 molecule with long driver on the xz plane without the driver. The orbitals are taken with an isosurface value equal to 0.015.

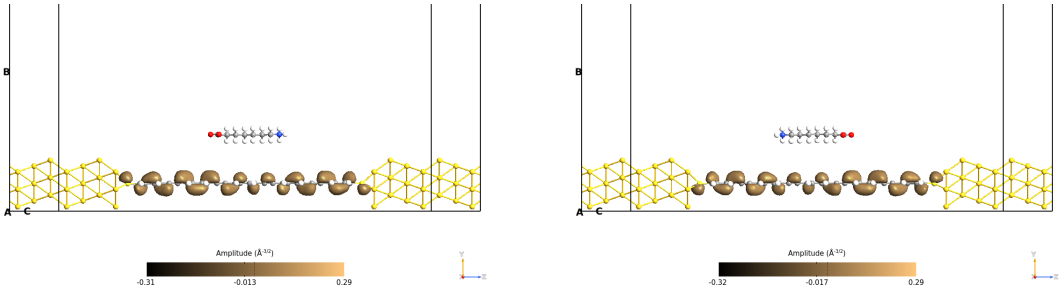

(a) logic '0'. (b) logic '1'.

Figure 6.112: Picture of the orbitals corresponding to the LUMO+1 level for the OPE5 molecule with long driver on the yz plane. The orbitals are taken with an isosurface value equal to 0.015.

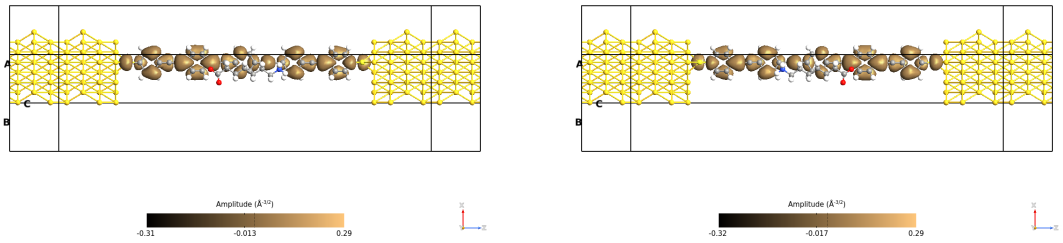

(a) logic '0'. (b) logic '1'.

Figure 6.113: Picture of the orbitals corresponding to the LUMO+1 level for the OPE5 molecule with long driver on the xz plane with the driver. The orbitals are taken with an isosurface value equal to 0.015.

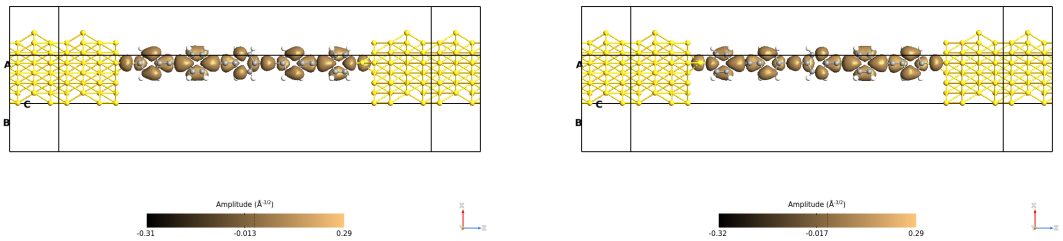

(a) logic '0'. (b) logic '1'.

Figure 6.114: Picture of the orbitals corresponding to the LUMO+1 level for the OPE5 molecule with long driver on the xz plane without the driver. The orbitals are taken with an isosurface value equal to 0.015.

6.3.4 Pathways

The transmission pathways concerning the angle between the arrows and the x-axis (figures 6.115, 6.116 and 6.117) don't present relevant surprises with respect to the initial thoughts. The electrons follow the carbon chain, and when they arrive close to the benzene, they split into two branches, at the end of the benzene's path they rejoin in a single flow.

The weight transmission pathways confirm the TS results. For the 0.28 eV (figure 6.118) and 0.44 eV (figure 6.119) pictures, there are no significant differences between the two logic configurations. The 0.52 eV transmission pathway (figure 6.120) instead, presents significantly different magnitude values between the two cases, in particular, for the logic '0' the highest value in the scale is equal to 0.88 while for the logic '1' the highest value is 0.29. This behavior is consistent with the trend in the TS (figure 6.100) of the OPE5 molecular junction.

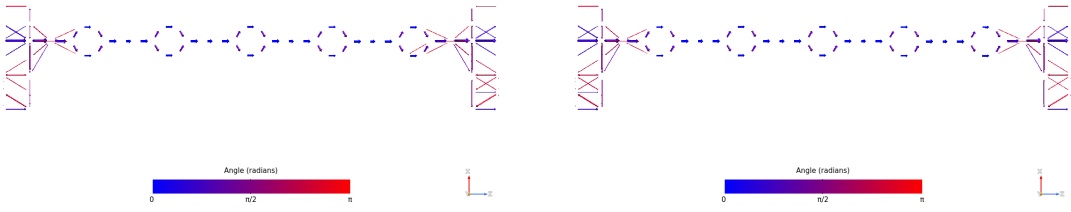

(a) logic '0'. (b) logic '1'.

Figure 6.115: Picture of the pathways corresponding to the energy 0.28 eV for the OPE5 with long driver on the xz plane. The blue arrows are in the same direction as the z-axis, while the red ones are in the opposite direction.

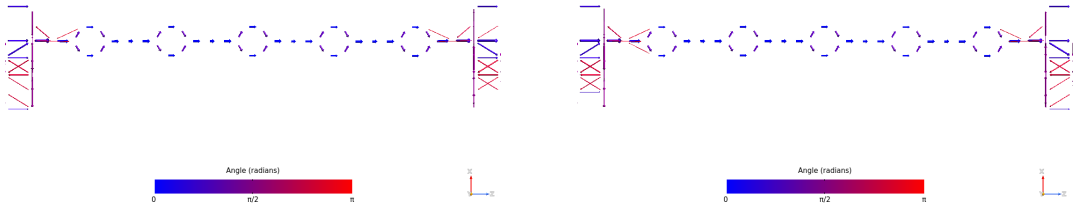

(a) logic '0'. (b) logic '1'.

Figure 6.116: Picture of the pathways corresponding to the energy 0.44 eV for the OPE5 with long driver on the xz plane. The blue arrows are in the same direction as the z-axis, while the red ones are in the opposite direction.

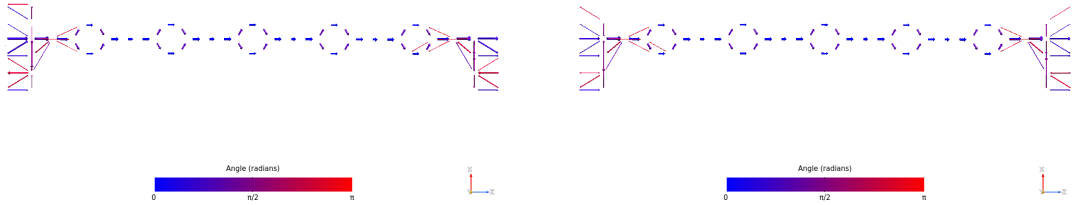

(a) logic '0'. (b) logic '1'.

Figure 6.117: Picture of the pathways corresponding to the energy 0.52 eV for the OPE5 with long driver on the xz plane. The blue arrows are in the same direction as the z-axis, while the red ones are in the opposite direction.

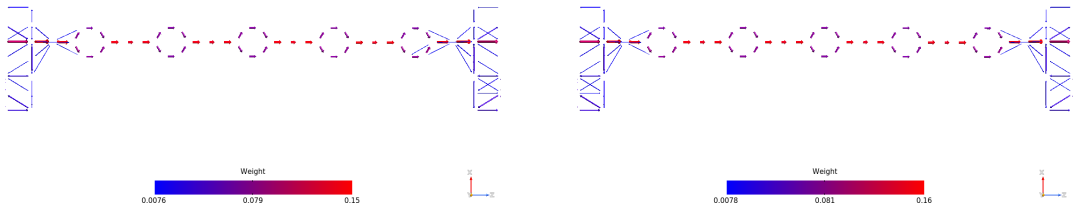

(a) logic '0'. (b) logic '1'.

Figure 6.118: Picture of the pathways corresponding to the energy 0.28 eV for the OPE5 molecule with long driver on the xz plane. The plots show the arrows' magnitude.

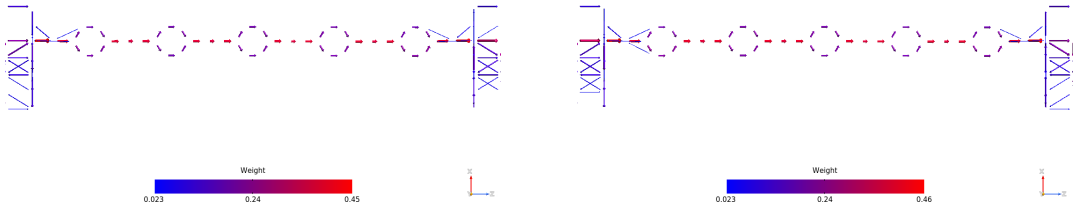

(a) logic '0'. (b) logic '1'.

Figure 6.119: Picture of the pathways corresponding to the energy 0.44 eV for the OPE5 molecule with long driver on the xz plane. The plots show the arrows' magnitude.

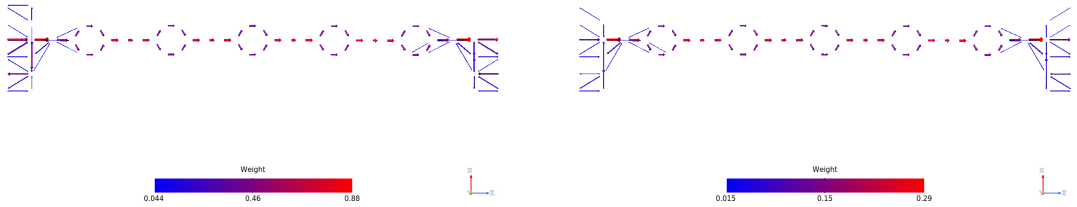

(a) logic '0'. (b) logic '1'.

Figure 6.120: Picture of the pathways corresponding to the energy 0.52 eV for the OPE5 molecule with long driver on the xz plane. The plots show the arrows' magnitude.

6.3.5 Different alignement

The OPE5 is the longest molecule between the selected ones, for this reason, a deeper analysis can be performed. The driver is moved from the left side to the right side, it is not always placed in the middle of the junction. This simulation cannot be performed with the other molecules because their channel lengths are comparable with the driver length.

The builder views of the simulations are reported in the pictures below, in particular, figure 6.121 refers to the left alignment of the driver molecule, while figure 6.122 to the right alignment.

In figure 6.123 are reported the TS of the two logic configurations, in particular, figure 6.123a refers to the logic '0' configuration, while figure 6.123b to the logic '1' one.

The TS behavior is unpredictable, for the same logic value the plot presents different trends, which is not good in terms of readout system robustness. A general trend could be seen looking at the configuration in which the positive pole of the driver is close to one electrode (left alignment in logic '0' configuration and right alignment in logic '1' case), in those cases the TS reveals a high and narrow peak close to the energy axis origin. Around 1 eV, the behavior is very close between the three different alignments.

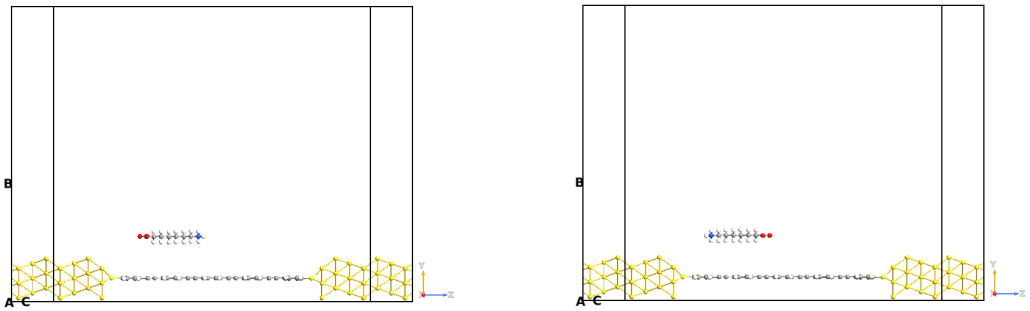

(a) logic '0'. (b) logic '1'.

Figure 6.121: Picture of the builter views for the OPE5 molecule with long driver placed on the left side of the junction.

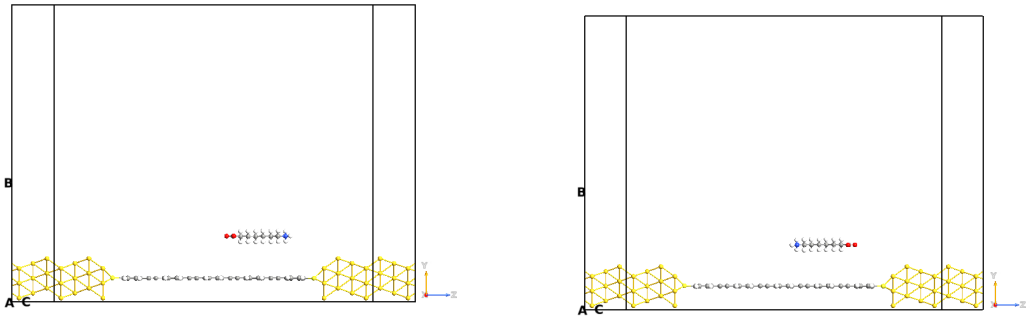

(a) logic '0'. (b) logic '1'.

Figure 6.122: Picture of the builter views for the OPE5 molecule with long driver placed on the right side of the junction.

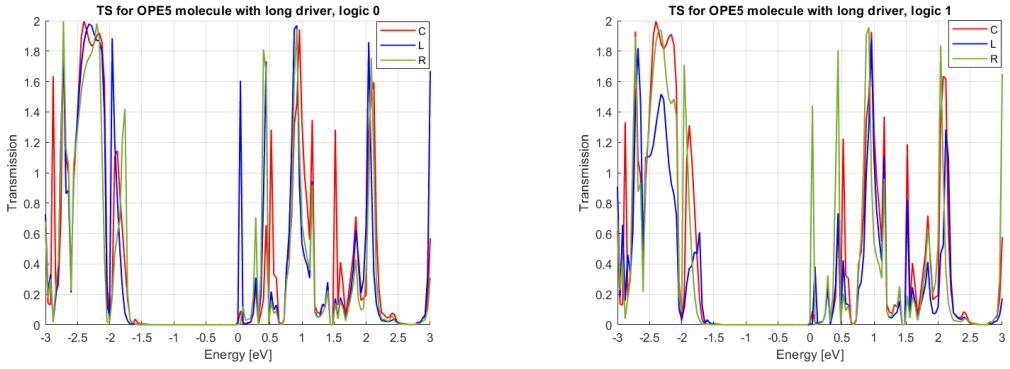

(a) logic '0'. (b) logic '1'.

Figure 6.123: Picture of the TS for the OPE5 molecule with the long driver placed at different alignments with respect to the junction, in particular, the C curve stands for central, the L one for left and the R line stands for right.

In figure 6.124 are shown the IV plot for the two configurations, figure 6.124a refers to the logic '0' one, while figure 6.124b to the logic '1'.

From the plots, it is possible to notice that the behaviors of the different alignment cases are different, which means that the system doesn't show good robustness against the not-perfect placement of the molecule. In particular, the left alignment in the logic '1' configuration presents a completely different trend with respect to the other two configurations. In the logic '1' IV picture, instead, the current for low applied voltages is very low in all the cases except for the central alignment, which reveals a high divable current also for low potentials.

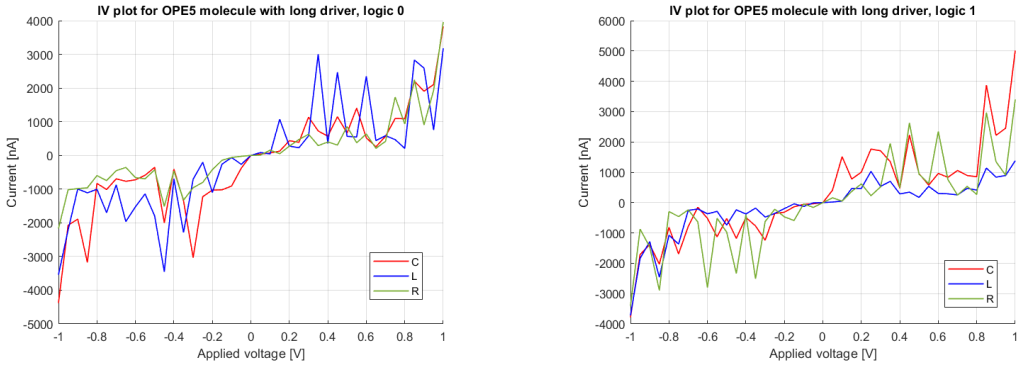

(a) logic '0'. (b) logic '1'.

Figure 6.124: Picture of the IV for the OPE5 molecule with the long driver placed at different alignments with respect to the junction, in particular, the C curve stands for central, the L one for left and the R line stands for right.

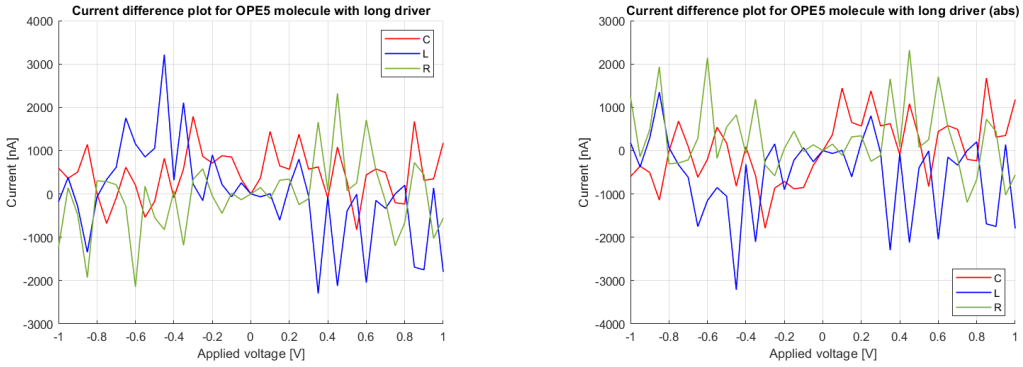

(a) logic '1' - logic '0'. (b) |logic '1'| - |logic '0'|.

Figure 6.125: Picture of the current difference for the OPE5 molecule with the long driver placed at different alignments with respect to the junction, in particular, the C curve stands for central, the L one for left and the R line stands for right.

Figure 6.125 shows the current difference between the two logic configurations, considering the conduction direction (therefore the sign) in figure 6.125a and not considering

it in figure 6.125b. It is possible to observe that the trends are quite different, therefore the readout system design in these conditions is more difficult. The junction molecule's length should be slightly larger than the molFCN one.

6.4 Phthalocyanine

The phthalocyanine molecule was selected for its high polarizability value. In these simulations, it has been bounded to the electrodes through sulfur atoms. The builder views of the device are reported in figure 6.126.

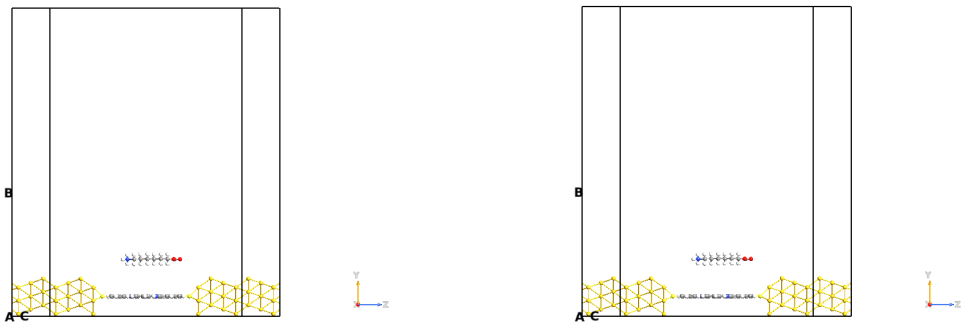

(a) logic '0' configuration. (b) logic '1' configuration.

Figure 6.126: Picture of the QuantumATK builder for the Pc molecule. The white atoms are the hydrogens, the yellow ones are gold atoms, the lighter yellow ones are the sulfurs, the blue ones are nitrogens, the reds are the oxygens and the grey atoms are carbons.

6.4.1 TS

The TS of the Pc molecular junction under the long driver influence is plotted in figure 6.127. Looking at it, it is possible to derive why the Pc molecular junctions are not considered by researchers, in fact, the peaks close to the origin of the energy axis have low transmission values. The HOMOs' energy levels are quite distant from the 0 eV, therefore they are not easily includible in a bias window. The first consistent peak corresponds to roughly 1 eV, thus means that a wide bias window is needed to include it (at least 2 V of applied voltage).

As for the OPV3 and OPE3 molecules, the Pc TS for the two configurations are practically the same, they have the same shape, the differences are related to the amplitude and wideness of the transmission peaks.

6.4.2 IV

As expected from the TS, the current is lower than the OPV3 and OPE3 ones, but it exhibits good properties. In the IV plot (figure 6.128) is possible to observe that the current of the two configurations have different values, thus means that it is readable by an electronic measurement system.

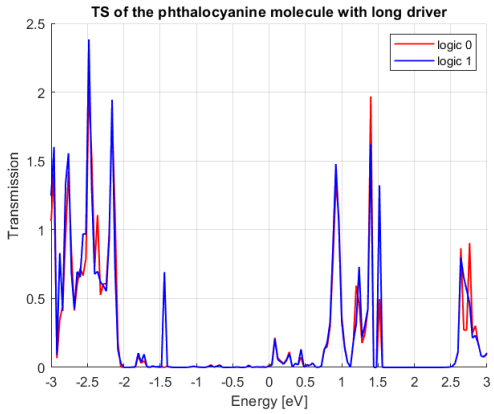

Figure 6.127: Picture of TS for the Pc molecule considering the long driver, the red curve represents the logic '0' configuration while the blue one the logic '1' configuration.

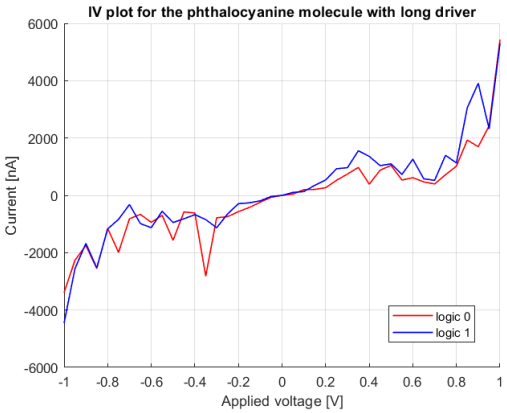

Figure 6.128: Picture of IV for the Pc molecule considering the long driver, the red curve represents the logic '0' configuration while the blue one the logic '1' configuration.

In figure 6.129 are reported the current difference graphs. They show the feasibility of a readout system, the current difference between the two configurations for some points (-0.35 V and 0.9 V) is about 2 μA, which is a measurable value. In absolute terms, the Pc molecule works worse than OPV3 and OPE3, but it works.

6.4.3 Orbitals

It is difficult to derive some information through the orbitals view, because there are two different behaviors, the first one is no changes between the two configurations, and the other one is the complementary shape between them. The HOMO-1 orbitals (figures 6.130, 6.131 and 6.132) are the only ones that show a complementary behavior between logic '0' and logic '1'. It has also the narrowest orbitals, the greater amount of them are close to the negative pole of the driver. The other three energy levels (figures 6.133, 6.134, 6.135, 6.136, 6.137, 6.138, 6.139, 6.140 and 6.141) present the same orbitals.

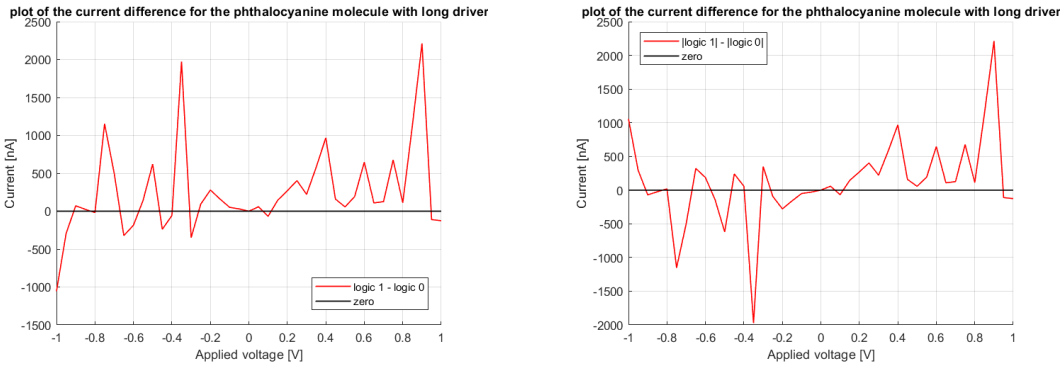

(a) logic '1' - logic '0'. (b) |logic '1'| - |logic '0'|.

Figure 6.129: Picture of the current difference for the Pc molecule considering the long driver.

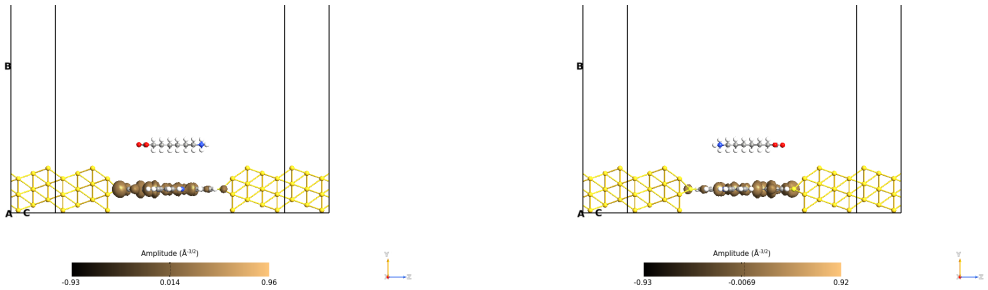

(a) logic '0'. (b) logic '1'.

Figure 6.130: Picture of the orbitals corresponding to the HOMO-1 level for the Pc molecule with long driver on the yz plane. The orbitals are taken with an isosurface value equal to 0.015.

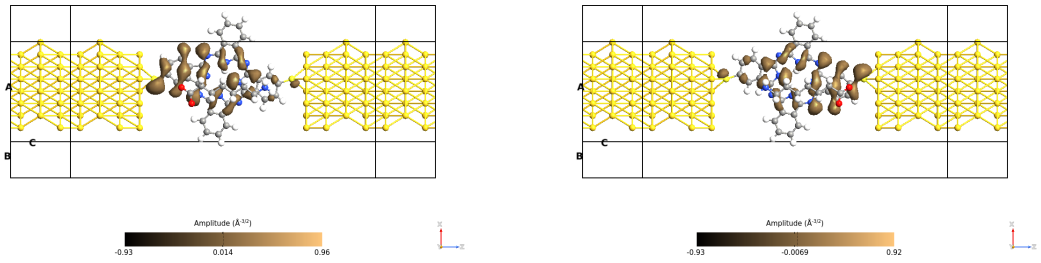

(a) logic '0'. (b) logic '1'.

Figure 6.131: Picture of the orbitals corresponding to the HOMO-1 level for the Pc molecule with long driver on the xz plane with the driver. The orbitals are taken with an isosurface value equal to 0.015.

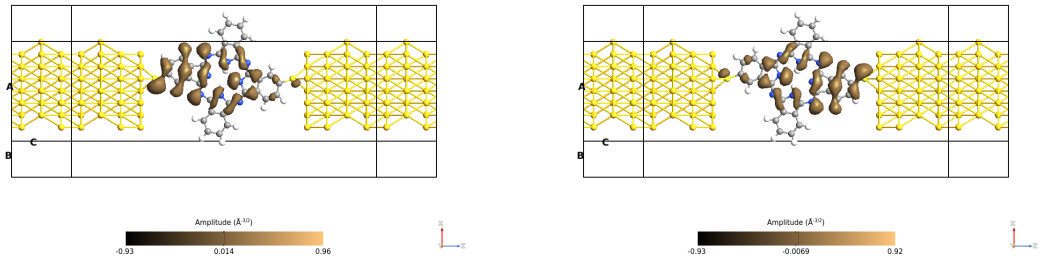

(a) logic '0'. (b) logic '1'.

Figure 6.132: Picture of the orbitals corresponding to the HOMO-1 level for the Pc molecule with long driver on the xz plane without the driver. The orbitals are taken with an isosurface value equal to 0.015.

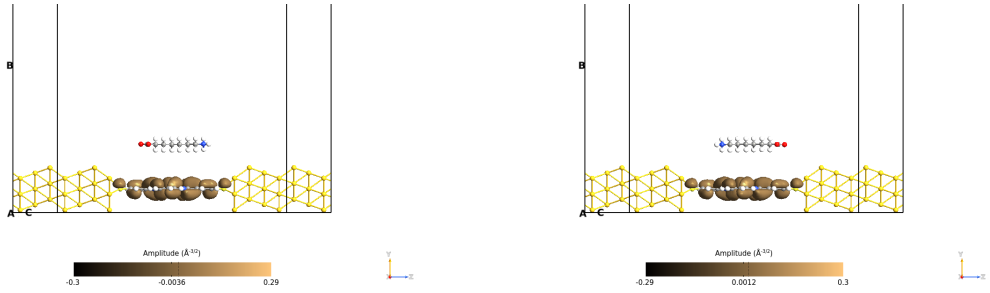

(a) logic '0'. (b) logic '1'.

Figure 6.133: Picture of the orbitals corresponding to the HOMO level for the Pc molecule with long driver on the yz plane. The orbitals are taken with an isosurface value equal to 0.015.

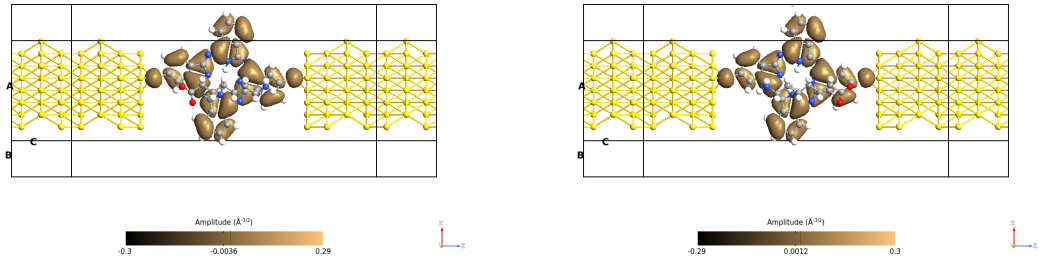

(a) logic '0'. (b) logic '1'.

Figure 6.134: Picture of the orbitals corresponding to the HOMO level for the Pc molecule with long driver on the xz plane with the driver. The orbitals are taken with an isosurface value equal to 0.015.

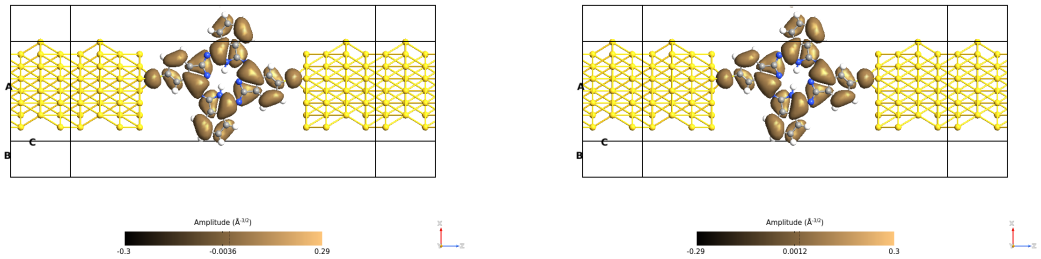

(a) logic '0'. (b) logic '1'.

Figure 6.135: Picture of the orbitals corresponding to the HOMO level for the Pc molecule with long driver on the xz plane without the driver. The orbitals are taken with an isosurface value equal to 0.015.

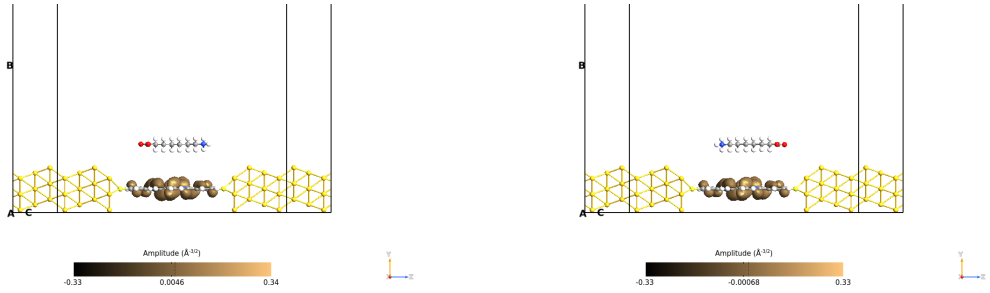

(a) logic '0'. (b) logic '1'.

Figure 6.136: Picture of the orbitals corresponding to the LUMO level for the Pc molecule with long driver on the yz plane. The orbitals are taken with an isosurface value equal to 0.015.

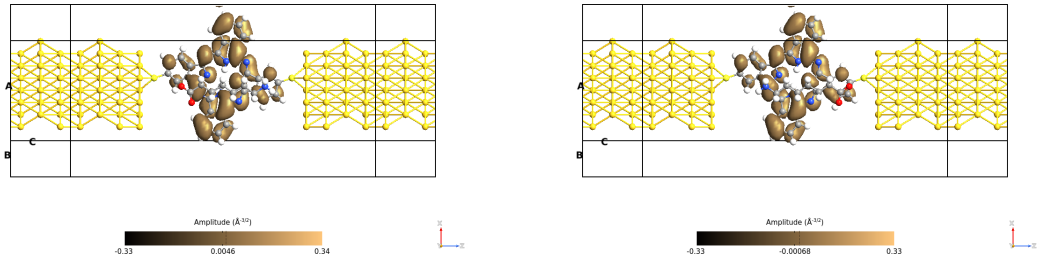

(a) logic '0'. (b) logic '1'.

Figure 6.137: Picture of the orbitals corresponding to the LUMO level for the Pc molecule with long driver on the xz plane with the driver. The orbitals are taken with an isosurface value equal to 0.015.

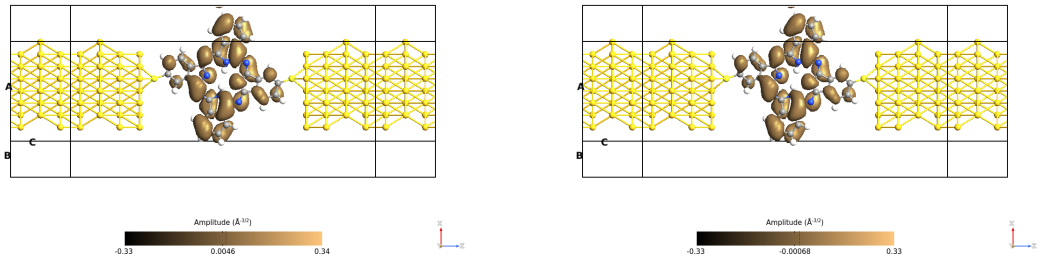

(a) logic '0'. (b) logic '1'.

Figure 6.138: Picture of the orbitals corresponding to the LUMO level for the Pc molecule with long driver on the xz plane without the driver. The orbitals are taken with an isosurface value equal to 0.015.

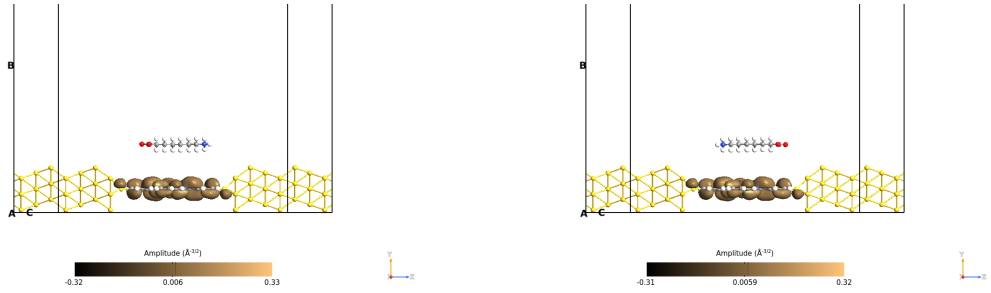

(a) logic '0'. (b) logic '1'.

Figure 6.139: Picture of the orbitals corresponding to the LUMO+1 level for the Pc molecule with long driver on the yz plane. The orbitals are taken with an isosurface value equal to 0.015.

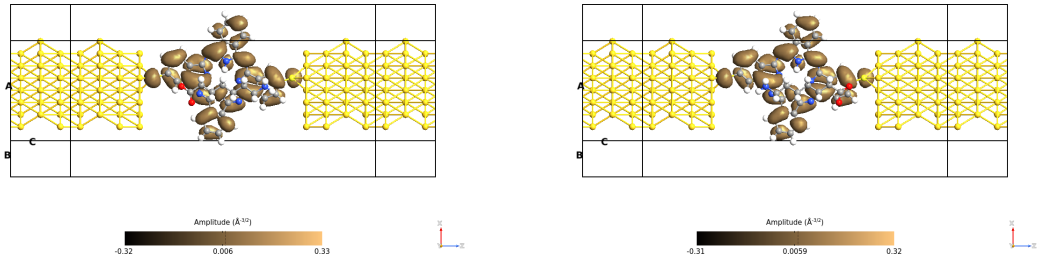

(a) logic '0'. (b) logic '1'.

Figure 6.140: Picture of the orbitals corresponding to the LUMO+1 level for the Pc molecule with long driver on the xz plane with the driver. The orbitals are taken with an isosurface value equal to 0.015.

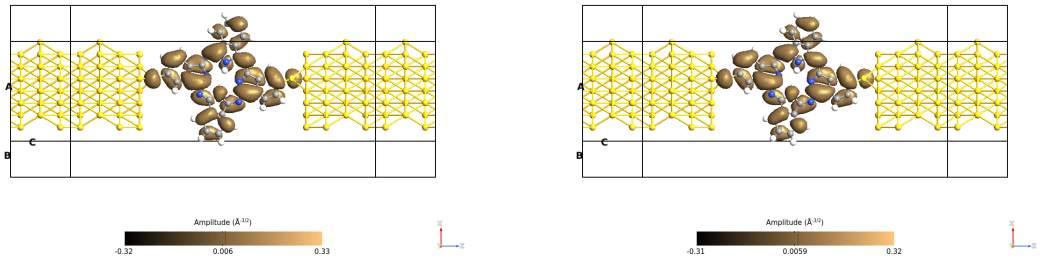

(a) logic '0'. (b) logic '1'.

Figure 6.141: Picture of the orbitals corresponding to the LUMO+1 level for the Pc molecule with long driver on the xz plane without the driver. The orbitals are taken with an isosurface value equal to 0.015.

6.4.4 Pathways

The Pc geometry is not the best for conduction, because it doesn't mimic a channel, it is more similar to a cross. The two sides orthogonal to the conduction direction don't contribute much to the conduction. It is possible to observe that for low energies the electron flow in the orthogonal branches is less important than the one for high energies. The transmission pathways corresponding to 0.08 eV (figure 6.142) tell us that only one of the two branches is effectively explored by the carriers, for the logic '0' it is the bottom one, while for the logic '1' is the upper one. In the other two transmission pathways (figures 6.143 and 6.144) is possible to notice the conduction in both the orthogonal branches. In general, in the conduction direction, there are red arrows which means that not all the electrons contribute positively at the conduction.

The weight transmission pathways highlight the poor conductivity of the Pc molecule. It is possible to derive it from the magnitude values, which are very low (0.06 - 0.09) except for the 0.06 eV case (figure 6.145) which exhibit higher values, but they are still lower than the OPE3 and OPV3 ones.

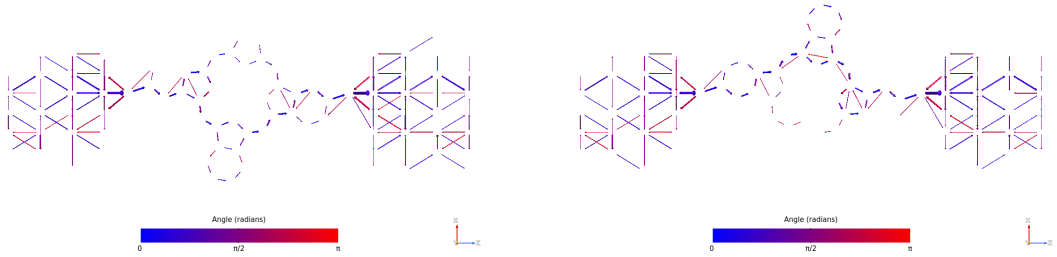

(a) logic '0'. (b) logic '1'.

Figure 6.142: Picture of the pathways corresponding to the energy 0.08 eV for the Pc with long driver on the xz plane. The blue arrows are in the same direction as the z-axis, while the red ones are in the opposite direction.

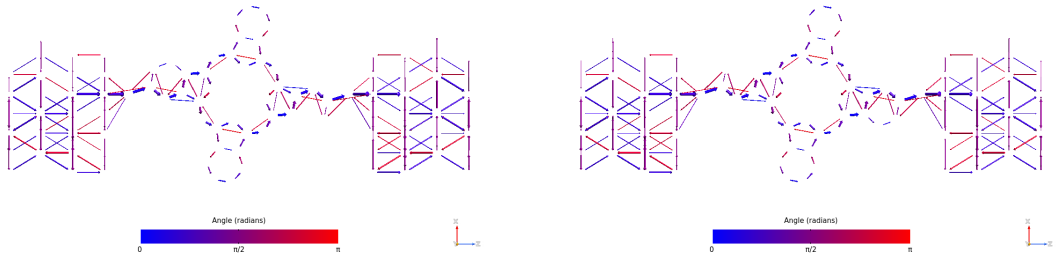

(a) logic '0'. (b) logic '1'.

Figure 6.143: Picture of the pathways corresponding to the energy 0.28 eV for the Pc with long driver on the xz plane. The blue arrows are in the same direction as the z-axis, while the red ones are in the opposite direction.

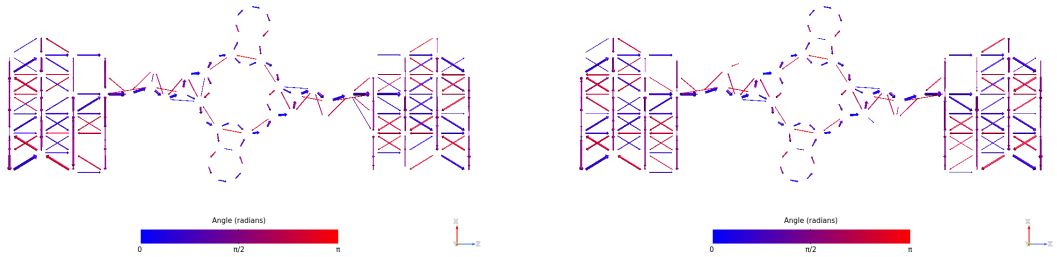

(a) logic '0'. (b) logic '1'.

Figure 6.144: Picture of the pathways corresponding to the energy 0.44 eV for the Pc with long driver on the xz plane. The blue arrows are in the same direction as the z-axis, while the red ones are in the opposite direction.

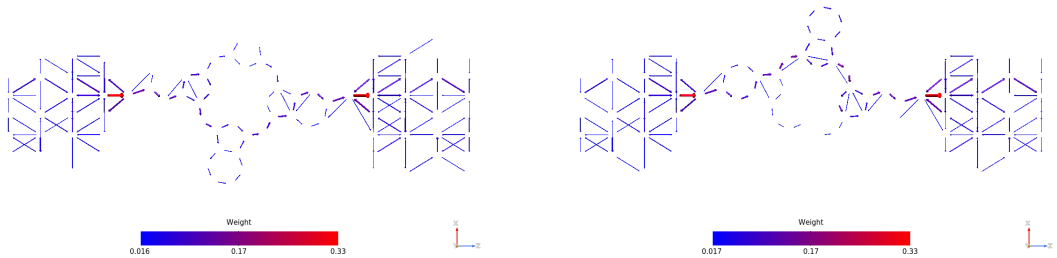

(a) logic '0'. (b) logic '1'.

Figure 6.145: Picture of the pathways corresponding to the energy 0.08 eV for the Pc molecule with long driver on the xz plane. The plots show the arrows' magnitude.

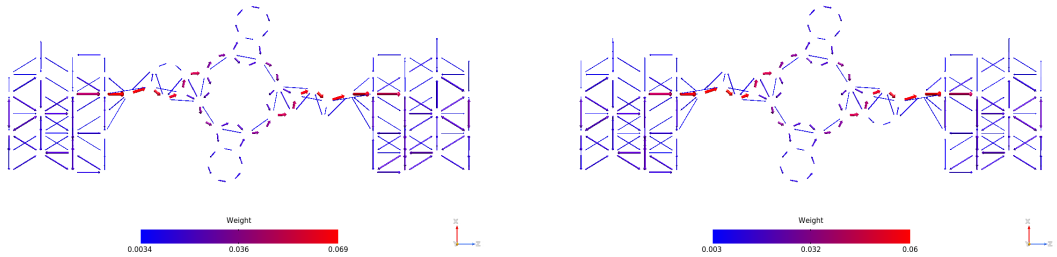

(a) logic '0'. (b) logic '1'.

Figure 6.146: Picture of the pathways corresponding to the energy 0.28 eV for the Pc molecule with long driver on the xz plane. The plots show the arrows' magnitude.

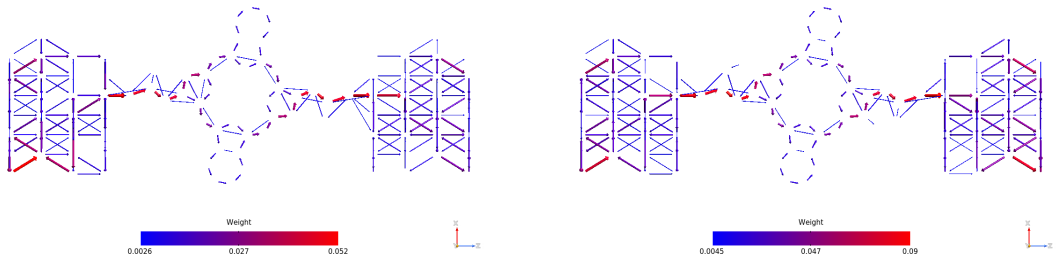

(a) logic '0'. (b) logic '1'.

Figure 6.147: Picture of the pathways corresponding to the energy 0.44 eV for the Pc molecule with long driver on the xz plane. The plots show the arrows' magnitude.

6.5 Zinc Phthalocyanine

The ZnPc molecule is very similar to the Pc one, the base is the same, but it contains a zinc atom in the middle of the molecule. The presence of the metal atom should improve the conduction properties of the molecular junction. The builder views of the ZnPc molecular junction are reported in figure 6.148.

6.5.1 TS

The TS plot is reported in figure 6.149. It is possible to notice that the zinc atom causes a HOMO-LUMO gap reduction because the LUMOs remain roughly in the same energy values, but the HOMO peak shifts towards the origin of the energy axis. Another difference is related to the amplitude of the HOMO peak, it is higher than the Pc one.

As for the molecules analyzed before, the ZnPc shows the same trend between the two logic configurations, the differences are related to the wideness and amplitude of the transmission peaks.

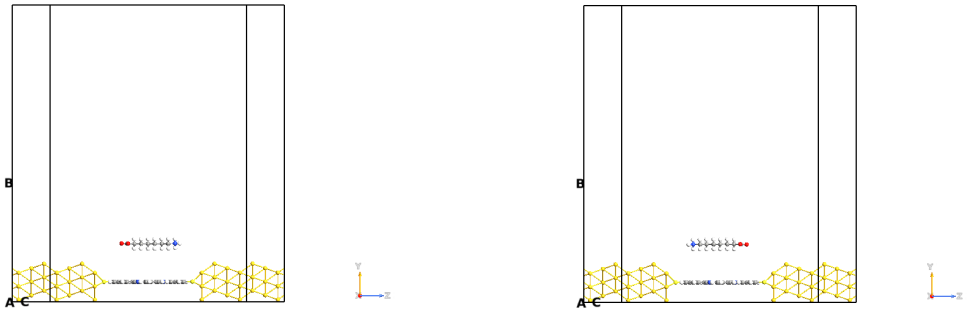

(a) logic '0' configuration. (b) logic '1' configuration.

Figure 6.148: Picture of the QuantumATK builder for the ZnPc molecule. The white atoms are the hydrogens, the yellow ones are gold atoms, the lighter yellow ones are the sulfurs, the blue ones are nitrogens, the reds are the oxygens and the grey atoms are carbons.

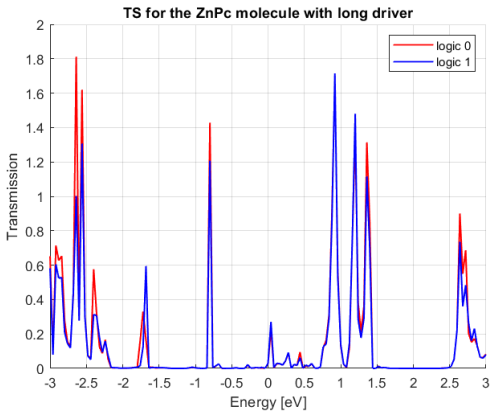

Figure 6.149: Picture of TS for the ZnPc molecule considering the long driver, the red curve represents the logic '0' configuration while the blue one the logic '1' configuration.

6.5.2 IV

The ZnPc molecule shows better conduction properties than the Pc one, as we can see in the figure 6.150. The amount of current that the molecule could drive is slightly lower than 5 μA.

The plots in figure 6.151 show the current difference between the two configurations, with and without considering the conduction direction. The readout system feasibility is assured by the peak around 0.35 V (greater than 3 μA). The problem could be related to the system robustness because the peak is narrow and if the voltage changes by 0.1 V the function becomes negative, therefore the logic values read are wrong.

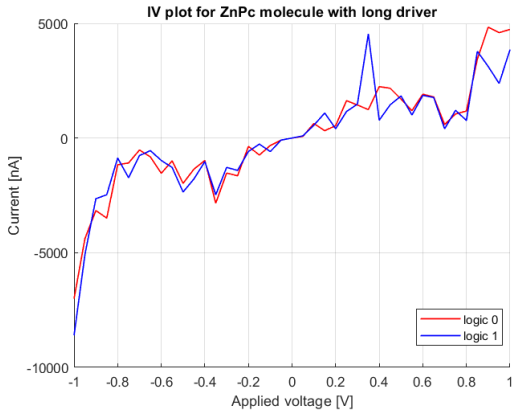

Figure 6.150: Picture of IV for the ZnPc molecule considering the long driver, the red curve represents the logic '0' configuration while the blue one the logic '1' configuration.

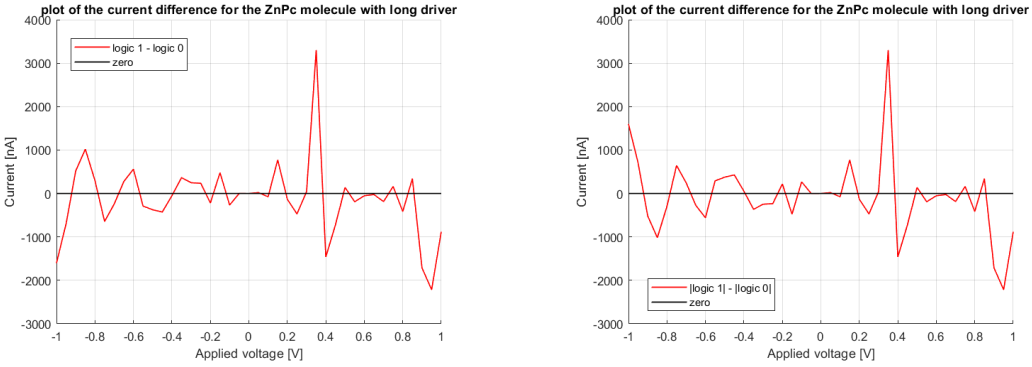

(a) logic '1' - logic '0'.

(b) |logic '1'| - |logic '0'|.

Figure 6.151: Picture of the current difference for the ZnPc molecule considering the long driver.

6.5.3 Orbitals

The ZnPc orbitals show a complementary behavior between the two logic configurations. All the analyzed energy levels (figures 6.152, 6.153, 6.154, 6.155, 6.156, 6.157, 6.158, 6.159, 6.160, 6.161, 6.162 and 6.163) present the same trend. The difference is related to the geometry of the orbitals, the HOMOs are thinner and they are closer to the driver's negative pole. On the other hand, the LUMOs are wider (they cover practically all the molecule) and their shape is similar to a bean.

A curious result can be noticed in the LUMO and LUMO+1 orbitals, no orbitals cover the zinc atom. We know that the electrons in a metal are below the Fermi's energy, in a molecule the Fermi's energy is placed between HOMO and LUMO (over the HOMO level and under the LUMO one). This behavior seems to be coherent with these information because the orbitals over the zinc atom are only present in the HOMO-1 and HOMO levels, which are below the Fermi's energy level.

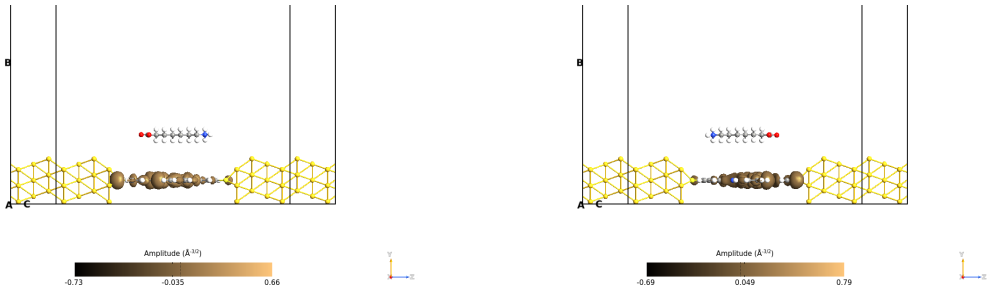

(a) logic '0'. (b) logic '1'.

Figure 6.152: Picture of the orbitals corresponding to the HOMO-1 level for the ZnPc molecule with long driver on the yz plane. The orbitals are taken with an isosurface value equal to 0.015.

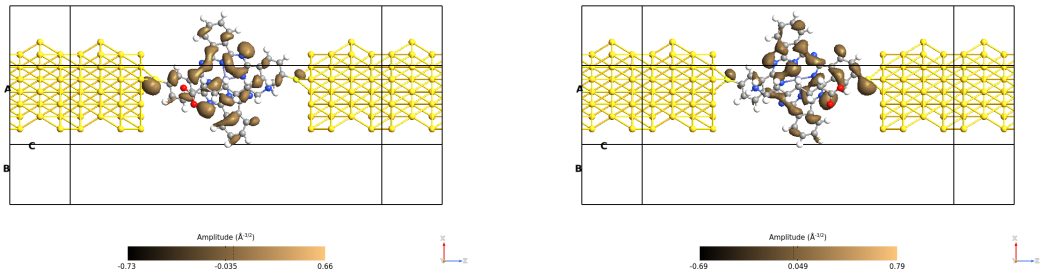

(a) logic '0'. (b) logic '1'.

Figure 6.153: Picture of the orbitals corresponding to the HOMO-1 level for the ZnPc molecule with long driver on the xz plane with the driver. The orbitals are taken with an isosurface value equal to 0.015.

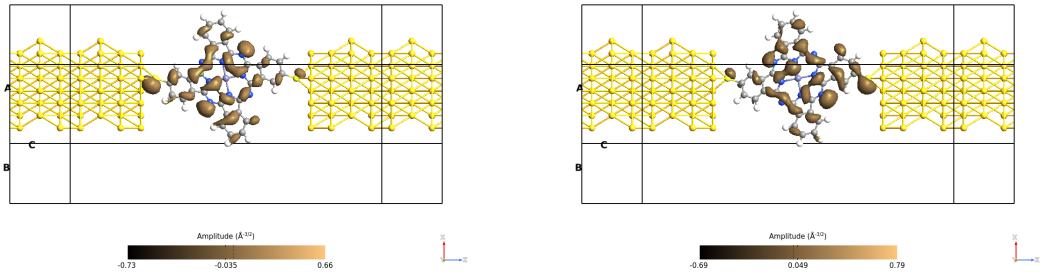

(a) logic '0'. (b) logic '1'.

Figure 6.154: Picture of the orbitals corresponding to the HOMO-1 level for the ZnPc molecule with long driver on the xz plane without the driver. The orbitals are taken with an isosurface value equal to 0.015.

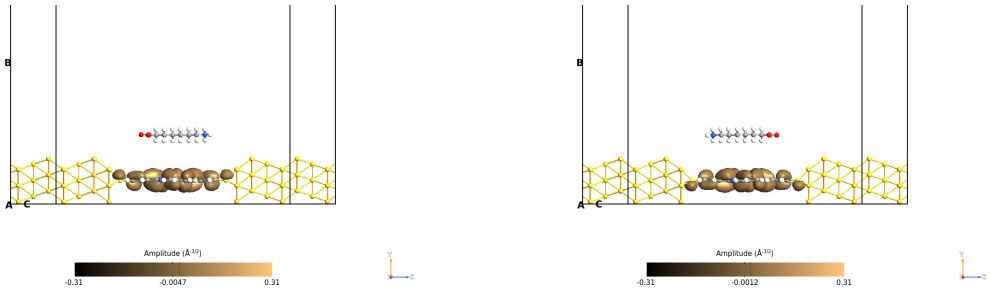

(a) logic '0'. (b) logic '1'.

Figure 6.155: Picture of the orbitals corresponding to the HOMO level for the ZnPc molecule with long driver on the yz plane. The orbitals are taken with an isosurface value equal to 0.015.

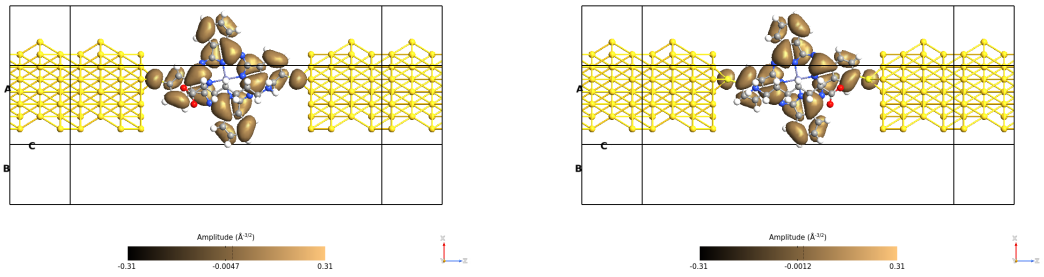

(a) logic '0'. (b) logic '1'.

Figure 6.156: Picture of the orbitals corresponding to the HOMO level for the ZnPc molecule with long driver on the xz plane with the driver. The orbitals are taken with an isosurface value equal to 0.015.

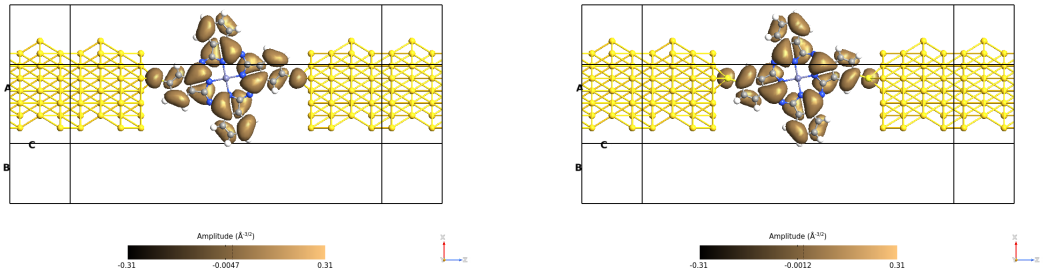

(a) logic '0'. (b) logic '1'.

Figure 6.157: Picture of the orbitals corresponding to the HOMO level for the ZnPc molecule with long driver on the xz plane without the driver. The orbitals are taken with an isosurface value equal to 0.015.

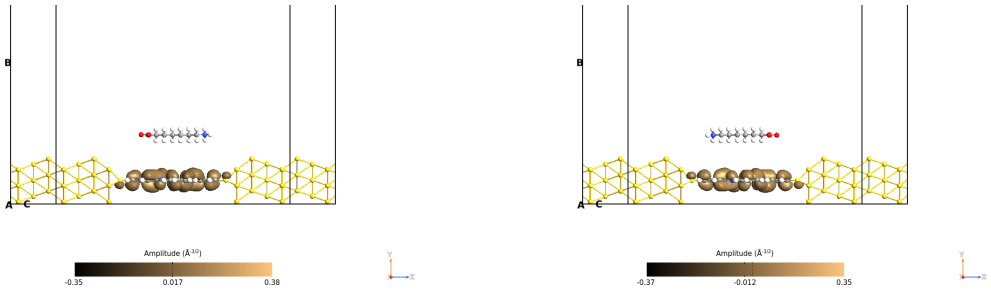

(a) logic '0'. (b) logic '1'.

Figure 6.158: Picture of the orbitals corresponding to the LUMO level for the ZnPc molecule with long driver on the yz plane. The orbitals are taken with an isosurface value equal to 0.015.

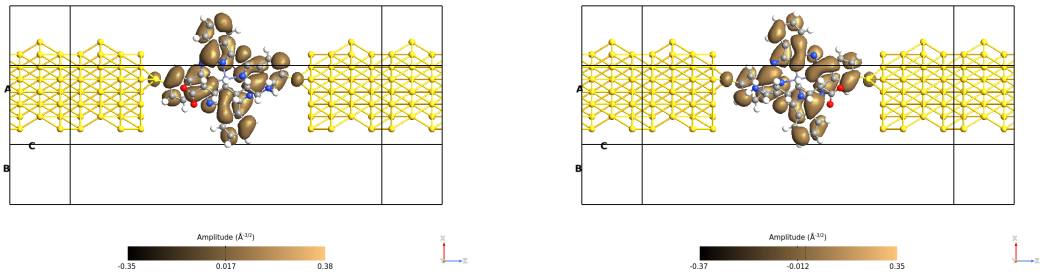

(a) logic '0'. (b) logic '1'.

Figure 6.159: Picture of the orbitals corresponding to the LUMO level for the ZnPc molecule with long driver on the xz plane with the driver. The orbitals are taken with an isosurface value equal to 0.015.

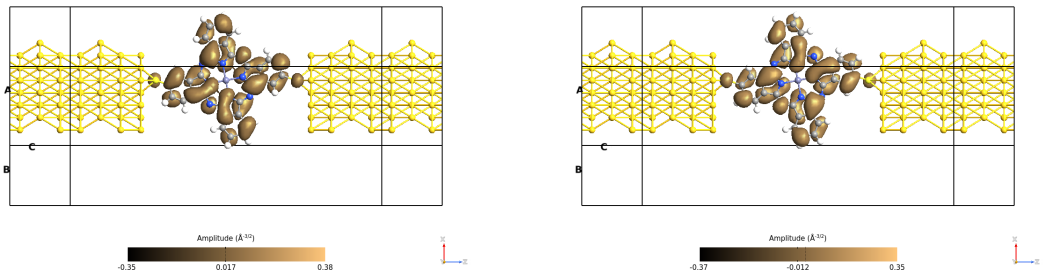

(a) logic '0'. (b) logic '1'.

Figure 6.160: Picture of the orbitals corresponding to the LUMO level for the ZnPc molecule with long driver on the xz plane without the driver. The orbitals are taken with an isosurface value equal to 0.015.

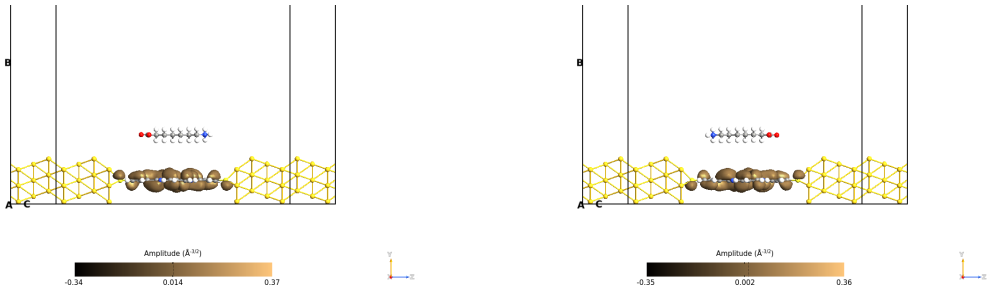

(a) logic '0'. (b) logic '1'.

Figure 6.161: Picture of the orbitals corresponding to the LUMO+1 level for the ZnPc molecule with long driver on the yz plane. The orbitals are taken with an isosurface value equal to 0.015.

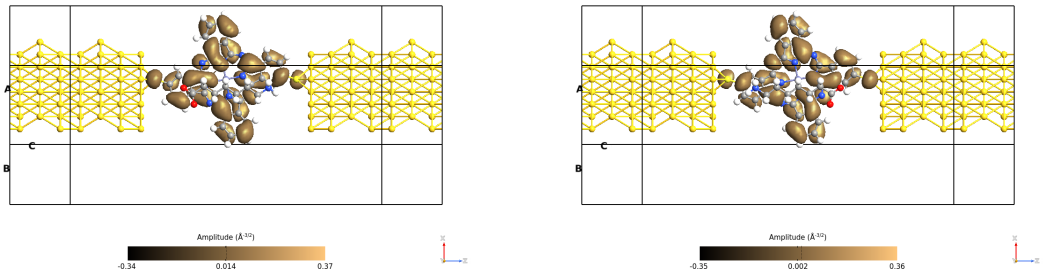

(a) logic '0'. (b) logic '1'.

Figure 6.162: Picture of the orbitals corresponding to the LUMO+1 level for the ZnPc molecule with long driver on the xz plane with the driver. The orbitals are taken with an isosurface value equal to 0.015.

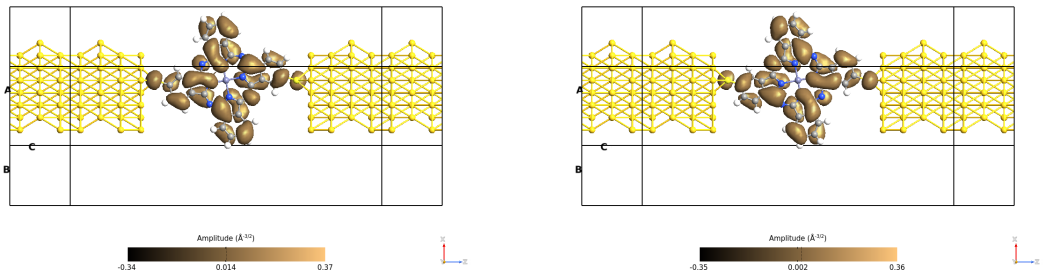

(a) logic '0'. (b) logic '1'.

Figure 6.163: Picture of the orbitals corresponding to the LUMO+1 level for the ZnPc molecule with long driver on the xz plane without the driver. The orbitals are taken with an isosurface value equal to 0.015.

6.5.4 Pathways

The transmission pathways reserve an important surprise, the zinc atom in the middle of the ZnPC doesn't help the conduction path, actually, it is an obstacle to the carriers. In the pictures, there are no arrows that pass through the molecule center, the only possible path is the larger one, thus the one that flows through the nitrogen atoms. The behavior is similar to the Pc one, the flow of carriers splits into two branches when it arrives near the center of the molecule, then it fuses together the two branches in the molecule's tail.

As before, it is possible to notice that increasing the energy, increases the electron flow in the orthogonal (to the conduction direction, which is the z-axis) branches.

Looking at the TS (figure 6.149) no significant differences are expected in the weight transmission pathways (figures 6.167, 6.168 and 6.169) because the amplitude of the peaks is the same, except for the 0.44 eV one that shows a little difference in terms of magnitude.

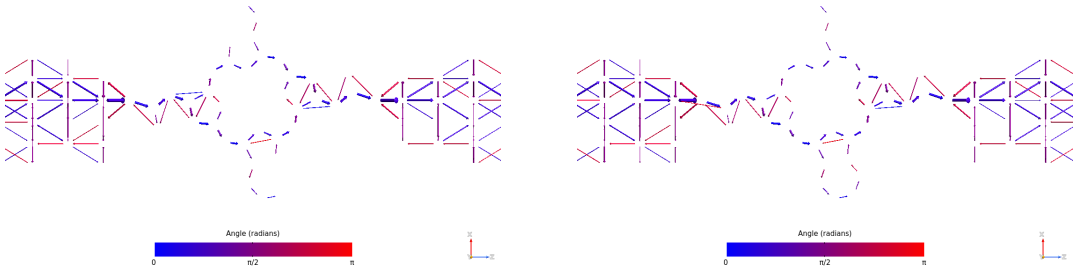

(a) logic '0'. (b) logic '1'.

Figure 6.164: Picture of the pathways corresponding to the energy 0.04 eV for the ZnPc with long driver on the xz plane. The blue arrows are in the same direction as the z-axis, while the red ones are in the opposite direction.

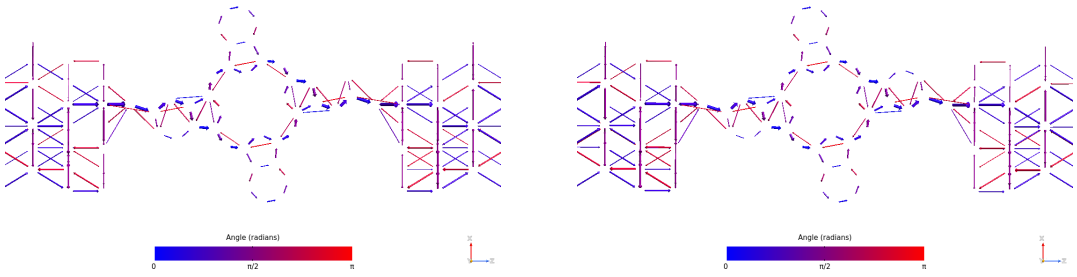

(a) logic '0'. (b) logic '1'.

Figure 6.165: Picture of the pathways corresponding to the energy 0.28 eV for the ZnPc with long driver on the xz plane. The blue arrows are in the same direction as the z-axis, while the red ones are in the opposite direction.

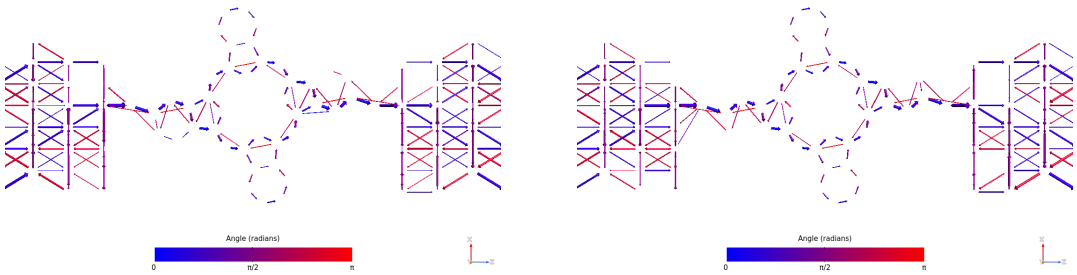

(a) logic '0'. (b) logic '1'.

Figure 6.166: Picture of the pathways corresponding to the energy 0.44 eV for the ZnPc with long driver on the xz plane. The blue arrows are in the same direction as the z-axis, while the red ones are in the opposite direction.

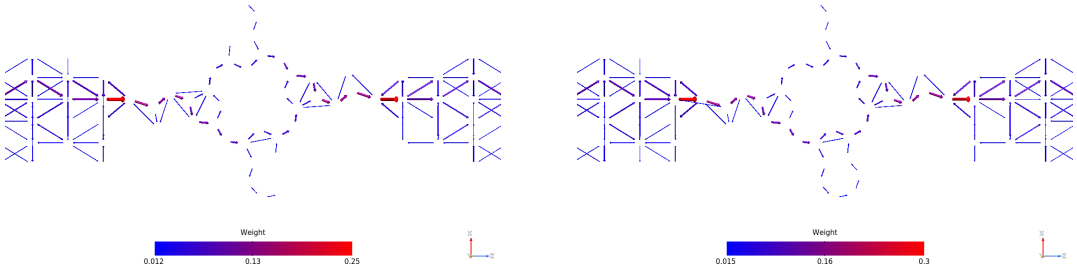

(a) logic '0'. (b) logic '1'.

Figure 6.167: Picture of the pathways corresponding to the energy 0.04 eV for the ZnPc molecule with long driver on the xz plane. The plots show the arrows' magnitude.

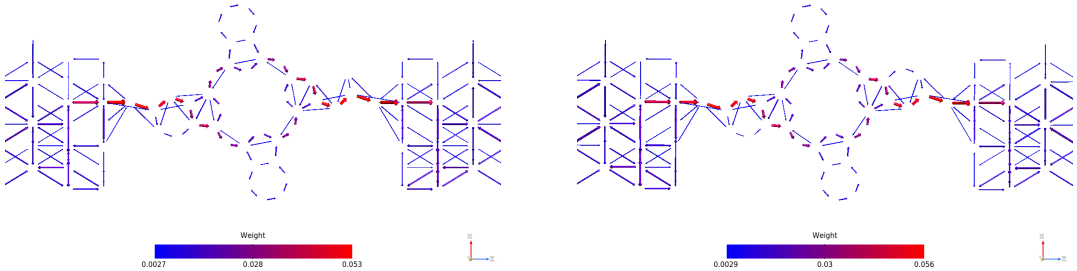

(a) logic '0'. (b) logic '1'.

Figure 6.168: Picture of the pathways corresponding to the energy 0.28 eV for the ZnPc molecule with long driver on the xz plane. The plots show the arrows' magnitude.

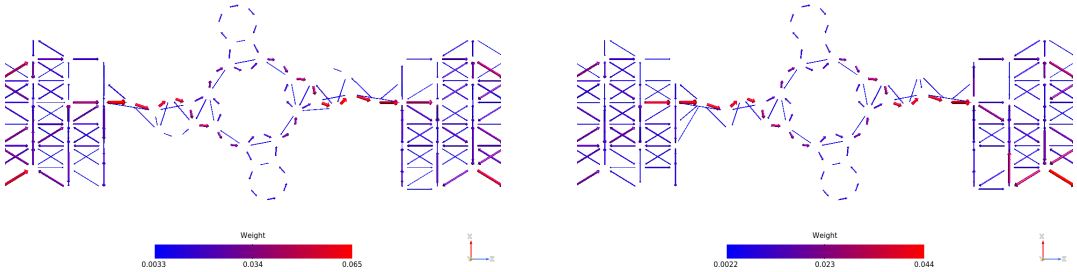

(a) logic '0'. (b) logic '1'.

Figure 6.169: Picture of the pathways corresponding to the energy 0.44 eV for the ZnPc molecule with long driver on the xz plane. The plots show the arrows' magnitude.

6.6 Zinc Phthalocyanine with thiol chains

The ZnPc with thiol chains works in low coupling conditions, therefore a low current is expected. The high polarizability value should provide to the system a high sensitivity to the logic configuration of the driver. A picture of the device in the simulation tool is reported in figure 6.170, where is possible to distinguish the junction molecule and the long driver, in particular the figure 6.170a refers to the logic '0' configuration while the figure 6.170b to the logic '1' one.

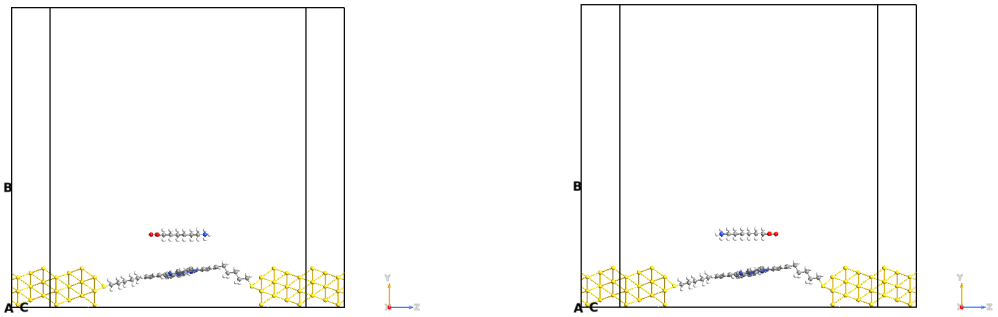

(a) logic '0' configuration. (b) logic '1' configuration.

Figure 6.170: Picture of the QuantumATK builder for the ZnPc molecule with thiol chains. The white atoms are the hydrogens, the yellow ones are gold atoms, the lighter yellow ones are the sulfurs, the blue ones are nitrogens, the reds are the oxygens, the grey atoms are carbons and the light grey one is the zinc.

6.6.1 TS

In figure 6.171 is reported the TS for the ZnPc with thiol chains molecular junction.

It was expected to a low values of transmission (due to the weak coupling) but they are smaller than we thought. This molecule seems not good as a readout system, because

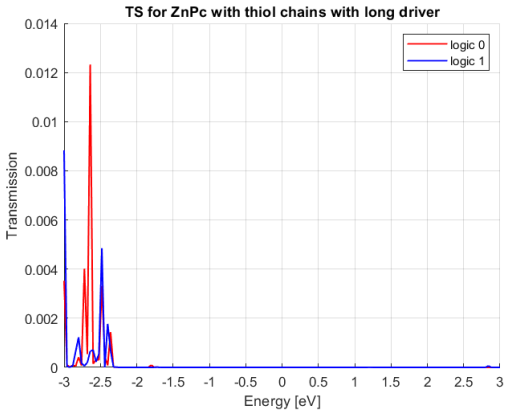

Figure 6.171: Picture of TS for the ZnPc with thiol chains molecule considering the long driver, the red curve represents the logic '0' configuration while the blue one the logic '1' configuration.

the HOMO peaks are distant from the origin of the energy axis and the LUMO ones don't even appear in the plot (they are beyond 3 eV).

6.6.2 IV

The IV plot (figure 6.172) confirms the feelings written in the section before, the current is extremely low in all the voltage ranges considered, and the only exception is close to -1 V in which the current is equal to few tens of nA.

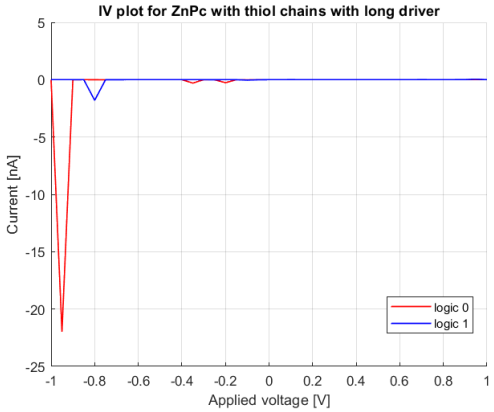

Figure 6.172: Picture of IV for the ZnPc with thiol chains molecule considering the long driver, the red curve represents the logic '0' configuration while the blue one the logic '1' configuration.

The figure 6.173 shows the current difference between logic '1' and logic '0' configurations. The plot tells us that the only detectable difference is close to -1 V, however, this difference is about 22 nA, well below the OPE3 and OPV3 ones. For the reasons

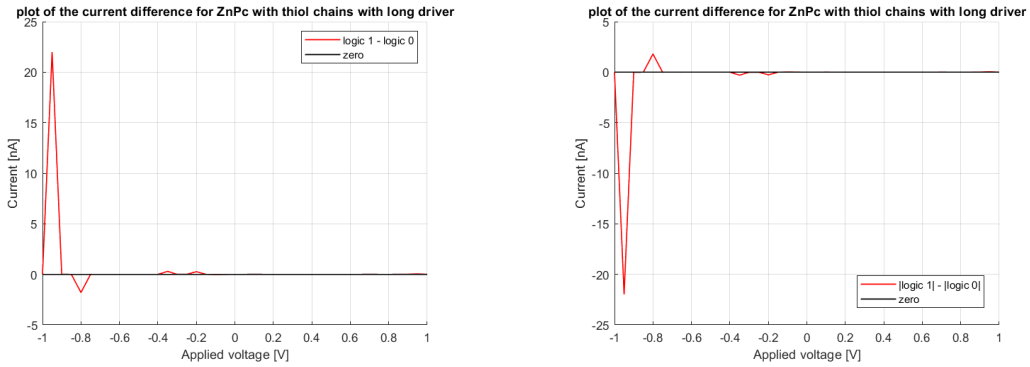

(a) logic '1' - logic '0'.

(b) |logic '1'| - |logic '0'|.

Figure 6.173: Picture of the current difference for the ZnPc with thiol chains molecule considering the long driver.

explained before the ZnPc with thiol chains in these conditions cannot be a good choice as a readout system.

6.6.3 Orbitals

The orbitals representation could be very interesting for seeing the influence of the electric field generated by the dipole moment of the driver on the junction molecule. For each energy level have been taken three different views corresponding to the yz plane, the xz plane with and without the driver (for a better and clearer understanding of the orbital shape). Below are reported the orbitals pictures for the HOMO-1 level (figures 6.174, 6.175 and 6.176), for the HOMO level (figures 6.177, 6.178 and 6.179), for the LUMO (figures 6.180, 6.181 and 6.182) and LUMO+1 (figures 6.183, 6.184 and 6.185). In general, it is possible to notice a dual behavior for the two configurations. In almost all the analyzed orbitals the two pictures seem to be the complementarity.

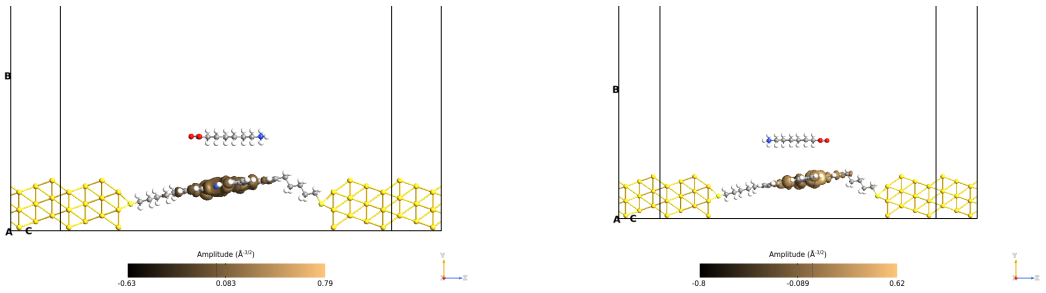

(a) logic '0'.

(b) logic '1'.

Figure 6.174: Picture of the orbitals corresponding to the HOMO-1 level for the ZnPc with thiol chains molecule with long driver on the yz plane. The orbitals are taken with an isosurface value equal to 0.015.

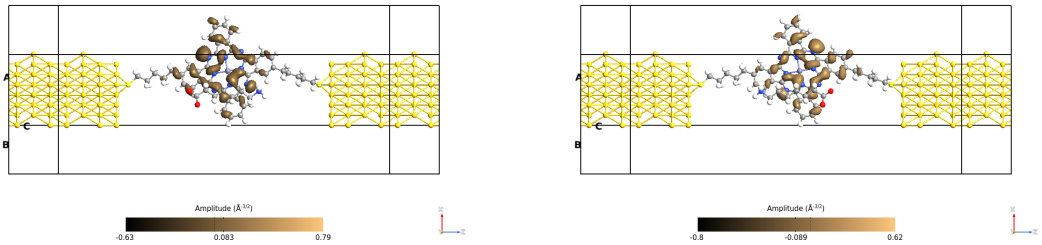

(a) logic '0'. (b) logic '1'.

Figure 6.175: Picture of the orbitals corresponding to the HOMO-1 level for the ZnPc with thiol chains molecule with long driver on the xz plane with the driver. The orbitals are taken with an isosurface value equal to 0.015.

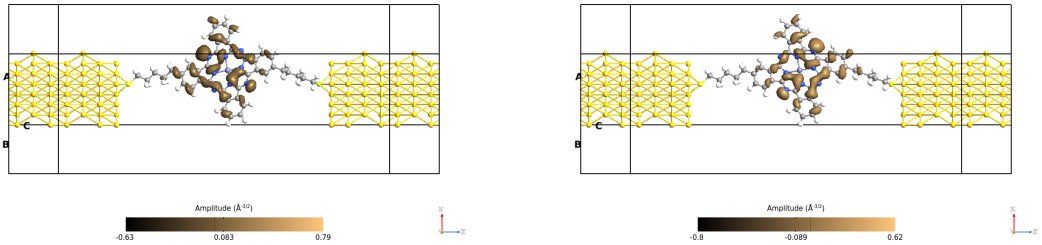

(a) logic '0'. (b) logic '1'.

Figure 6.176: Picture of the orbitals corresponding to the HOMO-1 level for the ZnPc with thiol chains molecule with long driver on the xz plane. The orbitals are taken with an isosurface value equal to 0.015.

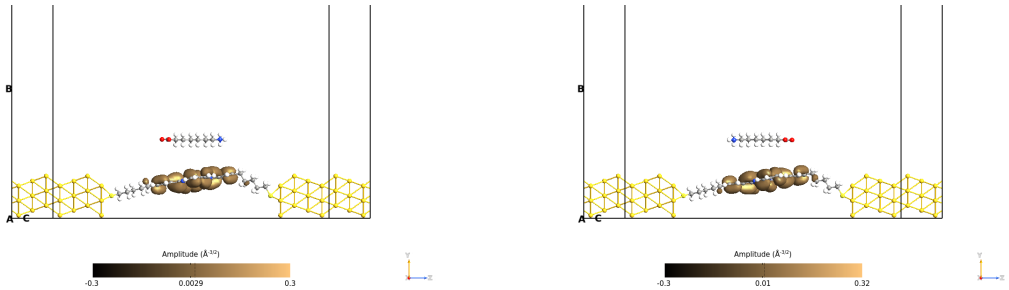

(a) logic '0'. (b) logic '1'.

Figure 6.177: Picture of the orbitals corresponding to the HOMO level for the ZnPc with thiol chains molecule with long driver on the yz plane. The orbitals are taken with an isosurface value equal to 0.015.

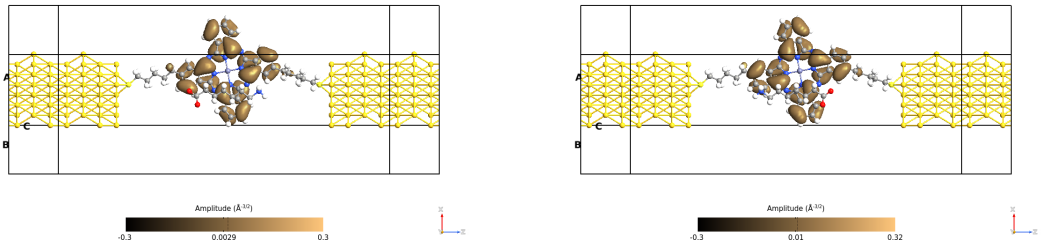

(a) logic '0'. (b) logic '1'.

Figure 6.178: Picture of the orbitals corresponding to the HOMO level for the ZnPc with thiol chains molecule with long driver on the xz plane with the driver. The orbitals are taken with an isosurface value equal to 0.015.

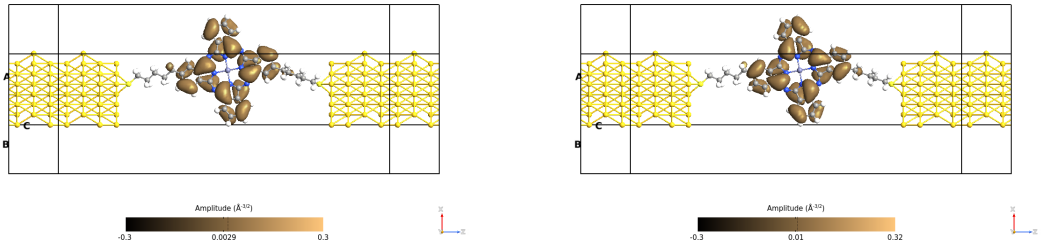

(a) logic '0'. (b) logic '1'.

Figure 6.179: Picture of the orbitals corresponding to the HOMO level for the ZnPc with thiol chains molecule with long driver on the xz plane. The orbitals are taken with an isosurface value equal to 0.015.

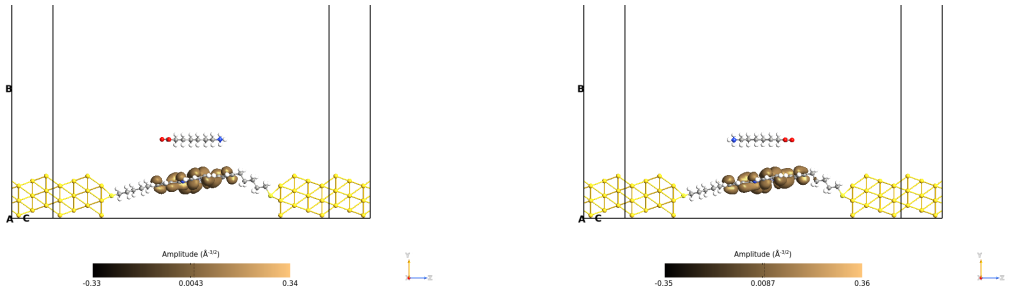

(a) logic '0'. (b) logic '1'.

Figure 6.180: Picture of the orbitals corresponding to the LUMO level for the ZnPc with thiol chains molecule with long driver on the yz plane. The orbitals are taken with an isosurface value equal to 0.015.

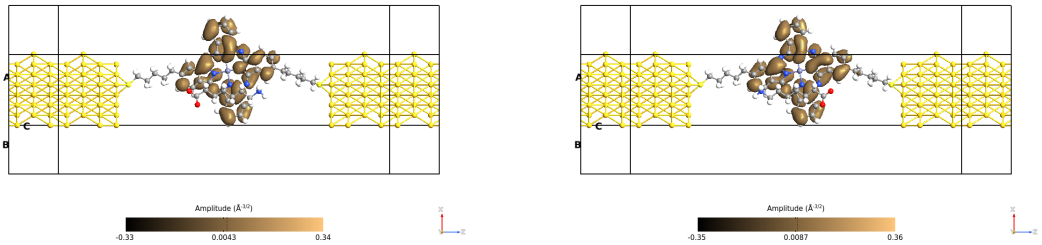

(a) logic '0'. (b) logic '1'.

Figure 6.181: Picture of the orbitals corresponding to the LUMO level for the ZnPc with thiol chains molecule with long driver on the xz plane with the driver. The orbitals are taken with an isosurface value equal to 0.015.

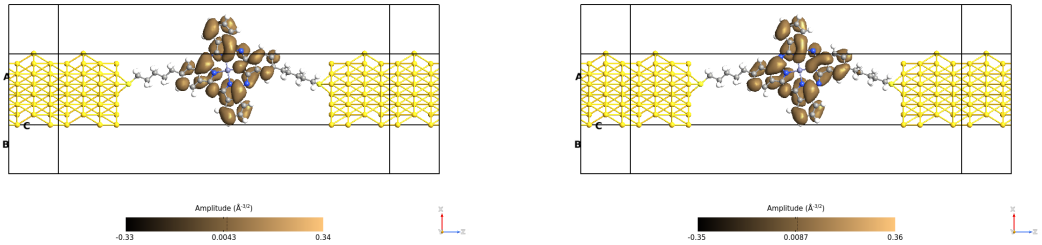

(a) logic '0'. (b) logic '1'.

Figure 6.182: Picture of the orbitals corresponding to the LUMO level for the ZnPc with thiol chains molecule with long driver on the xz plane. The orbitals are taken with an isosurface value equal to 0.015.

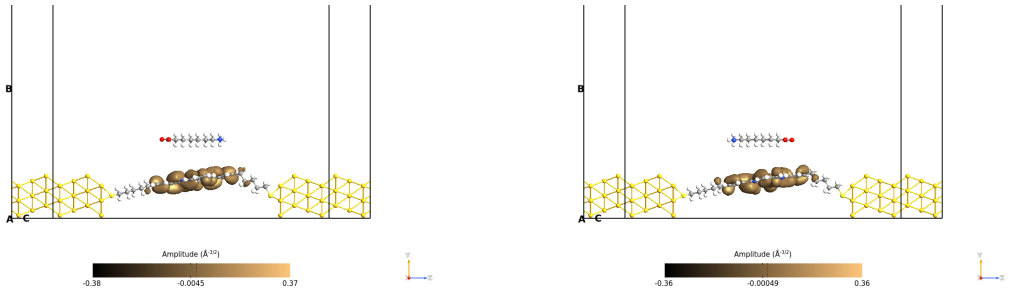

(a) logic '0'. (b) logic '1'.

Figure 6.183: Picture of the orbitals corresponding to the LUMO+1 level for the ZnPc with thiol chains molecule with long driver on the yz plane. The orbitals are taken with an isosurface value equal to 0.015.

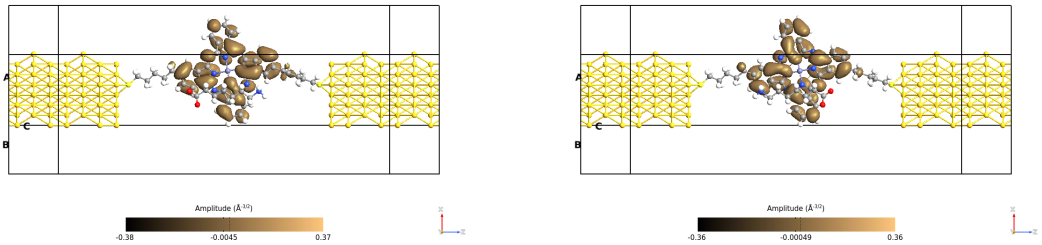

(a) logic '0'. (b) logic '1'.

Figure 6.184: Picture of the orbitals corresponding to the LUMO+1 level for the ZnPc with thiol chains molecule with long driver on the xz plane with the driver. The orbitals are taken with an isosurface value equal to 0.015.

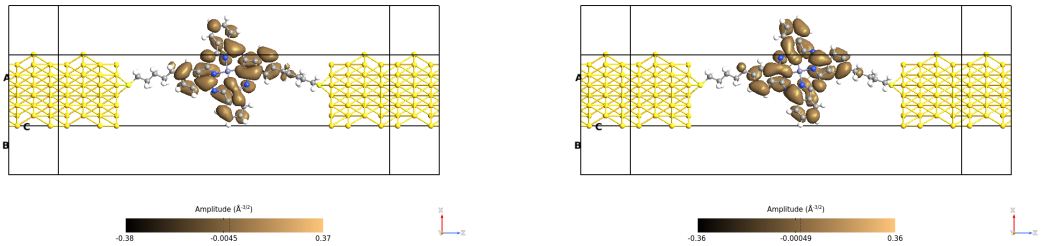

(a) logic '0'. (b) logic '1'.

Figure 6.185: Picture of the orbitals corresponding to the LUMO+1 level for the ZnPc with thiol chains molecule with long driver on the xz plane. The orbitals are taken with an isosurface value equal to 0.015.

6.6.4 Pathways

The pathways block allows us to see the conduction path. It is interesting to know where the electrons pass in order to analyze the effect of the driver on the conduction of the molecular junction. It has been selected 3 energies for the calculation of the pathways, and each of them was considered for a different aim.

The -0.5 eV has been chosen because it is in the bias window (for 1 V) and the TS at this point is extremely low. From the figures 6.186 and 6.189 is possible to derive that the two configurations in this point are very similar, as expected.

The figures 6.187 and 6.190 show the transmission pathways for the -2.48 eV of energy. In this point the TS (figure 6.171) has a higher value of the logic '1' configuration than the logic '0' one. The condition is well highlighted by the patways, the logic '0' picture (figure 6.187a) has not the thiol chains, while in the logic '1' (figure 6.187b) the chains are displayed. Another difference is related to the two sides corresponding to the z-direction of the ZnPc molecule, in both configurations the side close to the positive pole is less scattered (less red arrows) than the negative pole side. This last induces more problems

during the conduction path of the carriers.

The dual situation with respect to the -2.48 eV is the -2.64 eV in which the TS shows a higher value for the logic '0' configuration. The pathways corresponding to this energy are reported in the figures 6.188 and 6.191. In this case, all the considerations made before are reversed.

A difference with respect to the ZnPc molecule is the role of the zinc atom. In this case, it contributes to the conduction, it is possible to observe some arrows that interact with the molecule's center. The weight transmission pathways tell us that the zinc atom contribution is very low in terms of magnitude.

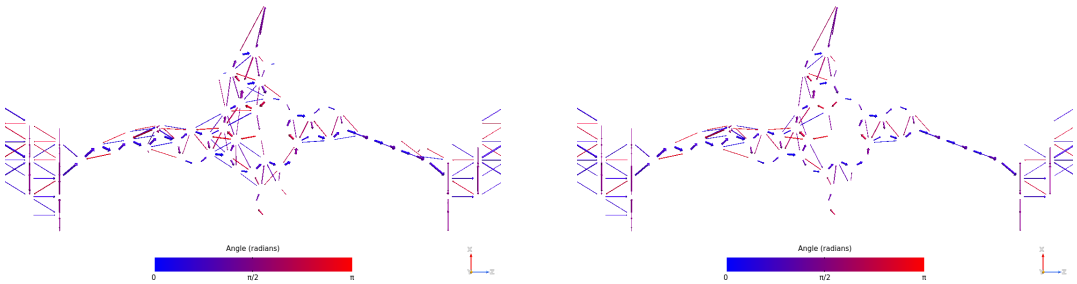

(a) logic '0'. (b) logic '1'.

Figure 6.186: Picture of the pathways corresponding to the energy -0.5 eV for the ZnPc with thiol chains molecule with long driver on the xz plane. The blue arrows are in the same direction of the z-axis, while the red ones are in the opposite direction.

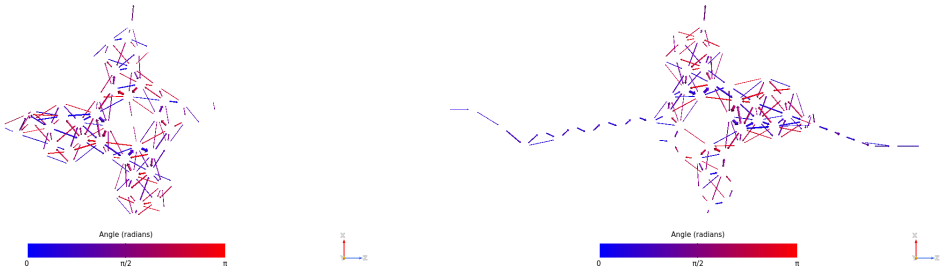

(a) logic '0'. (b) logic '1'.

Figure 6.187: Picture of the pathways corresponding to the energy -2.48 eV for the ZnPc with thiol chains molecule with long driver on the xz plane. The blue arrows are in the same direction of the z-axis, while the red ones are in the opposite direction.

(a) logic '0'. (b) logic '1'.

Figure 6.188: Picture of the pathways corresponding to the energy -2.64 eV for the ZnPc with thiol chains molecule with long driver on the xz plane. The blue arrows are in the same direction of the z-axis, while the red ones are in the opposite direction.

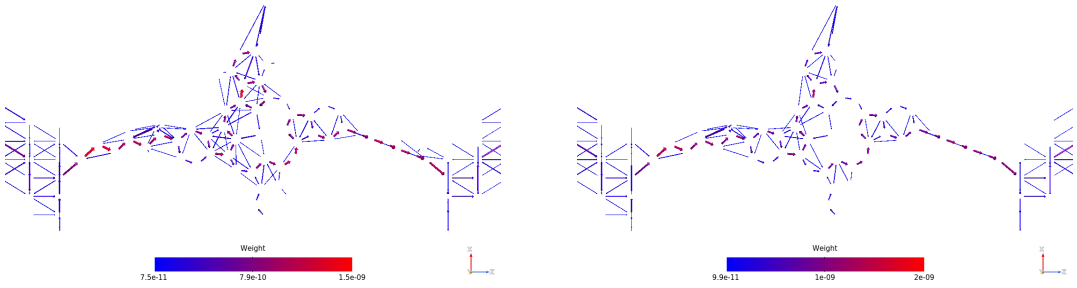

(a) logic '0'. (b) logic '1'.

Figure 6.189: Picture of the pathways corresponding to the energy -0.50 eV for the ZnPc with thiol chains molecule with long driver on the xz plane. The plots show the arrows magnitude.

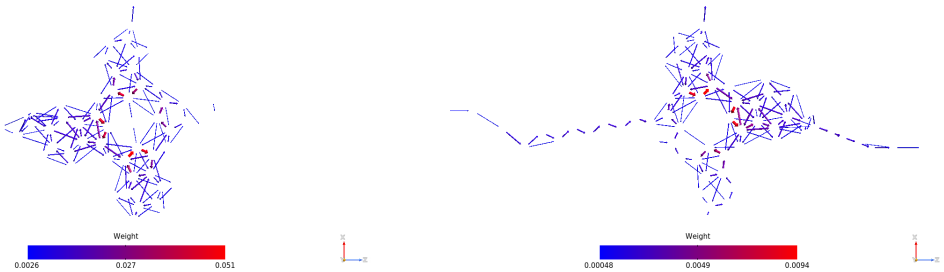

(a) logic '0'. (b) logic '1'.

Figure 6.190: Picture of the pathways corresponding to the energy -2.48 eV for the ZnPc with thiol chains molecule with long driver on the xz plane. The plots show the arrows magnitude.

(a) logic '0'.

(b) logic '1'.

Figure 6.191: Picture of the pathways corresponding to the energy -2.64 eV for the ZnPc with thiol chains molecule with long driver on the xz plane. The plots show the arrows magnitude.

6.7 4-Aminobenzoic acid

The 4-Aminobenzoic acid has been selected for its dipole moment and its geometrical shape. It is a benzene with a nitrogen and two oxygens which provide the polar behavior to the molecule. A picture of the device in the simulation tool is reported in the figure 6.192, where is possible to distinguish the junction molecule and the long driver, in particular the figure 6.192a refers to the logic '0' configuration while the figure 6.192b to the logic '1' one. The driver is placed at a distance of 7 Å to the junction, a reasonable value for today's technology.

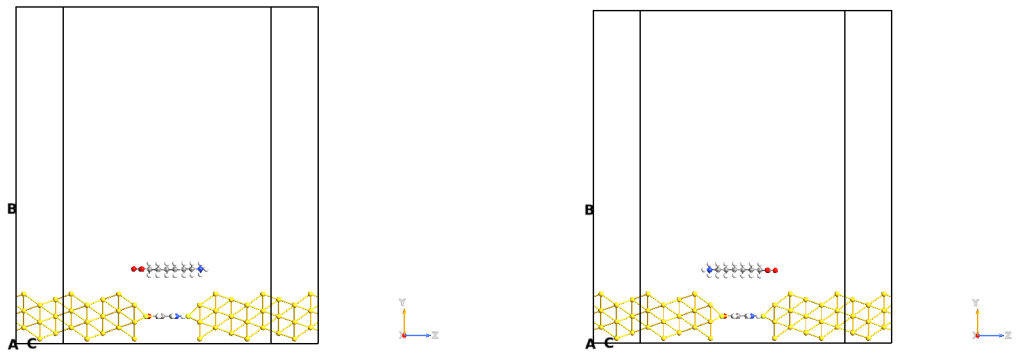

(a) logic '0' configuration.

(b) logic '1' configuration.

Figure 6.192: Picture of the QuantumATK builder for the 4-Aminobenzoic acid molecule. The white atoms are the hydrogens, the yellow ones are gold atoms, the lighter yellow ones are the sulphurs, the blue ones are nitrogens, the reds are the oxygens and the grey atoms are carbons.

The molecule is not currently used inside molecular junctions, but its similarity with benzene should help synthesis. If the results are satisfactory an accurate analysis of the molecule could be done.

6.7.1 TS

The TS in the figure 6.193 shows good conductivity properties for the 4-Aminobenzoic acid molecule. The reasons are linked to the position of the LUMO peaks, close to the energy axis' origin, while the HOMOs are more distant but the shape between LUMOs and HOMOs is not completely flat, it has some hills which provide some current; therefore the conduction in LUMO type. The expected current is not the same as OPE3 and OPV3, but the current should be greater than the ZnPc with thiol chains molecule.

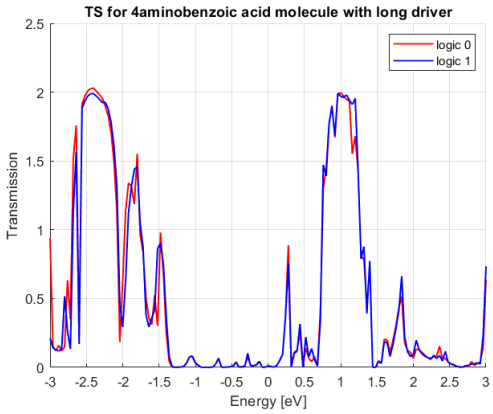

Figure 6.193: Picture of TS for the 4-Aminobenzoic acid molecule considering the long driver, the red curve represents the logic '0' configuration while the blue one the logic '1' configuration.

6.7.2 IV

The IV plot (figure 6.194) exhibits a different behavior for the two configurations, this phenomenon allows us to distinguish the two logic values. As expected the amount of current that the molecule can drive is not as high as OPE3 and OPV3, but it is also not bad (few μA).

The current difference plot (figure 6.195) highlights the feasibility of a readout system with a 4-Aminobenzoic acid molecular junction because near 0.35 V the current difference is beyond 1 μA. This configuration works worse than the OPV3 and OPE3 ones, but better than the ZnPc with thiol chains one. Near 1 V the 4-Aminobenzoic acid current difference plot has a peak of about 3 μA.

6.7.3 Orbitals

On the orbital view is possible to observe the influence of the dipole moment of the driver affecting the polar molecule in the junction. In the pictures below report the yz plane, xz plane with driver and xz plane without driver for each energy level selected. In particular the HOMO-1 levels is in the figures 6.196, 6.197 and 6.198; the HOMO one in the figures 6.199, 6.200 and 6.201; the LUMO one in the figures 6.202, 6.203 and 6.204; the LUMO+1 level in the figures 6.205, 6.206 and 6.207.

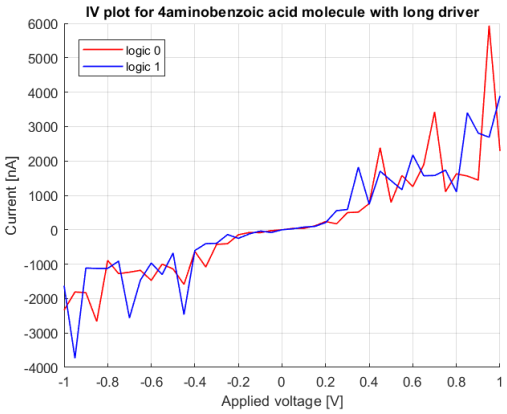

Figure 6.194: Picture of TS for the 4-Aminobenzoic acid molecule considering the long driver, the red curve represents the logic '0' configuration while the blue one the logic '1' configuration.

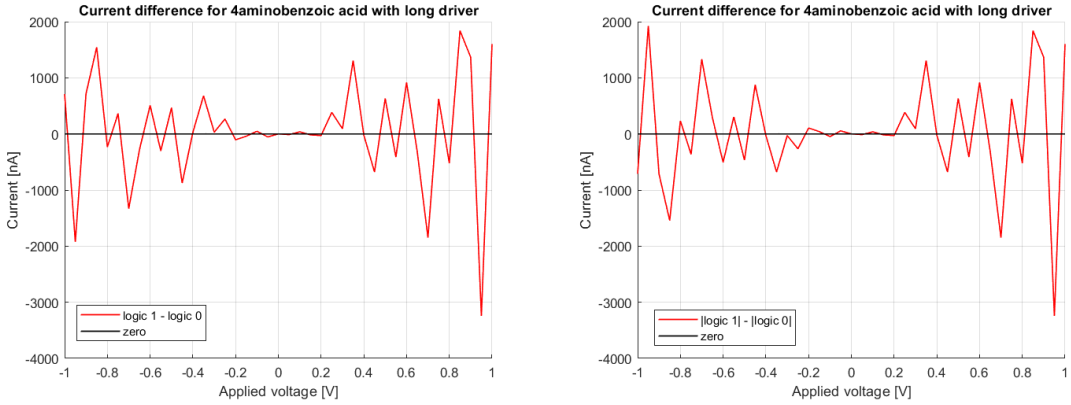

(a) logic 1 - logic 0.

(b) |logic 1| - |logic 0|.

Figure 6.195: Picture of current difference for the Ethyl4-(benzyl-methylamino) benzoate molecule considering the long driver.

For the HOMO-1 and HOMO levels the behavior is not the complementary one, the polar nature of the 4-Aminobenzoic acid influence itself the orbitals geometry.

The LUMO and LUMO+1, instead, show a complementary behavior, the driver influence is strong enough to deeply modify the orbitals' shape.

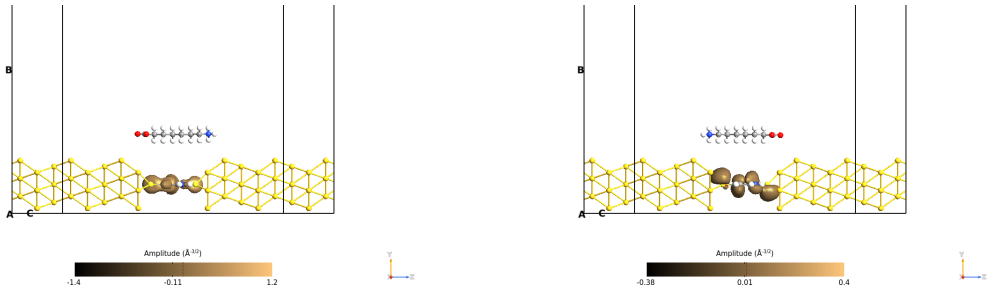

(a) logic '0'. (b) logic '1'.

Figure 6.196: Picture of the orbitals corresponding to the HOMO-1 level for the 4-Aminobenzoic acid molecule with long driver on the yz plane. The orbitals are taken with an isosurface value equal to 0.015.

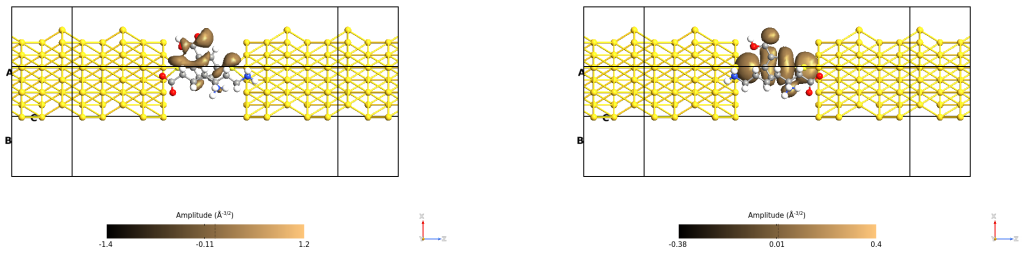

(a) logic '0'. (b) logic '1'.

Figure 6.197: Picture of the orbitals corresponding to the HOMO-1 level for the 4-Aminobenzoic acid molecule with long driver on the xz plane with the driver. The orbitals are taken with an isosurface value equal to 0.015.

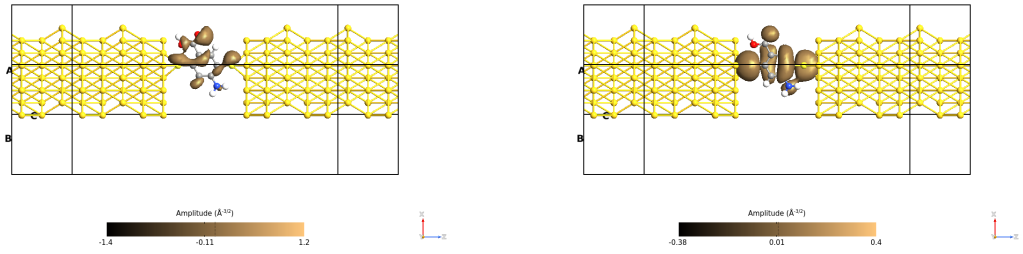

(a) logic '0'. (b) logic '1'.

Figure 6.198: Picture of the orbitals corresponding to the HOMO-1 level for the 4-Aminobenzoic acid molecule with long driver on the xz plane. The orbitals are taken with an isosurface value equal to 0.015.

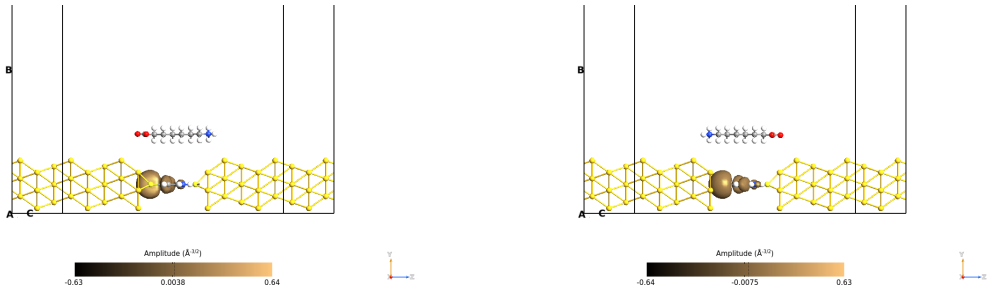

(a) logic '0'. (b) logic '1'.

Figure 6.199: Picture of the orbitals corresponding to the HOMO level for the 4-Aminobenzoic acid molecule with long driver on the yz plane. The orbitals are taken with an isosurface value equal to 0.015.

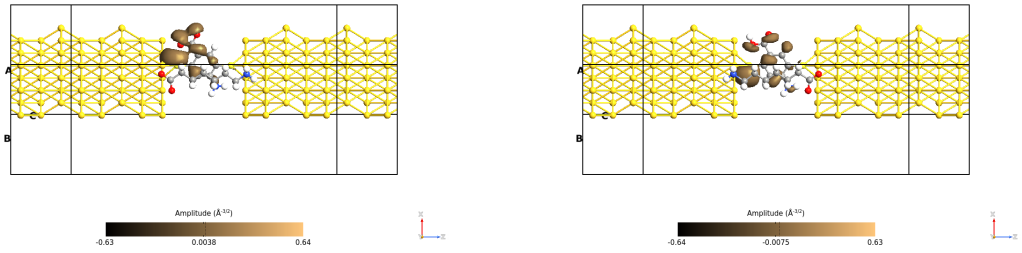

(a) logic '0'. (b) logic '1'.

Figure 6.200: Picture of the orbitals corresponding to the HOMO level for the 4-Aminobenzoic acid molecule with long driver on the xz plane with the driver. The orbitals are taken with an isosurface value equal to 0.015.

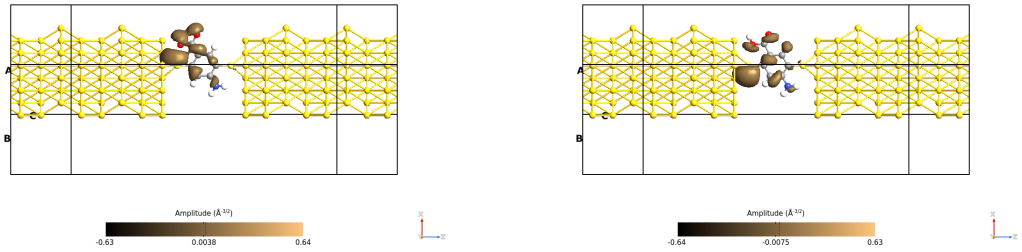

(a) logic '0'. (b) logic '1'.

Figure 6.201: Picture of the orbitals corresponding to the HOMO level for the 4-Aminobenzoic acid molecule with long driver on the xz plane. The orbitals are taken with an isosurface value equal to 0.015.

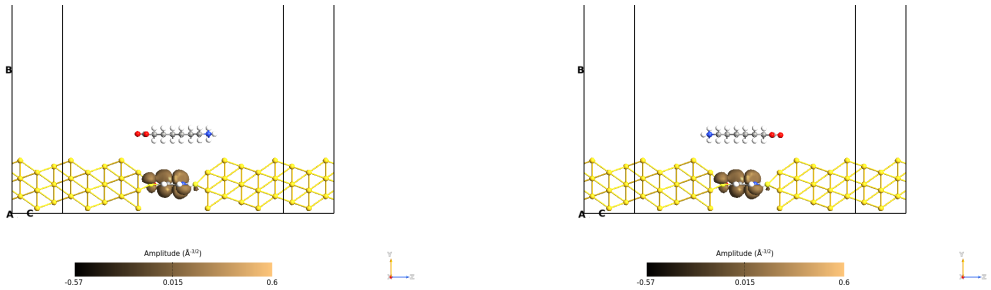

(a) logic '0'. (b) logic '1'.

Figure 6.202: Picture of the orbitals corresponding to the LUMO level for the 4-Aminobenzoic acid molecule with long driver on the yz plane. The orbitals are taken with an isosurface value equal to 0.015.

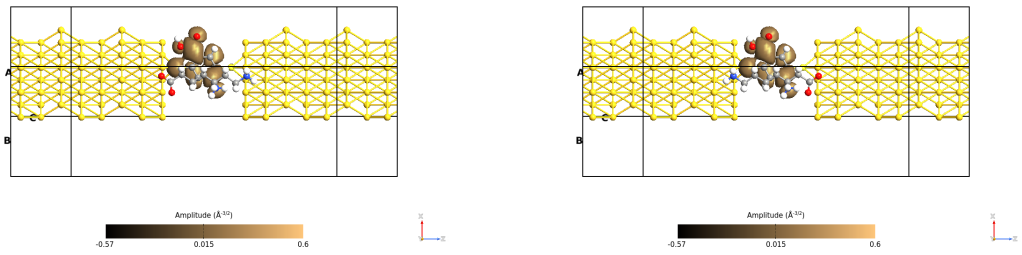

(a) logic '0'. (b) logic '1'.

Figure 6.203: Picture of the orbitals corresponding to the LUMO level for the 4-Aminobenzoic acid molecule with long driver on the xz plane with the driver. The orbitals are taken with an isosurface value equal to 0.015.

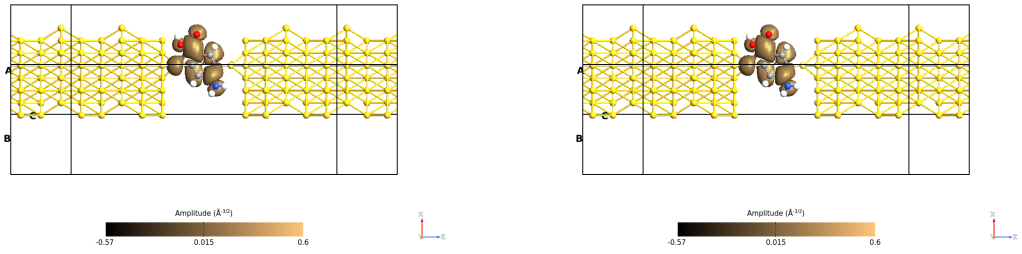

(a) logic '0'. (b) logic '1'.

Figure 6.204: Picture of the orbitals corresponding to the LUMO level for the 4-Aminobenzoic acid molecule with long driver on the xz plane. The orbitals are taken with an isosurface value equal to 0.015.

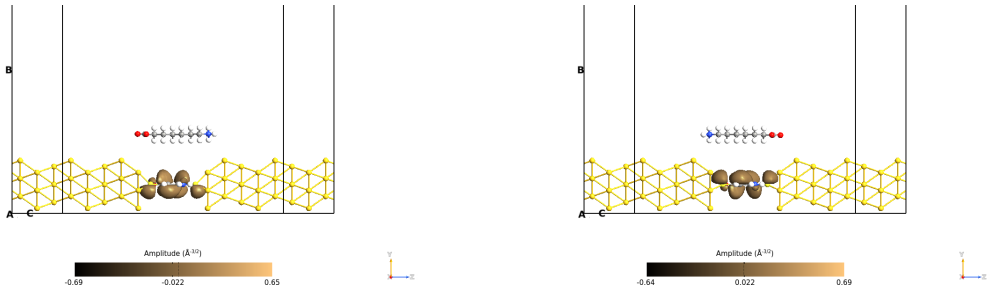

(a) logic '0'. (b) logic '1'.

Figure 6.205: Picture of the orbitals corresponding to the LUMO+1 level for the 4-Aminobenzoic acid molecule with long driver on the yz plane. The orbitals are taken with an isosurface value equal to 0.015.

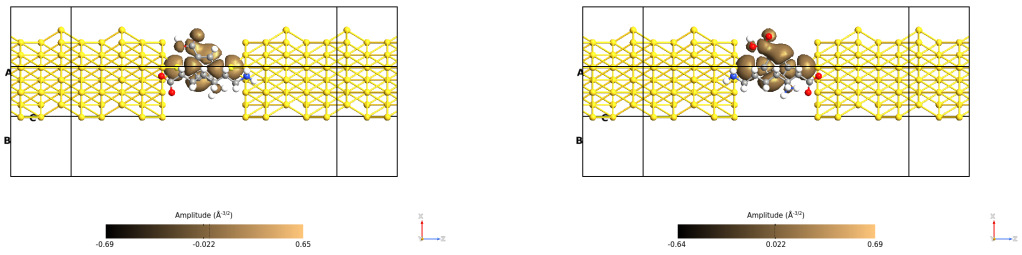

(a) logic '0'. (b) logic '1'.

Figure 6.206: Picture of the orbitals corresponding to the LUMO+1 level for the 4-Aminobenzoic acid molecule with long driver on the xz plane with the driver. The orbitals are taken with an isosurface value equal to 0.015.

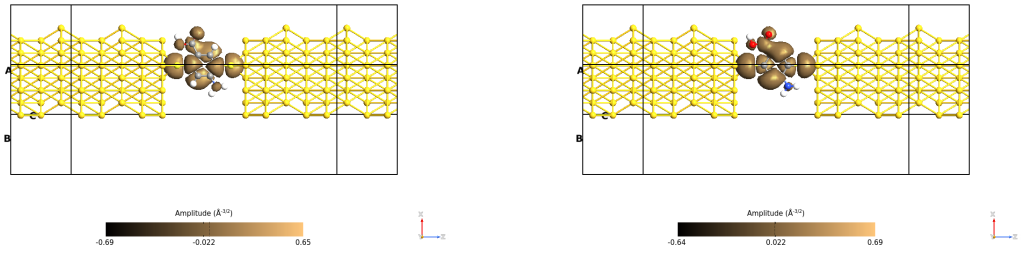

(a) logic '0'. (b) logic '1'.

Figure 6.207: Picture of the orbitals corresponding to the LUMO+1 level for the 4-Aminobenzoic acid molecule with long driver on the xz plane. The orbitals are taken with an isosurface value equal to 0.015.

6.7.4 Pathways

For the conduction pathways have been chosen three different energies; 0.28 eV because it corresponds to the first peak in the TS (figure 6.193), 0.44 eV because it is the second peak in the TS (very small) and 0.76 eV because it is placed on the first small peak of the wider mountain centered at 1 eV.

The pictures don't exhibit completely different behaviors, they are very close in any of the three energies considered.

An interesting result can be noticed in the 0.76 eV plots (figures 6.210 and 6.213) in which the conduction path in the benzene is coherent with the conduction direction in the bottom part of the benzene ring, while in the other cases (figures 6.208, 6.211, 6.209 and 6.212) it is coherent in the upper part of the ring.

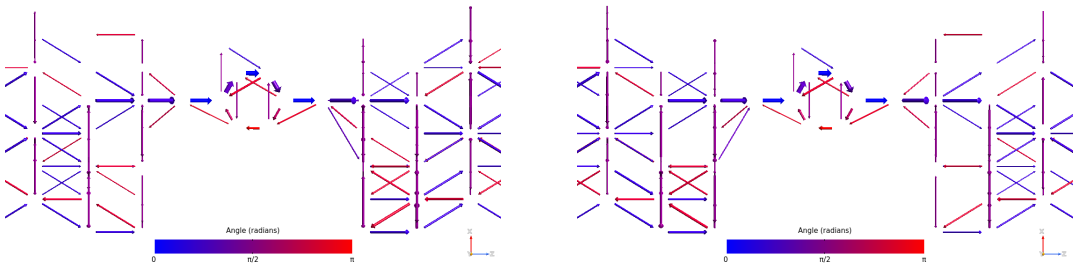

(a) logic '0'. (b) logic '1'.

Figure 6.208: Picture of the pathways corresponding to the energy 0.28 eV for the 4-Aminobenzoic acid molecule with long driver on the xz plane. The blue arrows are in the same direction as the z-axis, while the red ones are in the opposite direction.

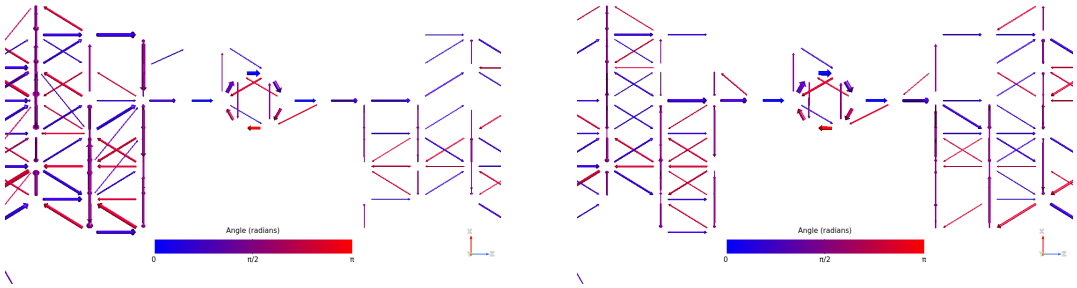

(a) logic '0'. (b) logic '1'.

Figure 6.209: Picture of the pathways corresponding to the energy 0.44 eV for the 4-Aminobenzoic acid molecule with long driver on the xz plane. The blue arrows are in the same direction as the z-axis, while the red ones are in the opposite direction.

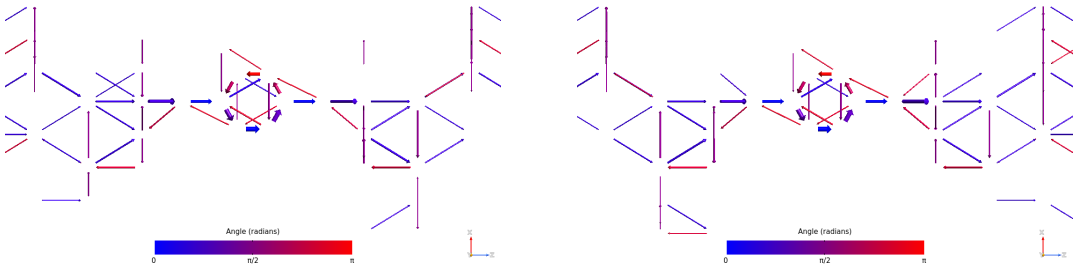

(a) logic '0'. (b) logic '1'.

Figure 6.210: Picture of the pathways corresponding to the energy 0.76 eV for the 4-Aminobenzoic acid molecule with long driver on the xz plane. The blue arrows are in the same direction as the z-axis, while the red ones are in the opposite direction.

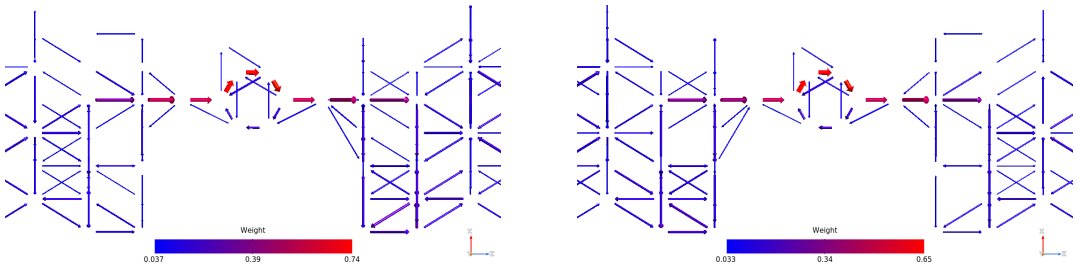

(a) logic '0'. (b) logic '1'.

Figure 6.211: Picture of the pathways corresponding to the energy 0.28 eV for the 4-Aminobenzoic acid molecule with long driver on the xz plane. The plots show the arrows' magnitude.

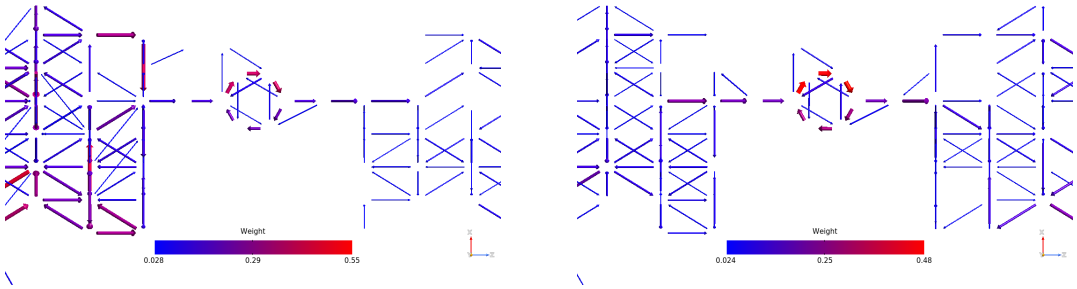

(a) logic '0'. (b) logic '1'.

Figure 6.212: Picture of the pathways corresponding to the energy 0.44 eV for the 4-Aminobenzoic acid molecule with long driver on the xz plane. The plots show the arrows' magnitude.

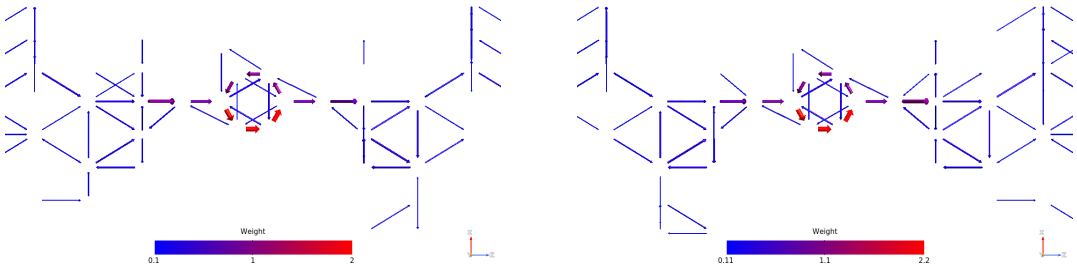

(a) logic '0'. (b) logic '1'.

Figure 6.213: Picture of the pathways corresponding to the energy 0.76 eV for the 4-Aminobenzoic acid molecule with long driver on the xz plane. The plots show the arrows' magnitude.

6.8 Ethyl4-(benzyl-methylamino)benzoate

The Ethyl4-(benzyl-methylamino) benzoate is not a common molecule used for MT applications, but it has been studied for its properties. The dipole moment is quite important and the molecule geometry is strongly not symmetric, thus can induce different behavior when subjected to different electric fields.

The QuantumATK builders are reported in the figure 6.214, in which is possible to observe the not flatness of the junction molecule. This phenomenon can cause a low current.

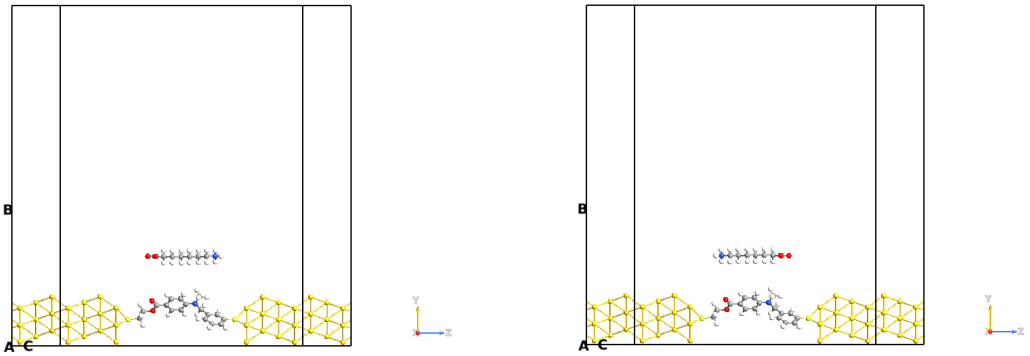

(a) logic '0' configuration. (b) logic '1' configuration.

Figure 6.214: Picture of the QuantumATK builder for the Ethyl4-(benzyl-methylamino) benzoate molecule. The white atoms are the hydrogens, the yellow ones are gold atoms, the lighter yellow ones are the sulfurs, the blue ones are nitrogens, the reds are the oxygens and the grey atoms are carbons.

6.8.1 TS

The TS is plotted in the figure 6.215. The molecule doesn't show good conduction properties, because the HOMO peak is at low energies (below 2 eV) and the LUMO peak is beyond the 3 eV (not present in the TS). For these reasons, the expected current is very low.

However, the TS shows an ON/OFF behavior, for an ON/OFF behavior I mean a plot in which there is at least one transmission peak in which the TS of the other logic configuration is practically zero. For example, the before-explained situation can be noticed at -2.5 eV, in which the logic '1' transmission is higher than 0.4 while the logic '0' one is lower than 0.05; at -2.75 eV it is possible to observe the dual case.

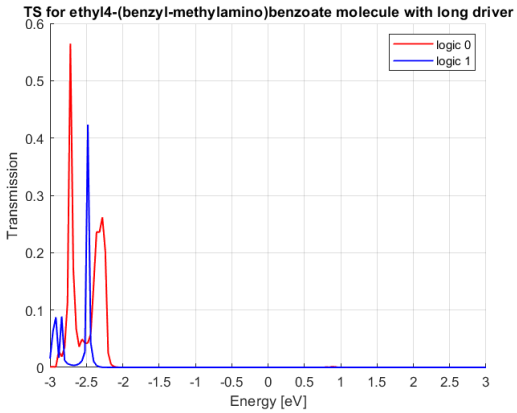

Figure 6.215: Picture of TS for the Ethyl4-(benzyl-methylamino) benzoate molecule considering the long driver, the red curve represents the logic '0' configuration while the blue one the logic '1' configuration.

6.8.2 IV

In figure 6.216 is possible to see the IV plot of the Ethyl4-(benzyl-methylamino) benzoate. As expected, the current is very low (tenths of nA, hence hundreds of pA). In the central region (form -0.8 V to 0.8 V) the current is practically zero, while in the extremes of the set is possible to catch the difference between the two configurations. Another problem is related to the high voltages which can detect the difference because it is about 1 V, this potential can influence the clock signal of the molFCN.

Figure 6.217 shows the current difference between the two configurations for the Ethyl4-(benzyl-methylamino) benzoate molecule. The limits highlighted in the previous section can be seen more easily with these plots. The figure 6.217a tells us that the difference between logic '1' and logic '0' is very low, in the orders of pA, it is difficult but not impossible to sense it. The figure 6.217b is plotted considering the absolute values of the current (it is the same as the figure 6.217a for positive potentials).

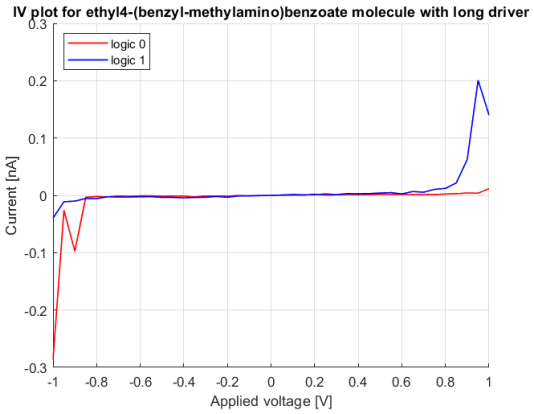

Figure 6.216: Picture of IV for the Ethyl4-(benzyl-methylamino) benzoate molecule considering the long driver, the red curve represents the logic '0' configuration while the blue one the logic '1' configuration.

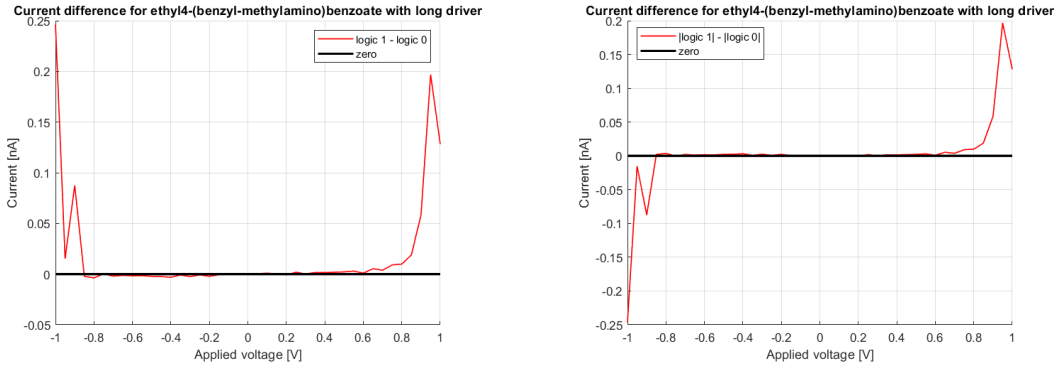

(a) logic 1 - logic 0.

(b) |logic 1| - |logic 0|.

Figure 6.217: Picture of current difference for the Ethyl4-(benzyl-methylamino) benzoate molecule considering the long driver.

6.8.3 Orbitals

The orbitals views of the Ethyl4-(benzyl-methylamino) benzoate are very interesting because they show different shape between the two configurations. The HOMO-1 (figures 6.218, 6.219 and 6.220), the LUMO (figures 6.224, 6.225 and 6.226) and LUMO+1 (figures 6.227, 6.228 and 6.229) views point out the driver influence on the junction molecular. The HOMO orbitals (figures 6.221, 6.222 and 6.223), instead, are practically the same for the two different logic values. The shape of the logic '1' plot retraces the same geometry of the logic '0' ones, but it is possible to notice that the dimension of the orbitals are slightly different, this behavior is possible to notice on the sulfur atom close to the left electrode. In general, the intrinsic asymmetry of the Ethyl4-(benzyl-methylamino) benzoate provides different interaction between the different driver configurations, the orbitals shape is one of the proof of the readout system feasability.

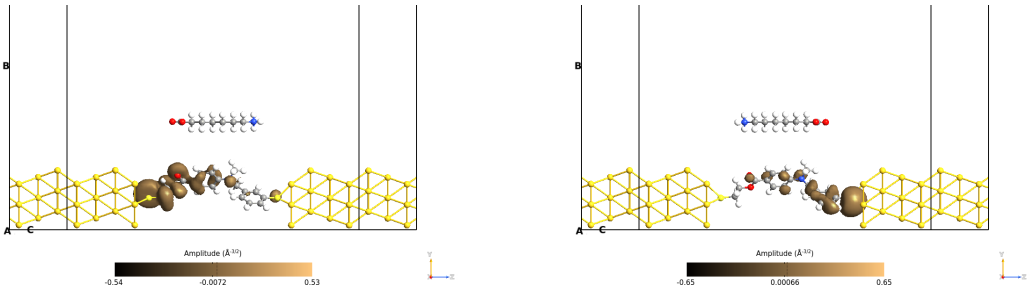

(a) logic '0'. (b) logic '1'.

Figure 6.218: Picture of the orbitals corresponding to the HOMO-1 level for the Ethyl4-(benzyl-methylamino) benzoate molecule with long driver on the yz plane. The orbitals are taken with an isosurface value equal to 0.015.

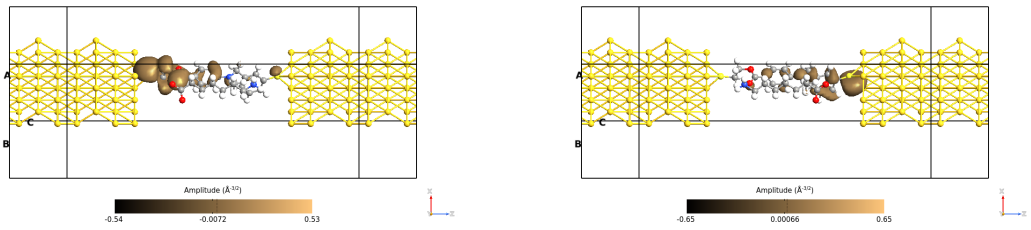

(a) logic '0'. (b) logic '1'.

Figure 6.219: Picture of the orbitals corresponding to the HOMO-1 level for the Ethyl4-(benzyl-methylamino) benzoate molecule with long driver on the xz plane with the driver. The orbitals are taken with an isosurface value equal to 0.015.

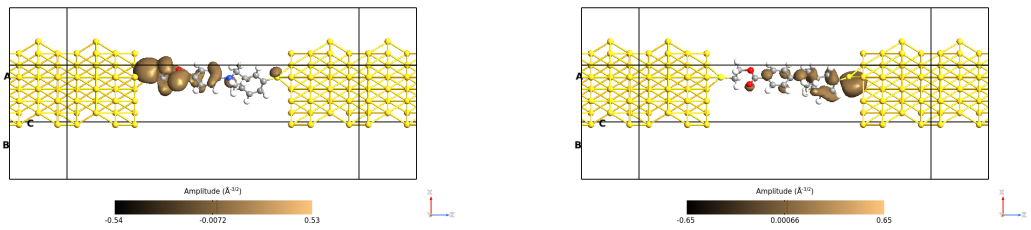

(a) logic '0'. (b) logic '1'.

Figure 6.220: Picture of the orbitals corresponding to the HOMO-1 level for the Ethyl4-(benzyl-methylamino) benzoate molecule with long driver on the xz plane. The orbitals are taken with an isosurface value equal to 0.015.

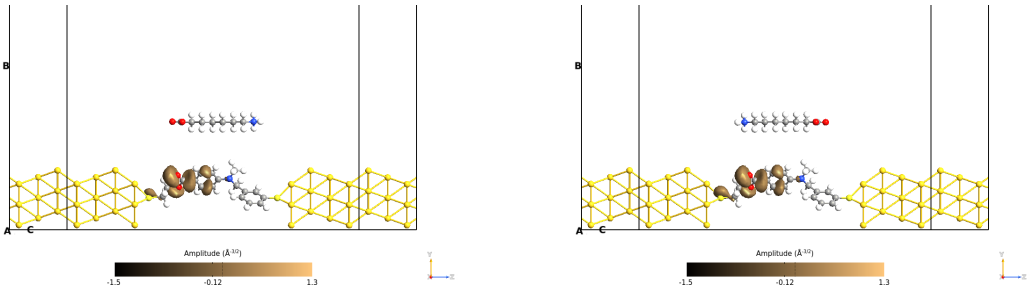

(a) logic '0'. (b) logic '1'.

Figure 6.221: Picture of the orbitals corresponding to the HOMO level for the Ethyl4-(benzyl-methylamino) benzoate molecule with long driver on the yz plane. The orbitals are taken with an isosurface value equal to 0.015.

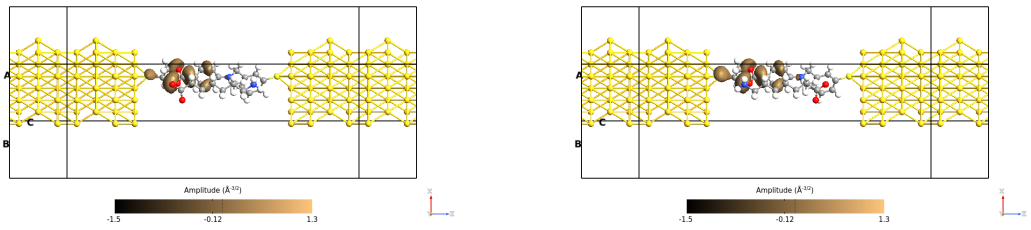

(a) logic '0'. (b) logic '1'.

Figure 6.222: Picture of the orbitals corresponding to the HOMO level for the Ethyl4-(benzyl-methylamino) benzoate molecule with long driver on the xz plane with the driver. The orbitals are taken with an isosurface value equal to 0.015.

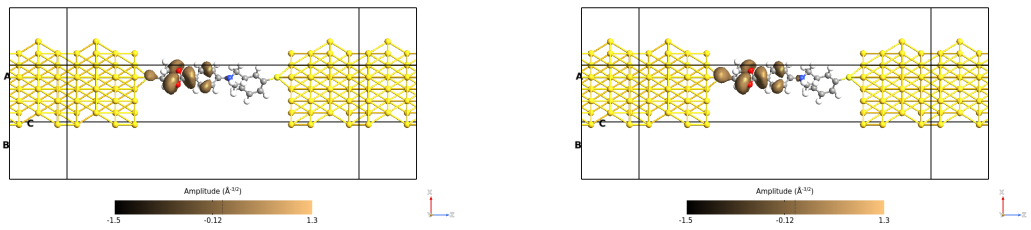

(a) logic '0'. (b) logic '1'.

Figure 6.223: Picture of the orbitals corresponding to the HOMO level for the Ethyl4-(benzyl-methylamino) benzoate molecule with long driver on the xz plane. The orbitals are taken with an isosurface value equal to 0.015.

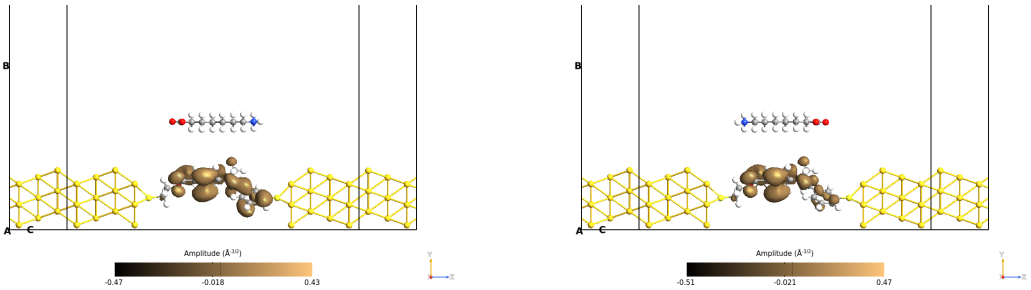

(a) logic '0'. (b) logic '1'.

Figure 6.224: Picture of the orbitals corresponding to the LUMO level for the Ethyl4-(benzyl-methylamino) benzoate molecule with long driver on the yz plane. The orbitals are taken with an isosurface value equal to 0.015.

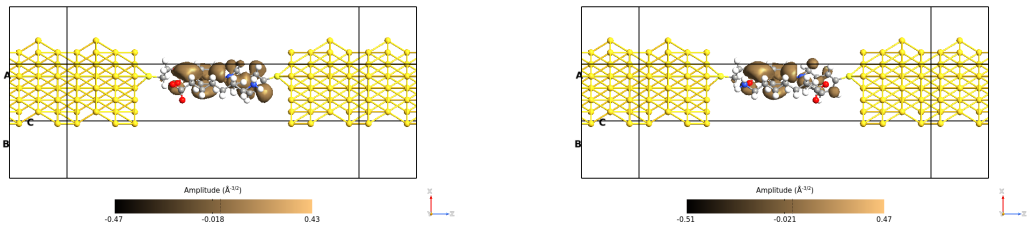

(a) logic '0'. (b) logic '1'.

Figure 6.225: Picture of the orbitals corresponding to the LUMO level for the Ethyl4-(benzyl-methylamino) benzoate molecule with long driver on the xz plane with the driver. The orbitals are taken with an isosurface value equal to 0.015.

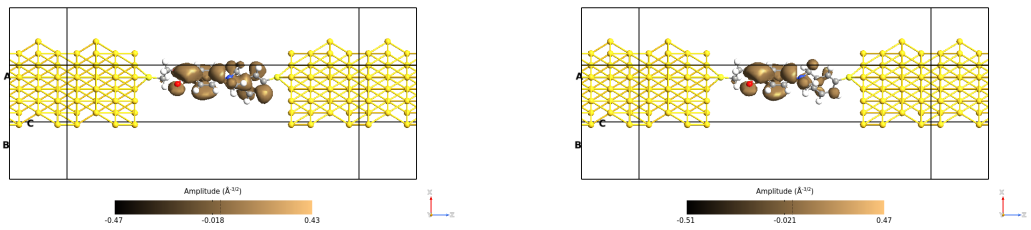

(a) logic '0'. (b) logic '1'.

Figure 6.226: Picture of the orbitals corresponding to the LUMO level for the Ethyl4-(benzyl-methylamino) benzoate molecule with long driver on the xz plane. The orbitals are taken with an isosurface value equal to 0.015.

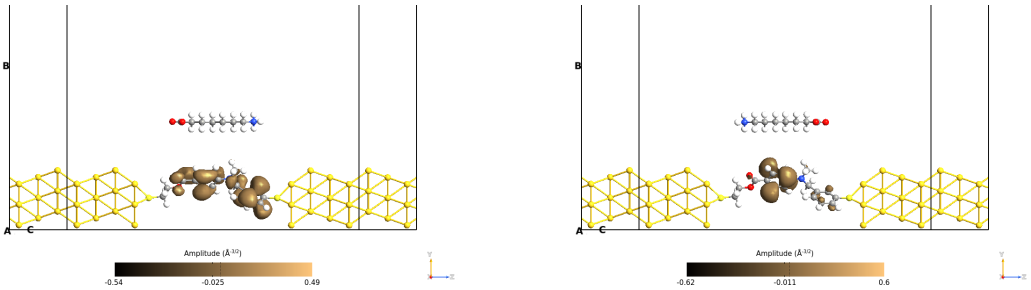

(a) logic '0'. (b) logic '1'.

Figure 6.227: Picture of the orbitals corresponding to the LUMO+1 level for the Ethyl4-(benzyl-methylamino) benzoate molecule with long driver on the yz plane. The orbitals are taken with an isosurface value equal to 0.015.

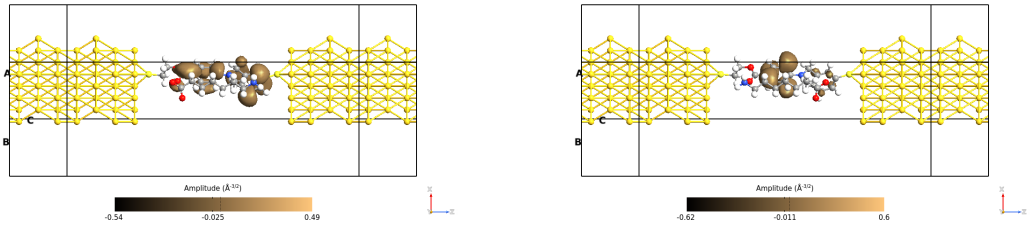

(a) logic '0'. (b) logic '1'.

Figure 6.228: Picture of the orbitals corresponding to the LUMO+1 level for the Ethyl4-(benzyl-methylamino) benzoate molecule with long driver on the xz plane with the driver. The orbitals are taken with an isosurface value equal to 0.015.

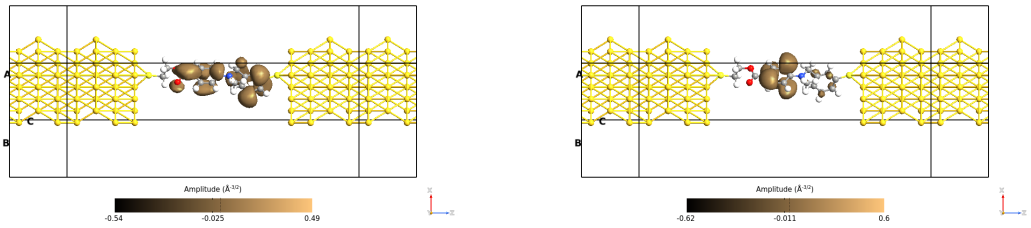

(a) logic '0'. (b) logic '1'.

Figure 6.229: Picture of the orbitals corresponding to the LUMO+1 level for the Ethyl4-(benzyl-methylamino) benzoate molecule with long driver on the xz plane. The orbitals are taken with an isosurface value equal to 0.015.

6.8.4 Pathways

The TS of the Ethyl4-(benzyl-methylamino) benzoate doesn't exibit significant peaks in the bias window (from -0.5 eV to 0.5 eV), for this reason only one transmission pathways point is taken inside the bias window. This point is at -0.25 eV (figures 6.230 and 6.233) and it doesn't show important result, because it has a very low magnitude value.

For the other two energy levels (figures 6.231, 6.234, 6.232 and 6.235) the transmission pathways reveal important results. The weight plots highlight the ON/OFF behavior cited in the TS section. For the -2.28 eV pathways we can notice that in the logic '0' (figure 6.231a) the maximum value of the scale is 0.18 while for the logic '1' it is 0.00014. This wide difference could be exploited with a gate electrode. The same consideration could be done for the path at -2.48 eV, but the roles are swapped, the logic '1' presents the higher magnitude value with respect to the logic '0' one.

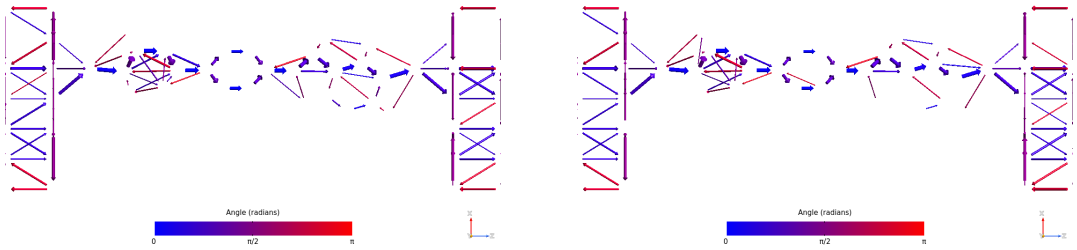

(a) logic '0'. (b) logic '1'.

Figure 6.230: Picture of the pathways at the energy -0.25 eV for the Ethyl4-(benzyl-methylamino) benzoate molecule with long driver on the xz plane. The blue arrows are in the same direction as the z-axis, while the red ones are in the opposite direction.

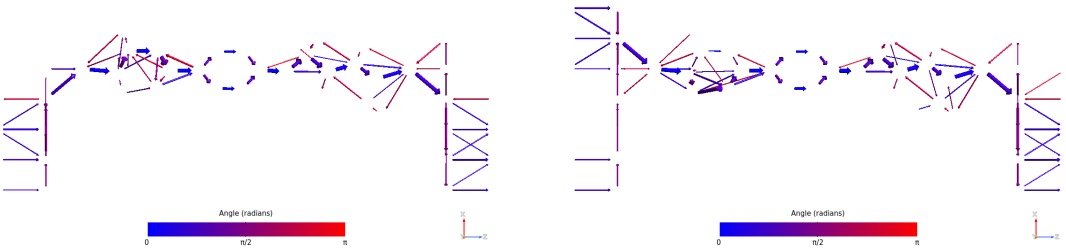

(a) logic '0'. (b) logic '1'.

Figure 6.231: Picture of the pathways at the energy -2.28 eV for the Ethyl4-(benzyl-methylamino) benzoate molecule with long driver on the xz plane. The blue arrows are in the same direction as the z-axis, while the red ones are in the opposite direction.

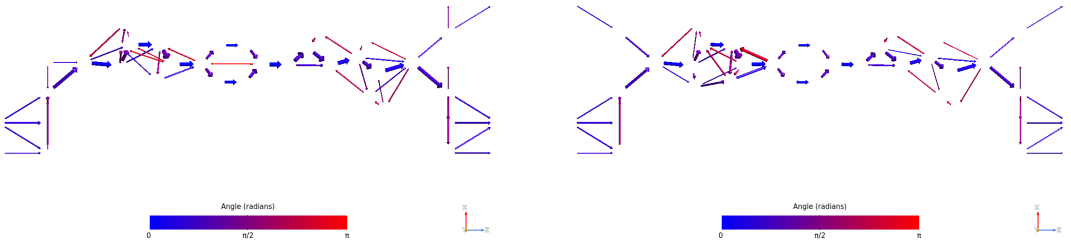

(a) logic '0'. (b) logic '1'.

Figure 6.232: Picture of the pathways at the energy -2.48 eV for the Ethyl4-(benzyl-methylamino) benzoate molecule with long driver on the xz plane. The blue arrows are in the same direction as the z-axis, while the red ones are in the opposite direction.

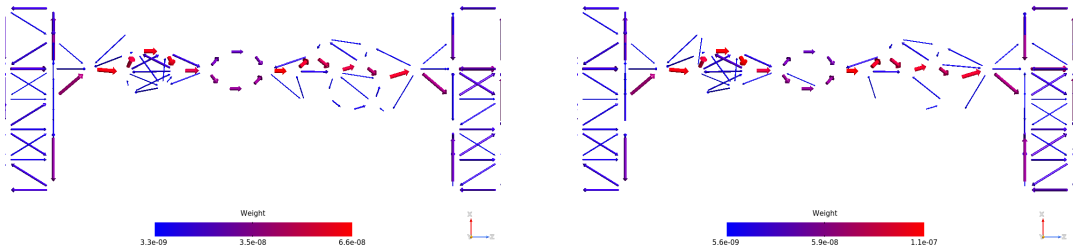

(a) logic '0'. (b) logic '1'.

Figure 6.233: Picture of the pathways corresponding to the energy -0.25 eV for the Ethyl4-(benzyl-methylamino) benzoate molecule with long driver on the xz plane. The plots show the arrows' magnitude.

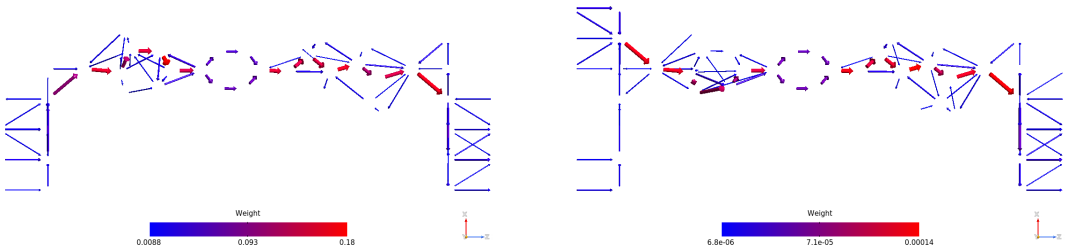

(a) logic '0'. (b) logic '1'.

Figure 6.234: Picture of the pathways corresponding to the energy -2.28 eV for the Ethyl4-(benzyl-methylamino) benzoate molecule with long driver on the xz plane. The plots show the arrows' magnitude.

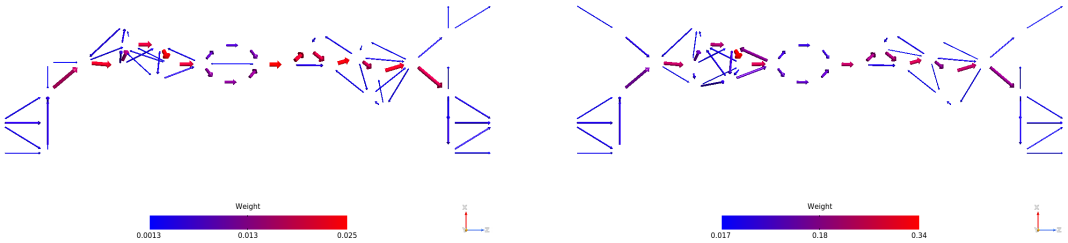

(a) logic '0'. (b) logic '1'.

Figure 6.235: Picture of the pathways corresponding to the energy -2.48 eV for the Ethyl4-(benzyl-methylamino) benzoate molecule with long driver on the xz plane. The plots show the arrows' magnitude.

6.9 Polar Molecule 2

The polar molecule 2 is a molecule designed ad hoc for this molecular junction. For this reason, no information about its conduction properties can be read in the literature. The geometry of the molecule is similar to the OPV3 and OPE3 ones, therefore a high current is expected.

The builder screens of the molecular junctions are reported in figure 6.236.

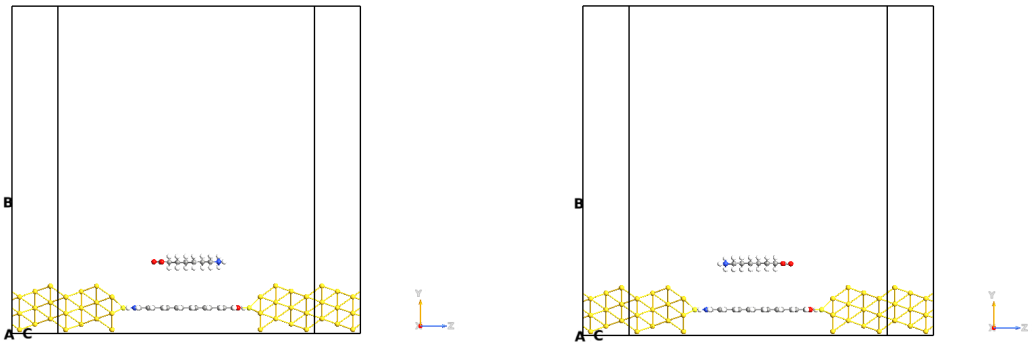

(a) logic '0' configuration. (b) logic '1' configuration.

Figure 6.236: Picture of the QuantumATK builder for the polar molecule 2. The white atoms are the hydrogens, the yellow ones are gold atoms, the lighter yellow ones are the sulfurs, the blue ones are nitrogens, the reds are the oxygens and the grey atoms are carbons.

6.9.1 TS

The TS (figure 6.237) highlights good conduction properties. The LUMO peaks are close to the energy axis's origine, therefore they are easily includable in the bias window. As for the OPV3 and OPE3, the shape is the same for the two logic configurations, the

differences are related to the wideness and amplitude of the peaks. The conduction is LUMO type because the HOMO peaks are distant from the 0 eV.

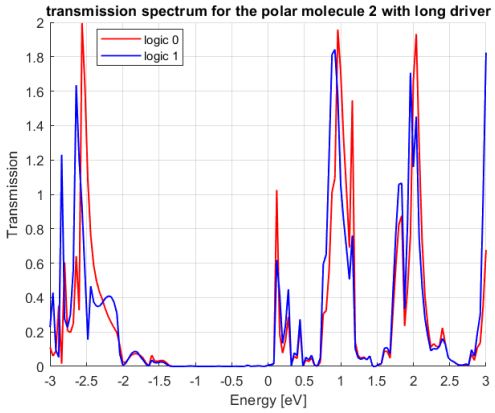

Figure 6.237: Picture of TS for the polar molecule 2 considering the long driver, the red curve represents the logic '0' configuration while the blue one the logic '1' configuration.

6.9.2 IV

The IV plot (figure 6.238) shows a not odd trend, this can be related to the polar behavior of the molecule. The current driven by the molecular junction is high, as expected, and thus is a very important feature for the readout system, the higher is the current, higher is the difference between the two configurations.

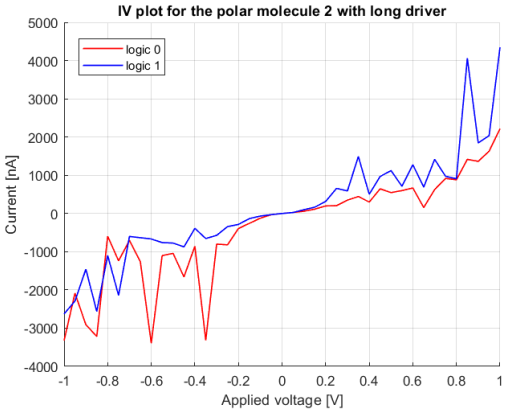

Figure 6.238: Picture of IV for the polar molecule 2 considering the long driver, the red curve represents the logic '0' configuration while the blue one the logic '1' configuration.

The current difference graph (figure 6.239) points out the feasibility of the readout system, in particular, the point at -0.35 V presents a current difference higher than 2.5 μA, which is easily detectable by a measurement system. The molecule is a good candidate for the readout system based on molecular junctions.

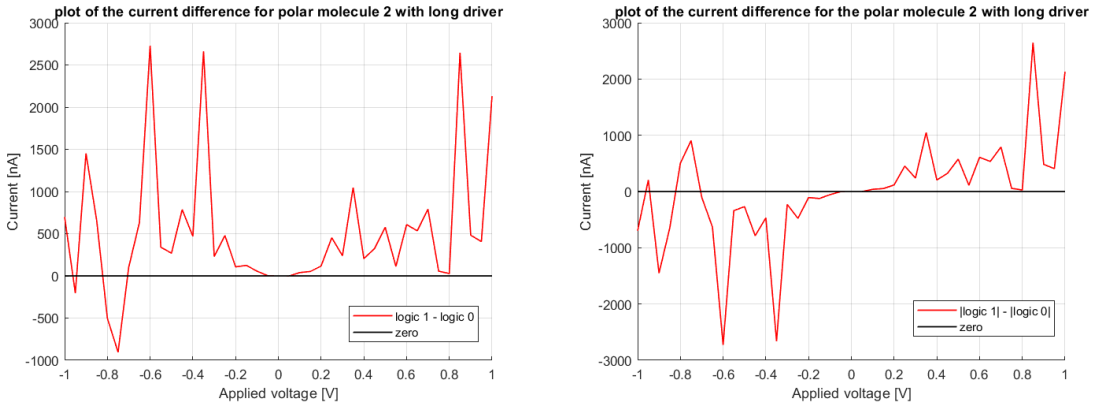

(a) logic '1' - logic '0'.

(b) |logic '1'| - |logic '0'|.

Figure 6.239: Picture of current difference for the polar molecule 2 considering the long driver.

6.9.3 Orbitals

The orbital views are quite different for the analyzed energy levels. In the HOMO-1 case (figures 6.240, 6.241 and 6.242) is easily noticeable the diversity between the two logic configurations, in particular, close to the electrode the orbital shapes present significant differences related to wideness and form. For the HOMO (figures 6.243, 6.244 and 6.245) and LUMO (figures 6.246, 6.247 and 6.248) levels the results confirm the previously analyzed trend.

The LUMO+1 energy level (figures 6.249, 6.250 and 6.251) shows the same behavior for the two logic configurations. The high polarizability value of the polar molecule 2 provides the same behavior of the OPV3 and OPE3 to the molecule.

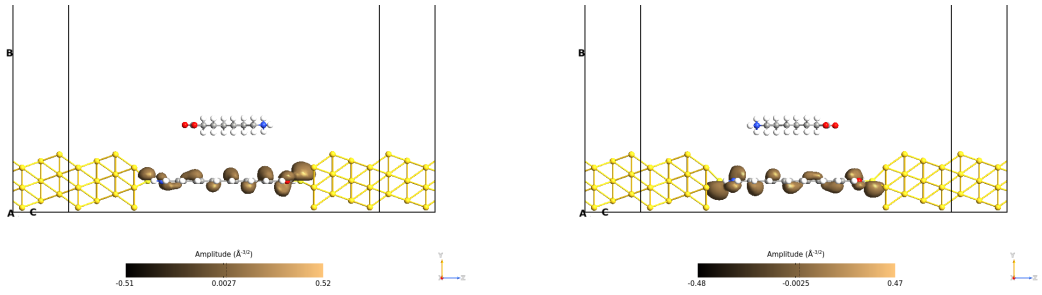

(a) logic '0'.

(b) logic '1'.

Figure 6.240: Picture of the orbitals corresponding to the HOMO-1 level for the polar molecule 2 with long driver on the yz plane. The orbitals are taken with an isosurface value equal to 0.015.

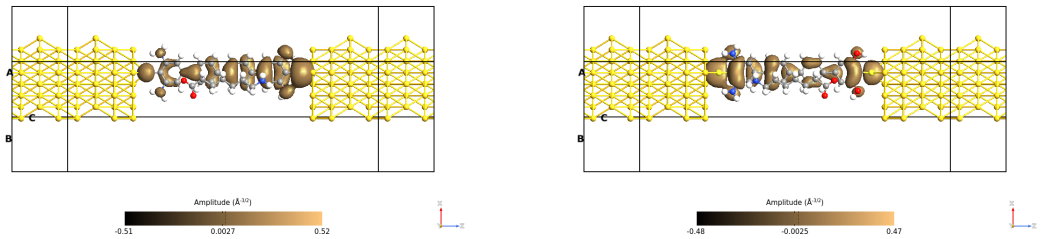

(a) logic '0'. (b) logic '1'.

Figure 6.241: Picture of the orbitals corresponding to the HOMO-1 level for the polar molecule 2 with long driver on the xz plane with the driver. The orbitals are taken with an isosurface value equal to 0.015.

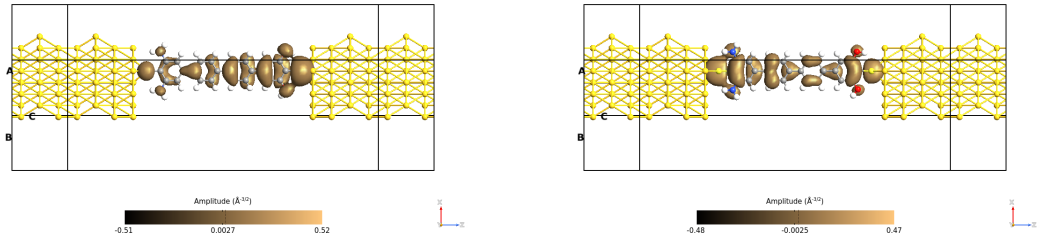

(a) logic '0'. (b) logic '1'.

Figure 6.242: Picture of the orbitals corresponding to the HOMO-1 level for the polar molecule 2 with long driver on the xz plane. The orbitals are taken with an isosurface value equal to 0.015.

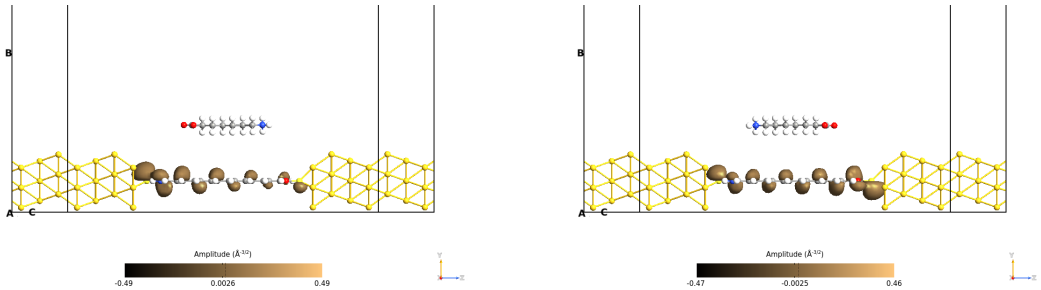

(a) logic '0'. (b) logic '1'.

Figure 6.243: Picture of the orbitals corresponding to the HOMO level for the polar molecule 2 with long driver on the yz plane. The orbitals are taken with an isosurface value equal to 0.015.

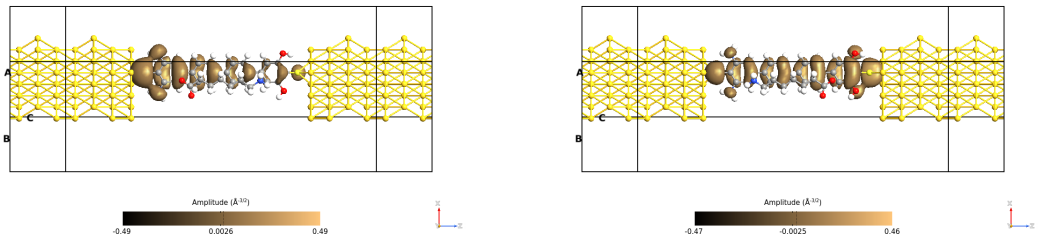

(a) logic '0'. (b) logic '1'.

Figure 6.244: Picture of the orbitals corresponding to the HOMO level for the polar molecule 2 with long driver on the xz plane with the driver. The orbitals are taken with an isosurface value equal to 0.015.

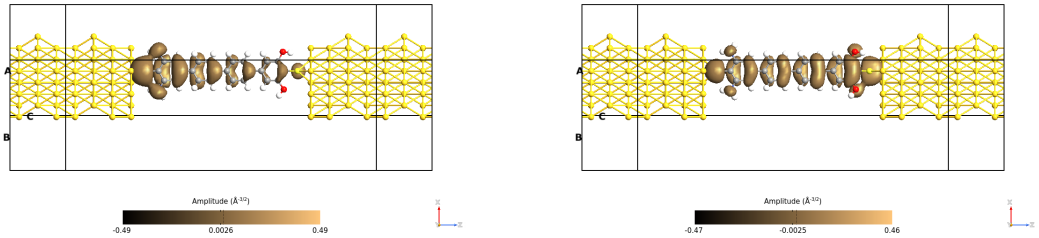

(a) logic '0'. (b) logic '1'.

Figure 6.245: Picture of the orbitals corresponding to the HOMO level for the polar molecule 2 with long driver on the xz plane. The orbitals are taken with an isosurface value equal to 0.015.

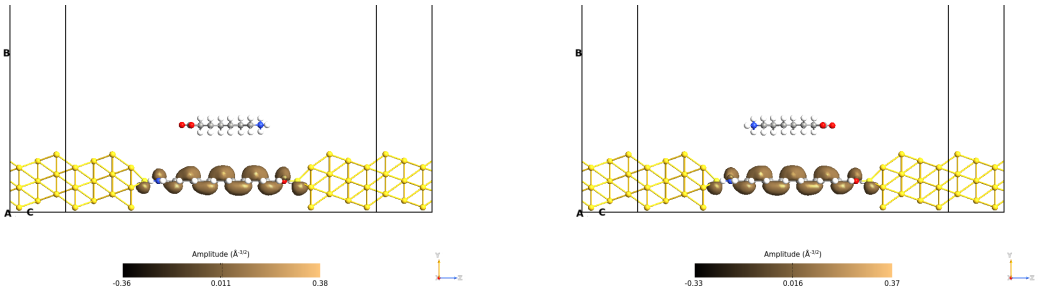

(a) logic '0'. (b) logic '1'.

Figure 6.246: Picture of the orbitals corresponding to the LUMO level for the polar molecule 2 with long driver on the yz plane. The orbitals are taken with an isosurface value equal to 0.015.

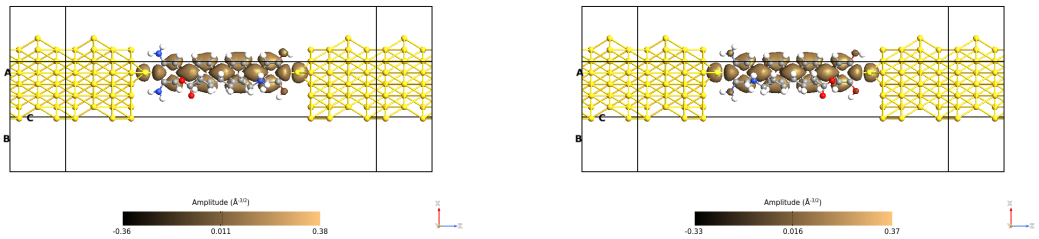

(a) logic '0'. (b) logic '1'.

Figure 6.247: Picture of the orbitals corresponding to the LUMO level for the polar molecule 2 with long driver on the xz plane with the driver. The orbitals are taken with an isosurface value equal to 0.015.

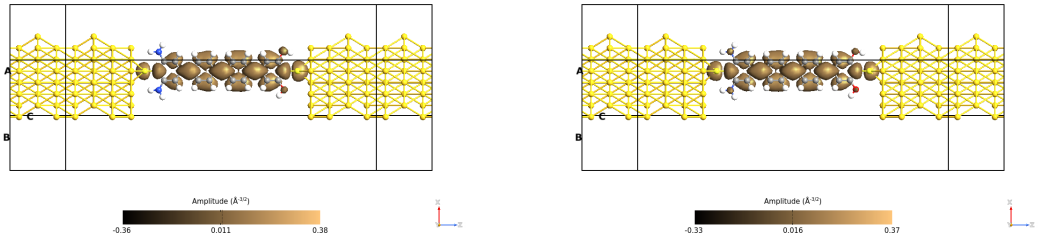

(a) logic '0'. (b) logic '1'.

Figure 6.248: Picture of the orbitals corresponding to the LUMO level for the polar molecule 2 with long driver on the xz plane. The orbitals are taken with an isosurface value equal to 0.015.

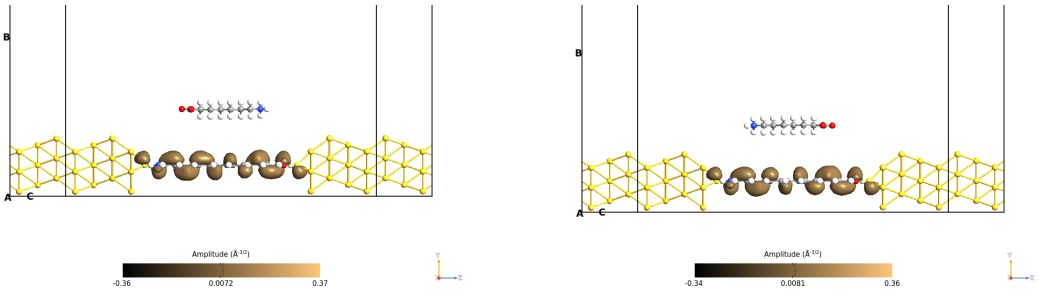

(a) logic '0'. (b) logic '1'.

Figure 6.249: Picture of the orbitals corresponding to the LUMO+1 level for the polar molecule 2 with long driver on the yz plane. The orbitals are taken with an isosurface value equal to 0.015.

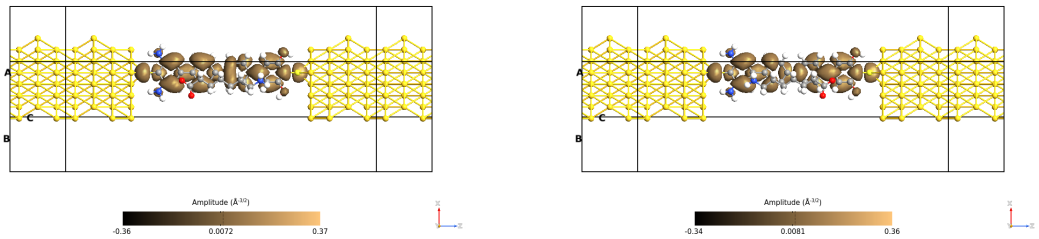

(a) logic '0'. (b) logic '1'.

Figure 6.250: Picture of the orbitals corresponding to the LUMO+1 level for the polar molecule 2 with long driver on the xz plane with the driver. The orbitals are taken with an isosurface value equal to 0.015.

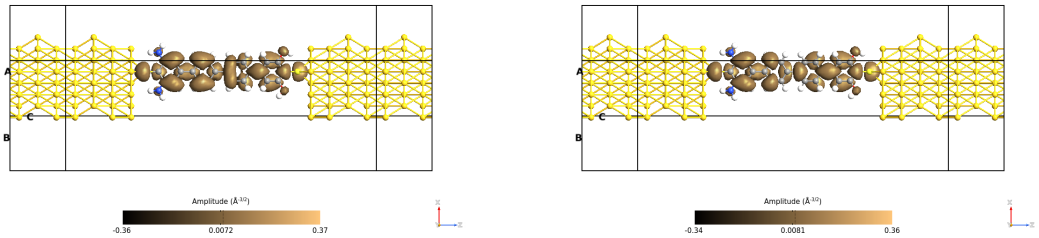

(a) logic '0'. (b) logic '1'.

Figure 6.251: Picture of the orbitals corresponding to the LUMO+1 level for the polar molecule 2 with long driver on the xz plane. The orbitals are taken with an isosurface value equal to 0.015.

6.9.4 Pathways

From the transmission pathways regarding the angle (figures 6.252, 6.253 and 6.254) it is possible to notice the same tendency, the higher is the energy, the higher is the amount of electrons that flow in the opposite direction of the conduction direction.

The weight transmission pathways (figures 6.252, 6.253 and 6.254) cofirms the conclusions derived from the TS (figure 6.237). The 0.12 eV plot shows the highest distance in terms of magnitude (0.94 for the logic '0' against 0.57 for the logic '1') considering the three selected energy values, in fact on the TS it correspond to the larger amplitude difference between the three peaks considered. The pathways at 0.28 eV tells us the opposite behavior with respect to the 0.12 eV, the logic '1' configuratio presents a higher magnitude value than the other one. In the third plot, instead, is posible to observe that the values are practically the same for the two cases.

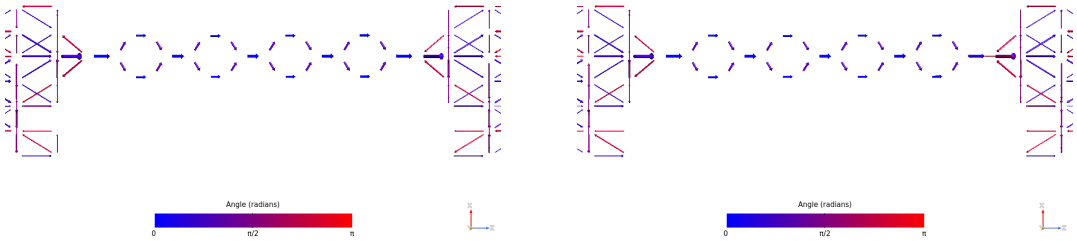

(a) logic '0'. (b) logic '1'.

Figure 6.252: Picture of the pathways corresponding to the energy 0.12 eV for the polar molecule 2 with long driver on the xz plane. The blue arrows are in the same direction as the z-axis, while the red ones are in the opposite direction.

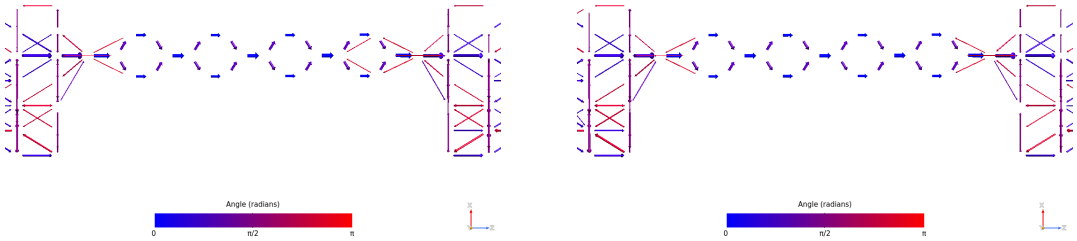

(a) logic '0'. (b) logic '1'.

Figure 6.253: Picture of the pathways corresponding to the energy 0.28 eV for the polar molecule 2 with long driver on the xz plane. The blue arrows are in the same direction as the z-axis, while the red ones are in the opposite direction.

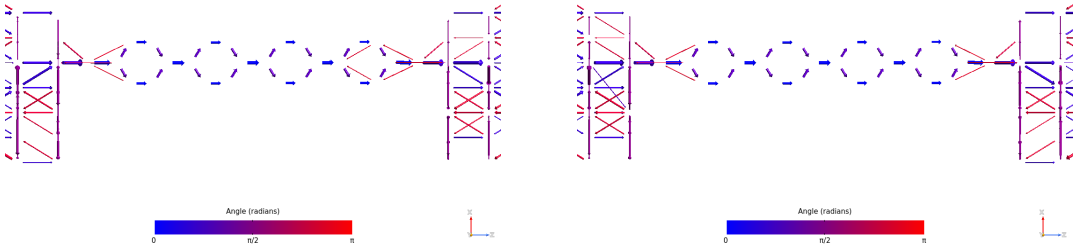

(a) logic '0'. (b) logic '1'.

Figure 6.254: Picture of the pathways corresponding to the energy 0.44 eV for the polar molecule 2 with long driver on the xz plane. The blue arrows are in the same direction as the z-axis, while the red ones are in the opposite direction.

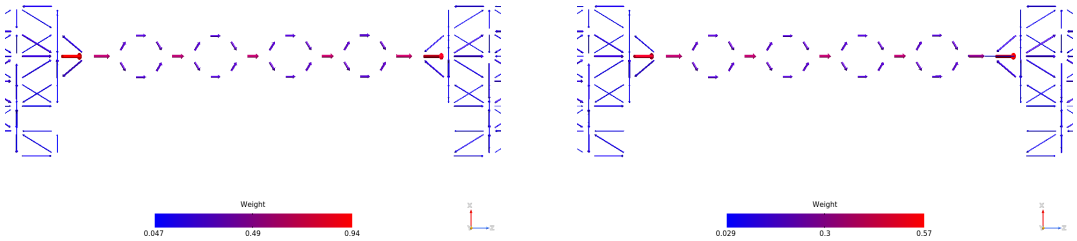

(a) logic '0'. (b) logic '1'.

Figure 6.255: Picture of the pathways corresponding to the energy 0.12 eV for the polar molecule 2 with long driver on the xz plane. The plots show the arrows' magnitude.

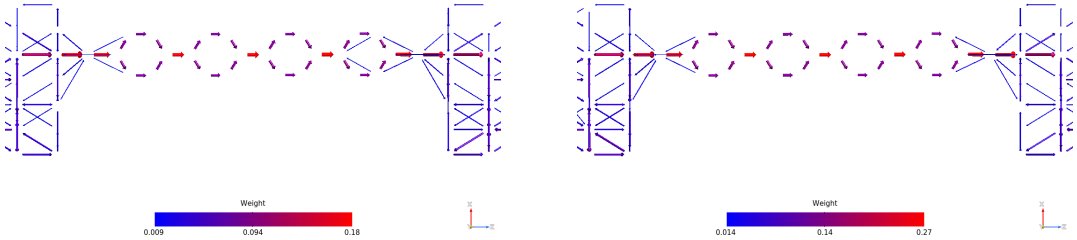

(a) logic '0'. (b) logic '1'.

Figure 6.256: Picture of the pathways corresponding to the energy 0.28 eV for the polar molecule 2 with long driver on the xz plane. The plots show the arrows' magnitude.

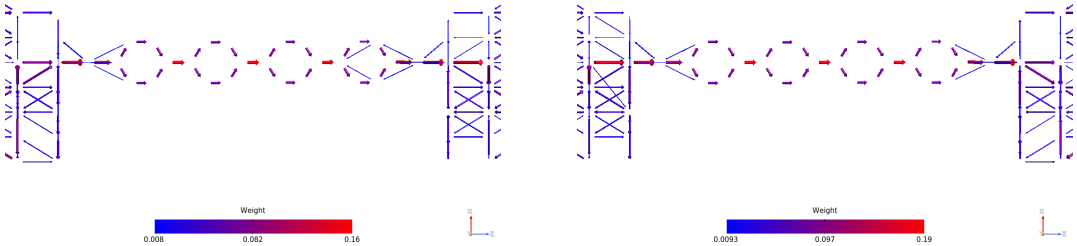

(a) logic '0'. (b) logic '1'.

Figure 6.257: Picture of the pathways corresponding to the energy 0.44 eV for the polar molecule 2 with long driver on the xz plane. The plots show the arrows' magnitude.

6.10 Polar Molecule 7

The polar molecule 7 is a molecule designed ad hoc for this molecular junction. For this reason, no information about its conduction properties can be read in the literature. The

base of the molecule is the OPE3, in which OH and NH_2 groups are added to provide the polar behavior of the molecule. The builder views are displayed in the figure 6.258.

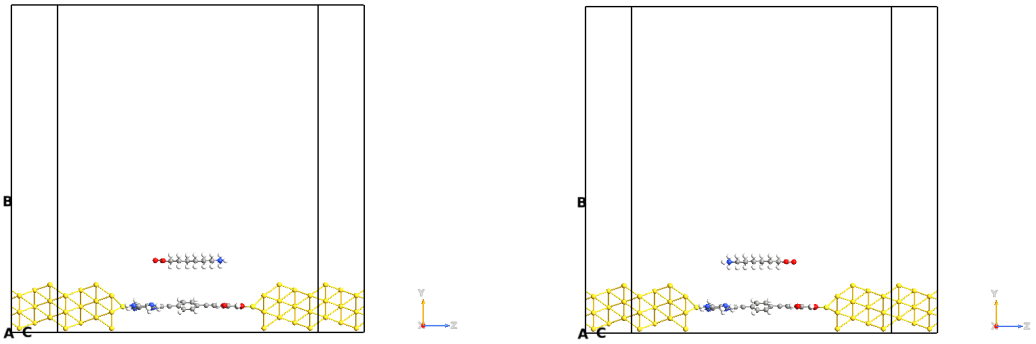

(a) logic '0' configuration. (b) logic '1' configuration.

Figure 6.258: Picture of the QuantumATK builder for the polar molecule 7. The white atoms are the hydrogens, the yellow ones are gold atoms, the lighter yellow ones are the sulfurs, the blue ones are nitrogens, the reds are the oxygens and the grey atoms are carbons.

6.10.1 TS

The TS plot (figure 6.259) is similar to the OPE3 one (figure 6.52a), the differences are mostly related to the trend at high energies (below -2 eV and over 1.5 eV). In general the polar molecule 7 seems to be a molecule with good conduction properties, the conduction is LUMO type because the HOMO peaks are very distant from the origin of the energy axis.

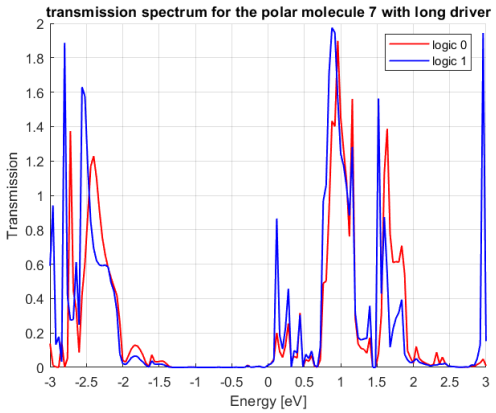

Figure 6.259: Picture of TS for the polar molecule 7 considering the long driver, the red curve represents the logic '0' configuration while the blue one the logic '1' configuration.

The polar molecule 7 is not strongly asymmetric, because the base is the OPE3

molecule, which is symmetrical, and the added groups provide asymmetry but not in a deep way. This can be the reason for the not ON/OFF TS.

6.10.2 IV

The IV plot (figure 6.260) tells us the goodness in terms of conduction properties of the polar molecule 7. The amount of current that the molecule can drive is quite high, this is an important feature of the readout system. Especially for negative voltages, the molecule behavior is largely different for the two configurations.

Figure 6.260: Picture of IV for the polar molecule 7 considering the long driver, the red curve represents the logic '0' configuration while the blue one the logic '1' configuration.

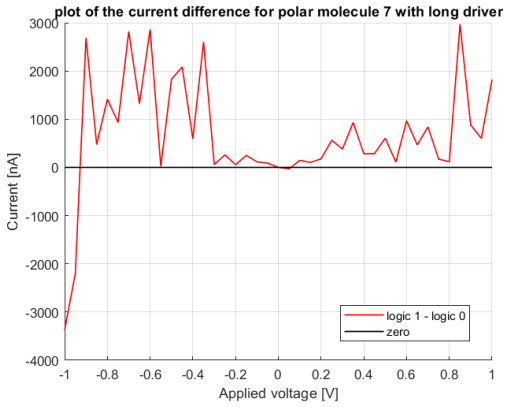

(a) logic 1 - logic 0.

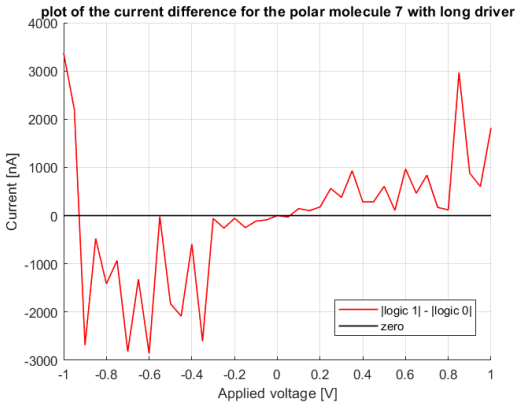

(b) |logic 1| - |logic 0|.

Figure 6.261: Picture of current difference for the polar molecule 7 considering the long driver.

The current difference graphs (figure 6.261) highlight the feasibility of the readout system. From the -0.3 V to the -0.9 V the logic '0' current is higher (in absolute value, so

not considering the current direction) than the logic '1' one. The difference reaches high values, they are higher than 2 μA and lower than 3 μA.

6.10.3 Orbitals

The orbital views of the polar molecule 7 reveal a completely different trend between the two logic configurations. The HOMO-1 (figures 6.262, 6.263 and 6.264) is completely diverse between the logic '0' and logic '1', the only common property that is possible to notice is the high concentration of the orbitals close to the driver's negative pole. The LUMO+1 (figures 6.271, 6.272 and 6.273) energy level presents the more similar orbital trend between the two configurations with respect to the other three selected energy levels. In general, the molecule's asymmetrical geometry provides it different behavior when subjected to the driver's influence.

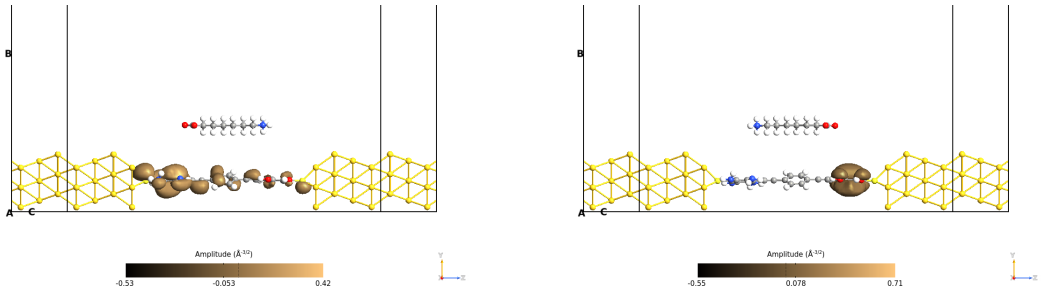

(a) logic '0'. (b) logic '1'.

Figure 6.262: Picture of the orbitals corresponding to the HOMO-1 level for the polar molecule 7 with long driver on the yz plane. The orbitals are taken with an isosurface value equal to 0.015.

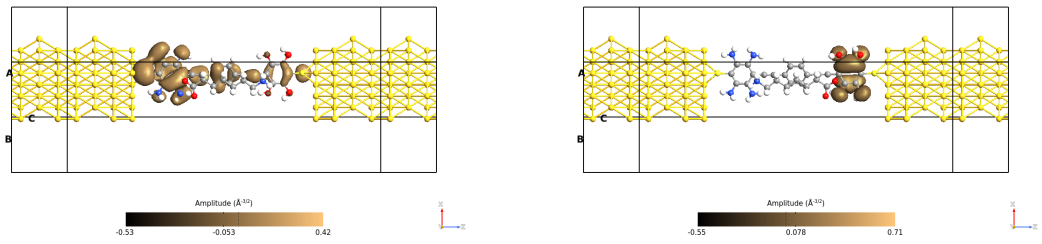

(a) logic '0'. (b) logic '1'.

Figure 6.263: Picture of the orbitals corresponding to the HOMO-1 level for the polar molecule 7 with long driver on the xz plane with the driver. The orbitals are taken with an isosurface value equal to 0.015.

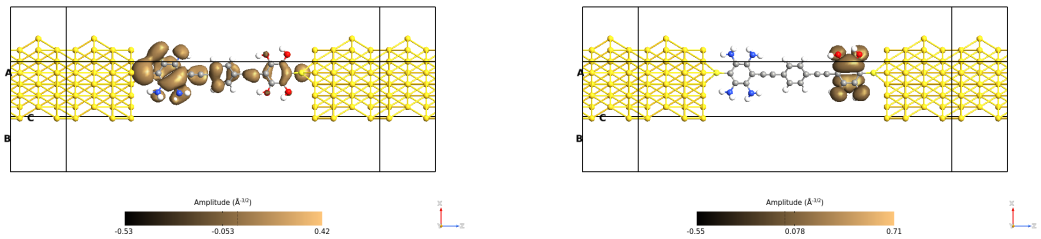

(a) logic '0'. (b) logic '1'.

Figure 6.264: Picture of the orbitals corresponding to the HOMO-1 level for the polar molecule 7 with long driver on the xz plane. The orbitals are taken with an isosurface value equal to 0.015.

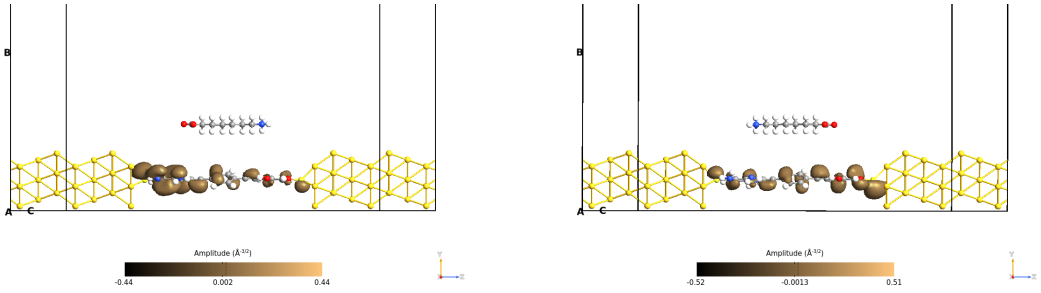

(a) logic '0'. (b) logic '1'.

Figure 6.265: Picture of the orbitals corresponding to the HOMO level for the polar molecule 7 with long driver on the yz plane. The orbitals are taken with an isosurface value equal to 0.015.

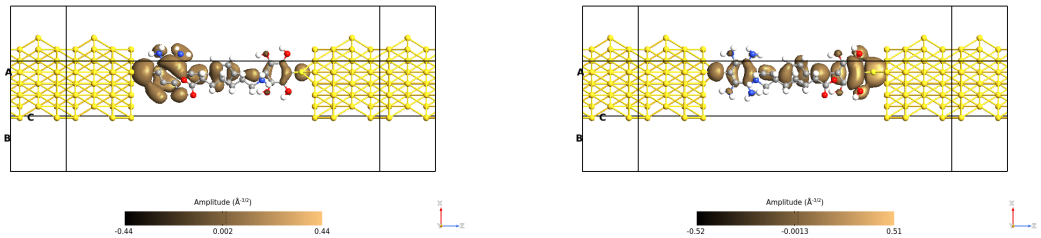

(a) logic '0'. (b) logic '1'.

Figure 6.266: Picture of the orbitals corresponding to the HOMO level for the polar molecule 7 with long driver on the xz plane with the driver. The orbitals are taken with an isosurface value equal to 0.015.

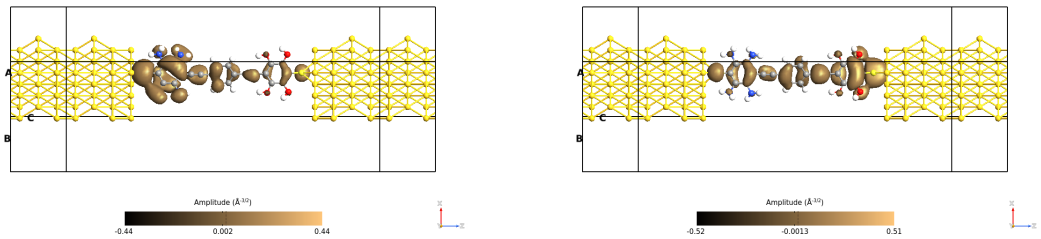

(a) logic '0'. (b) logic '1'.

Figure 6.267: Picture of the orbitals corresponding to the HOMO level for the polar molecule 7 with long driver on the xz plane. The orbitals are taken with an isosurface value equal to 0.015.

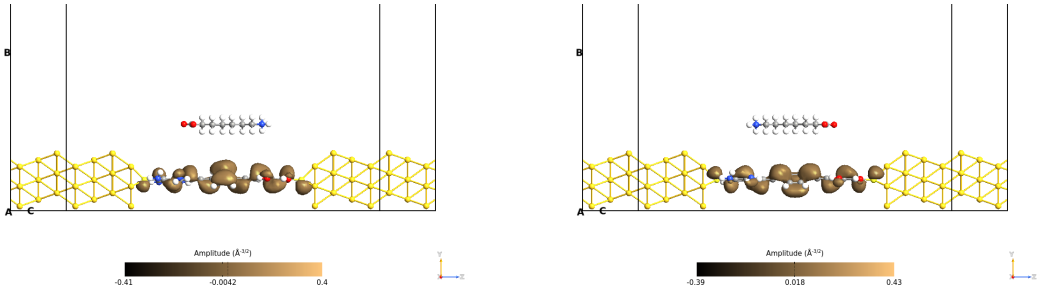

(a) logic '0'. (b) logic '1'.

Figure 6.268: Picture of the orbitals corresponding to the LUMO level for the polar molecule 7 with long driver on the yz plane. The orbitals are taken with an isosurface value equal to 0.015.

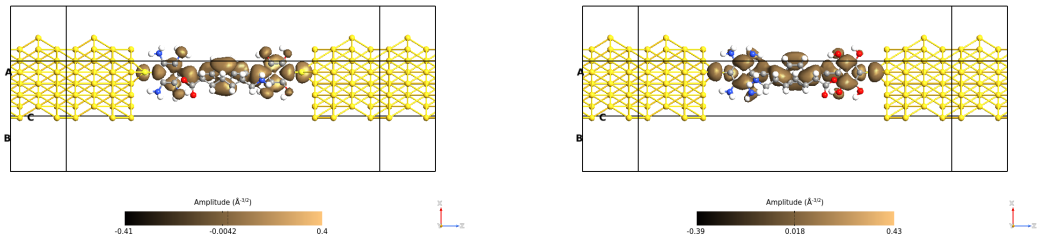

(a) logic '0'. (b) logic '1'.

Figure 6.269: Picture of the orbitals corresponding to the LUMO level for the polar molecule 7 with long driver on the xz plane with the driver. The orbitals are taken with an isosurface value equal to 0.015.

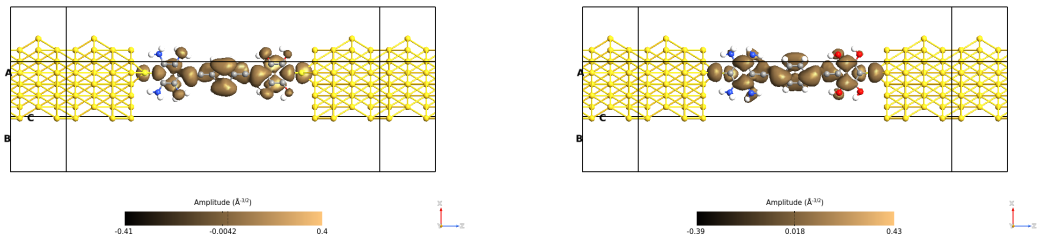

(a) logic '0'. (b) logic '1'.

Figure 6.270: Picture of the orbitals corresponding to the LUMO level for the polar molecule 7 with long driver on the xz plane. The orbitals are taken with an isosurface value equal to 0.015.

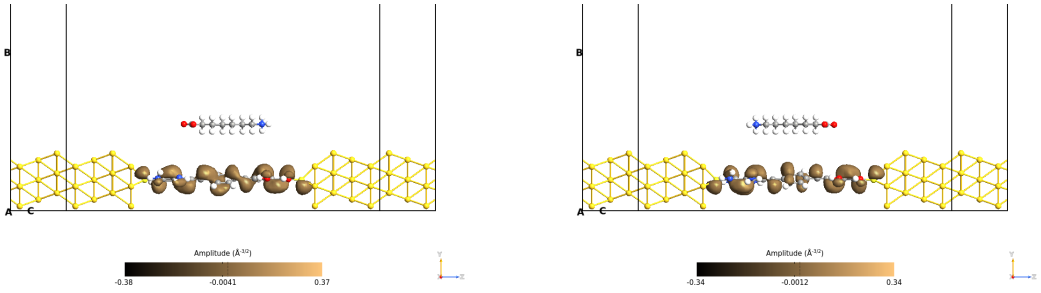

(a) logic '0'. (b) logic '1'.

Figure 6.271: Picture of the orbitals corresponding to the LUMO+1 level for the polar molecule 7 with long driver on the yz plane. The orbitals are taken with an isosurface value equal to 0.015.

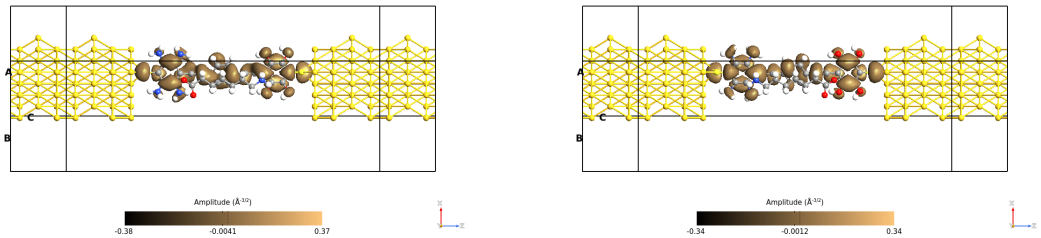

(a) logic '0'. (b) logic '1'.

Figure 6.272: Picture of the orbitals corresponding to the LUMO+1 level for the polar molecule 7 with long driver on the xz plane with the driver. The orbitals are taken with an isosurface value equal to 0.015.

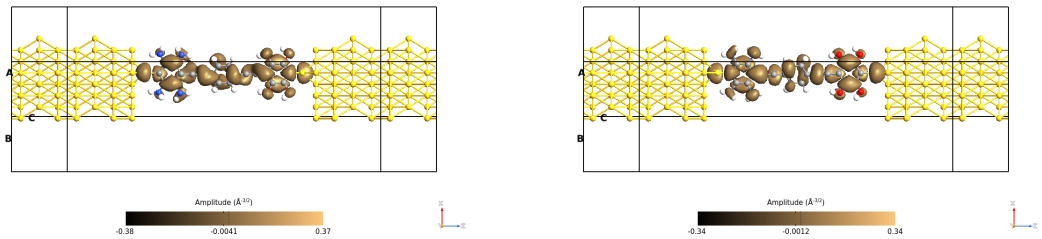

(a) logic '0'. (b) logic '1'.

Figure 6.273: Picture of the orbitals corresponding to the LUMO+1 level for the polar molecule 7 with long driver on the xz plane. The orbitals are taken with an isosurface value equal to 0.015.

6.10.4 Pathways

The polar molecule 7's transmission pathways don't reserve surprises, the angle plots (figures 6.274, 6.275 and 6.276) confirm the same behavior as the previously analyzed molecules.

Figures 6.277, 6.278 and 6.279 show the weight transmission pathways. They exhibit the expected trend knowing the TS (figure 6.259). In the 0.12 eV path, the magnitude value presents the highest difference between the two configurations, 0.18 for the logic '0' against 0.82 for the logic '1'. The 0.44 eV plots are the most similar ones, 0.2 for the logic '0' against the 0.25 for the logic '1'. The 0.28 eV pathways show intermediate behavior with respect to the other two selected energy levels.

In general, the pathways reveal different behaviors between the two logic configurations, this is a fundamental property for the feasibility of the readout system for molFCN.

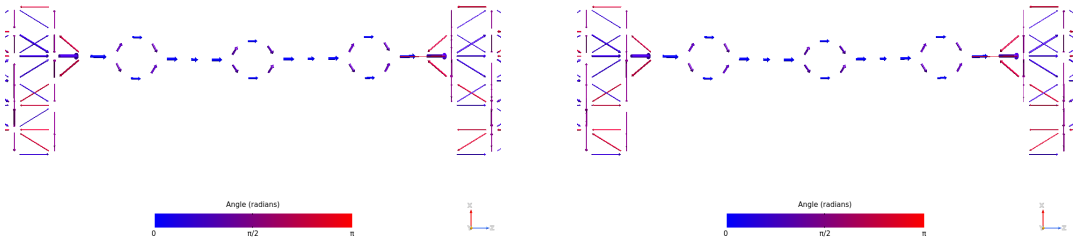

(a) logic '0'. (b) logic '1'.

Figure 6.274: Picture of the pathways corresponding to the energy 0.12 eV for the polar molecule 7 with long driver on the xz plane. The blue arrows are in the same direction as the z-axis, while the red ones are in the opposite direction.

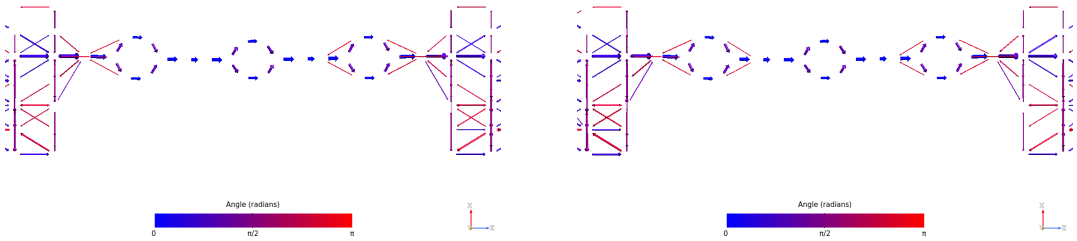

(a) logic '0'. (b) logic '1'.

Figure 6.275: Picture of the pathways corresponding to the energy 0.28 eV for the polar molecule 7 with long driver on the xz plane. The blue arrows are in the same direction as the z-axis, while the red ones are in the opposite direction.

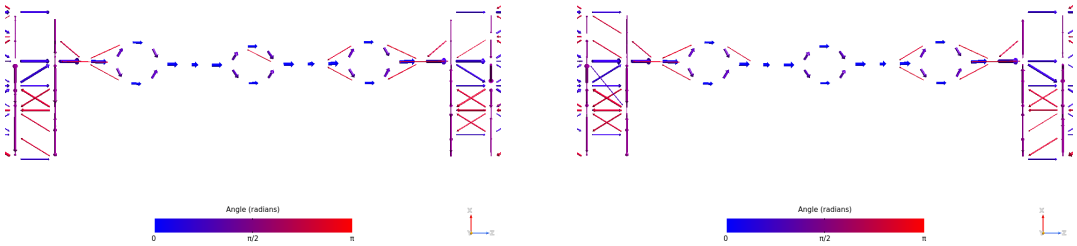

(a) logic '0'. (b) logic '1'.

Figure 6.276: Picture of the pathways corresponding to the energy 0.44 eV for the polar molecule 7 with long driver on the xz plane. The blue arrows are in the same direction as the z-axis, while the red ones are in the opposite direction.

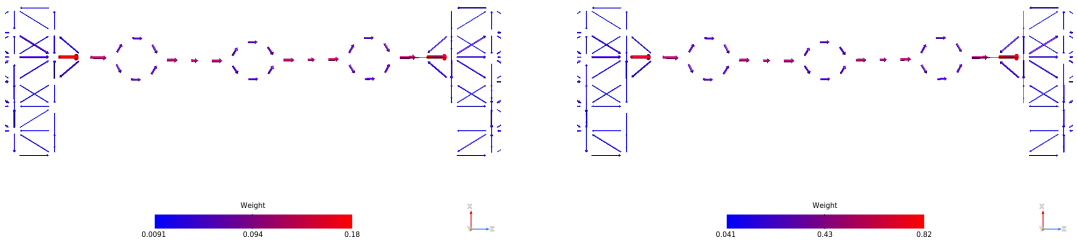

(a) logic '0'. (b) logic '1'.

Figure 6.277: Picture of the pathways corresponding to the energy 0.12 eV for the polar molecule 7 with long driver on the xz plane. The plots show the arrows' magnitude.

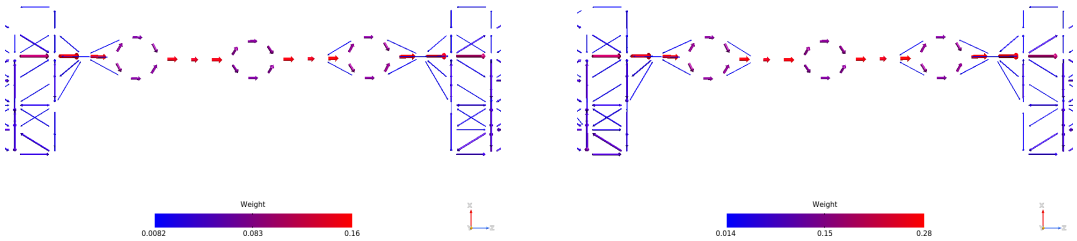

(a) logic '0'. (b) logic '1'.

Figure 6.278: Picture of the pathways corresponding to the energy 0.28 eV for the polar molecule 7 with long driver on the xz plane. The plots show the arrows' magnitude.

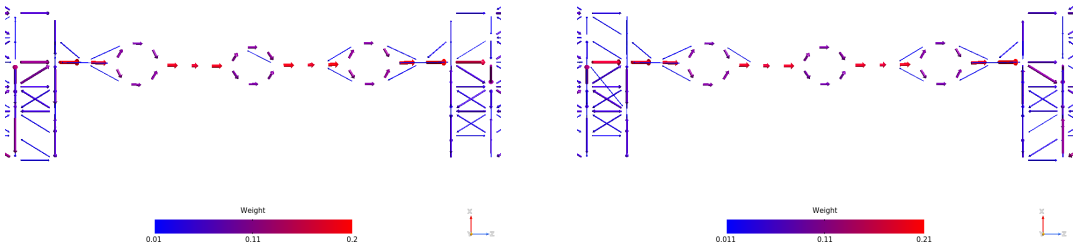

(a) logic '0'. (b) logic '1'.

Figure 6.279: Picture of the pathways corresponding to the energy 0.44 eV for the polar molecule 7 with long driver on the xz plane. The plots show the arrows' magnitude.

6.11 Molecules comparison

The analyzed molecules are many, it is difficult to compare all of them in a single plot. Two main categories have been selected for dividing the molecules:

- *High polarizability*: OPE3, OPV3, ZnPc, Pc and ZnPc with thiol chains;
- *High dipole moment*: 4-Aminobenzoic acid, ethyl4-(benzyl-methylamino) benzoate, polar molecule 2 and polar molecule 7.

6.11.1 High polarizability molecules

The IV plots (figure 6.280) show important conduction properties for all the molecules, except for the ZnPc with thiol chains. This phenomenon was expected because this molecule works in the weak coupling, therefore the current driven is quite low with respect to the molecules that allow the strong coupling conditions.

The current difference plot (figure 6.281) is the most interesting graph because it shows clearly the feasibility and goodness of the readout system. The picture tells us that the OPV3 molecule is the best one in terms of current difference between the two

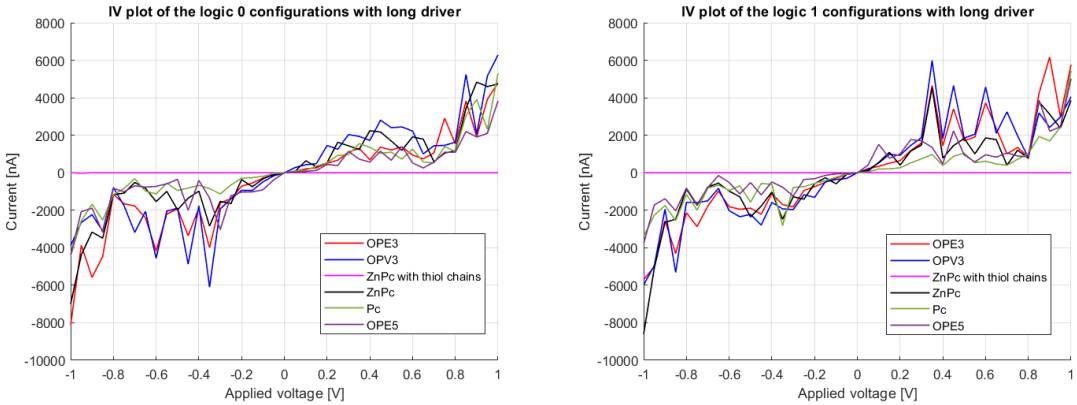

(a) Logic '0'.

(b) Logic '1'.

Figure 6.280: Picture of IV plot for all the molecules with a high polarizability value considering the long driver, the red curve represents the OPE3, the blue one the OPV3, the magenta curve stands for the ZnPc with thiol chains, the black one is for the ZnPC, the green line for the Pc molecule and the purple curve is for the OPE5.

logic configurations. The OPE3 and ZnPc molecular junctions present the same value at 0.35 V, but the OPE3 one is more robust because it has a wide interval in which the logic '1' current is always higher than the logic '0' one. The Pc molecule shows a significant current difference, but lower than the molecule cited before, while the ZnPc with thiol chains is not suitable for the readout purpose.

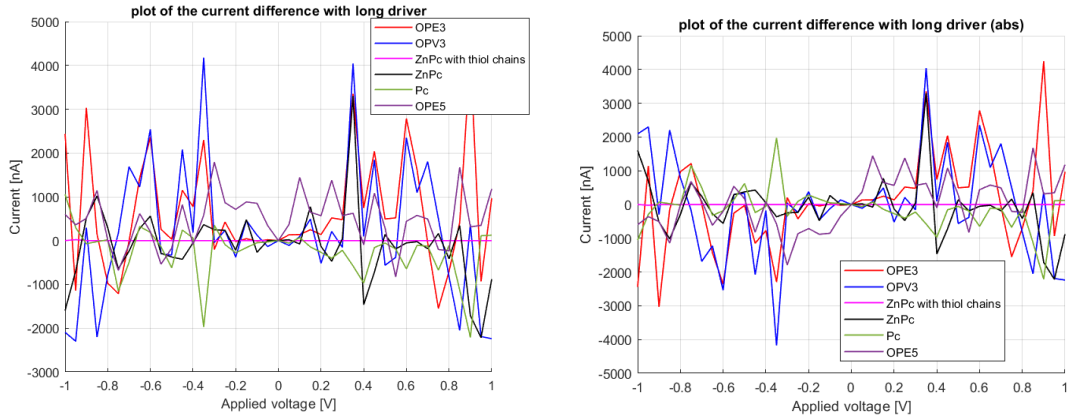

(a) logic '1' - logic '0'.

(b) |logic '1'|-|logic'0'|.

Figure 6.281: Picture of current difference for all the molecules with a high polarizability value considering the long driver, the red curve represents the OPE3, the blue one the OPV3, the magenta curve stands for the ZnPc with thiol chains, the black one is for the ZnPC, the green line for the Pc molecule and the purple curve is for the OPE5.

6.11.2 High dipole moment molecules

The IV plots are reported in the figure 6.282. The ethyl4-(benzyl-methylamino) benzoate is the molecule with the worst conduction properties with respect to the other three polar molecules. The polar molecule 2 and polar molecule 7 present different behavior between the two configurations, particularly for negative voltages, while the 4-Amino benzoic acid for the positive voltages.

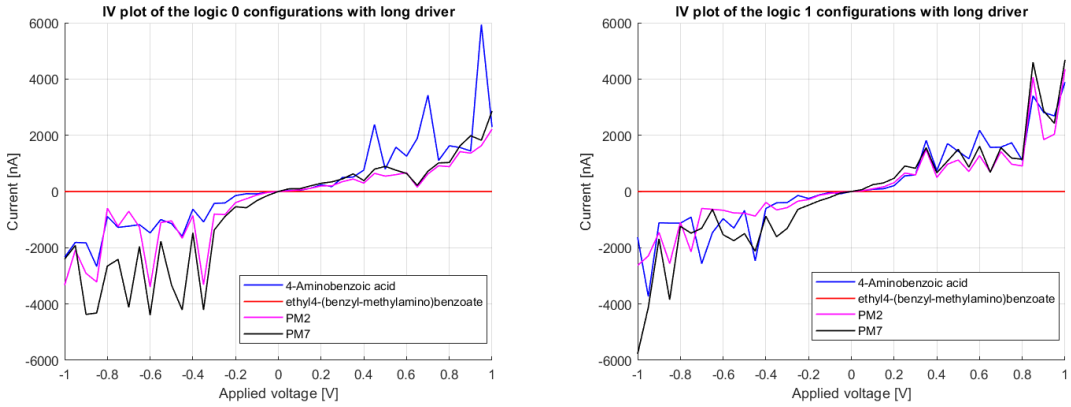

(a) Logic '0'.

(b) Logic '1'.

Figure 6.282: Picture of IV plot for all the molecules with a high dipole moment considering the long driver, the red curve represents the ethyl4-(benzyl-methylamino) benzoate, the blue one the 4-Aminobenzoic acid, the magenta curve stands for the polar molecule 2, the black one is for the polar molecule 7.

Figure 6.283 shows the current difference between the two logic configurations. It is a significant plot because it tells us clearly how easy can be (or not) to determine the logic value encoded in the molFCN. The polar molecule 7 is the one that fits in a better way our task, it presents the highest current difference and it has a wide interval (from -0.3 V to -0.9 V) in which the logic '0' is higher than the logic '1' in absolute value (not considering the current direction). The polar molecule 2 is the second better molecule, it has high current difference values but it exhibits a narrower interval in which one current prevails over the other. The 4-Amino benzoic acid can be used as a readout system because it shows a current difference higher than 1 μA (current detectable with today's measurement system) but it works in a worse way than the other two cited before.

The ethyl4-(benzyl-methylamino) benzoate could not work in these conditions as a readout system, but its TS allows us to think of a gate electrode in order to highlight the current difference between the two logic configurations.

6.11.3 Conclusions

As said before, it is not convenient to plot all the molecule's results in a single graph because it becomes understandable. All the presented molecules have their strengths and

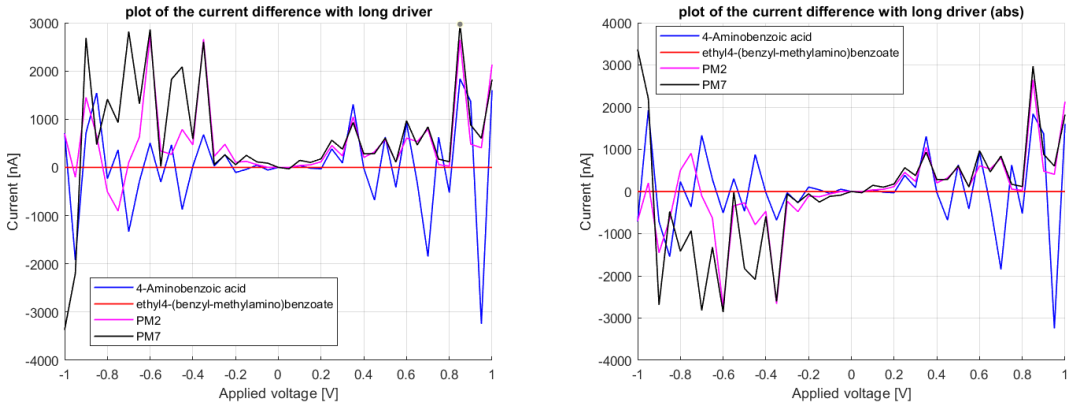

(a) logic '1' - logic '0'.

(b) |logic '1'|-|logic'0'|.

Figure 6.283: Picture of current difference for all the molecules with a high dipole moment considering the long driver, the red curve represents the ethyl4-(benzyl-methylamino) benzoate, the blue one the 4-Aminobenzoic acid, the magenta curve stands for the polar molecule 2, the black one is for the polar molecule 7.

their drawbacks, the best molecule must be chosen according to the molFCN specifications.

The more symmetric molecules require high conduction properties in order to amplify the current difference between the two configurations. The asymmetric molecules, instead, present different behavior when subjected to different electric fields, the conduction is more relevant, but in any case, it helps to distinguish the two logic values.

In the table 6.1 are reported the voltage points in which the molecules exhibit their largest current difference. It has been done to summarize clearly the comparison between all the selected molecules.

Table 6.1: The table shows the current ratio and difference for the different molecules in a specific voltage point.

Molecule	V_{point} **[V]**	$I_1 - I_0$ **[nA]**	I_1/I_0
OPV3	0.35	4042.3	5.747
OPE3	0.35	3352.93	4.245
Pc	0.9	2212.29	2.304
ZnPc	0.35	3300.11	3.665
ZnPc thiol chains	-0.95	21.9809	96833
4Aminobenzoic acid	0.35	1306.56	3.545
Ethyl4-(benzyl-methylamino) benzoate	-1	0.246315	1.382
Polar molecule 2	-0.35	2661.71	5.065
Polar molecule 7	-0.6	2859.23	2.861

6.12 Gate

The ethy4-(benzyl-methylamino) benzoate has been tested with the gate electrode due to its ON/OFF TS (figure 6.215). The builder views are reported in figure 6.284, in which is possible to notice the light grey electrode in the bottom part of the picture that is the gate electrode.

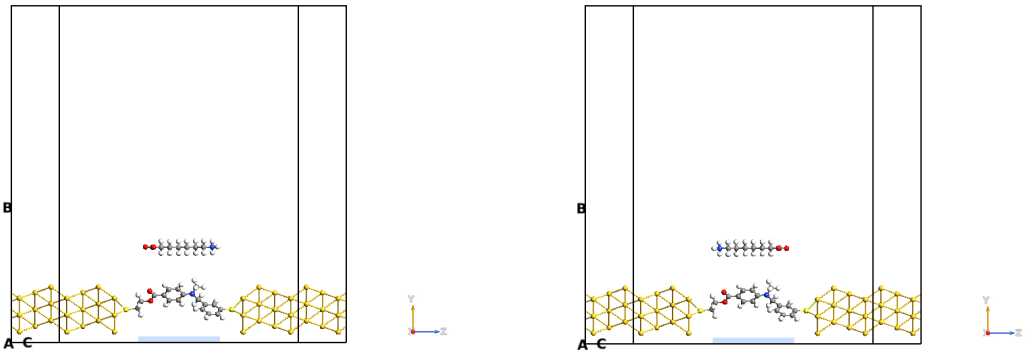

(a) Logic '0'. (b) Logic '1'.

Figure 6.284: Picture of the QuantumATK builder for the ehtyl4-(benzyl-methylamino) benzoate molecule with the gate electrode. The white atoms are the hydrogens, the yellow ones are gold atoms, the lighter yellow ones are the sulfurs, the blue ones are nitrogens, the reds are the oxygens and the grey atoms are carbons.

6.12.1 TS

In the TS plot (figure 6.285) is possible to observe easily the gate influence. The HOMO peaks move close to the energy axis' origine for negative gate voltages, while they move away for positive voltages. A particular behavior is exhibited from the -5 curve for the logic '0' plot, the peaks are not moving closer to the 0 eV and the amplitude of the peaks rises to very high values.

6.12.2 IV

The IV plot (figure 6.286) highlights the bad conduction properties of the molecule. There are only a few spikes in which the driven current is significant. The most relevant plots are the ones obtained with a gate voltage of 5 V, which can be too high for some applications.

The current difference plot (6.287) confirms the thoughts said before. The molecule with a gate voltage equal to 5 V can be used as a readout system because it exhibits a current difference slightly lower than 400 nA for an applied voltage of -0.65 V. The importance of a gate voltage can be noticed by looking at the red curve in the plot (the red curve stands for $V_G = 0$ V), it is practically impossible to see it because it drives a very low current with respect to the other curves. This means that a gate electrode can be very important for some applications because it shifts the TS.

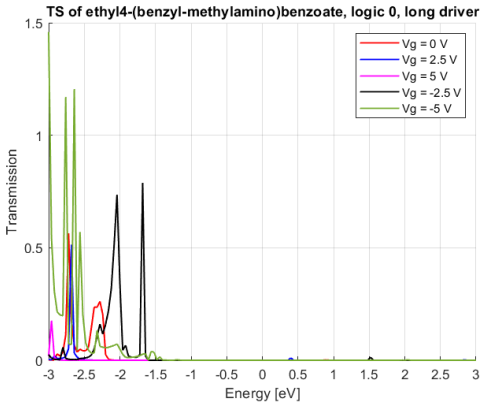

(a) logic '0' configuration.

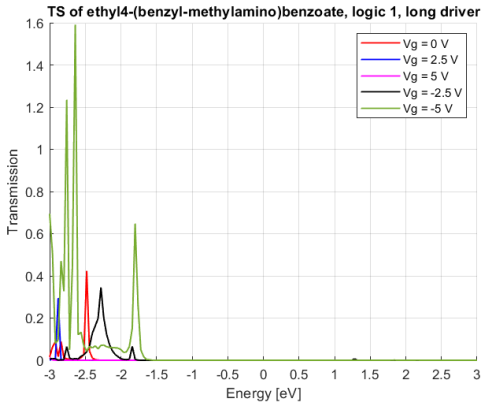

(b) logic '1' configuration.

Figure 6.285: Picture of TS for the Ethyl4-(benzyl-methylamino) benzoate molecule varying the gate voltage. The red curve represents the V_G=0V, the blue one V_G=2.5V, the magenta V_G=5V, the black line V_G=-2.5V and the green stands for V_G=-5V.

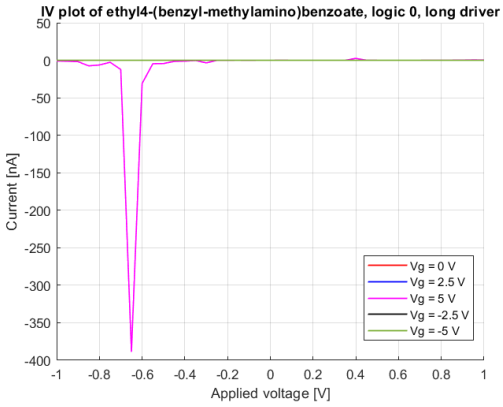

(a) logic '0' configuration.

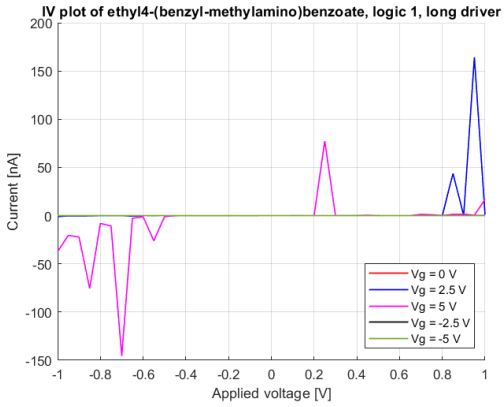

(b) logic '1' configuration.

Figure 6.286: Picture of IV for the Ethyl4-(benzyl-methylamino) benzoate molecule varying the gate voltage. The red curve represents the V_G=0V, the blue one V_G=2.5V, the magenta V_G=5V, the black line V_G=-2.5V and the green stands for V_G=-5V.

In general, an asymmetric molecule fits well for the gate electrode because it has a higher probability of ON/OFF TS with respect to the symmetric molecules. The Ethyl4-(benzyl-methylamino) benzoate molecule is not able to drive a consistent amount of current, it must be studied as a strongly asymmetric molecule that exhibits good conduction properties.

The polar molecules have not yet been studied within molecular junctions but for the readout system for molFCN they should be investigated for they asymmetric geometries.

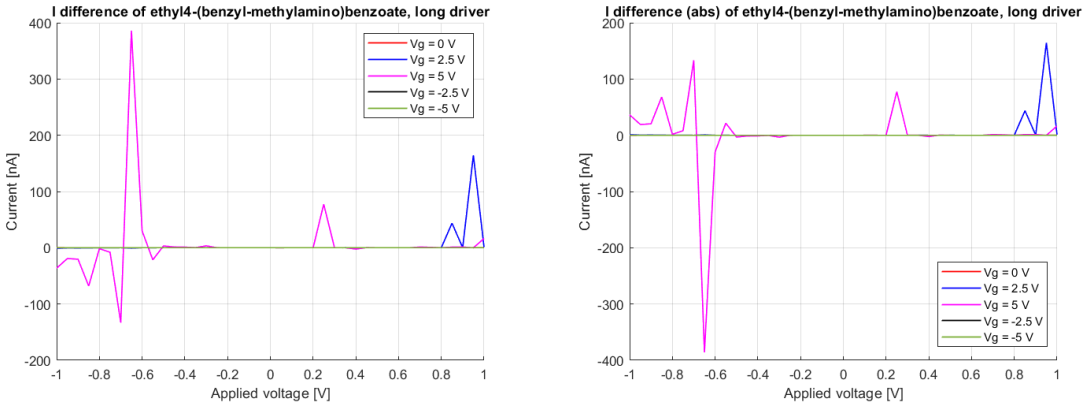

(a) logic '1' - logic '0'.

(b) |logic '1'| - |logic '0'|.

Figure 6.287: Picture of current difference for the Ethyl4-(benzyl-methylamino) benzoate molecule varying the gate voltage. The red curve represents the V_G=0V, the blue one V_G=2.5V, the magenta V_G=5V, the black line V_G=-2.5V and the green stands for V_G=-5V.

6.13 Different distances to the junction

These analyses have been performed to investigate the robustness of the readout system at the fabrication tolerances. In particular, the driver has been shifted at longer distances to observe the current trend. A decrement of the current is expected, but if it is small the readout system can work even considering fabrication tolerances. The OPV3 and OPE3 molecules show interesting results, therefore they have been simulated with the driver at different distances for testing their flexibility to the non-idealities. These two molecules have been selected not only for their property but also because they are currently employed in molecular junctions.

6.13.1 OPV3: long driver

In the four builders in figures 6.288 (logic '0' configuration) and 6.289 (logic '1' configuration) can be noticed the driver distance with respect to the junction molecule. In addition to the simulation with a distance of 7 Å, two additional cases have been selected, the two distances are respectively 10.5 Å and 14 Å.

In the figure 6.290 is possible to observe the TS for the two logic values. The trend of the curves remains the same in each case, the difference is related to the amplitude of the peaks. In particular, the LUMO peak from 7 Å to 10.5 Å sees a decrease in the maximum value, while it shifts to higher energies for the 14 Å one.

As expected the current becomes smaller as the distance between the driver and junction increases, we can notice it in the figure 6.291. For low values of voltage (below 0.2 V) the current assumes the same value (roughly) for all three cases, while when the voltage is higher the current difference is more relevant.

Figure 6.292 is a fundamental proof of the feasibility of the readout system because it

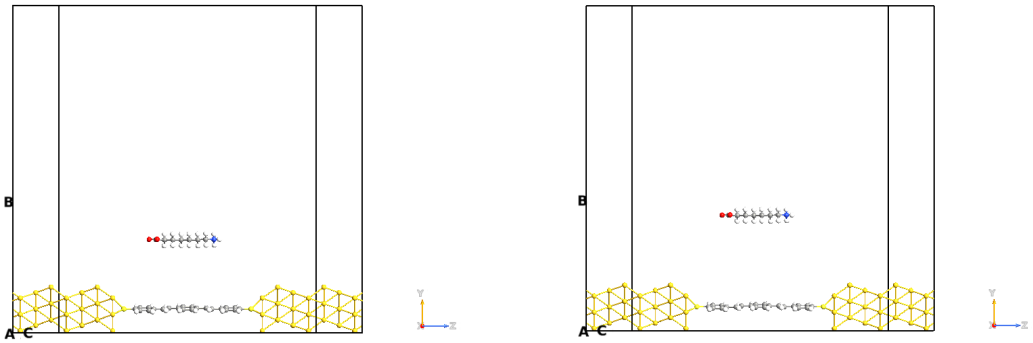

(a) Distance between junction molecule and driver equal to 10.5 Å.

(b) Distance between junction molecule and driver equal to 14 Å.

Figure 6.288: Picture of the QuantumATK builder for the OPV3 molecule, logic '0' configuration with the long driver at a different distance. The white atoms are the hydrogens, the yellow ones are gold atoms, the lighter yellow ones are the sulfurs, the blue ones are nitrogens, the reds are the oxygens and the grey atoms are carbons.

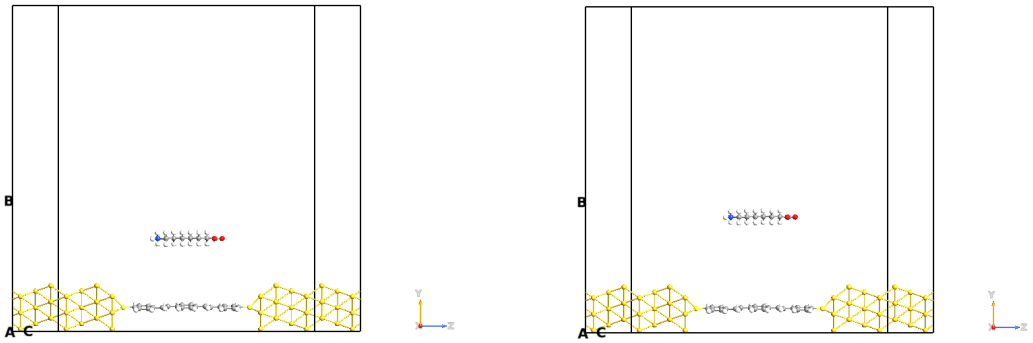

(a) Distance between junction molecule and driver equal to 10.5 Å.

(b) Distance between junction molecule and driver equal to 14 Å.

Figure 6.289: Picture of the QuantumATK builder for the OPV3 molecule, logic '1' configuration with the long driver at a different distance. The white atoms are the hydrogens, the yellow ones are gold atoms, the lighter yellow ones are the sulfurs, the blue ones are nitrogens, the reds are the oxygens and the grey atoms are carbons.

is possible to observe that around the 0.35 V (the peak with the largest difference between the two configurations) the current difference in the worst case (14 Å of distance) is higher than 2 μA, which can be detected easily for the modern electronic. The results are more than satisfactory.

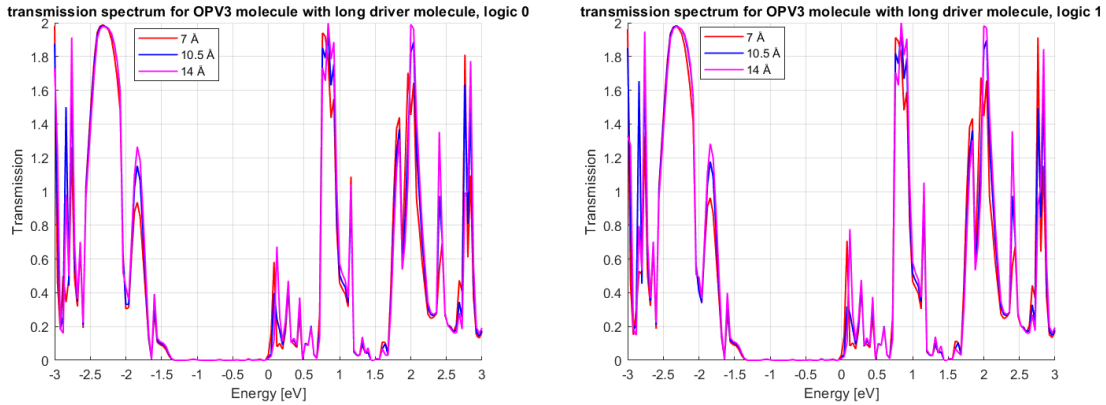

(a) logic '0' configuration.

(b) logic '1' configuration.

Figure 6.290: Picture of the TS for the OPV3 molecule considering the long driver at different distances, in particular, the red curve is obtained with the driver at a distance of 7 Å, the blue one at a distance 10.5 Å and the magenta one at 14 Å.

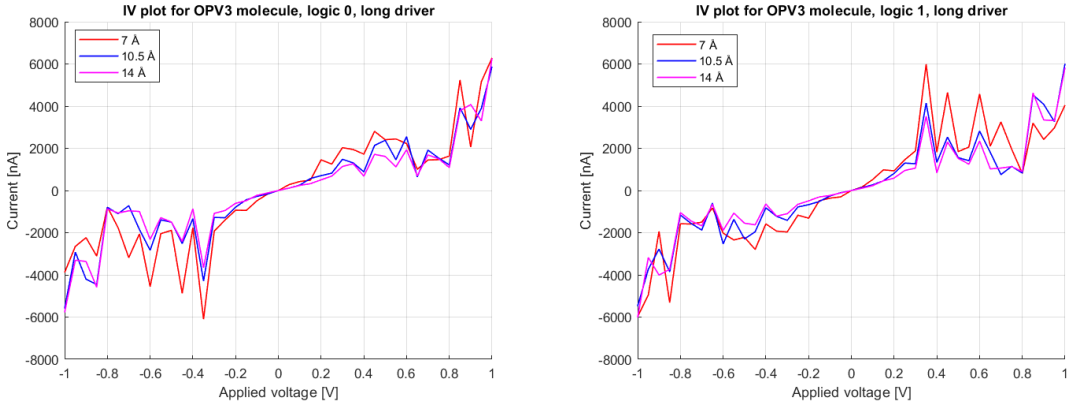

(a) logic 0 configuration.

(b) logic 1 configuration.

Figure 6.291: Picture of the IV for the OPV3 molecule considering the long driver at different distances, in particular, the red curve is obtained with the driver at a distance of 7 Å, the blue one at a distance 10.5 Å and the magenta one at 14 Å.

The orbital views confirm the trend seen in the previous cases. The aim of this section is to compare the different distance influences on the molecular junction, for this reason, the pictures in the figure are for the same logic value but at different distances. The figures from 6.293 to 6.304 refer to the logic '0' configuration, while from 6.305 to 6.316 refer to the logic '1'.

The orbital behavior reveals two main cases, the same trend between the two configurations or the complementary geometry. It is difficult to derive some comclusions considering the orbital plots.

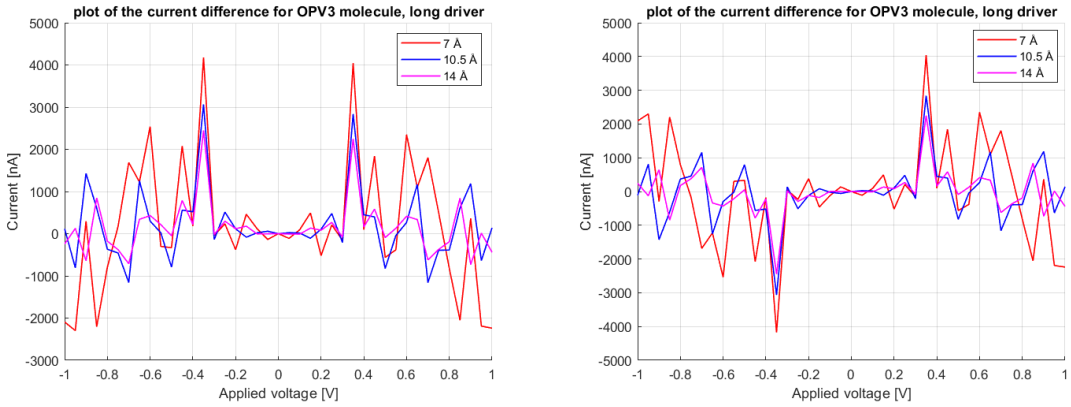

(a) logic '1' - logic '0'.

(b) |logic '1'| - |logic '0'|.

Figure 6.292: Picture of the current difference between the two configurations for the OPV3 molecule considering the long driver at different distances, in particular, the red curve is obtained with the driver at a distance of 7 Å, the blue one at a distance 10.5 Å and the magenta one at 14 Å.

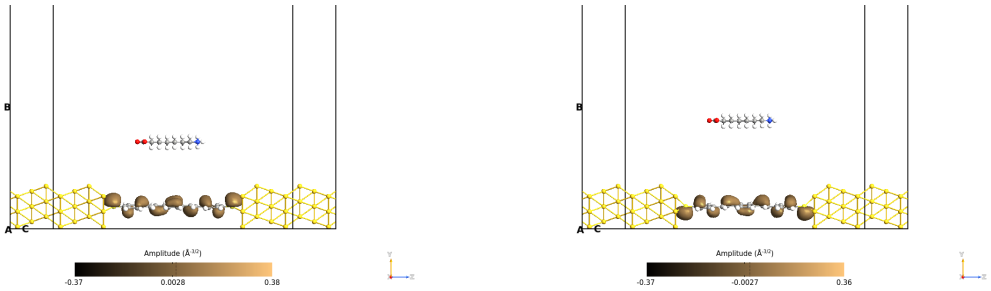

(a) Distance 10.5 Å.

(b) Distance 14 Å.

Figure 6.293: Picture of the orbitals corresponding to the HOMO-1 level for the OPV3 molecule with long driver at different distances, logic '0' configuration, on the yz plane. The orbitals are taken with an isosurface value equal to 0.015.

The transmission pathways don't reveal surprises, they confirm the previous trend. The figures from 6.317 to 6.322 refer to the logic '0' configuration, while from 6.323 to 6.328 to the logic '1' one.

For the plots concerning the angle, as expected, the higher the energy, the higher the amount of electrons that flow in the opposite direction with respect to the conduction direction.

The weight graphs show the same trend that the TS (figure 6.290) tells us. Higher is the magnitude value according to the amplitude of the peak in the TS.

The OPV3 molecule LUMO peaks shift to higher energies when the electric field is lower (small driver or long distance), for this reason, four plots (figures 6.317, 6.320, 6.323 and 6.326) are taken for different energies.

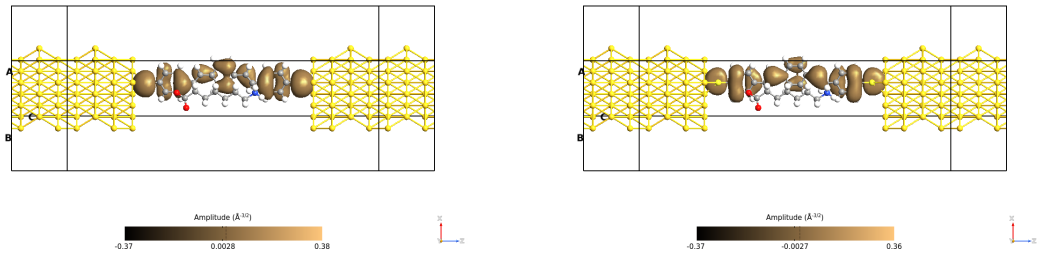

(a) Distance 10.5 Å. (b) Distance 14 Å.

Figure 6.294: Picture of the orbitals corresponding to the HOMO-1 level for the OPV3 molecule with long driver at different distances, logic '0' configuration, on the xz plane with the driver. The orbitals are taken with an isosurface value equal to 0.015.

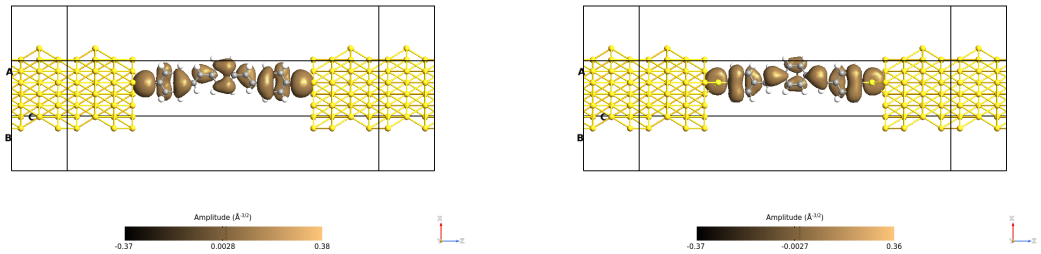

(a) Distance 10.5 Å. (b) Distance 14 Å.

Figure 6.295: Picture of the orbitals corresponding to the HOMO-1 level for the OPV3 molecule with long driver at different distances, logic '0' configuration, on the xz plane without the driver. The orbitals are taken with an isosurface value equal to 0.015.

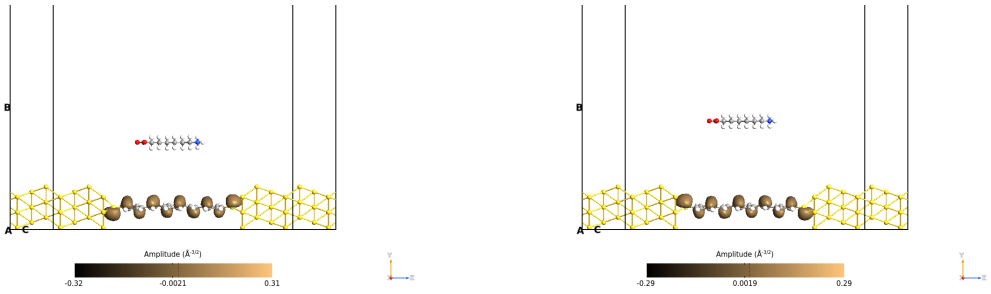

(a) Distance 10.5 Å. (b) Distance 14 Å.

Figure 6.296: Picture of the orbitals corresponding to the HOMO level for the OPV3 molecule with long driver at different distances, logic '0' configuration, on the yz plane. The orbitals are taken with an isosurface value equal to 0.015.

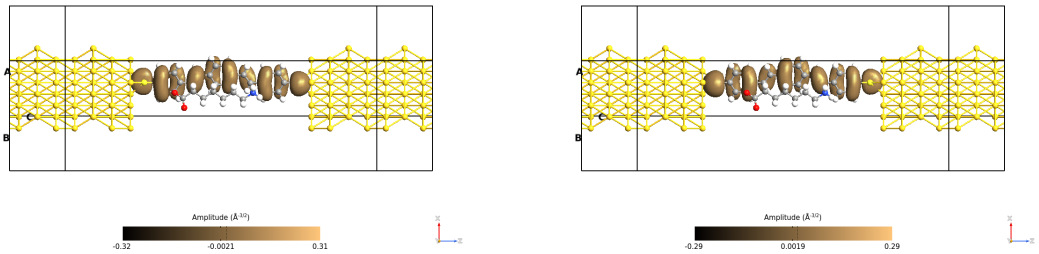

(a) Distance 10.5 Å. (b) Distance 14 Å.

Figure 6.297: Picture of the orbitals corresponding to the HOMO level for the OPV3 molecule with long driver at different distances, logic '0' configuration, on the xz plane with the driver. The orbitals are taken with an isosurface value equal to 0.015.

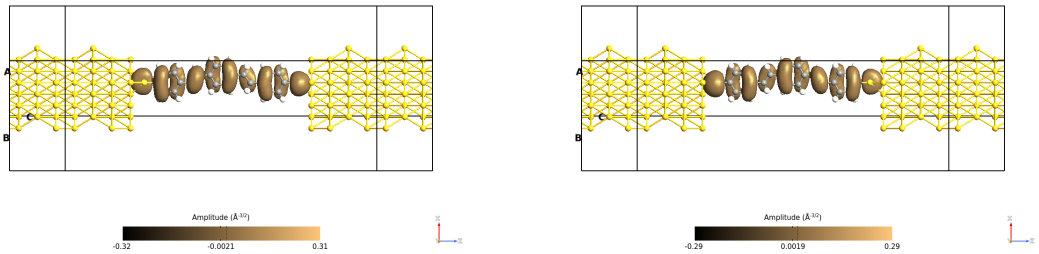

(a) Distance 10.5 Å. (b) Distance 14 Å.

Figure 6.298: Picture of the orbitals corresponding to the HOMO level for the OPV3 molecule with long driver at different distances, logic '0' configuration, on the xz plane without the driver. The orbitals are taken with an isosurface value equal to 0.015.

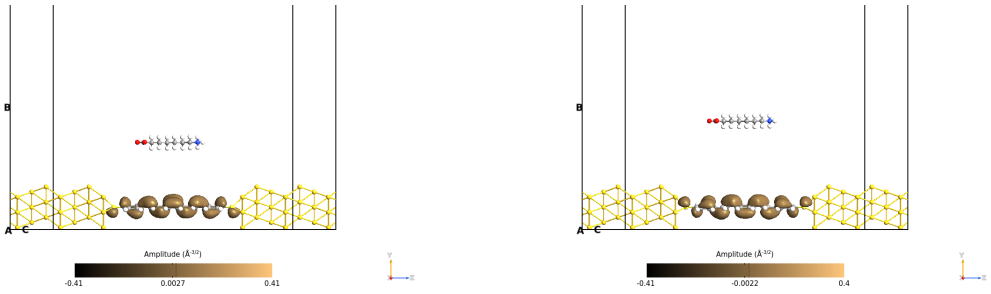

(a) Distance 10.5 Å. (b) Distance 14 Å.

Figure 6.299: Picture of the orbitals corresponding to the LUMO level for the OPV3 molecule with long driver at different distances, logic '0' configuration, on the yz plane. The orbitals are taken with an isosurface value equal to 0.015.

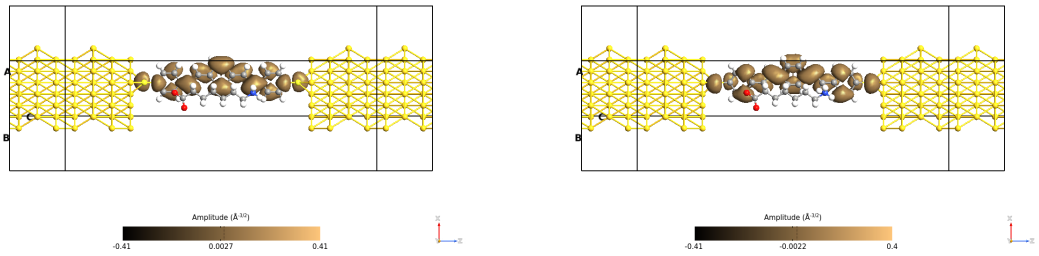

(a) Distance 10.5 Å. (b) Distance 14 Å.

Figure 6.300: Picture of the orbitals corresponding to the LUMO level for the OPV3 molecule with long driver at different distances, logic '0' configuration, on the xz plane with the driver. The orbitals are taken with an isosurface value equal to 0.015.

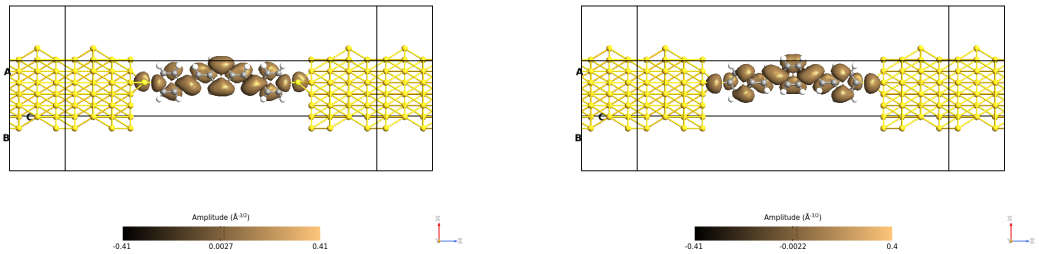

(a) Distance 10.5 Å. (b) Distance 14 Å.

Figure 6.301: Picture of the orbitals corresponding to the LUMO level for the OPV3 molecule with long driver at different distances, logic '0' configuration, on the xz plane without the driver. The orbitals are taken with an isosurface value equal to 0.015.

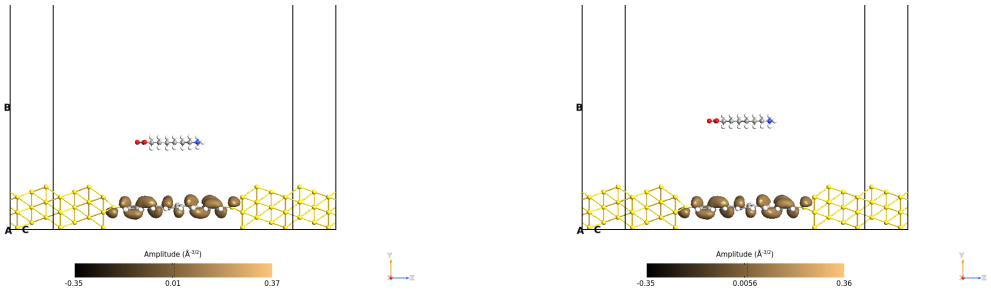

(a) Distance 10.5 Å. (b) Distance 14 Å.

Figure 6.302: Picture of the orbitals corresponding to the LUMO+1 level for the OPV3 molecule with long driver at different distances, logic '0' configuration, on the yz plane. The orbitals are taken with an isosurface value equal to 0.015.

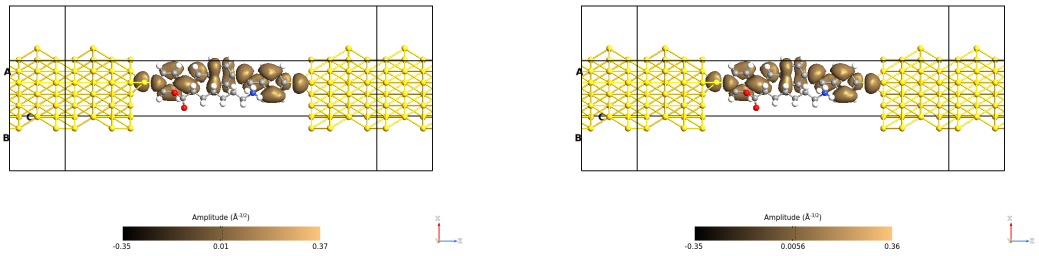

(a) Distance 10.5 Å. (b) Distance 14 Å.

Figure 6.303: Picture of the orbitals corresponding to the LUMO+1 level for the OPV3 molecule with long driver at different distances, logic '0' configuration, on the xz plane with the driver. The orbitals are taken with an isosurface value equal to 0.015.

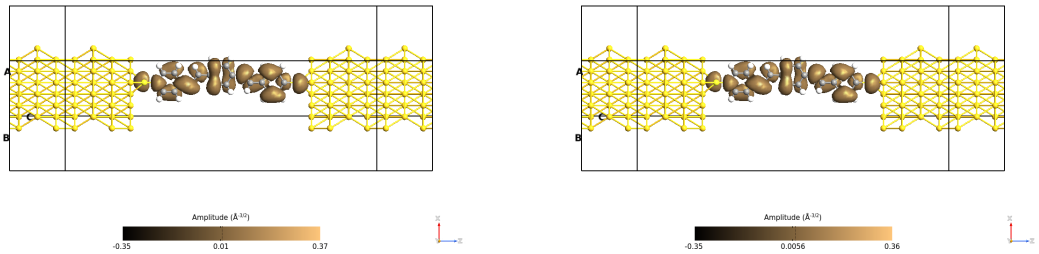

(a) Distance 10.5 Å. (b) Distance 14 Å.

Figure 6.304: Picture of the orbitals corresponding to the LUMO+1 level for the OPV3 molecule with long driver at different distances, logic '0' configuration, on the xz plane without the driver. The orbitals are taken with an isosurface value equal to 0.015.

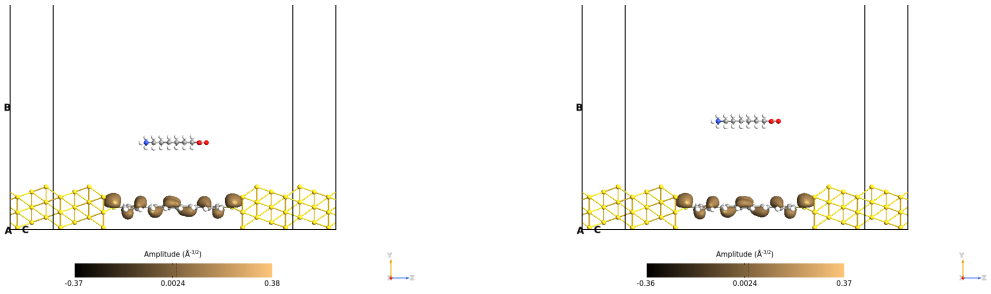

(a) Distance 10.5 Å. (b) Distance 14 Å.

Figure 6.305: Picture of the orbitals corresponding to the HOMO-1 level for the OPV3 molecule with long driver at different distances, logic '1' configuration, on the yz plane. The orbitals are taken with an isosurface value equal to 0.015.

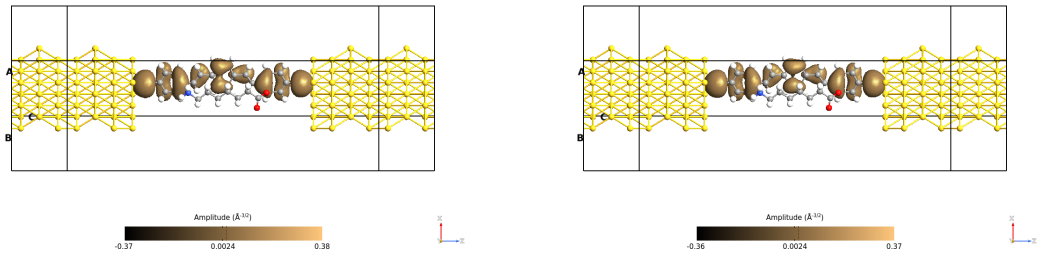

(a) Distance 10.5 Å. (b) Distance 14 Å.

Figure 6.306: Picture of the orbitals corresponding to the HOMO-1 level for the OPV3 molecule with long driver at different distances, logic '1' configuration, on the xz plane with the driver. The orbitals are taken with an isosurface value equal to 0.015.

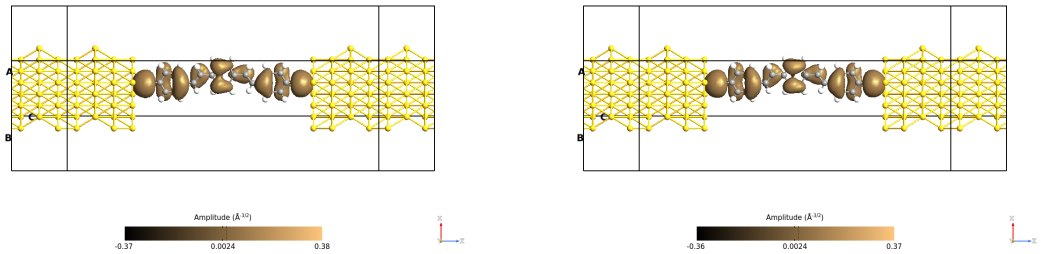

(a) Distance 10.5 Å. (b) Distance 14 Å.

Figure 6.307: Picture of the orbitals corresponding to the HOMO-1 level for the OPV3 molecule with long driver at different distances, logic '1' configuration, on the xz plane without the driver. The orbitals are taken with an isosurface value equal to 0.015.

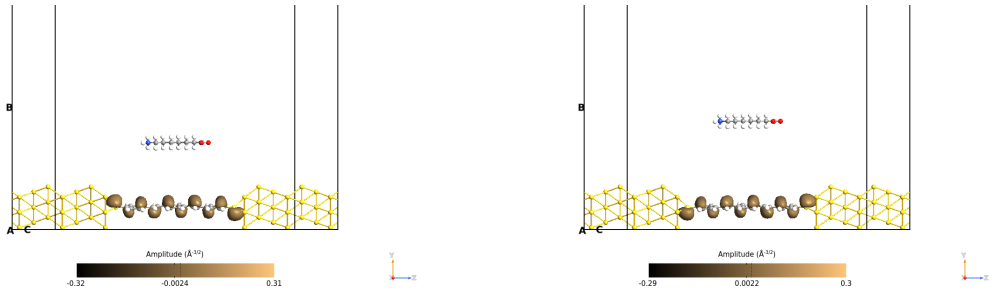

(a) Distance 10.5 Å. (b) Distance 14 Å.

Figure 6.308: Picture of the orbitals corresponding to the HOMO level for the OPV3 molecule with long driver at different distances, logic '1' configuration, on the yz plane. The orbitals are taken with an isosurface value equal to 0.015.

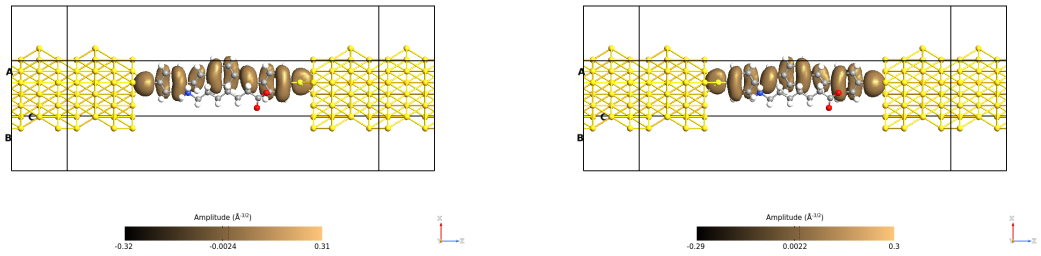

(a) Distance 10.5 Å. (b) Distance 14 Å.

Figure 6.309: Picture of the orbitals corresponding to the HOMO level for the OPV3 molecule with long driver at different distances, logic '1' configuration, on the xz plane with the driver. The orbitals are taken with an isosurface value equal to 0.015.

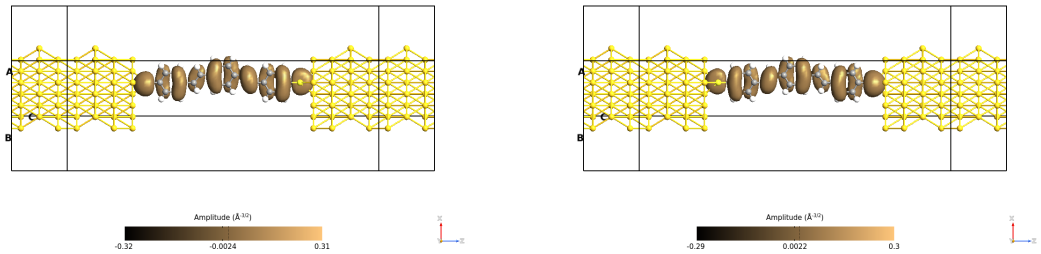

(a) Distance 10.5 Å. (b) Distance 14 Å.

Figure 6.310: Picture of the orbitals corresponding to the HOMO level for the OPV3 molecule with long driver at different distances, logic '1' configuration, on the xz plane without the driver. The orbitals are taken with an isosurface value equal to 0.015.

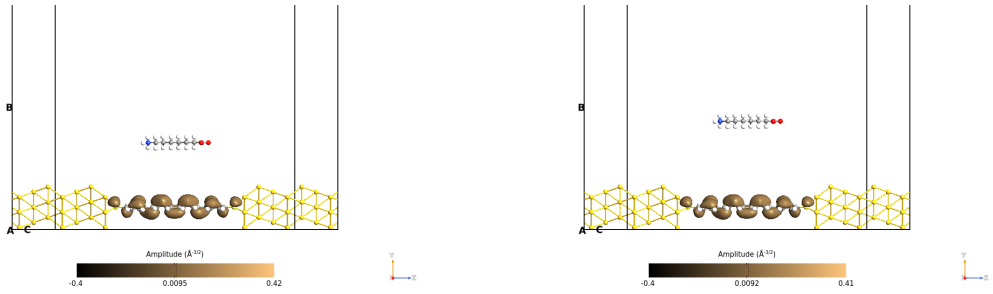

(a) Distance 10.5 Å. (b) Distance 14 Å.

Figure 6.311: Picture of the orbitals corresponding to the LUMO level for the OPV3 molecule with long driver at different distances, logic '1' configuration, on the yz plane. The orbitals are taken with an isosurface value equal to 0.015.

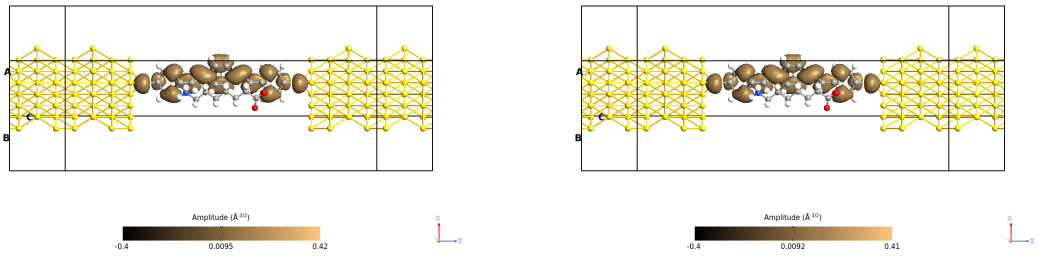

(a) Distance 10.5 Å. (b) Distance 14 Å.

Figure 6.312: Picture of the orbitals corresponding to the LUMO level for the OPV3 molecule with long driver at different distances, logic '1' configuration, on the xz plane with the driver. The orbitals are taken with an isosurface value equal to 0.015.

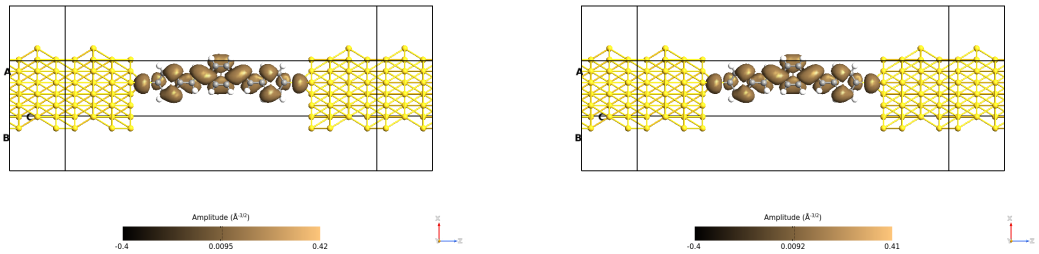

(a) Distance 10.5 Å. (b) Distance 14 Å.

Figure 6.313: Picture of the orbitals corresponding to the LUMO level for the OPV3 molecule with long driver at different distances, logic '1' configuration, on the xz plane without the driver. The orbitals are taken with an isosurface value equal to 0.015.

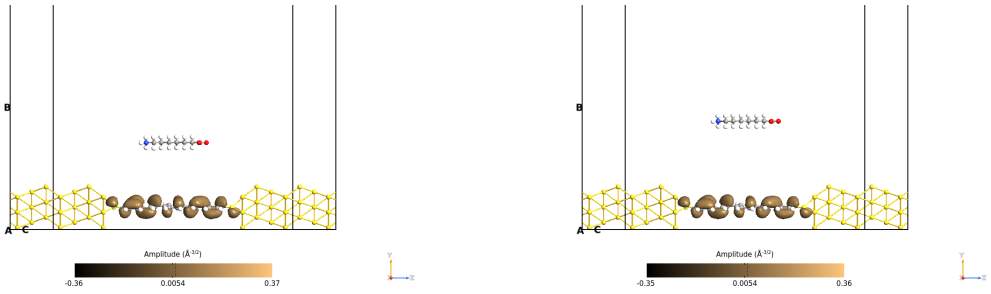

(a) Distance 10.5 Å. (b) Distance 14 Å.

Figure 6.314: Picture of the orbitals corresponding to the LUMO+1 level for the OPV3 molecule with long driver at different distances, logic '1' configuration, on the yz plane. The orbitals are taken with an isosurface value equal to 0.015.

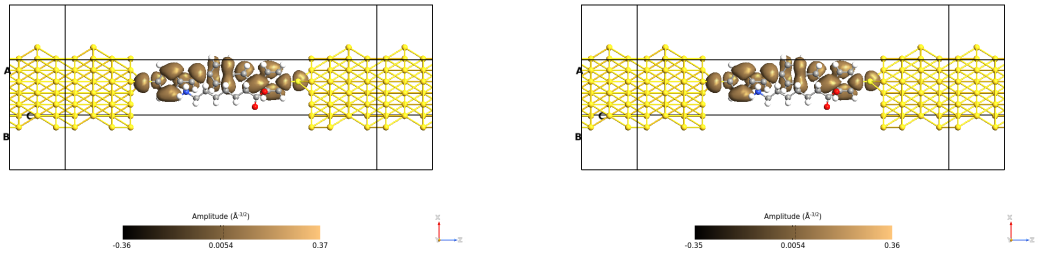

(a) Distance 10.5 Å. (b) Distance 14 Å.

Figure 6.315: Picture of the orbitals corresponding to the LUMO+1 level for the OPV3 molecule with long driver at different distances, logic '1' configuration, on the xz plane with the driver. The orbitals are taken with an isosurface value equal to 0.015.

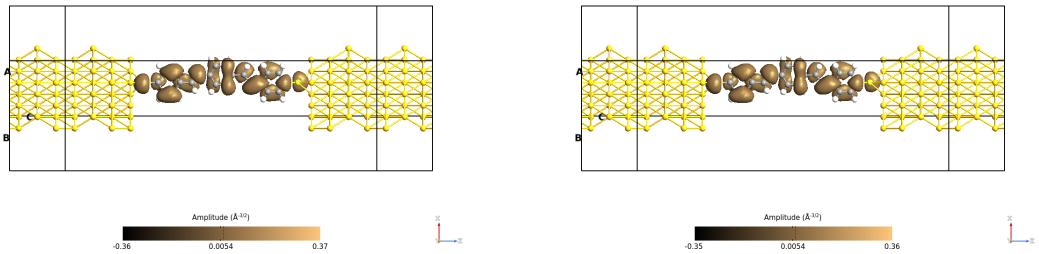

(a) Distance 10.5 Å. (b) Distance 14 Å.

Figure 6.316: Picture of the orbitals corresponding to the LUMO+1 level for the OPV3 molecule with long driver at different distances, logic '1' configuration, on the xz plane without the driver. The orbitals are taken with an isosurface value equal to 0.015.

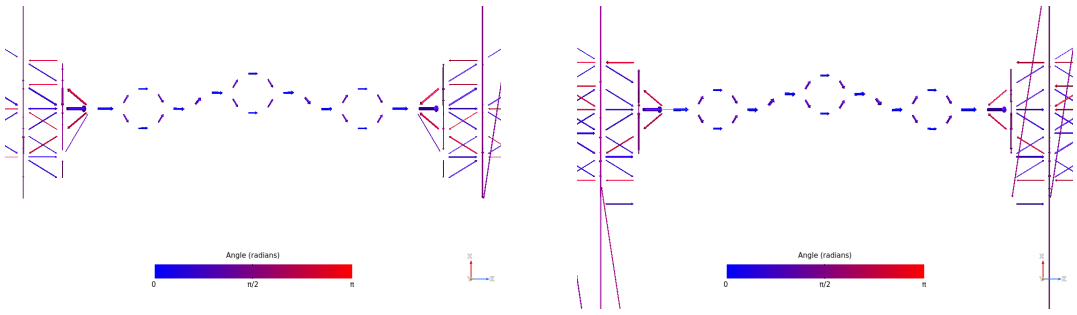

(a) Distance 10.5 Å, energy 0.08 eV. (b) Distance 14 Å, energy 0.12 eV.

Figure 6.317: Picture of the transmission pathways for the OPV3 molecule with long driver at different distances concerning the angle, logic '0' configuration, on the xz plane.

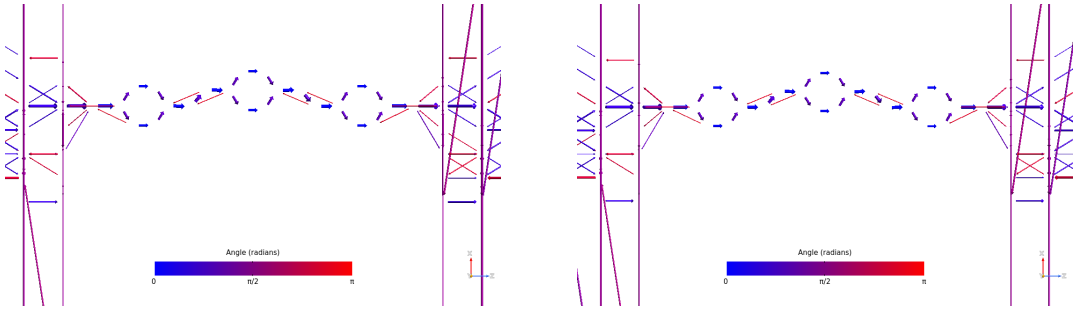

(a) Distance 10.5 Å. (b) Distance 14 Å.

Figure 6.318: Picture of the transmission pathways corresponding to the energy 0.28 eV concerning the angle, for the OPV3 molecule with long driver at different distances, logic '0' configuration, on the xz plane.

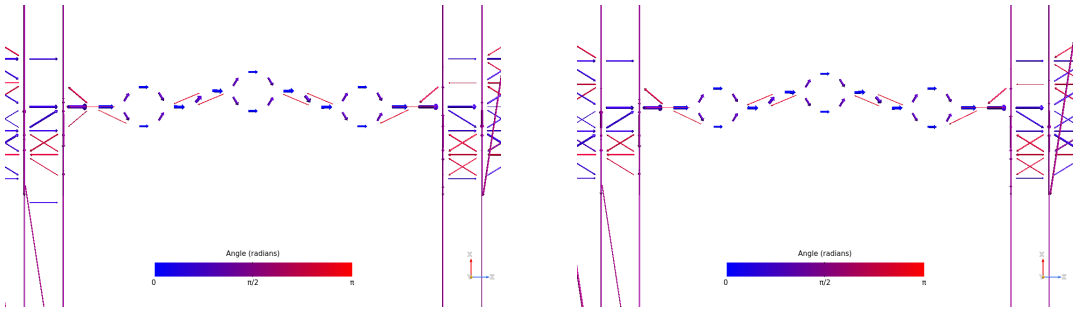

(a) Distance 10.5 Å. (b) Distance 14 Å.

Figure 6.319: Picture of the transmission pathways corresponding to the energy 0.44 eV concerning the angle, for the OPV3 molecule with long driver at different distances, logic '0' configuration, on the xz plane.

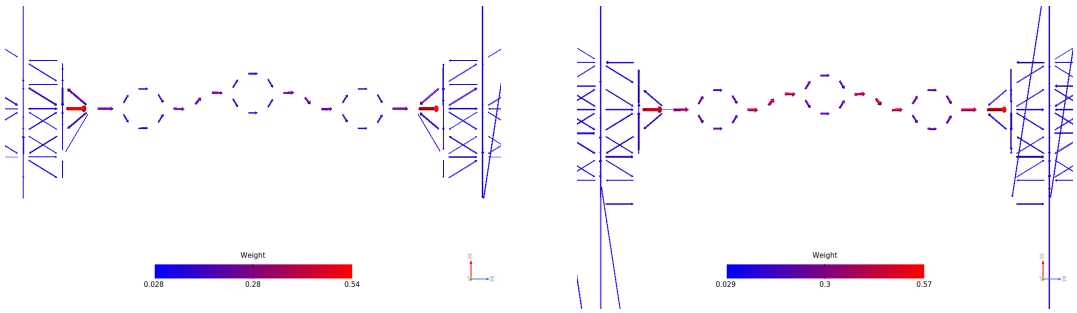

(a) Distance 10.5 Å, energy 0.08 eV. (b) Distance 14 Å, energy 0.12 eV.

Figure 6.320: Picture of the pathways for the OPV3 molecule with long driver at different distance, logic '0' configuration, on the xz plane. The plots show the arrows' magnitude.

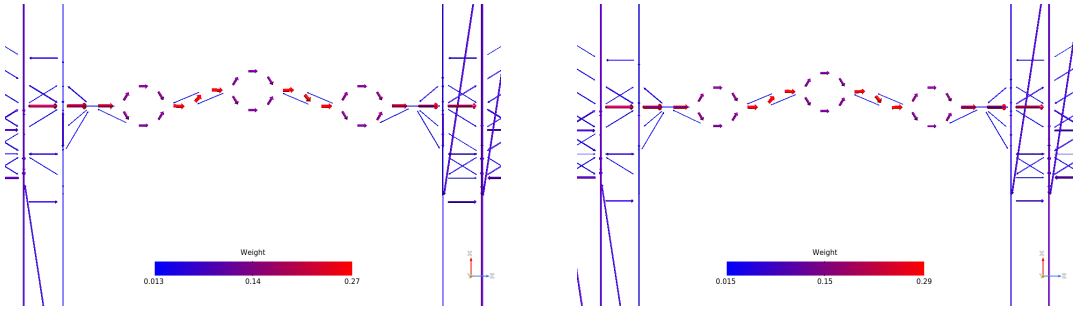

(a) Distance 10.5 Å. (b) Distance 14 Å.

Figure 6.321: Picture of the pathways corresponding to the energy 0.28 eV for the OPV3 molecule with long driver at different distance, logic '0' configuration, on the xz plane. The plots show the arrows' magnitude.

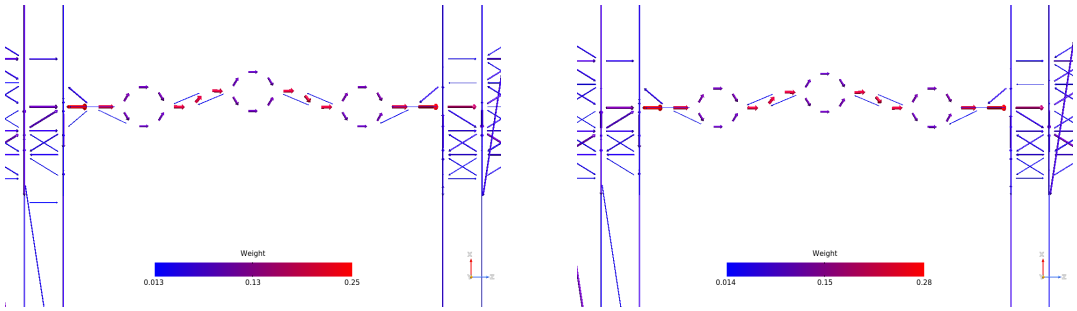

(a) Distance 10.5 Å. (b) Distance 14 Å.

Figure 6.322: Picture of the pathways corresponding to the energy 0.44 eV for the OPV3 molecule with long driver at different distance, logic '0' configuration, on the xz plane. The plots show the arrows' magnitude.

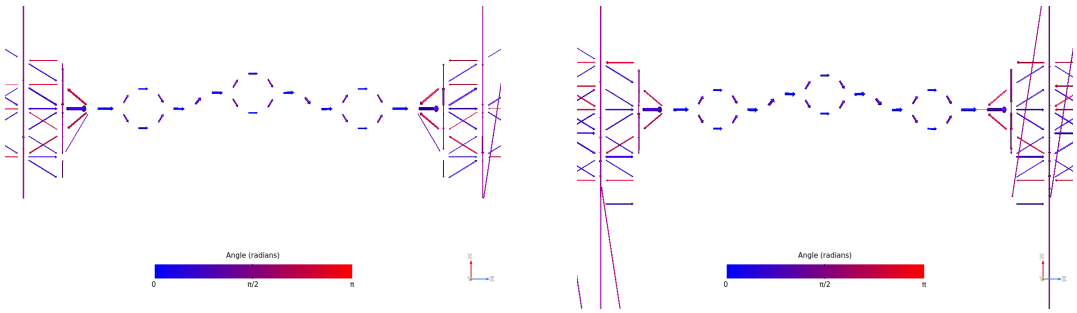

(a) Distance 10.5 Å, energy 0.08 eV. (b) Distance 14 Å, energy 0.12 eV.

Figure 6.323: Picture of the transmission pathways concerning the angle, for the OPV3 molecule with long driver at different distances, logic '1' configuration, on the xz plane.

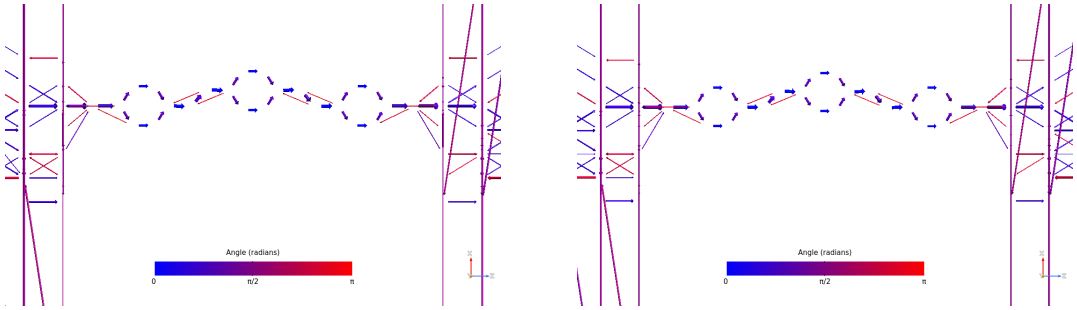

(a) Distance 10.5 Å. (b) Distance 14 Å.

Figure 6.324: Picture of the transmission pathways corresponding to the energy 0.28 eV concerning the angle, for the OPV3 molecule with long driver at different distances, logic '1' configuration, on the xz plane.

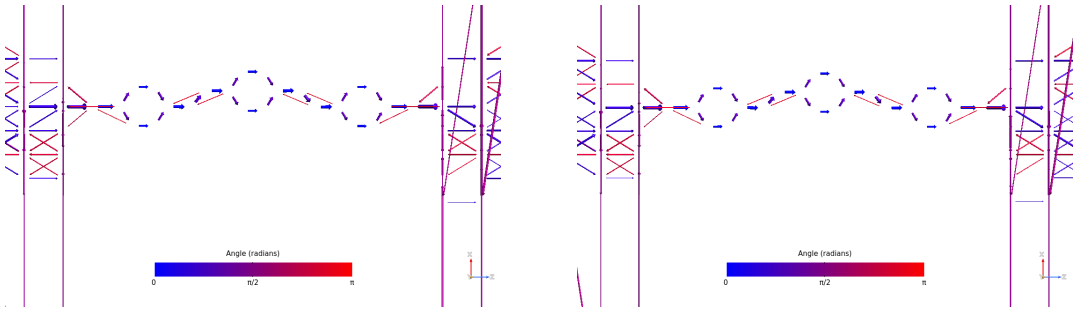

(a) Distance 10.5 Å. (b) Distance 14 Å.

Figure 6.325: Picture of the transmission pathways corresponding to the energy 0.44 eV concerning the angle, for the OPV3 molecule with long driver at different distances, logic '1' configuration, on the xz plane.

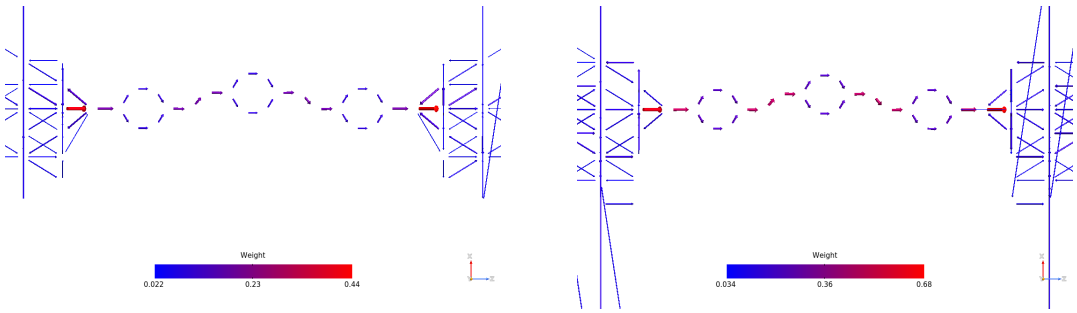

(a) Distance 10.5 Å, energy 0.08 eV. (b) Distance 14 Å, energy 0.12 eV.

Figure 6.326: Picture of the pathways for the OPV3 molecule with long driver at different distance, logic '1' configuration, on the xz plane. The plots show the arrows' magnitude.

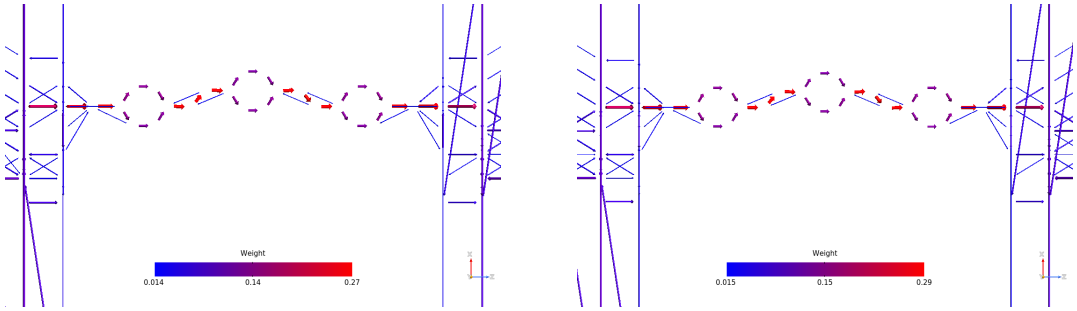

(a) Distance 10.5 Å. (b) Distance 14 Å.

Figure 6.327: Picture of the pathways corresponding to the energy 0.28 eV for the OPV3 molecule with long driver at different distance, logic '1' configuration, on the xz plane. The plots show the arrows' magnitude.

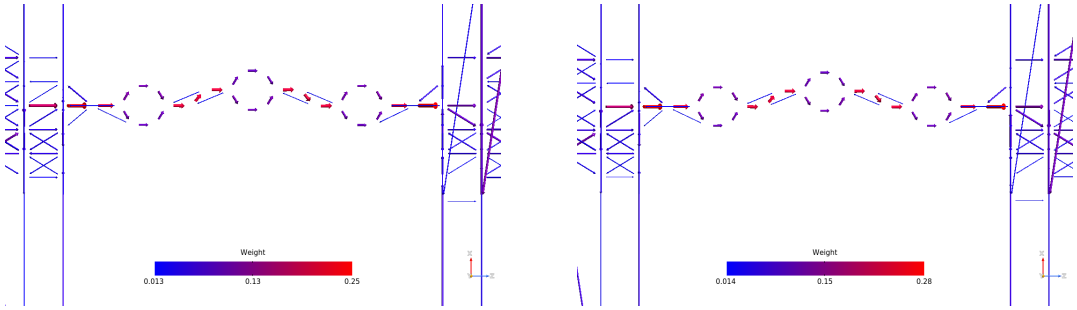

(a) Distance 10.5 Å. (b) Distance 14 Å.

Figure 6.328: Picture of the pathways corresponding to the energy 0.44 eV for the OPV3 molecule with long driver at different distance, logic '1' configuration, on the xz plane. The plots show the arrows' magnitude.

6.13.2 OPV3: small driver

The OPV3 builders with the small driver at different distances are reported in the figures 6.329 and 6.330, in particular, the figure 6.329 regards the logic '0' configuration, while the figure 6.330 for the logic '1' one.

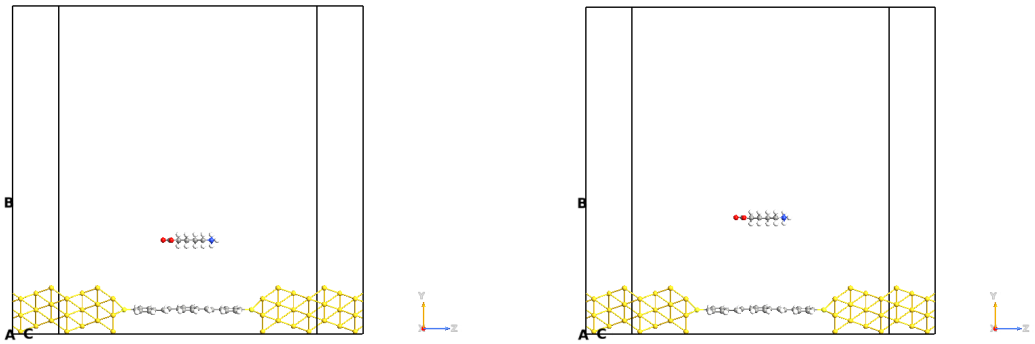

(a) Distance between junction molecule and driver equal to 10.5 Å.

(b) Distance between junction molecule and driver equal to 14 Å.

Figure 6.329: Picture of the QuantumATK builder for the OPV3 molecule, logic '0' configuration with the small driver at a different distance. The white atoms are the hydrogens, the yellow ones are gold atoms, the lighter yellow ones are the sulfurs, the blue ones are nitrogens, the reds are the oxygens and the grey atoms are carbons.

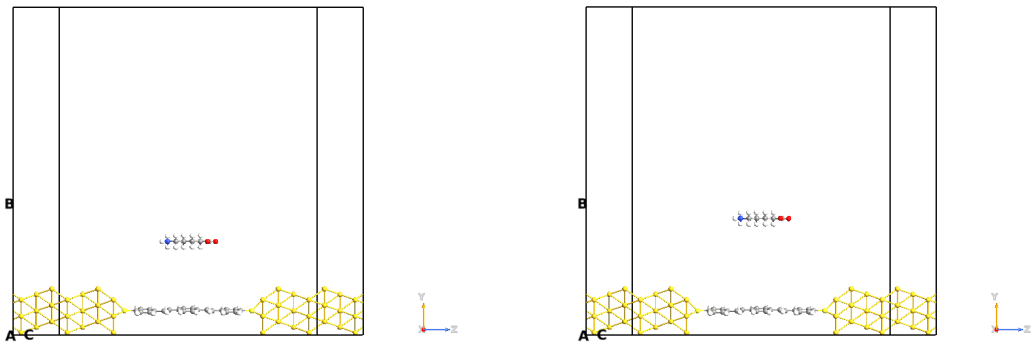

(a) Distance between junction molecule and driver equal to 10.5 Å.

(b) Distance between junction molecule and driver equal to 14 Å.

Figure 6.330: Picture of the QuantumATK builder for the OPV3 molecule, logic '1' configuration with the small driver at a different distance. The white atoms are the hydrogens, the yellow ones are gold atoms, the lighter yellow ones are the sulfurs, the blue ones are nitrogens, the reds are the oxygens and the grey atoms are carbons.

As for the long driver, the small driver results confirm the possibility of performing the readout system through a molecular junction. In figure 6.331 are reported the TS for the two logic values. Also in this case it is possible to see the LUMO peak decrease and

shift for larger distances.

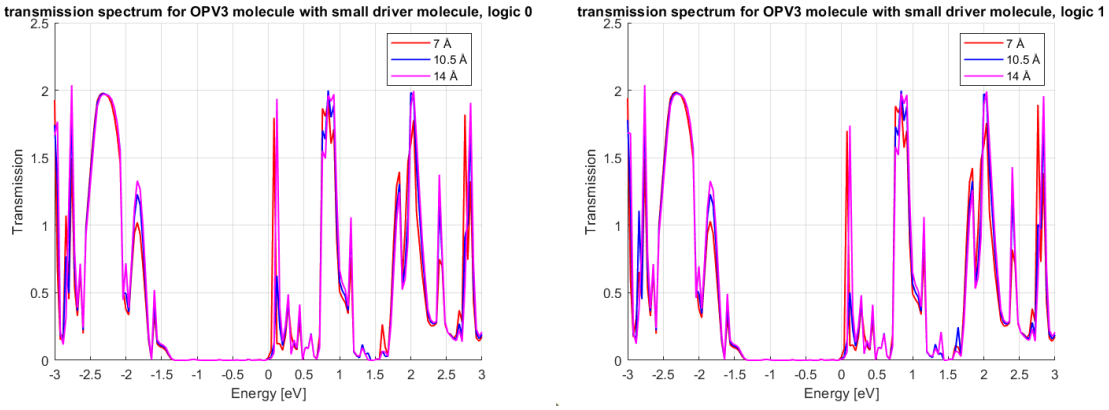

(a) logic 0 configuration.

(b) logic 1 configuration.

Figure 6.331: Picture of the TS for the OPV3 molecule considering the small driver at different distances, in particular the red curve is obtained with the driver at a distance of 7 Å, the blue one at a distance 10.5 Å and the magenta one at 14 Å.

For the IV plots (figure 6.332) can be made the same considerations than the long driver case, the only difference is that also for low values of voltage the current is different between the three cases.

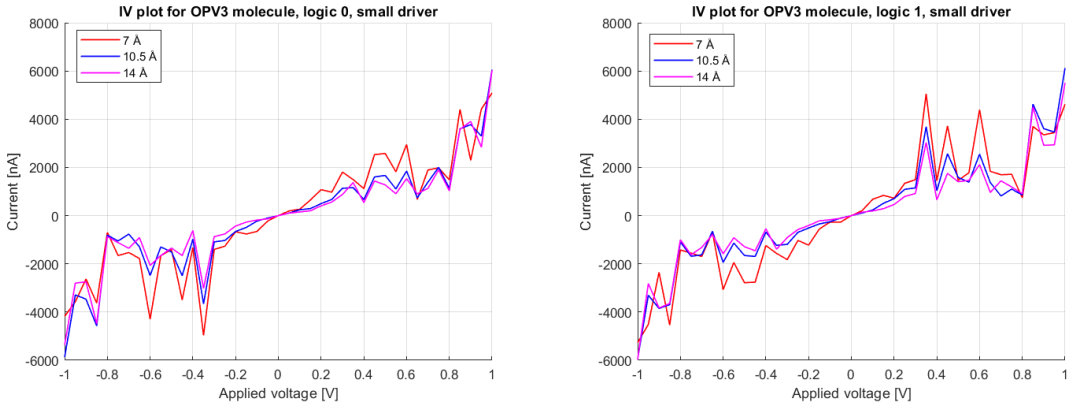

(a) logic 0 configuration.

(b) logic 1 configuration.

Figure 6.332: Picture of the IV for the OPV3 molecule considering the small driver at different distances, in particular the red curve is obtained with the driver at a distance of 7 Å, the blue one at a distance 10.5 Å and the magenta one at 14 Å.

The figure 6.333 shows the current difference between logic '1' and logic '0' configurations. In this case, the minimum value (of course it is associated to the 14 Å of distance) is about 1.5 μA, lower than the long driver cases, but it is still detectable easily by today's technology.

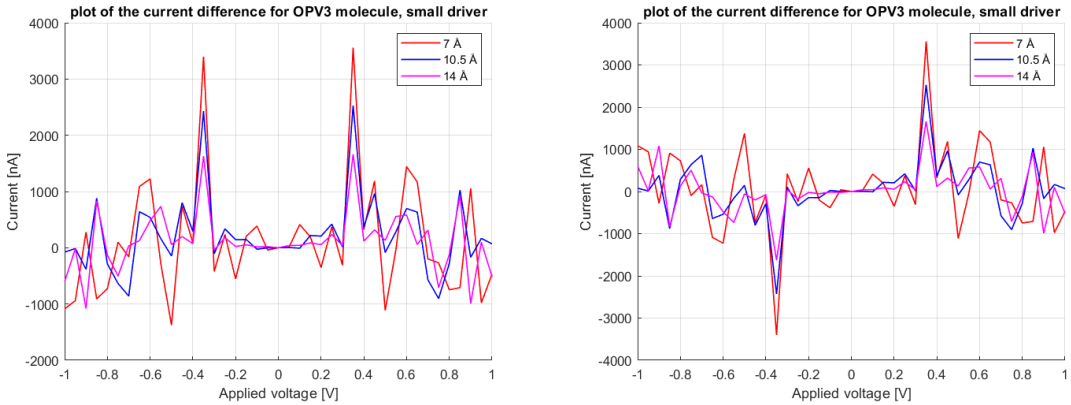

(a) logic '1' - logic '0'.

(b) |logic '1'| - |logic '0'|.

Figure 6.333: Picture of the current difference between the two configurations for the OPV3 molecule considering the small driver at different distances, in particular, the red curve is obtained with the driver at a distance of 7 Å, the blue one at a distance 10.5 Å and the magenta one at 14 Å.

The orbital views of the logic '0' configuration reveal the same behavior for the HOMO-1 (figures 6.334, 6.335 and 6.336), HOMO (figures 6.337, 6.338 and 6.339) and LUMO (figures 6.340, 6.341 and 6.342) levels, while the complementary one for the LUMO+1 energy level (figures 6.343, 6.344 and 6.345).

The logic '1' orbitals, instead, show the same behavior for the HOMO-1 (figures 6.346, 6.347 and 6.348) and HOMO (figures 6.349, 6.350 and 6.351), while the LUMO (figures 6.352, 6.353 and 6.354) and LUMO+1 (figures 6.355, 6.356 and 6.357) exhibit complementary trend.

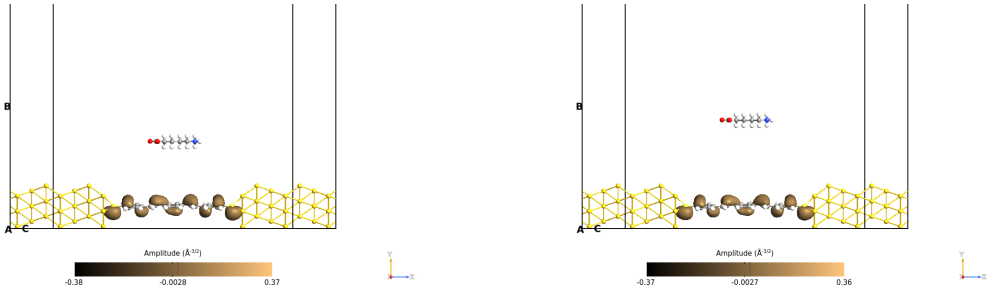

(a) Distance 10.5 Å.

(b) Distance 14 Å.

Figure 6.334: Picture of the orbitals corresponding to the HOMO-1 level for the OPV3 molecule with small driver at different distances, logic '0' configuration, on the yz plane. The orbitals are taken with an isosurface value equal to 0.015.

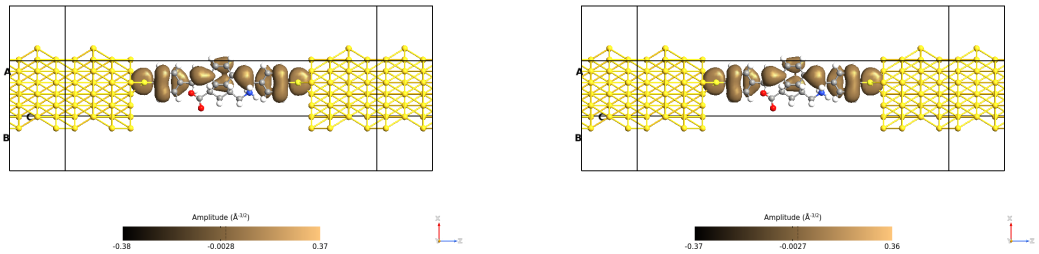

(a) Distance 10.5 Å. (b) Distance 14 Å.

Figure 6.335: Picture of the orbitals corresponding to the HOMO-1 level for the OPV3 molecule with small driver at different distances, logic '0' configuration, on the xz plane with the driver. The orbitals are taken with an isosurface value equal to 0.015.

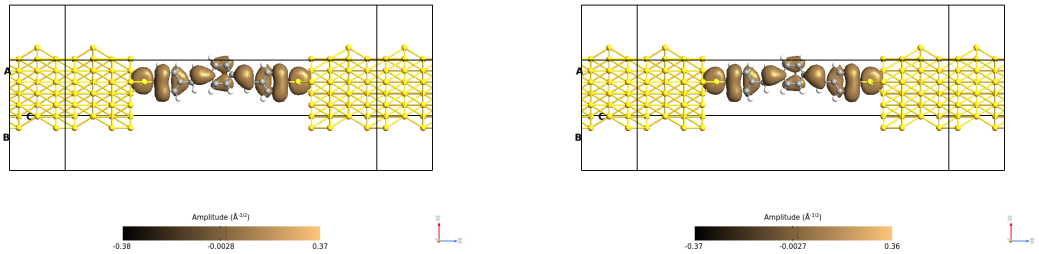

(a) Distance 10.5 Å. (b) Distance 14 Å.

Figure 6.336: Picture of the orbitals corresponding to the HOMO-1 level for the OPV3 molecule with small driver at different distances, logic '0' configuration, on the xz plane without the driver. The orbitals are taken with an isosurface value equal to 0.015.

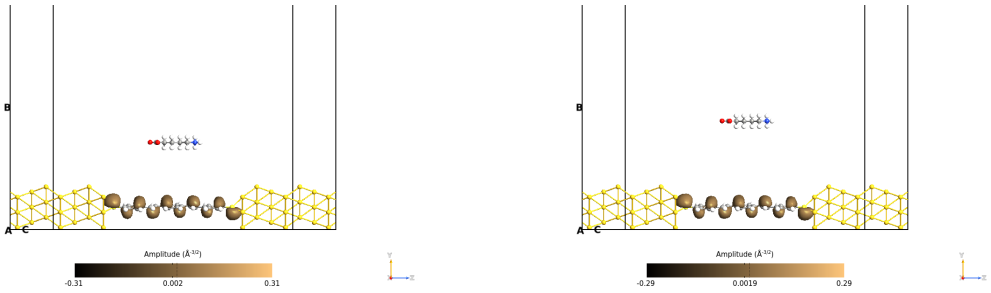

(a) Distance 10.5 Å. (b) Distance 14 Å.

Figure 6.337: Picture of the orbitals corresponding to the HOMO level for the OPV3 molecule with small driver at different distances, logic '0' configuration, on the yz plane. The orbitals are taken with an isosurface value equal to 0.015.

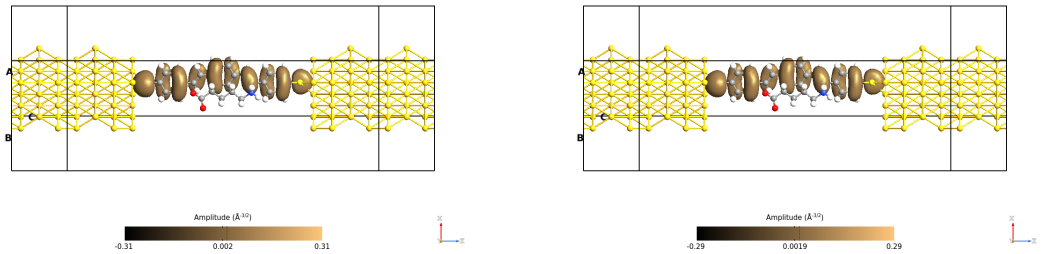

(a) Distance 10.5 Å. (b) Distance 14 Å.

Figure 6.338: Picture of the orbitals corresponding to the HOMO level for the OPV3 molecule with small driver at different distances, logic '0' configuration, on the xz plane with the driver. The orbitals are taken with an isosurface value equal to 0.015.

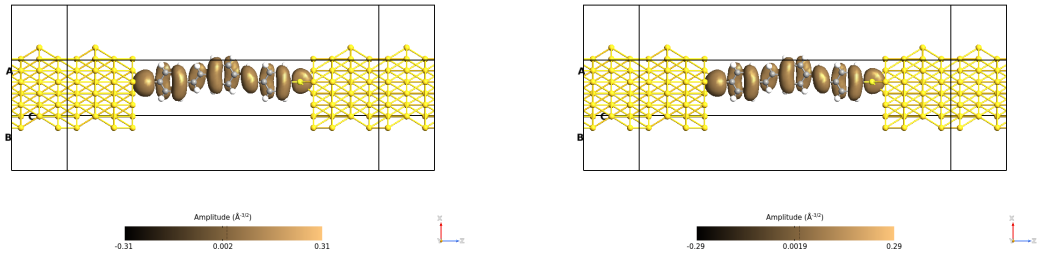

(a) Distance 10.5 Å. (b) Distance 14 Å.

Figure 6.339: Picture of the orbitals corresponding to the HOMO level for the OPV3 molecule with small driver at different distances, logic '0' configuration, on the xz plane without the driver. The orbitals are taken with an isosurface value equal to 0.015.

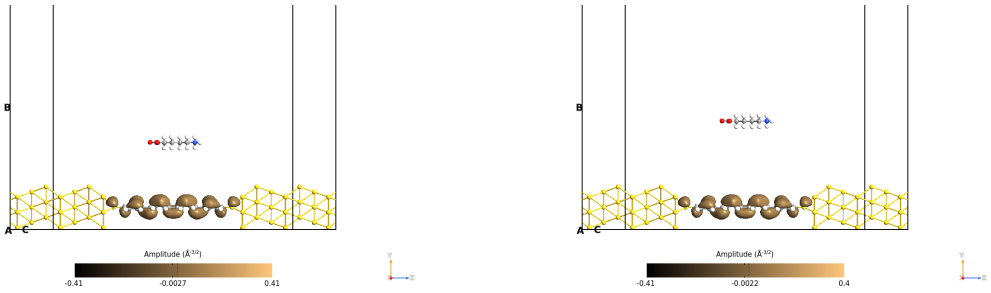

(a) Distance 10.5 Å. (b) Distance 14 Å.

Figure 6.340: Picture of the orbitals corresponding to the LUMO level for the OPV3 molecule with small driver at different distances, logic '0' configuration, on the yz plane. The orbitals are taken with an isosurface value equal to 0.015.

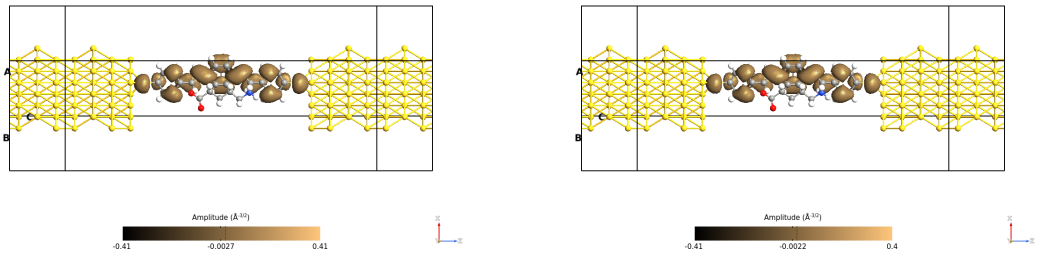

(a) Distance 10.5 Å. (b) Distance 14 Å.

Figure 6.341: Picture of the orbitals corresponding to the LUMO level for the OPV3 molecule with small driver at different distances, logic '0' configuration, on the xz plane with the driver. The orbitals are taken with an isosurface value equal to 0.015.

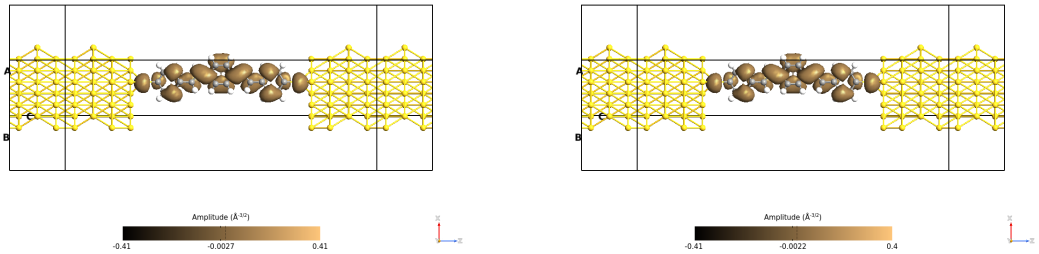

(a) Distance 10.5 Å. (b) Distance 14 Å.

Figure 6.342: Picture of the orbitals corresponding to the LUMO level for the OPV3 molecule with small driver at different distances, logic '0' configuration, on the xz plane without the driver. The orbitals are taken with an isosurface value equal to 0.015.

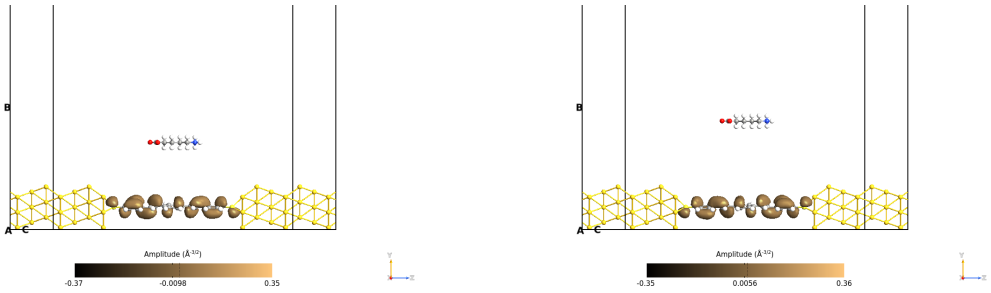

(a) Distance 10.5 Å. (b) Distance 14 Å.

Figure 6.343: Picture of the orbitals corresponding to the LUMO+1 level for the OPV3 molecule with small driver at different distances, logic '0' configuration, on the yz plane. The orbitals are taken with an isosurface value equal to 0.015.

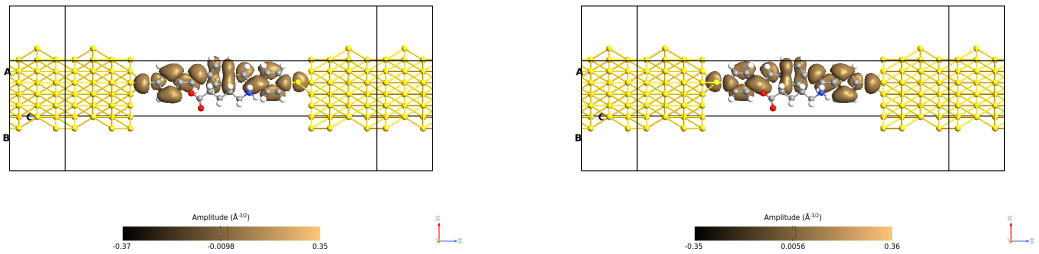

(a) Distance 10.5 Å. (b) Distance 14 Å.

Figure 6.344: Picture of the orbitals corresponding to the LUMO+1 level for the OPV3 molecule with small driver at different distances, logic '0' configuration, on the xz plane with the driver. The orbitals are taken with an isosurface value equal to 0.015.

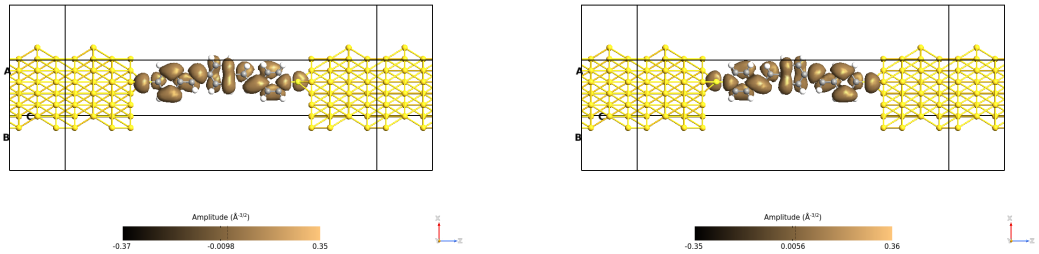

(a) Distance 10.5 Å. (b) Distance 14 Å.

Figure 6.345: Picture of the orbitals corresponding to the LUMO+1 level for the OPV3 molecule with small driver at different distances, logic '0' configuration, on the xz plane without the driver. The orbitals are taken with an isosurface value equal to 0.015.

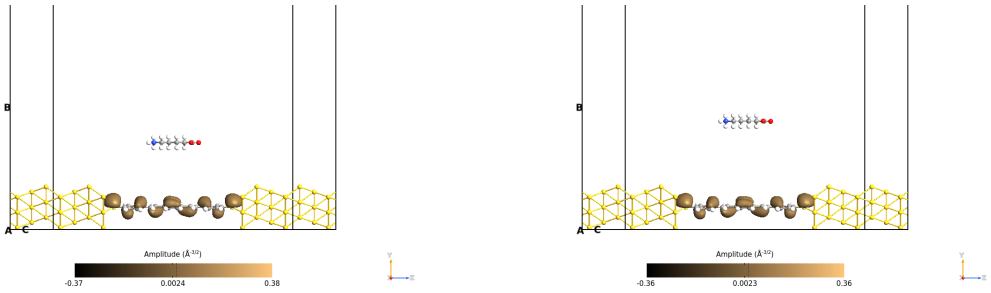

(a) Distance 10.5 Å. (b) Distance 14 Å.

Figure 6.346: Picture of the orbitals corresponding to the HOMO-1 level for the OPV3 molecule with small driver at different distances, logic '1' configuration, on the yz plane. The orbitals are taken with an isosurface value equal to 0.015.

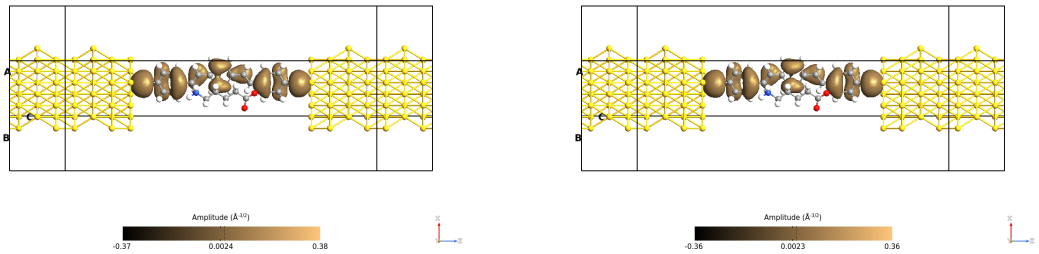

(a) Distance 10.5 Å. (b) Distance 14 Å.

Figure 6.347: Picture of the orbitals corresponding to the HOMO-1 level for the OPV3 molecule with small driver at different distances, logic '1' configuration, on the xz plane with the driver. The orbitals are taken with an isosurface value equal to 0.015.

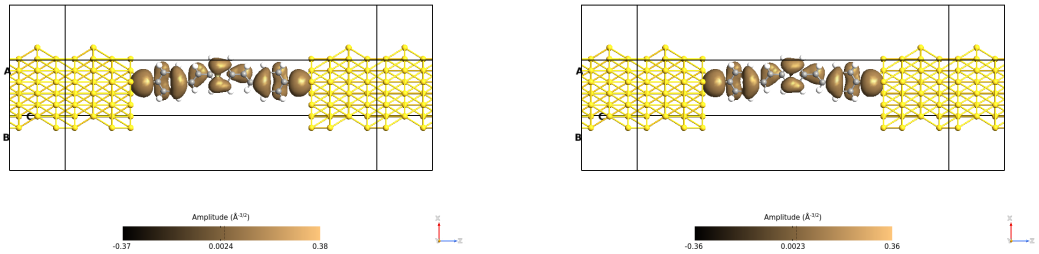

(a) Distance 10.5 Å. (b) Distance 14 Å.

Figure 6.348: Picture of the orbitals corresponding to the HOMO-1 level for the OPV3 molecule with small driver at different distances, logic '1' configuration, on the xz plane without the driver. The orbitals are taken with an isosurface value equal to 0.015.

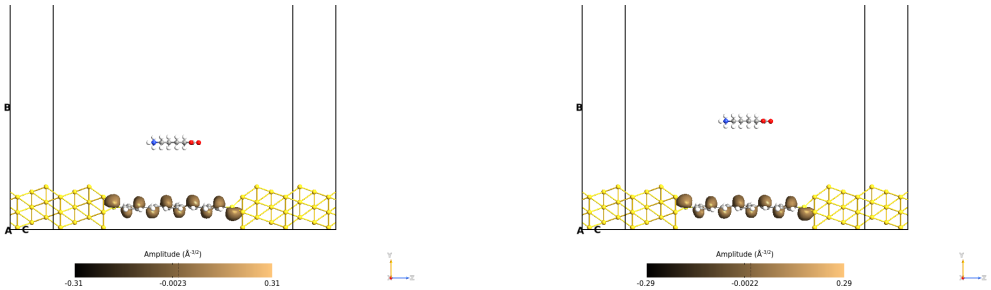

(a) Distance 10.5 Å. (b) Distance 14 Å.

Figure 6.349: Picture of the orbitals corresponding to the HOMO level for the OPV3 molecule with the small driver at different distances, logic '1' configuration, on the yz plane. The orbitals are taken with an isosurface value equal to 0.015.

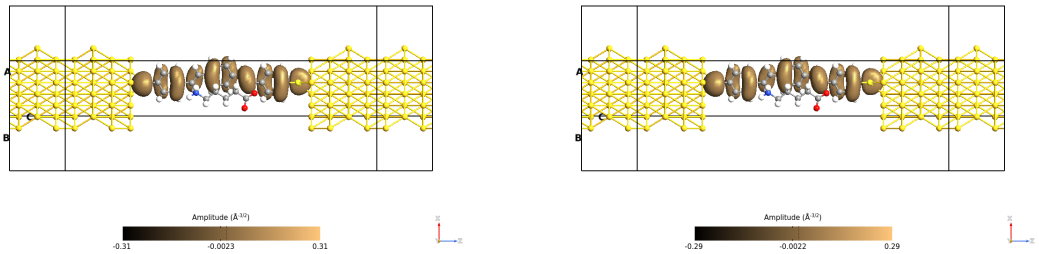

(a) Distance 10.5 Å. (b) Distance 14 Å.

Figure 6.350: Picture of the orbitals corresponding to the HOMO level for the OPV3 molecule with the small driver at different distances, logic '1' configuration, on the xz plane with the driver. The orbitals are taken with an isosurface value equal to 0.015.

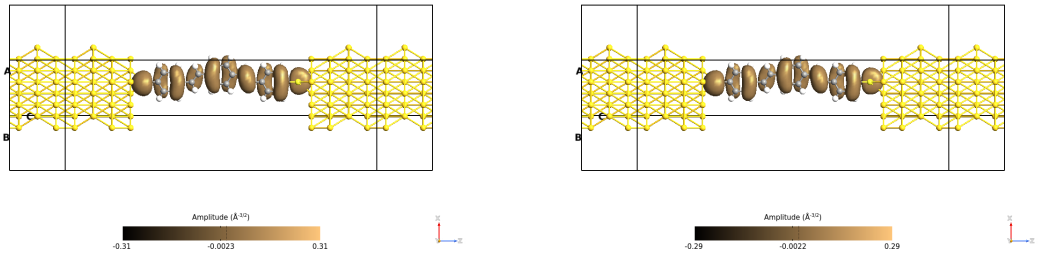

(a) Distance 10.5 Å. (b) Distance 14 Å.

Figure 6.351: Picture of the orbitals corresponding to the HOMO level for the OPV3 molecule with the small driver at different distances, logic '1' configuration, on the xz plane without the driver. The orbitals are taken with an isosurface value equal to 0.015.

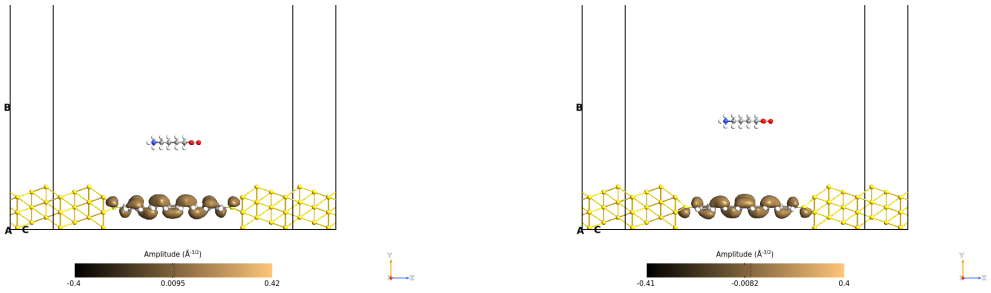

(a) Distance 10.5 Å. (b) Distance 14 Å.

Figure 6.352: Picture of the orbitals corresponding to the LUMO level for the OPV3 molecule with the small driver at different distances, logic '1' configuration, on the yz plane. The orbitals are taken with an isosurface value equal to 0.015.

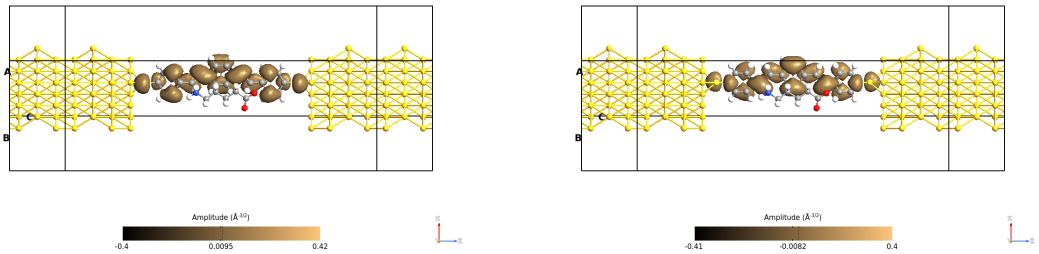

(a) Distance 10.5 Å. (b) Distance 14 Å.

Figure 6.353: Picture of the orbitals corresponding to the LUMO level for the OPV3 molecule with the small driver at different distances, logic '1' configuration, on the xz plane with the driver. The orbitals are taken with an isosurface value equal to 0.015.

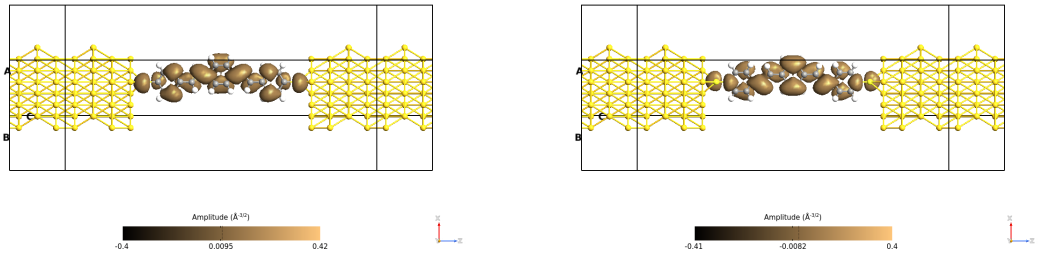

(a) Distance 10.5 Å. (b) Distance 14 Å.

Figure 6.354: Picture of the orbitals corresponding to the LUMO level for the OPV3 molecule with the small driver at different distances, logic '1' configuration, on the xz plane without the driver. The orbitals are taken with an isosurface value equal to 0.015.

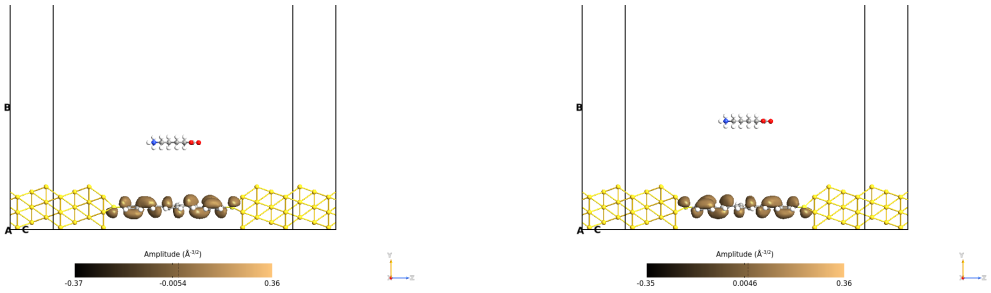

(a) Distance 10.5 Å. (b) Distance 14 Å.

Figure 6.355: Picture of the orbitals corresponding to the LUMO+1 level for the OPV3 molecule with the small driver at different distances, logic '1' configuration, on the yz plane. The orbitals are taken with an isosurface value equal to 0.015.

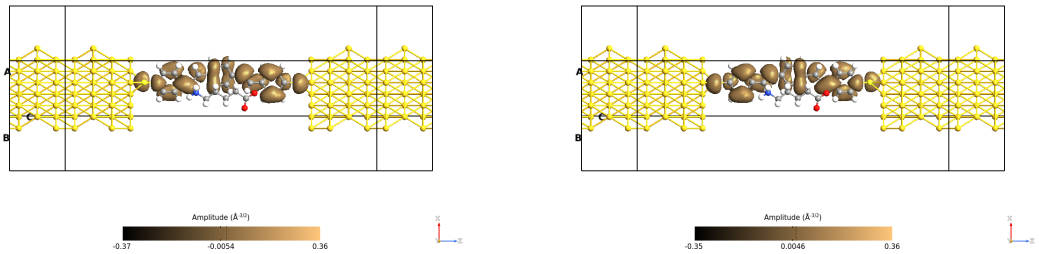

(a) Distance 10.5 Å.

(b) Distance 14 Å.

Figure 6.356: Picture of the orbitals corresponding to the LUMO+1 level for the OPV3 molecule with the small driver at different distances, logic '1' configuration, on the xz plane with the driver. The orbitals are taken with an isosurface value equal to 0.015.

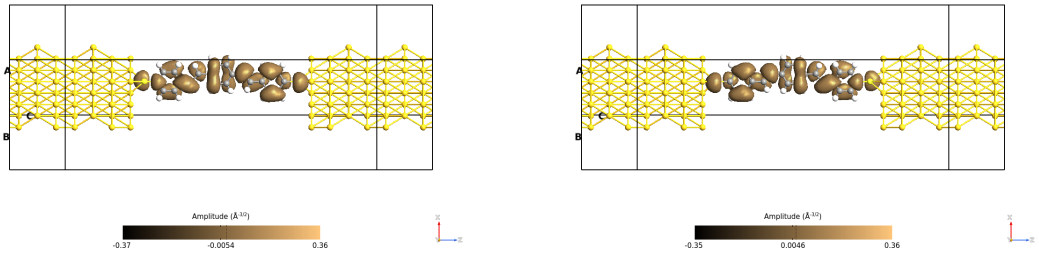

(a) Distance 10.5 Å.

(b) Distance 14 Å.

Figure 6.357: Picture of the orbitals corresponding to the LUMO+1 level for the OPV3 molecule with the small driver at different distances, logic '1' configuration, on the xz plane without the driver. The orbitals are taken with an isosurface value equal to 0.015.

The transmission pathways don't reveal surprises, they confirm the previous trend. The figures from 6.358 to 6.363 refer to the logic '0' configuration, while from 6.364 to 6.369 to the logic '1' one.

For the plots concerning the angle, as expected, the higher the energy, the higher the amount of electrons that flow in the opposite direction with respect to the conduction direction.

The weight graphs show the same trend that the TS (figure 6.331) tells us. Higher is the magnitude value according to the amplitude of the peak in the TS.

The small driver analysis with 14 Å of distance between the junction molecule and the driver plays a relevant role because it modelizes the not-perfect charge localization in the molFCN molecule (small driver) and the fabrication tolerances (accuracy in the deposition).

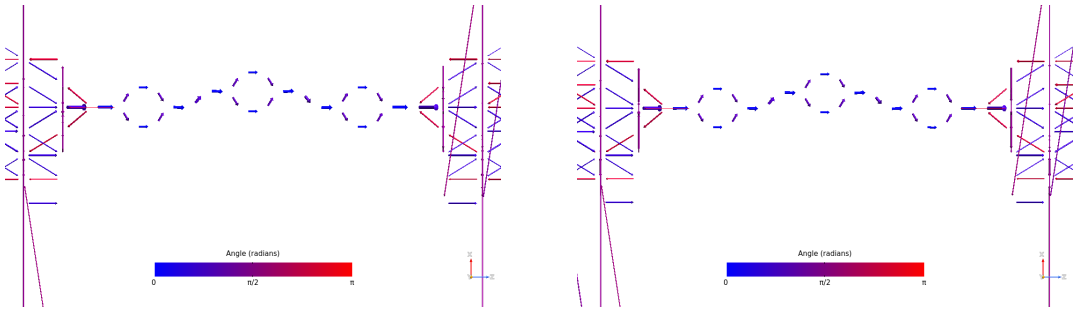

(a) Distance 10.5 Å. (b) Distance 14 Å.

Figure 6.358: Picture of the pathways corresponding to the energy 0.12 eV for the OPV3 molecule with the small driver at different distances, logic '0' configuration, on the xz plane. The blue arrows are in the same direction as the z-axis, while the red ones are in the opposite direction.

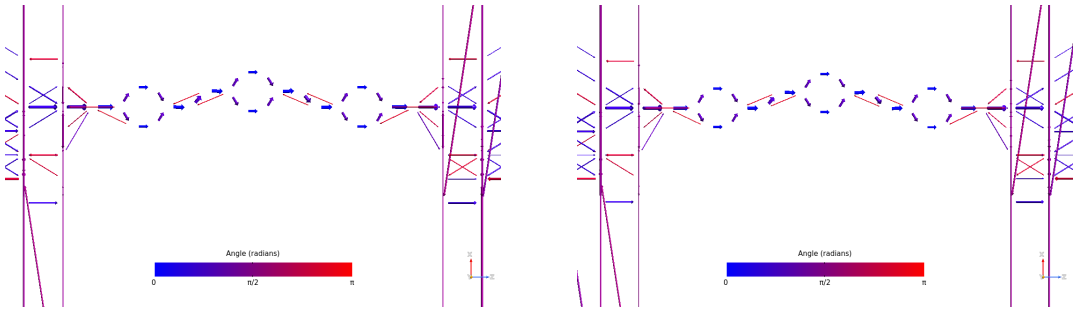

(a) Distance 10.5 Å. (b) Distance 14 Å.

Figure 6.359: Picture of the pathways corresponding to the energy 0.12 eV for the OPV3 molecule with the small driver at different distances, logic '0' configuration, on the xz plane. The blue arrows are in the same direction as the z-axis, while the red ones are in the opposite direction.

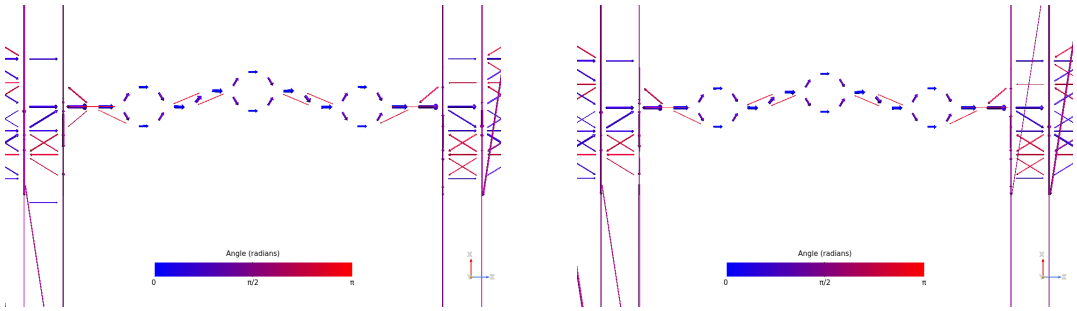

(a) Distance 10.5 Å. (b) Distance 14 Å.

Figure 6.360: Picture of the pathways corresponding to the energy 0.44 eV for the OPV3 molecule with the small driver at different distances, logic '0' configuration, on the xz plane. The blue arrows are in the same direction as the z-axis, while the red ones are in the opposite direction.

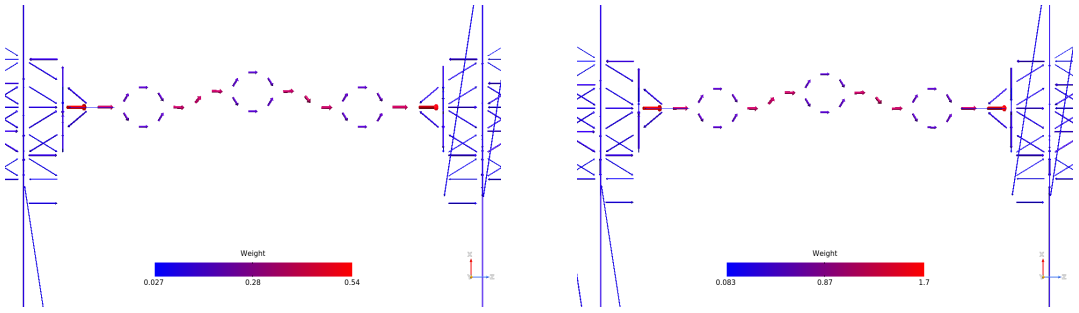

(a) Distance 10.5 Å. (b) Distance 14 Å.

Figure 6.361: Picture of the pathways corresponding to the energy 0.12 eV for the OPV3 molecule with the small driver at different distance, logic '0' configuration, on the xz plane. The plots show the arrows' magnitude.

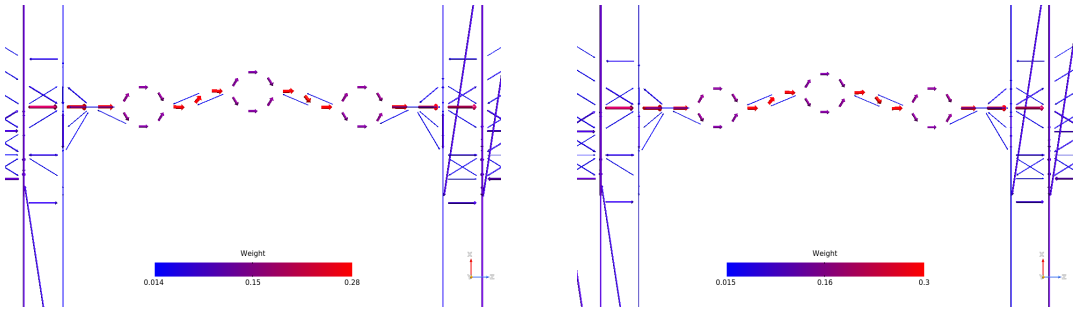

(a) Distance 10.5 Å. (b) Distance 14 Å.

Figure 6.362: Picture of the pathways corresponding to the energy 0.28 eV for the OPV3 molecule with the small driver at different distance, logic '0' configuration, on the xz plane. The plots show the arrows' magnitude.

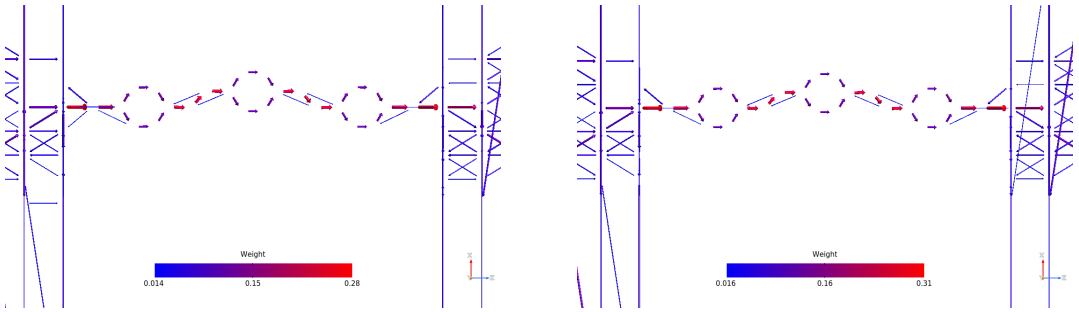

(a) Distance 10.5 Å. (b) Distance 14 Å.

Figure 6.363: Picture of the pathways corresponding to the energy 0.44 eV for the OPV3 molecule with the small driver at different distance, logic '0' configuration, on the xz plane. The plots show the arrows' magnitude.

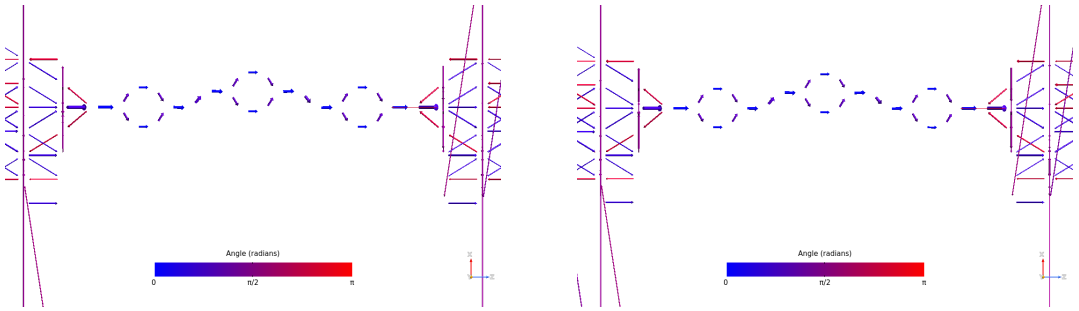

(a) Distance 10.5 Å. (b) Distance 14 Å.

Figure 6.364: Picture of the pathways corresponding to the energy 0.12 eV for the OPV3 molecule with the small driver at different distances, logic '1' configuration, on the xz plane. The blue arrows are in the same direction as the z-axis, while the red ones are in the opposite direction.

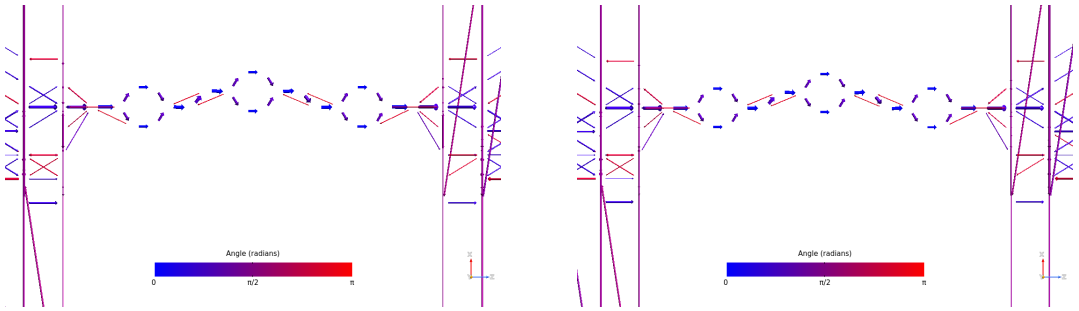

(a) Distance 10.5 Å. (b) Distance 14 Å.

Figure 6.365: Picture of the pathways corresponding to the energy 0.28 eV for the OPV3 molecule with the small driver at different distances, logic '1' configuration, on the xz plane. The blue arrows are in the same direction as the z-axis, while the red ones are in the opposite direction.

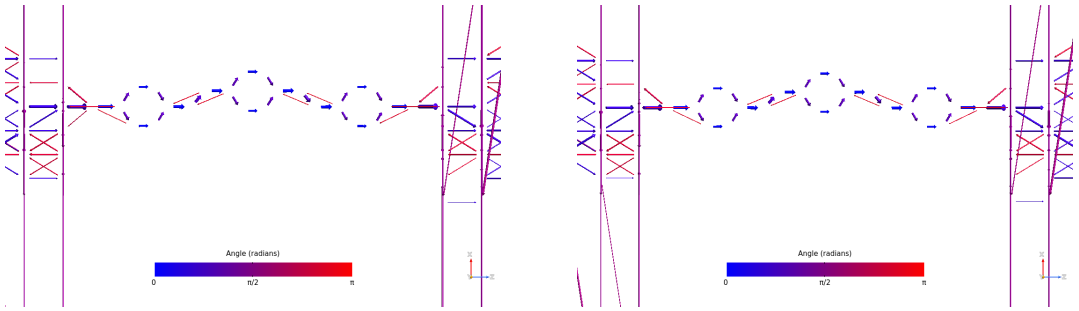

(a) Distance 10.5 Å. (b) Distance 14 Å.

Figure 6.366: Picture of the pathways corresponding to the energy 0.44 eV for the OPV3 molecule with the small driver at different distances, logic '1' configuration, on the xz plane. The blue arrows are in the same direction as the z-axis, while the red ones are in the opposite direction.

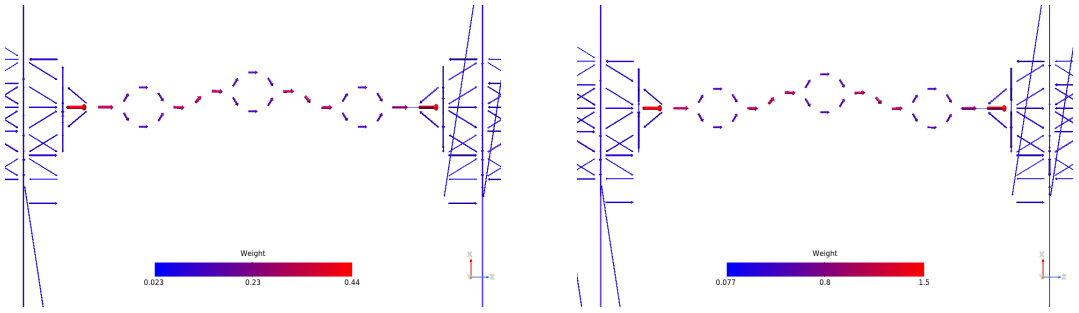

(a) Distance 10.5 Å. (b) Distance 14 Å.

Figure 6.367: Picture of the pathways corresponding to the energy 0.12 eV for the OPV3 molecule with the small driver at different distance, logic '1' configuration, on the xz plane. The plots show the arrows' magnitude.

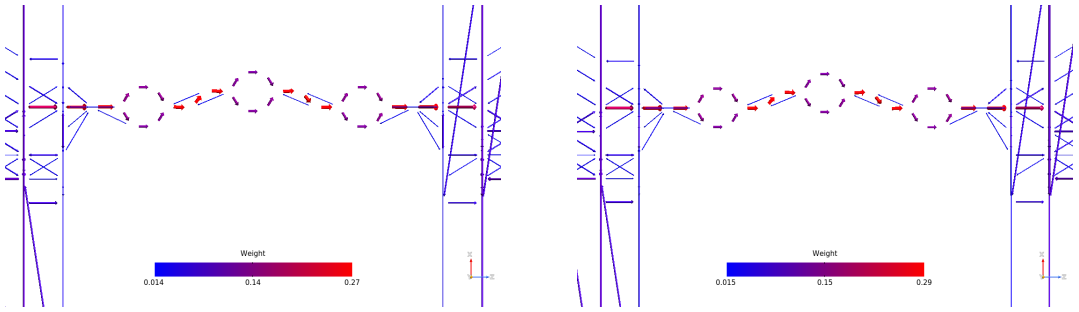

(a) Distance 10.5 Å. (b) Distance 14 Å.

Figure 6.368: Picture of the pathways corresponding to the energy 0.28 eV for the OPV3 molecule with the small driver at a different distance, logic '1' configuration, on the xz plane. The plots show the arrows' magnitude.

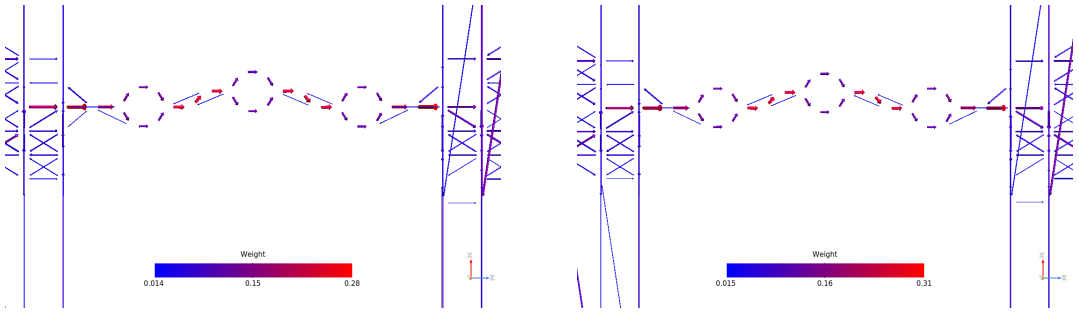

(a) Distance 10.5 Å. (b) Distance 14 Å.

Figure 6.369: Picture of the pathways corresponding to the energy 0.44 eV for the OPV3 molecule with the small driver at a different distance, logic '1' configuration, on the xz plane. The plots show the arrows' magnitude.

6.13.3 OPE3: long driver

The OPE3 molecule has been simulated at 11 Å and 14.5 Å (plus the 7.5 Å made in the previous analysis) as the distance between the junction molecule and the driver. The builders are reported below, in particular, the logic '0' configuration is displayed in figure 6.370 while the logic '1' one is shown in figure 6.371.

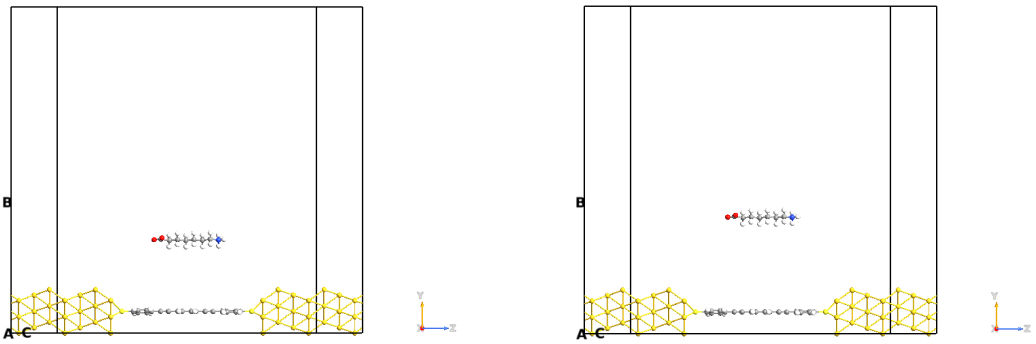

(a) Distance between junction molecule and driver equal to 11 Å.

(b) Distance between junction molecule and driver equal to 14.5 Å.

Figure 6.370: Picture of the QuantumATK builder for the OPV3 molecule, logic '0' configuration with the long driver at a different distance. The white atoms are the hydrogens, the yellow ones are gold atoms, the lighter yellow ones are the sulfurs, the blue ones are nitrogens, the reds are the oxygens and the grey atoms are carbons.

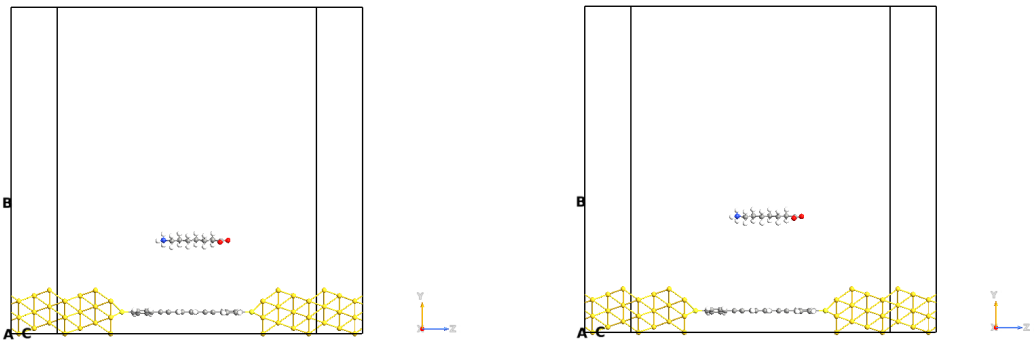

(a) Distance between junction molecule and driver equal to 11 Å.

(b) Distance between junction molecule and driver equal to 14.5 Å.

Figure 6.371: Picture of the QuantumATK builder for the OPV3 molecule, logic '1' configuration with the long driver at a different distance. The white atoms are the hydrogens, the yellow ones are gold atoms, the lighter yellow ones are the sulfurs, the blue ones are nitrogens, the reds are the oxygens and the grey atoms are carbons.

The OPE3 molecule exhibits an interesting behavior in the previous analysis, for testing its robustness to the distance variations more accurate simulations have been

performed. In figure 6.372 are shown the TS for the two configurations at different distances. The trend is very similar for each case, the differences are related to the amplitude and the shift of some peaks.

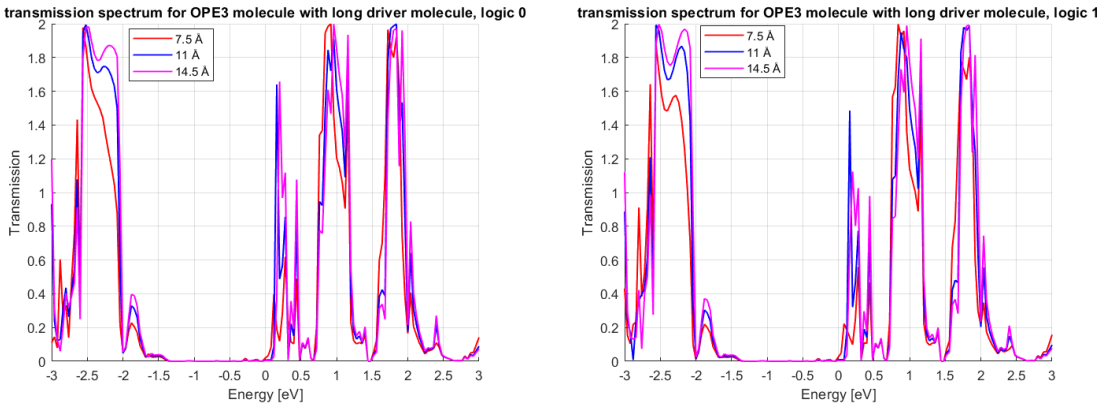

(a) logic 0 configuration.

(b) logic 1 configuration.

Figure 6.372: Picture of the TS for the OPE3 molecule considering the long driver at different distances, in particular, the red curve is obtained with the driver at a distance of 7.5 Å, the blue one at a distance 11 Å and the magenta one at 14.5 Å.

The IV plot (figure 6.373) confirms the possible detection of the two different configurations. Unlike the OPV3, the OPE3 sees a more relevant lowering of the current as the distance between the junction and the driver increases.

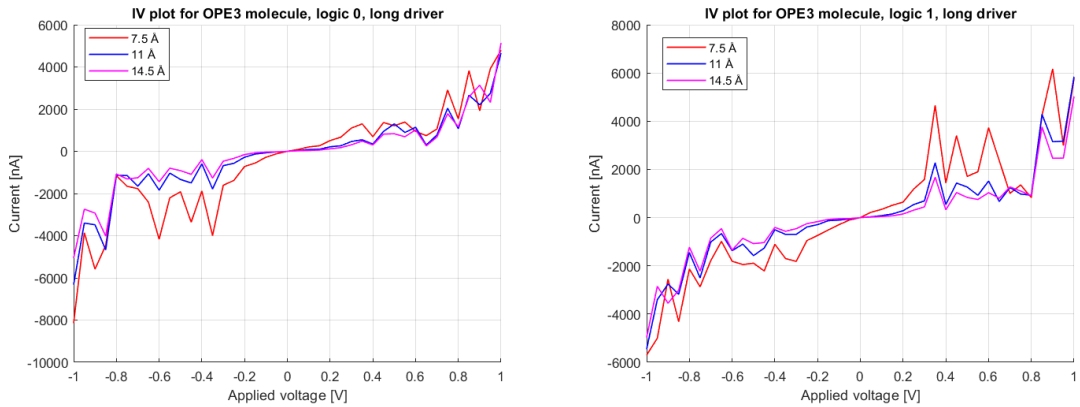

(a) logic 0 configuration.

(b) logic 1 configuration.

Figure 6.373: Picture of the IV for the OPE3 molecule considering the long driver at different distances, in particular, the red curve is obtained with the driver at a distance of 7.5 Å, the blue one at a distance 11 Å and the magenta one at 14.5 Å.

The feasibility of the readout system based on an OPE3 molecular junction is confirmed by the figure 6.374, in which the current difference in teh worst case is about 1 μA. This value is large enough to be detected by an electronic device.

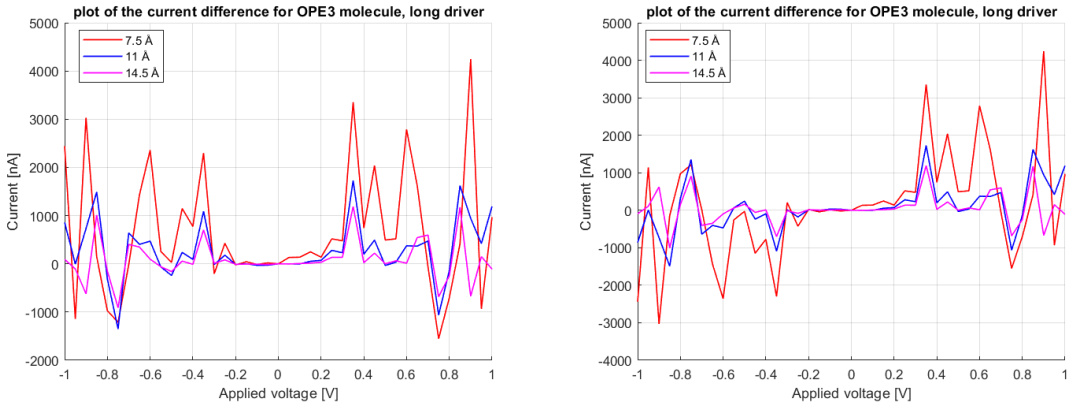

(a) logic '1' - logic '0'.

(b) |logic '1'| - |logic '0'|.

Figure 6.374: Picture of the current difference between the two configurations for the OPE3 molecule considering the long driver at different distances, in particular, the red curve is obtained with the driver at a distance of 7.5 Å, the blue one at a distance 11 Å and the magenta one at 14.5 Å.

As before, the orbitals show two different behavior, the same trend for the two considered distances and complementary geometries between them.

The figures from 6.375 to 6.386 concerns the logic '0' configuration. It can be noticed that the HOMO-1 (figures 6.375, 6.376 and 6.377) and HOMO (figures 6.378, 6.379 and 6.380) energy levels present the same trend between the two simulations, while the LUMO (figures 6.381, 6.382 and 6.383) and LUMO+1 (figures 6.384, 6.385 and 6.386) reveal the complementary behavior.

For the logic '1' configuration, instead, all the analyzed orbitals exhibit the complementary behavior between the two distances. The figures regarding the logic '1' configuration are the ones from 6.387 to 6.398.

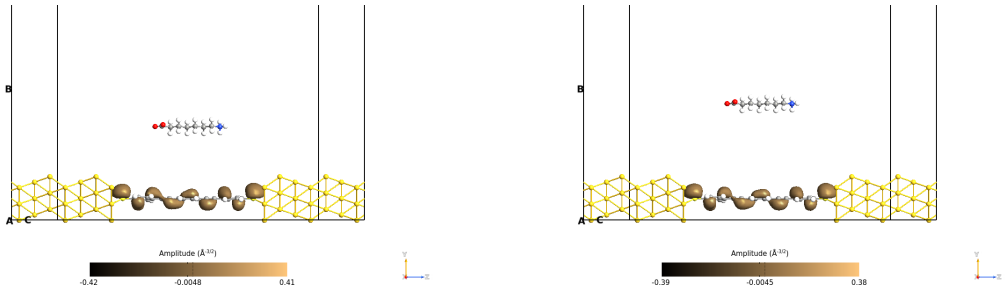

(a) Distance 11 Å.

(b) Distance 14.5 Å.

Figure 6.375: Picture of the orbitals corresponding to the HOMO-1 level for the OPE3 molecule with long driver at different distances, logic '0' configuration, on the yz plane. The orbitals are taken with an isosurface value equal to 0.015.

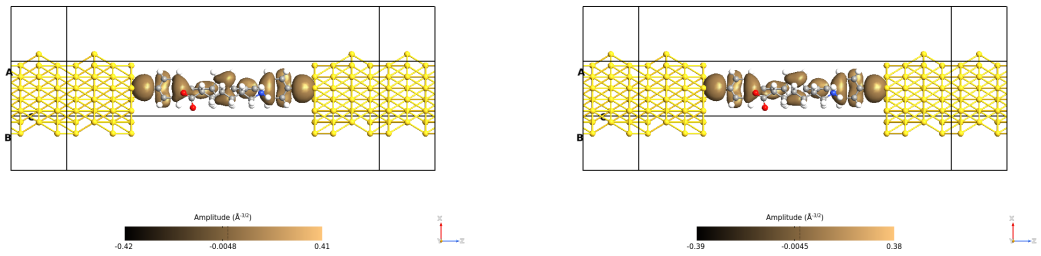

(a) Distance 11 Å. (b) Distance 14.5 Å.

Figure 6.376: Picture of the orbitals corresponding to the HOMO-1 level for the OPE3 molecule with long driver at different distances, logic '0' configuration, on the xz plane with the driver. The orbitals are taken with an isosurface value equal to 0.015.

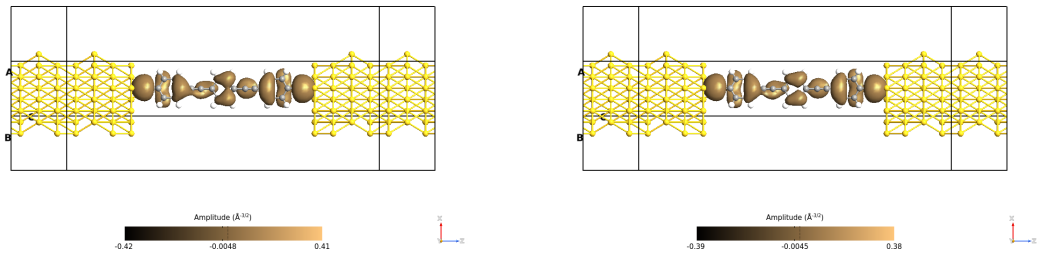

(a) Distance 11 Å. (b) Distance 14.5 Å.

Figure 6.377: Picture of the orbitals corresponding to the HOMO-1 level for the OPE3 molecule with long driver at different distances, logic '0' configuration, on the xz plane without the driver. The orbitals are taken with an isosurface value equal to 0.015.

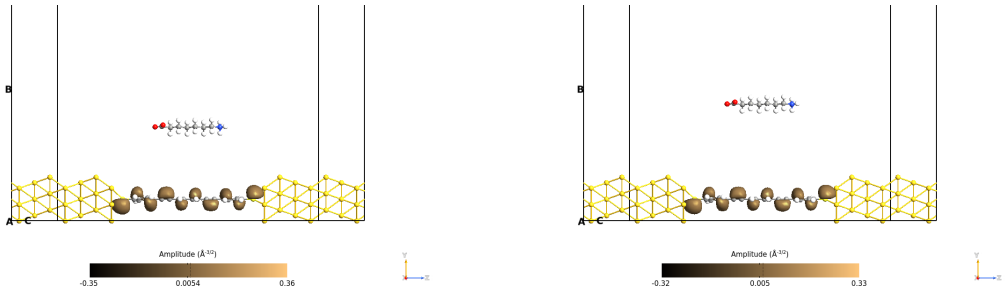

(a) Distance 11 Å. (b) Distance 14.5 Å.

Figure 6.378: Picture of the orbitals corresponding to the HOMO level for the OPE3 molecule with long driver at different distances, logic '0' configuration, on the yz plane. The orbitals are taken with an isosurface value equal to 0.015.

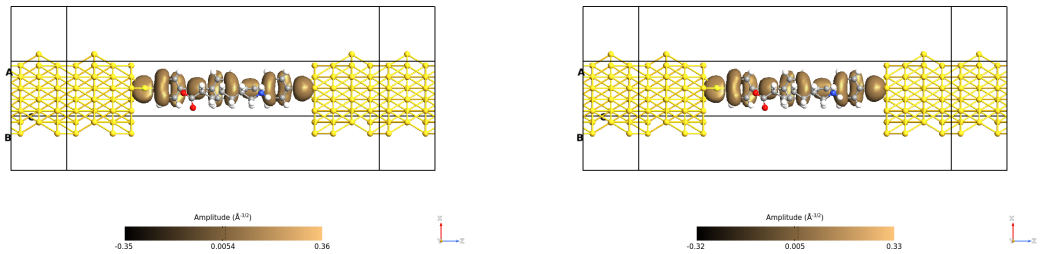

(a) Distance 11 Å. (b) Distance 14.5 Å.

Figure 6.379: Picture of the orbitals corresponding to the HOMO level for the OPE3 molecule with long driver at different distances, logic '0' configuration, on the xz plane with the driver. The orbitals are taken with an isosurface value equal to 0.015.

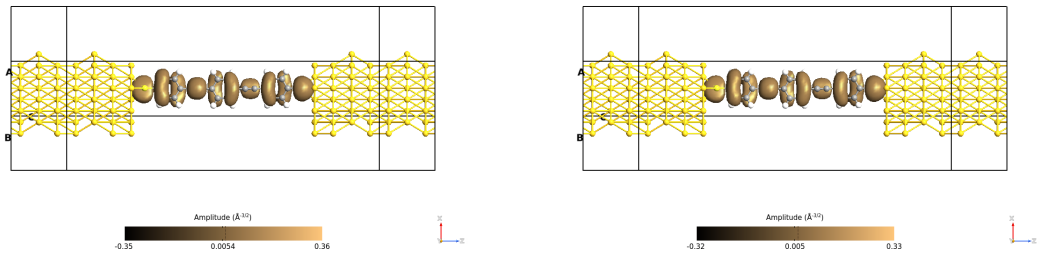

(a) Distance 11 Å. (b) Distance 14.5 Å.

Figure 6.380: Picture of the orbitals corresponding to the HOMO level for the OPE3 molecule with long driver at different distances, logic '0' configuration, on the xz plane without the driver. The orbitals are taken with an isosurface value equal to 0.015.

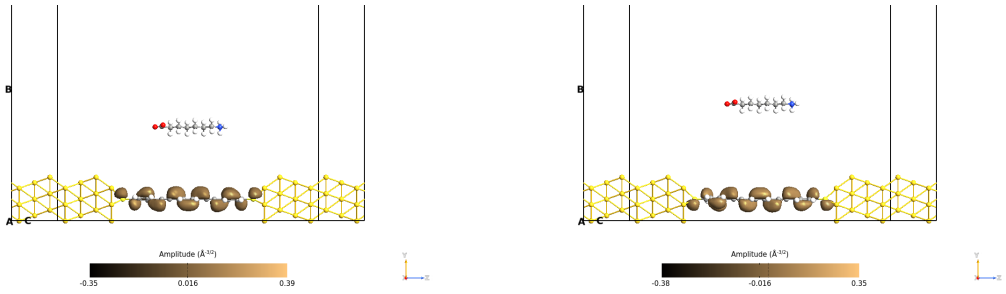

(a) Distance 11 Å. (b) Distance 14.5 Å.

Figure 6.381: Picture of the orbitals corresponding to the LUMO level for the OPE3 molecule with long driver at different distances, logic '0' configuration, on the yz plane. The orbitals are taken with an isosurface value equal to 0.015.

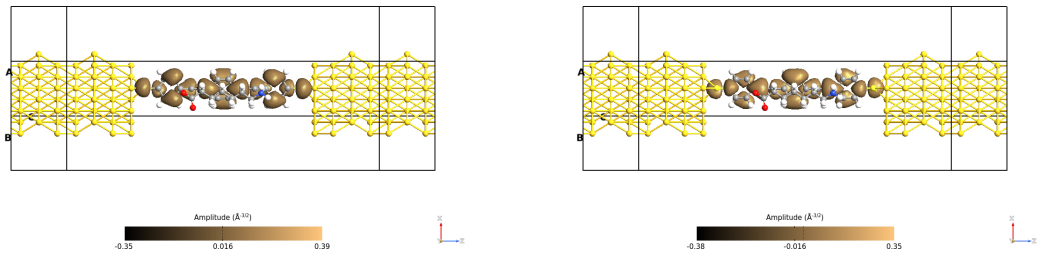

(a) Distance 11 Å. (b) Distance 14.5 Å.

Figure 6.382: Picture of the orbitals corresponding to the LUMO level for the OPE3 molecule with long driver at different distances, logic '0' configuration, on the xz plane with the driver. The orbitals are taken with an isosurface value equal to 0.015.

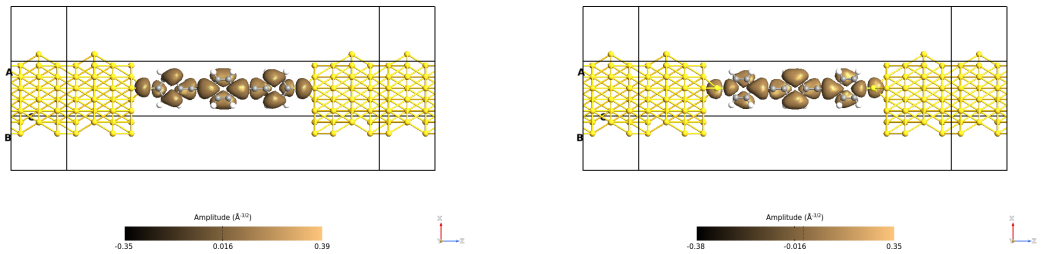

(a) Distance 11 Å. (b) Distance 14.5 Å.

Figure 6.383: Picture of the orbitals corresponding to the LUMO level for the OPE3 molecule with long driver at different distances, logic '0' configuration, on the xz plane without the driver. The orbitals are taken with an isosurface value equal to 0.015.

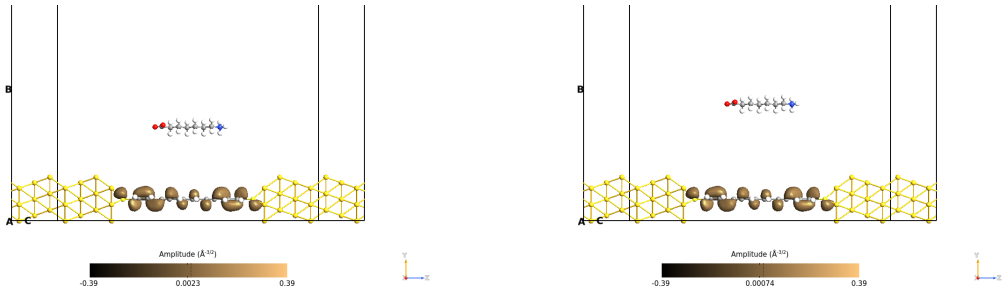

(a) Distance 11 Å. (b) Distance 14.5 Å.

Figure 6.384: Picture of the orbitals corresponding to the LUMO+1 level for the OPE3 molecule with long driver at different distances, logic '0' configuration, on the yz plane. The orbitals are taken with an isosurface value equal to 0.015.

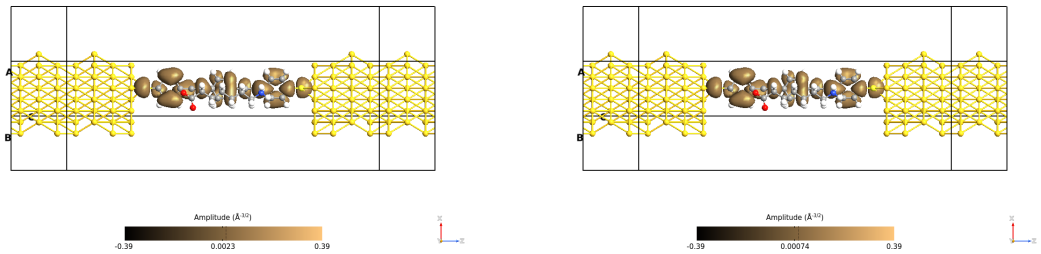

(a) Distance 11 Å. (b) Distance 14.5 Å.

Figure 6.385: Picture of the orbitals corresponding to the LUMO+1 level for the OPE3 molecule with long driver at different distances, logic '0' configuration, on the xz plane with the driver. The orbitals are taken with an isosurface value equal to 0.015.

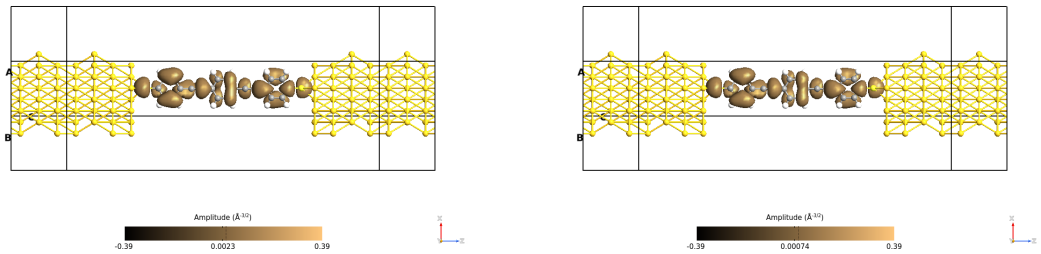

(a) Distance 11 Å. (b) Distance 14.5 Å.

Figure 6.386: Picture of the orbitals corresponding to the LUMO+1 level for the OPE3 molecule with long driver at different distances, logic '0' configuration, on the xz plane without the driver. The orbitals are taken with an isosurface value equal to 0.015.

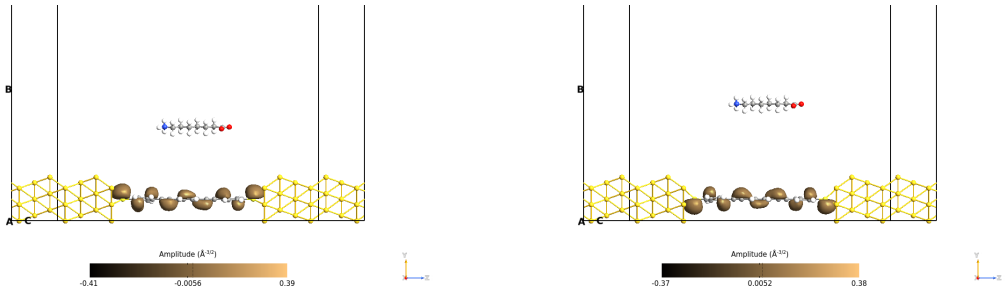

(a) Distance 11 Å. (b) Distance 14.5 Å.

Figure 6.387: Picture of the orbitals corresponding to the HOMO-1 level for the OPE3 molecule with long driver at different distances, logic '1' configuration, on the yz plane. The orbitals are taken with an isosurface value equal to 0.015.

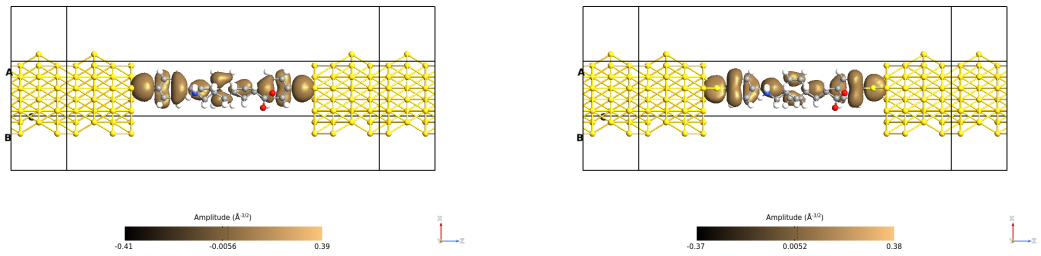

(a) Distance 11 Å. (b) Distance 14.5 Å.

Figure 6.388: Picture of the orbitals corresponding to the HOMO-1 level for the OPE3 molecule with long driver at different distances, logic '1' configuration, on the xz plane with the driver. The orbitals are taken with an isosurface value equal to 0.015.

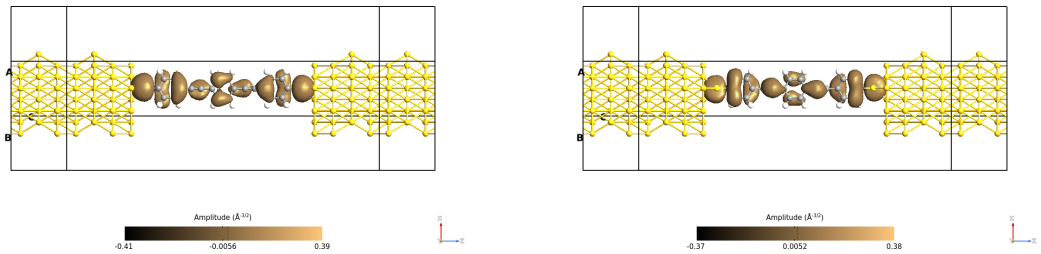

(a) Distance 11 Å. (b) Distance 14.5 Å.

Figure 6.389: Picture of the orbitals corresponding to the HOMO-1 level for the OPE3 molecule with long driver at different distances, logic '1' configuration, on the xz plane without the driver. The orbitals are taken with an isosurface value equal to 0.015.

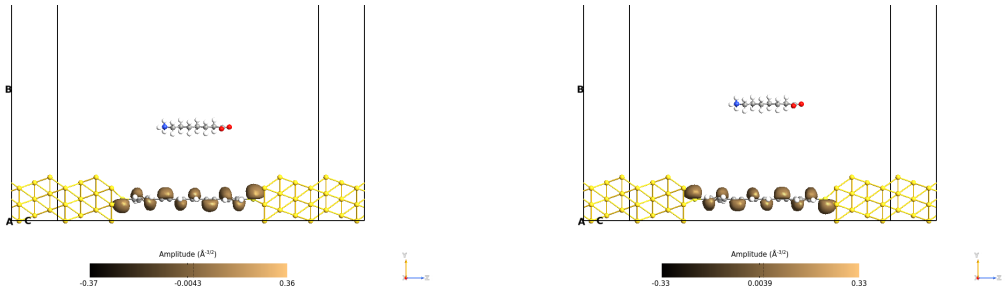

(a) Distance 11 Å. (b) Distance 14.5 Å.

Figure 6.390: Picture of the orbitals corresponding to the HOMO level for the OPE3 molecule with long driver at different distances, logic '1' configuration, on the yz plane. The orbitals are taken with an isosurface value equal to 0.015.

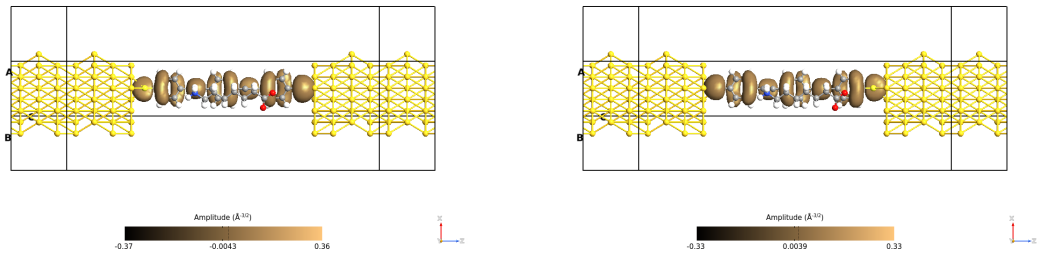

(a) Distance 11 Å. (b) Distance 14.5 Å.

Figure 6.391: Picture of the orbitals corresponding to the HOMO level for the OPE3 molecule with long driver at different distances, logic '1' configuration, on the xz plane with the driver. The orbitals are taken with an isosurface value equal to 0.015.

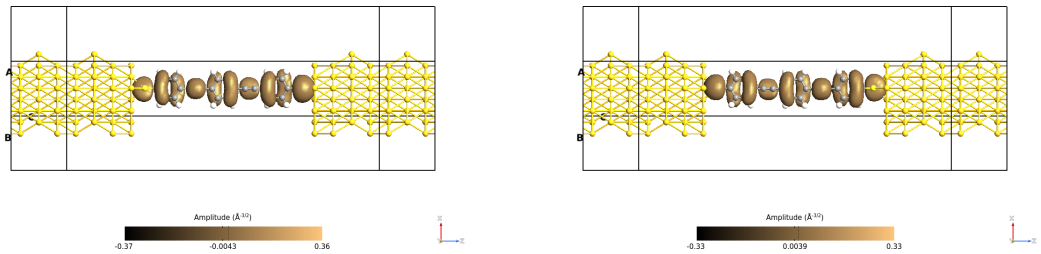

(a) Distance 11 Å. (b) Distance 14.5 Å.

Figure 6.392: Picture of the orbitals corresponding to the HOMO level for the OPE3 molecule with long driver at different distances, logic '1' configuration, on the xz plane without the driver. The orbitals are taken with an isosurface value equal to 0.015.

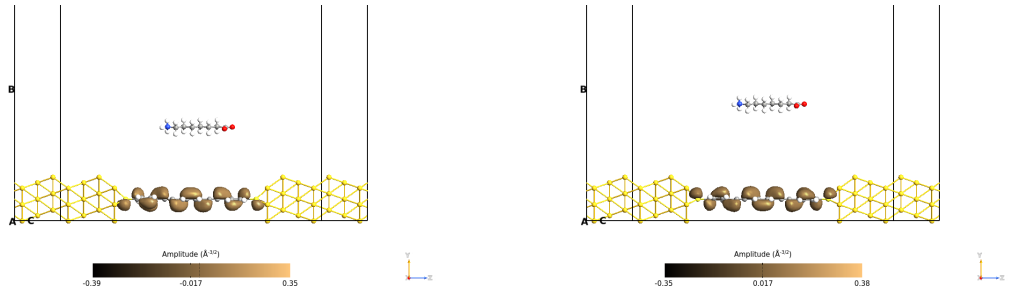

(a) Distance 11 Å. (b) Distance 14.5 Å.

Figure 6.393: Picture of the orbitals corresponding to the LUMO level for the OPE3 molecule with long driver at different distances, logic '1' configuration, on the yz plane. The orbitals are taken with an isosurface value equal to 0.015.

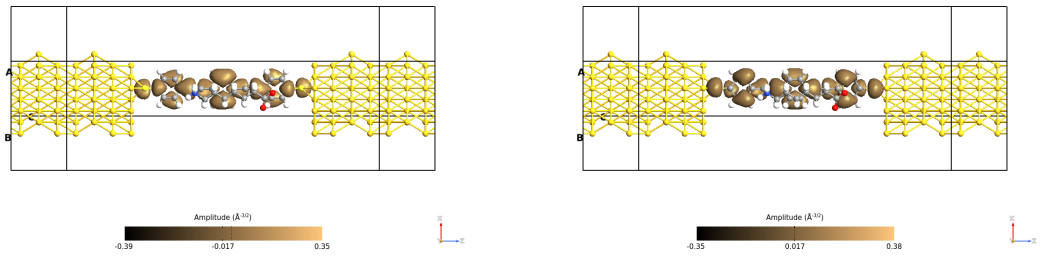

(a) Distance 11 Å. (b) Distance 14.5 Å.

Figure 6.394: Picture of the orbitals corresponding to the LUMO level for the OPE3 molecule with long driver at different distances, logic '1' configuration, on the xz plane with the driver. The orbitals are taken with an isosurface value equal to 0.015.

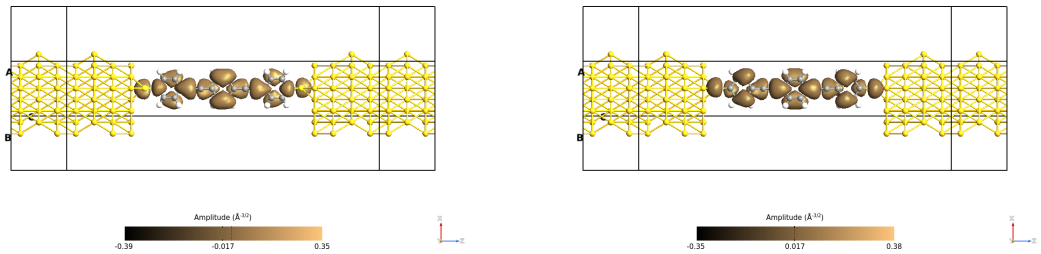

(a) Distance 11 Å. (b) Distance 14.5 Å.

Figure 6.395: Picture of the orbitals corresponding to the LUMO level for the OPE3 molecule with long driver at different distances, logic '1' configuration, on the xz plane without the driver. The orbitals are taken with an isosurface value equal to 0.015.

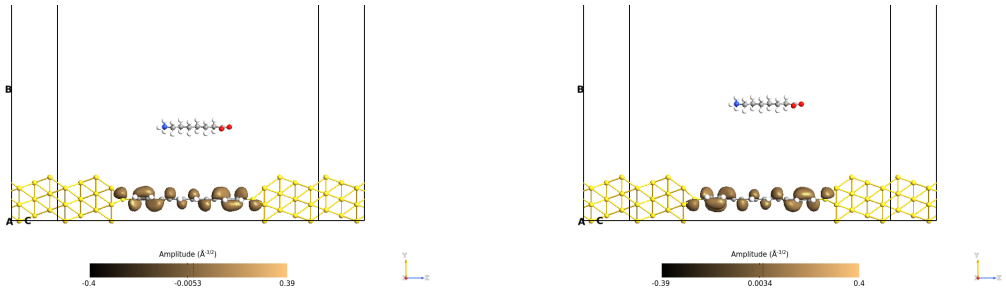

(a) Distance 11 Å. (b) Distance 14.5 Å.

Figure 6.396: Picture of the orbitals corresponding to the LUMO+1 level for the OPE3 molecule with long driver at different distances, logic '1' configuration, on the yz plane. The orbitals are taken with an isosurface value equal to 0.015.

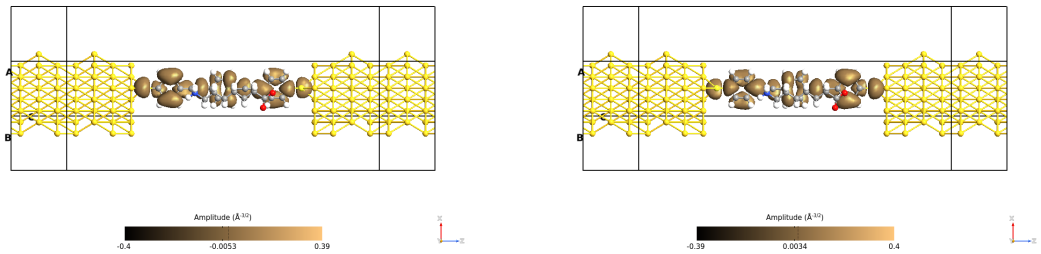

(a) Distance 11 Å. (b) Distance 14.5 Å.

Figure 6.397: Picture of the orbitals corresponding to the LUMO+1 level for the OPE3 molecule with long driver at different distances, logic '1' configuration, on the xz plane with the driver. The orbitals are taken with an isosurface value equal to 0.015.

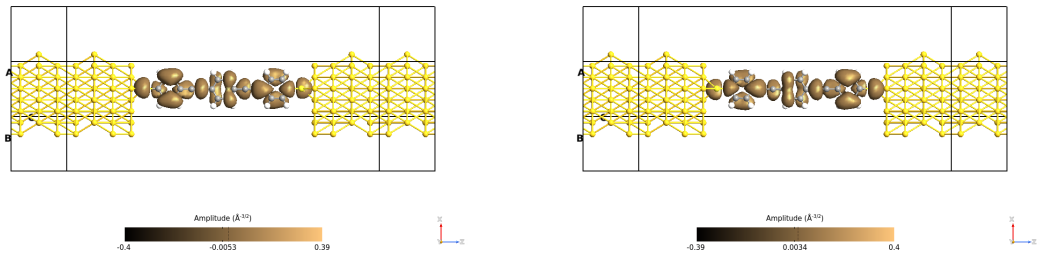

(a) Distance 11 Å. (b) Distance 14.5 Å.

Figure 6.398: Picture of the orbitals corresponding to the LUMO+1 level for the OPE3 molecule with long driver at different distances, logic '1' configuration, on the xz plane without the driver. The orbitals are taken with an isosurface value equal to 0.015.

The transmission pathways don't reveal surprises, they confirm the previous trend. The figures from 6.399 to 6.404 refer to the logic '0' configuration, while from 6.405 to 6.407 to the logic '1' one.

For the plots concerning the angle, as expected, the higher the energy, the higher the amount of electrons that flow in the opposite direction with respect to the conduction direction. This behavior is a mark for the symmetric molecules with good conduction properties.

The weight graphs show the same trend that the TS (figure 6.52a) tells us. Higher is the magnitude value according to the amplitude of the peak in the TS.

The transmission pathways show clearly the electron path, they are interesting because they could exhibit important differences between the two selected distances. In this case, it is important that the two plots for the same energy level are close enough in order to not evidence significant problems related to the not-perfect molecule positioning.

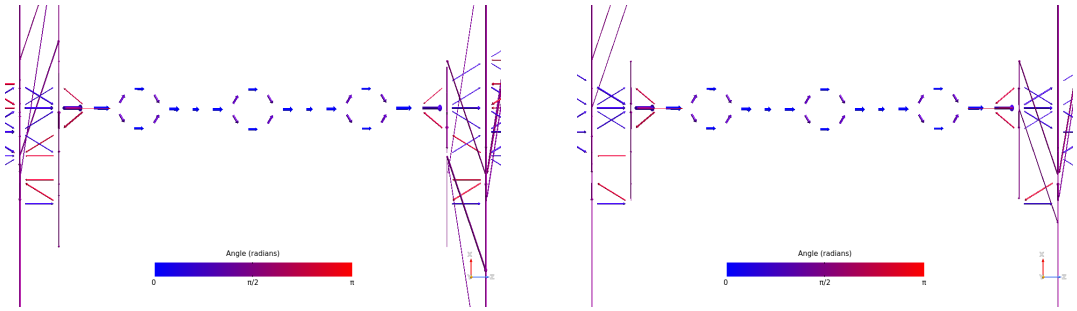

(a) Distance 11 Å, energy 0.16 eV. (b) Distance 14.5 Å, energy 0.12 eV.

Figure 6.399: Picture of the pathways for the OPE3 molecule with long driver at different distances, logic '0' configuration. The blue arrows are in the same direction as the z-axis, while the red ones are in the opposite direction.

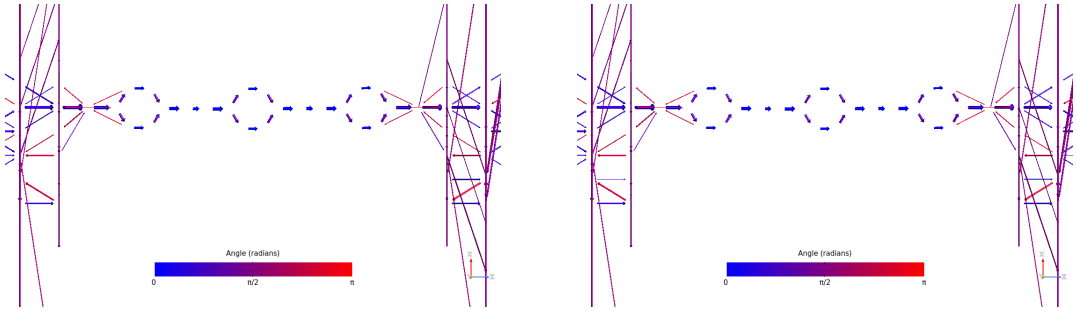

(a) Distance 11 Å. (b) Distance 14.5 Å.

Figure 6.400: Picture of the pathways corresponding to the energy 0.28 eV for the OPE3 molecule with long driver at different distances, logic '0' configuration. The blue arrows are in the same direction as the z-axis, while the red ones are in the opposite direction.

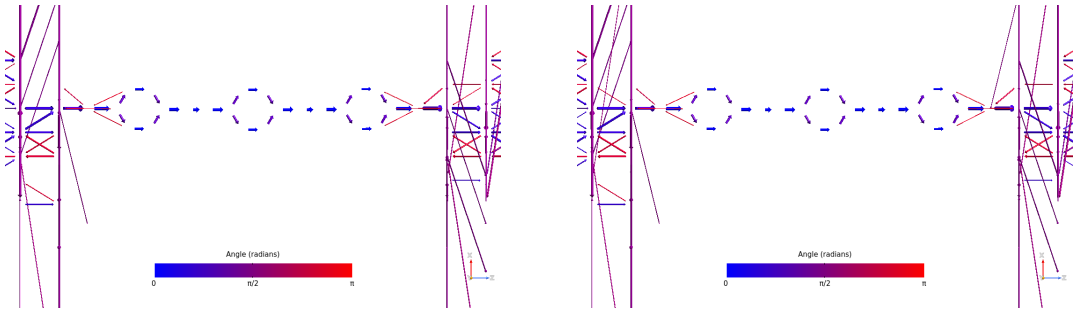

(a) Distance 11 Å. (b) Distance 14.5 Å.

Figure 6.401: Picture of the pathways corresponding to the energy 0.44 eV for the OPE3 molecule with long driver at different distances, logic '0' configuration. The blue arrows are in the same direction as the z-axis, while the red ones are in the opposite direction.

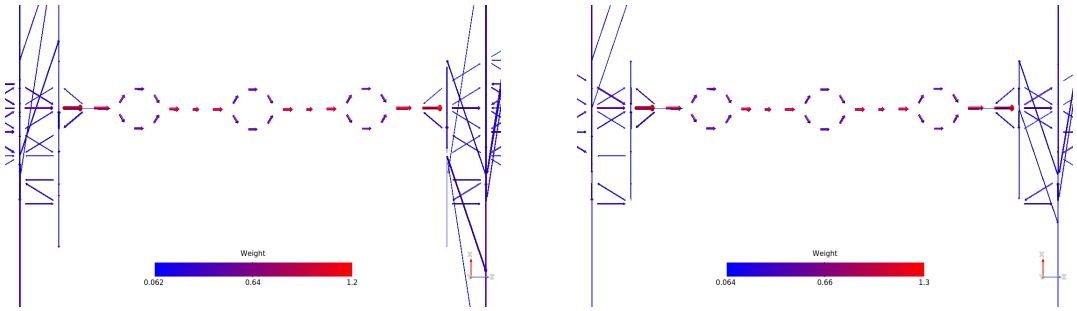

(a) Distance 11 Å, energy 0.16 eV.

(b) Distance 14.5 Å, energy 0.20 eV.

Figure 6.402: Picture of the pathways for the OPE3 molecule with long driver at different distance, logic '0' configuration, on the xz plane. The plots show the arrows' magnitude.

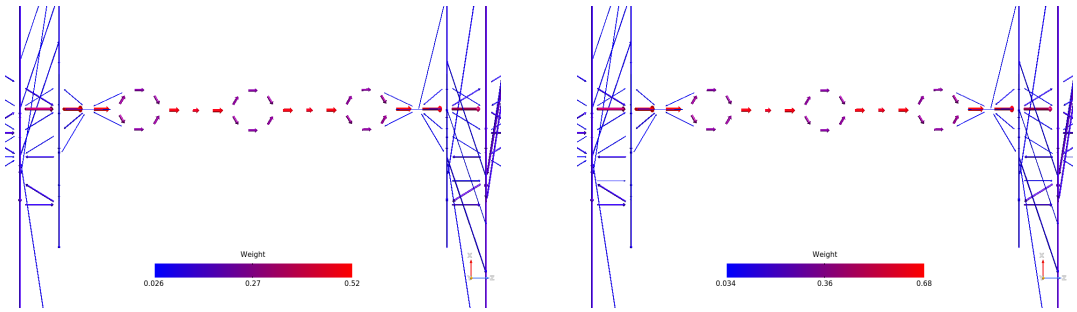

(a) Distance 11 Å.

(b) Distance 14.5 Å.

Figure 6.403: Picture of the pathways corresponding to the energy 0.28 eV for the OPE3 molecule with long driver at different distance, logic '0' configuration, on the xz plane. The plots show the arrows' magnitude.

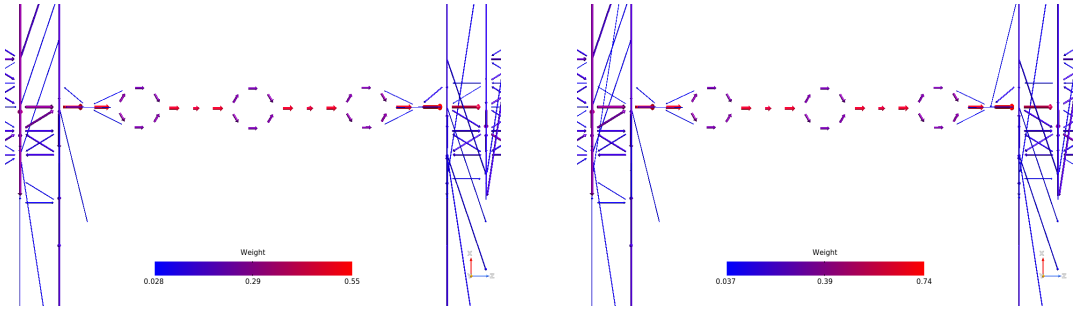

(a) Distance 11 Å.

(b) Distance 14.5 Å.

Figure 6.404: Picture of the pathways corresponding to the energy 0.44 eV for the OPE3 molecule with long driver at different distance, logic '0' configuration, on the xz plane. The plots show the arrows' magnitude.

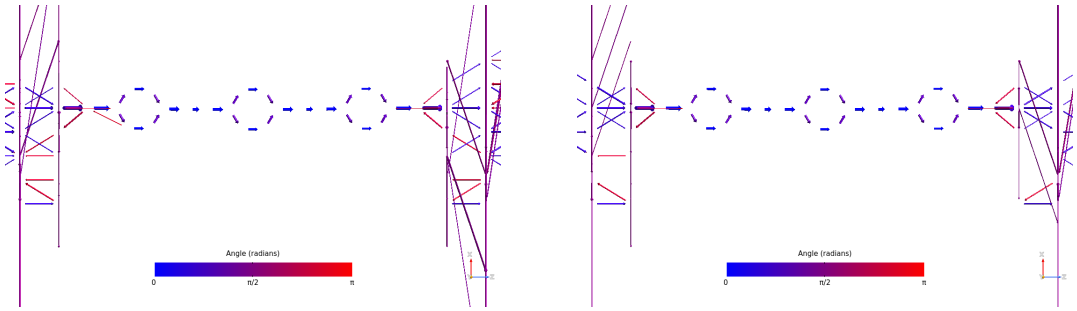

(a) Distance 11 Å, energy 0.16 eV.

(b) Distance 14.5 Å, energy 0.12 eV.

Figure 6.405: Picture of the pathways for the OPE3 molecule with long driver at different distances, logic '1' configuration, on the xz plane. The blue arrows are in the same direction as the z-axis, while the red ones are in the opposite direction.

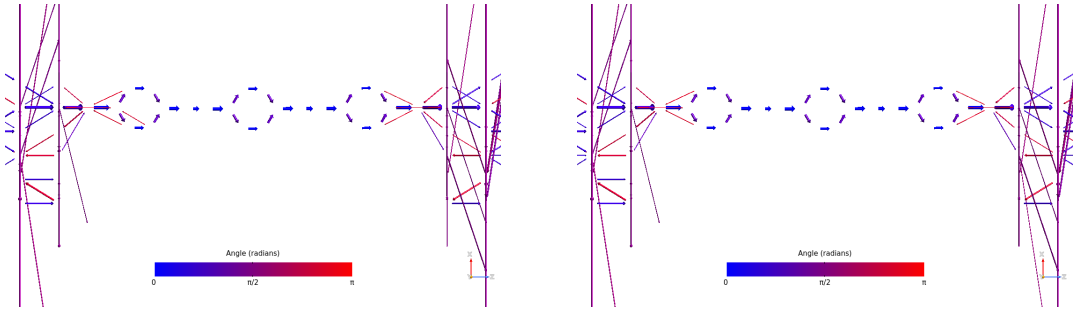

(a) Distance 11 Å.

(b) Distance 14.5 Å.

Figure 6.406: Picture of the pathways corresponding to the energy 0.28 eV for the OPE3 molecule with long driver at different distances, logic '1' configuration. The blue arrows are in the same direction as the z-axis, while the red ones are in the opposite direction.

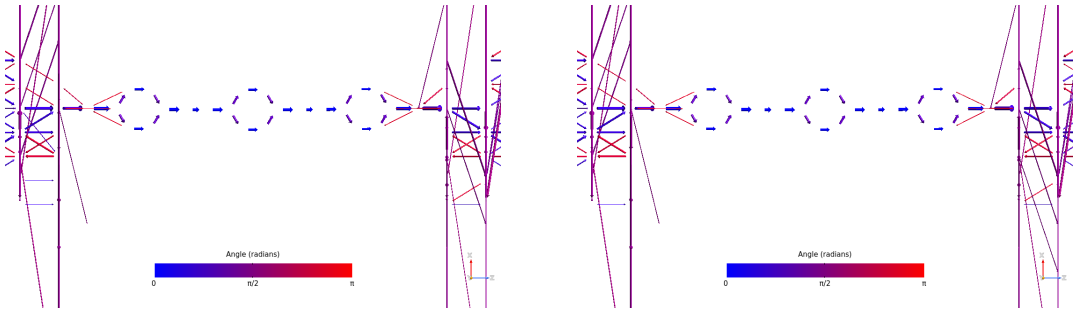

(a) Distance 11 Å.

(b) Distance 14.5 Å.

Figure 6.407: Picture of the pathways corresponding to the energy 0.44 eV for the OPE3 molecule with long driver at different distances, logic '1' configuration. The blue arrows are in the same direction as the z-axis, while the red ones are in the opposite direction.

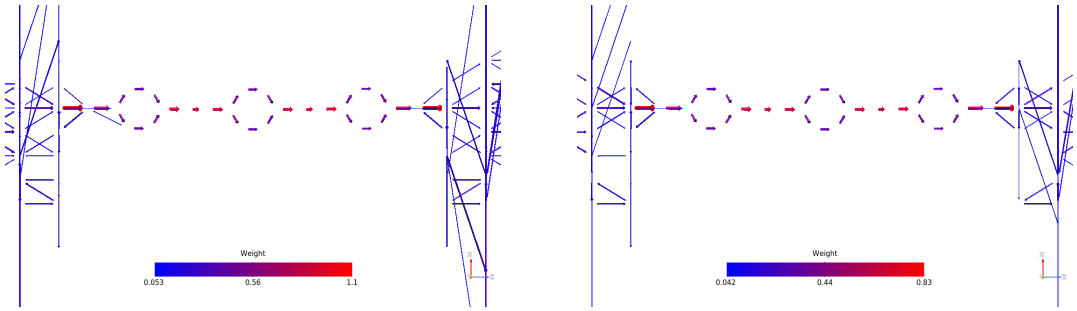

(a) Distance 11 Å, energy 0.16 eV.

(b) Distance 14.5 Å, energy 0.20 eV.

Figure 6.408: Picture of the pathways for the OPE3 molecule with long driver at different distance, logic '1' configuration, on the xz plane. The plots show the arrows' magnitude.

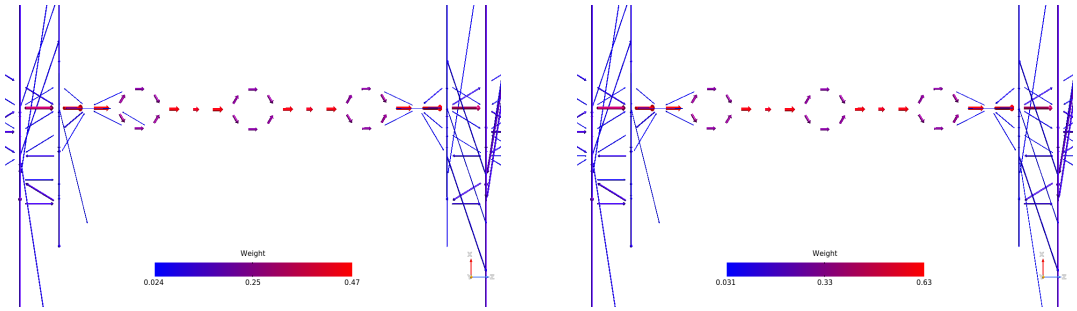

(a) Distance 11 Å.

(b) Distance 14.5 Å.

Figure 6.409: Picture of the pathways corresponding to the energy 0.28 eV for the OPE3 molecule with long driver at different distance, logic '1' configuration, on the xz plane. The plots show the arrows' magnitude.

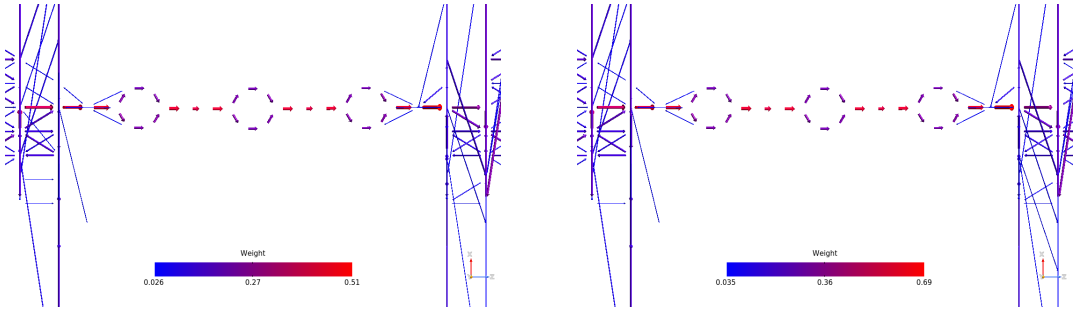

(a) Distance 11 Å.

(b) Distance 14.5 Å.

Figure 6.410: Picture of the pathways corresponding to the energy 0.44 eV for the OPE3 molecule with long driver at different distance, logic '1' configuration, on the xz plane. The plots show the arrows' magnitude.

6.13.4 OPE3: small driver

The OPE3 small driver builder views at different distances are reported in the figures 6.411 (logic '0') and 6.412 (logic '1').

These simulations are important for the tolerances' robustness. The small driver could be seen as a molFCN with the not completely charge localized. For this reason, it is fundamental that the small driver at 14.5 Å works properly in order to provide a readout system that works also considering non-idealities.

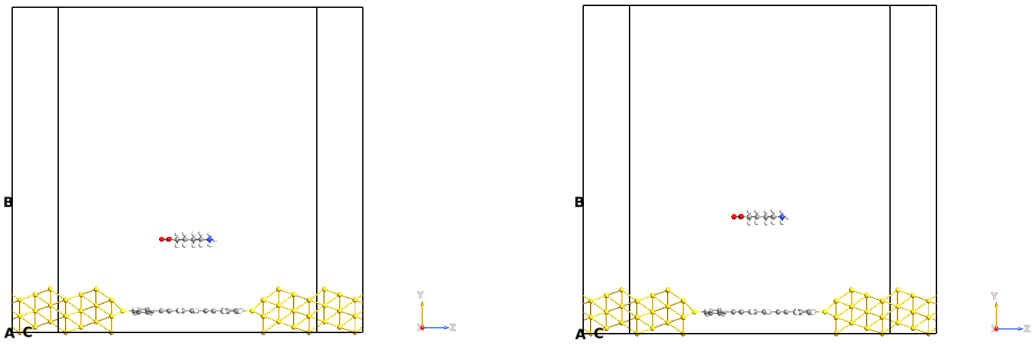

(a) Distance between junction molecule and driver equal to 11 Å.

(b) Distance between junction molecule and driver equal to 14.5 Å.

Figure 6.411: Picture of the QuantumATK builder for the OPV3 molecule, logic '0' configuration with the small driver at a different distance. The white atoms are the hydrogens, the yellow ones are gold atoms, the lighter yellow ones are the sulfurs, the blue ones are nitrogens, the reds are the oxygens and the grey atoms are carbons.

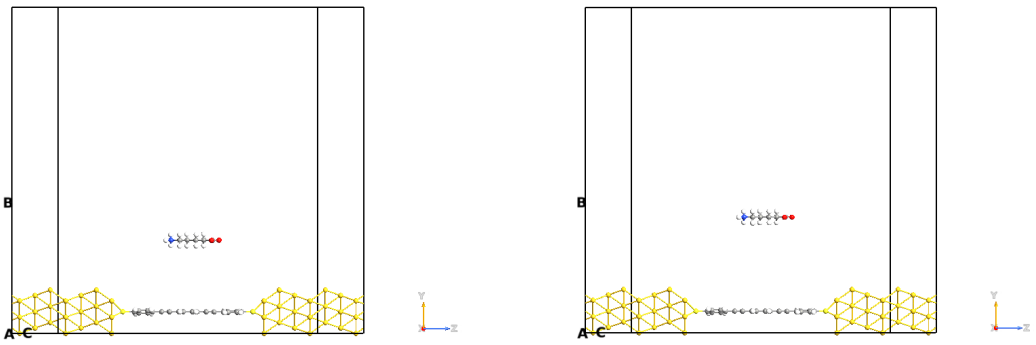

(a) Distance between junction molecule and driver equal to 11 Å.

(b) Distance between junction molecule and driver equal to 14.5 Å.

Figure 6.412: Picture of the QuantumATK builder for the OPV3 molecule, logic '1' configuration with the small driver at a different distance. The white atoms are the hydrogens, the yellow ones are gold atoms, the lighter yellow ones are the sulfurs, the blue ones are nitrogens, the reds are the oxygens and the grey atoms are carbons.

The small driver analysis was performed to increase the knowledge of the fabrication tolerance response. The lower dipole moment can refer to the not perfectly localization of the charge in the molFCN or some defects in the molecule synthesis. In the figure 6.413 are reported the TS for the different cases. The same considerations made for the long

driver can be done for the small driver.

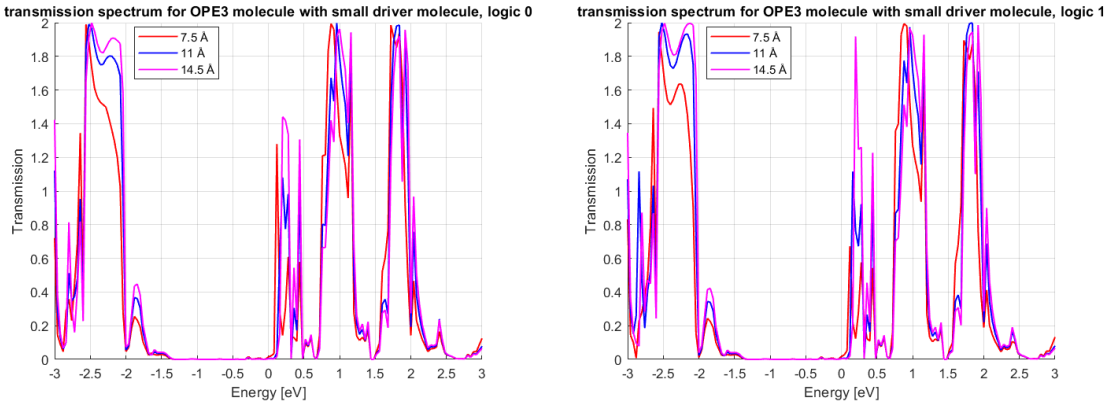

(a) logic 0 configuration.

(b) logic 1 configuration.

Figure 6.413: Picture of the TS for the OPE3 molecule considering the small driver at different distances, in particular the red curve is obtained with the driver at a distance of 7.5 Å, the blue one at a distance 11 Å and the magenta one at 14.5 Å.

The IV plot (figure 6.414) tells us that larger is the distance between the molecular junction and the driver and lower is the current. This result is consitent with the knowledge learned so far, lower is the elctric field at the junction, lower is the current.

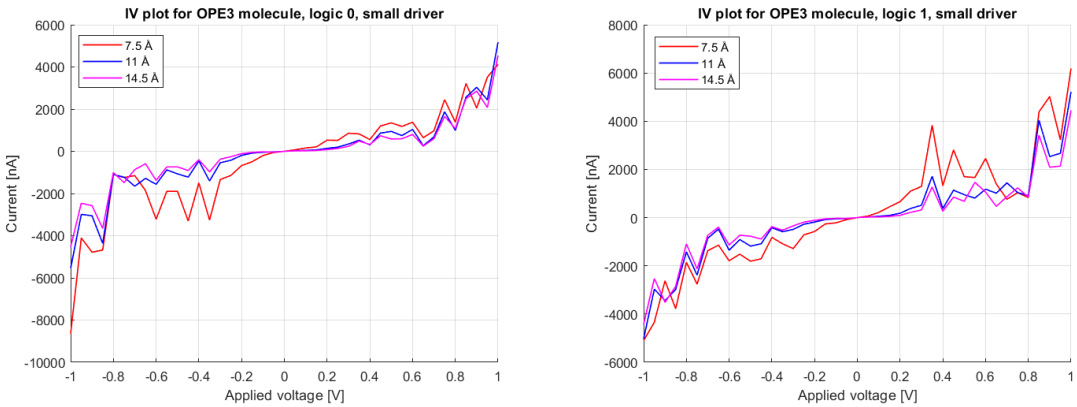

(a) logic 0 configuration.

(b) logic 1 configuration.

Figure 6.414: Picture of the IV for the OPE3 molecule considering the small driver at different distances, in particular the red curve is obtained with the driver at a distance of 7.5 Å, the blue one at a distance 11 Å and the magenta one at 14.5 Å.

The figure 6.415 highlights the feasibility of the readout system with the OPE3 molecule, because in the worst case the current difference is about hundreds of nA. This value is detectable by modern electronic devices.

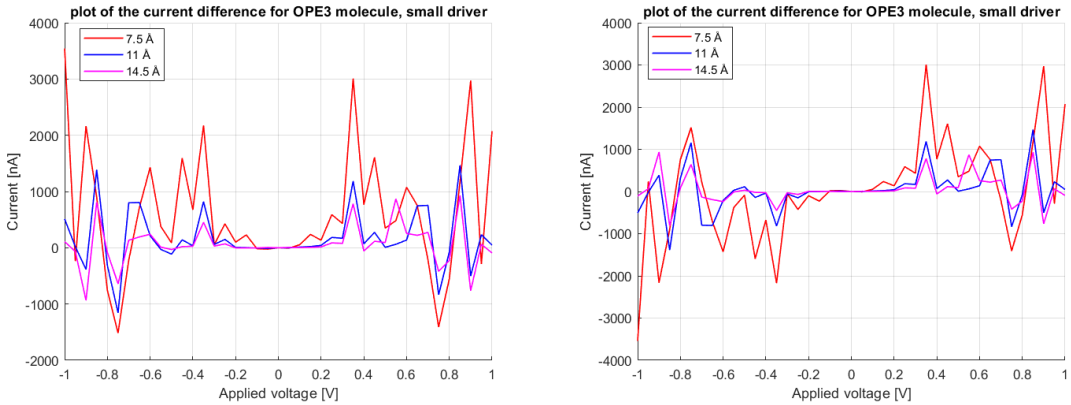

(a) logic '1' - logic '0'.

(b) |logic '1'| - |logic '0'|.

Figure 6.415: Picture of the current difference between the two configurations for the OPE3 molecule considering the small driver at different distances, in particular, the red curve is obtained with the driver at a distance of 7.5 Å, the blue one at a distance 11 Å and the magenta one at 14.5 Å.

As before, the orbitals show two different behavior, the same trend for the two considered distances and complementary geometries between them. The small driver confirms the same results as the long driver.

Concerning the logic '0', it can be noticed that the HOMO-1 (figures 6.416b, 6.417b and 6.418b) and HOMO (figures 6.419b, 6.420b and 6.421b) energy levels present the same trend between the two simulations, while the LUMO (figures 6.422b, 6.423b and 6.424b) and LUMO+1 (figures 6.425b, 6.426b and 6.427b) reveal the complementary behavior. These results are the same as the long driver.

For the logic '1' configuration, instead, all the analyzed orbitals exhibit the same behavior between the two distances, except for the LUMO+1 energy level. The figures regarding the logic '1' configuration are the ones from 6.387 to 6.398.

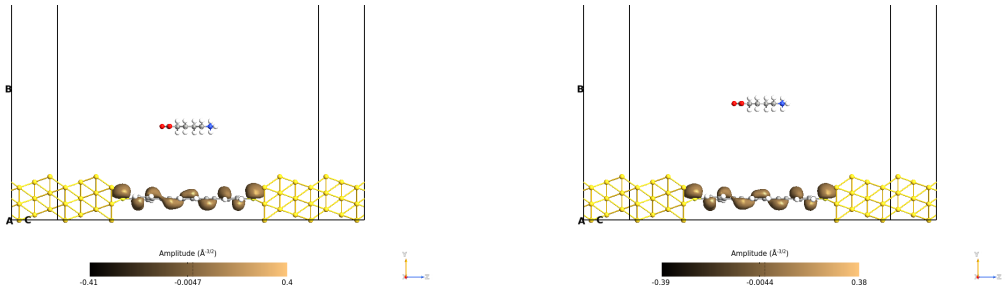

(a) Distance 11 Å.

(b) Distance 14.5 Å.

Figure 6.416: Picture of the orbitals corresponding to the HOMO-1 level for the OPE3 molecule with the small driver at different distances, logic '0' configuration, on the yz plane. The orbitals are taken with an isosurface value equal to 0.015.

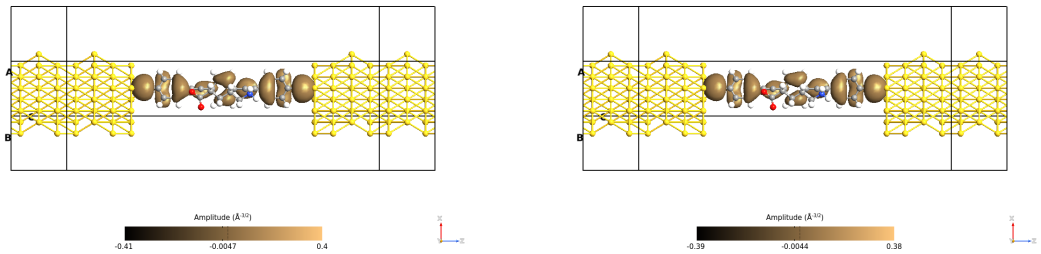

(a) Distance 11 Å. (b) Distance 14.5 Å.

Figure 6.417: Picture of the orbitals corresponding to the HOMO-1 level for the OPE3 molecule with the small driver at different distances, logic '0' configuration, on the xz plane with the driver. The orbitals are taken with an isosurface value equal to 0.015.

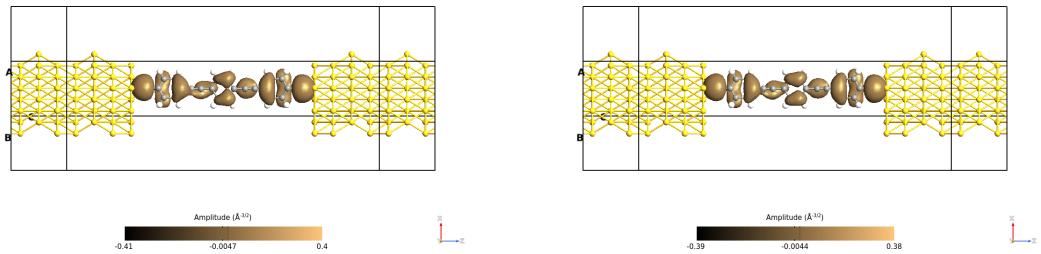

(a) Distance 11 Å. (b) Distance 14.5 Å.

Figure 6.418: Picture of the orbitals corresponding to the HOMO-1 level for the OPE3 molecule with the small driver at different distances, logic '0' configuration, on the xz plane without the driver. The orbitals are taken with an isosurface value equal to 0.015.

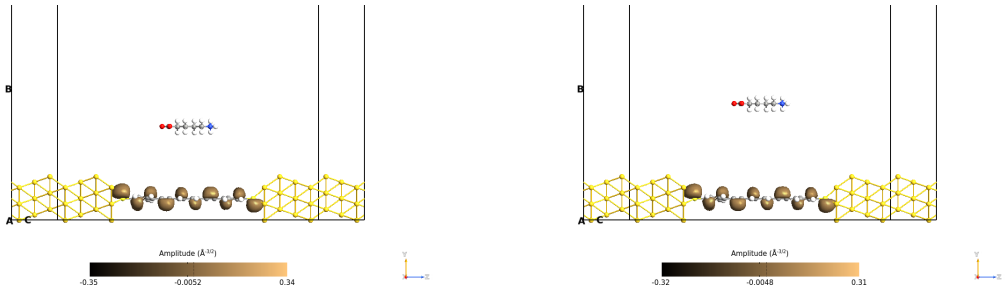

(a) Distance 11 Å. (b) Distance 14.5 Å.

Figure 6.419: Picture of the orbitals corresponding to the HOMO level for the OPE3 molecule with the small driver at different distances, logic '0' configuration, on the yz plane. The orbitals are taken with an isosurface value equal to 0.015.

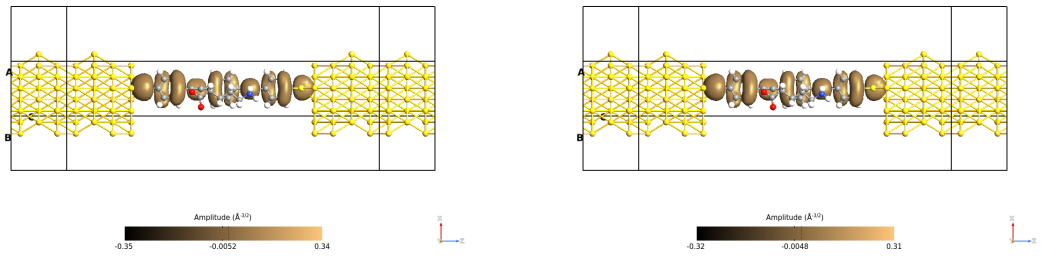

(a) Distance 11 Å. (b) Distance 14.5 Å.

Figure 6.420: Picture of the orbitals corresponding to the HOMO level for the OPE3 molecule with the small driver at different distances, logic '0' configuration, on the xz plane with the driver. The orbitals are taken with an isosurface value equal to 0.015.

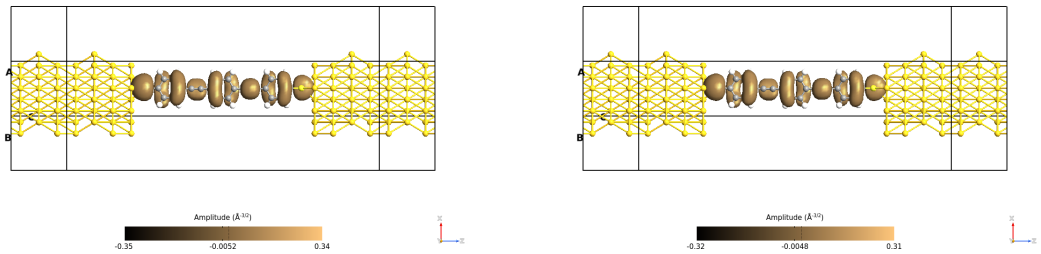

(a) Distance 11 Å. (b) Distance 14.5 Å.

Figure 6.421: Picture of the orbitals corresponding to the HOMO level for the OPE3 molecule with the small driver at different distances, logic '0' configuration, on the xz plane without the driver. The orbitals are taken with an isosurface value equal to 0.015.

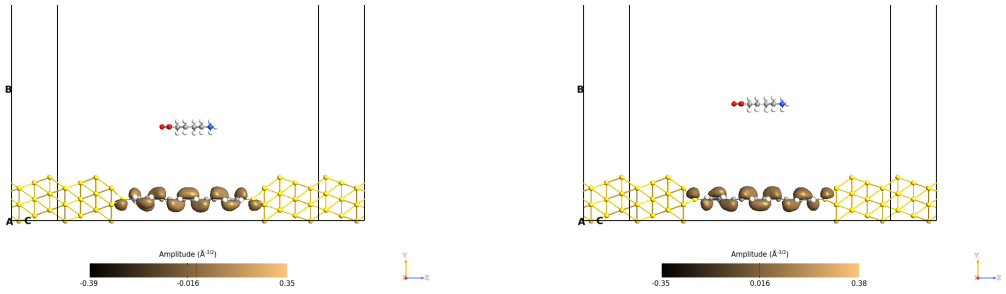

(a) Distance 11 Å. (b) Distance 14.5 Å.

Figure 6.422: Picture of the orbitals corresponding to the LUMO level for the OPE3 molecule with the small driver at different distances, logic '0' configuration, on the yz plane. The orbitals are taken with an isosurface value equal to 0.015.

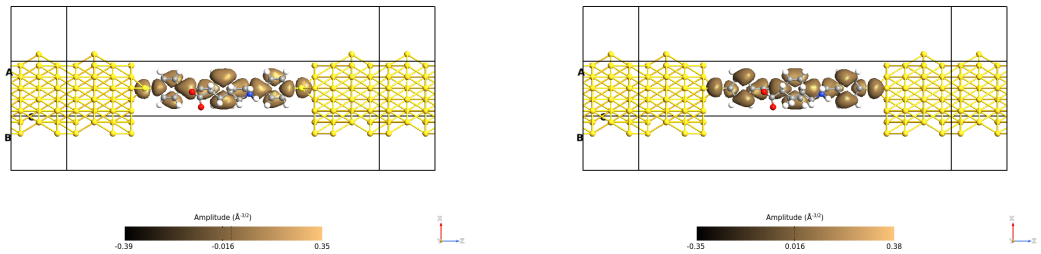

(a) Distance 11 Å. (b) Distance 14.5 Å.

Figure 6.423: Picture of the orbitals corresponding to the LUMO level for the OPE3 molecule with the small driver at different distances, logic '0' configuration, on the xz plane with the driver. The orbitals are taken with an isosurface value equal to 0.015.

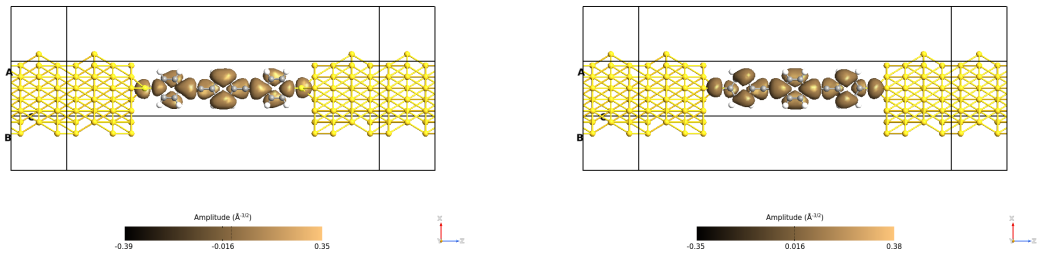

(a) Distance 11 Å. (b) Distance 14.5 Å.

Figure 6.424: Picture of the orbitals corresponding to the LUMO level for the OPE3 molecule with the small driver at different distances, logic '0' configuration, on the xz plane without the driver. The orbitals are taken with an isosurface value equal to 0.015.

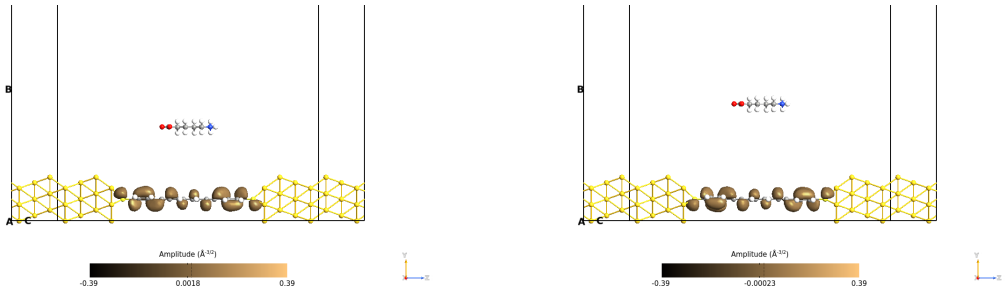

(a) Distance 11 Å. (b) Distance 14.5 Å.

Figure 6.425: Picture of the orbitals corresponding to the LUMO+1 level for the OPE3 molecule with the small driver at different distances, logic '0' configuration, on the yz plane. The orbitals are taken with an isosurface value equal to 0.015.

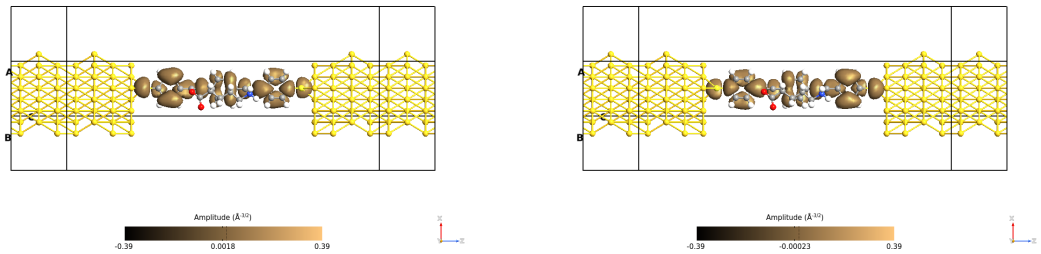

(a) Distance 11 Å. (b) Distance 14.5 Å.

Figure 6.426: Picture of the orbitals corresponding to the LUMO+1 level for the OPE3 molecule with the small driver at different distances, logic '0' configuration, on the xz plane with the driver. The orbitals are taken with an isosurface value equal to 0.015.

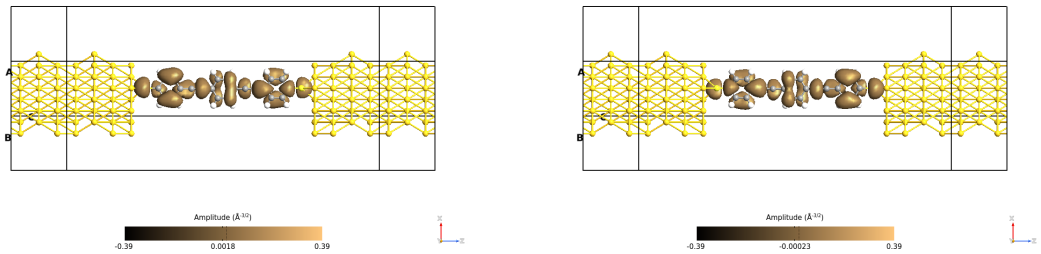

(a) Distance 11 Å. (b) Distance 14.5 Å.

Figure 6.427: Picture of the orbitals corresponding to the LUMO+1 level for the OPE3 molecule with the small driver at different distances, logic '0' configuration, on the xz plane without the driver. The orbitals are taken with an isosurface value equal to 0.015.

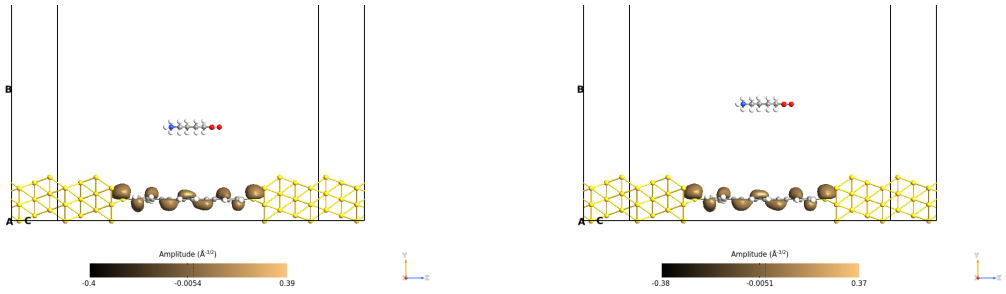

(a) Distance 11 Å. (b) Distance 14.5 Å.

Figure 6.428: Picture of the orbitals corresponding to the HOMO-1 level for the OPE3 molecule with the small driver at different distances, logic '1' configuration, on the yz plane. The orbitals are taken with an isosurface value equal to 0.015.

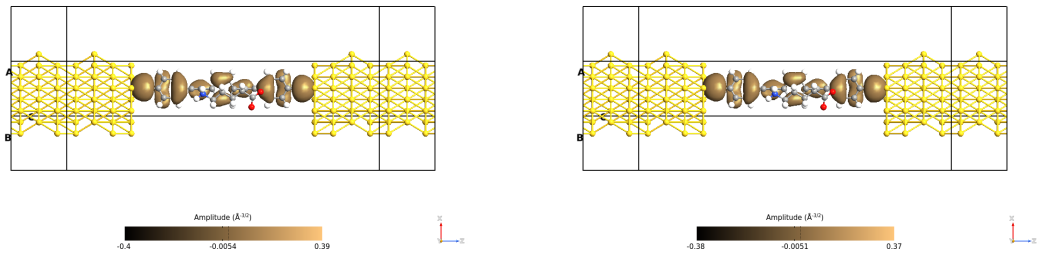

(a) Distance 11 Å. (b) Distance 14.5 Å.

Figure 6.429: Picture of the orbitals corresponding to the HOMO-1 level for the OPE3 molecule with the small driver at different distances, logic '1' configuration, on the xz plane with the driver. The orbitals are taken with an isosurface value equal to 0.015.

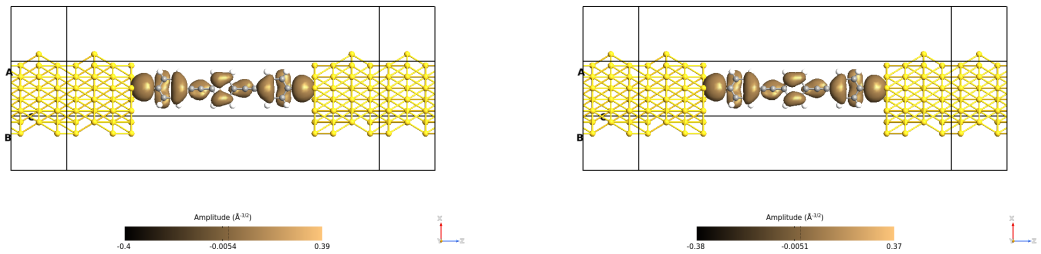

(a) Distance 11 Å. (b) Distance 14.5 Å.

Figure 6.430: Picture of the orbitals corresponding to the HOMO-1 level for the OPE3 molecule with the small driver at different distances, logic '1' configuration, on the xz plane without the driver. The orbitals are taken with an isosurface value equal to 0.015.

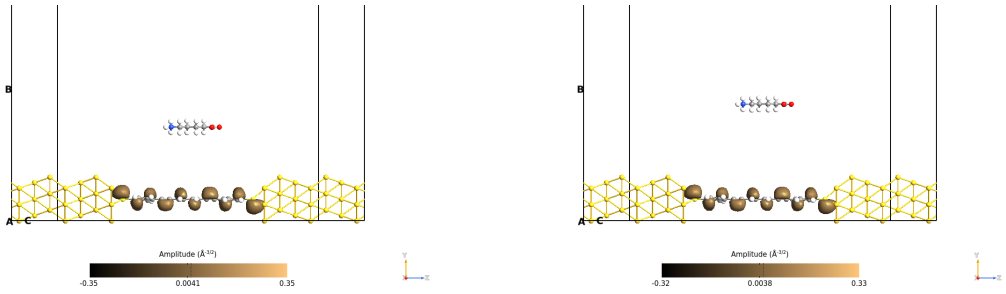

(a) Distance 11 Å. (b) Distance 14.5 Å.

Figure 6.431: Picture of the orbitals corresponding to the HOMO level for the OPE3 molecule with the small driver at different distances, logic '1' configuration, on the yz plane. The orbitals are taken with an isosurface value equal to 0.015.

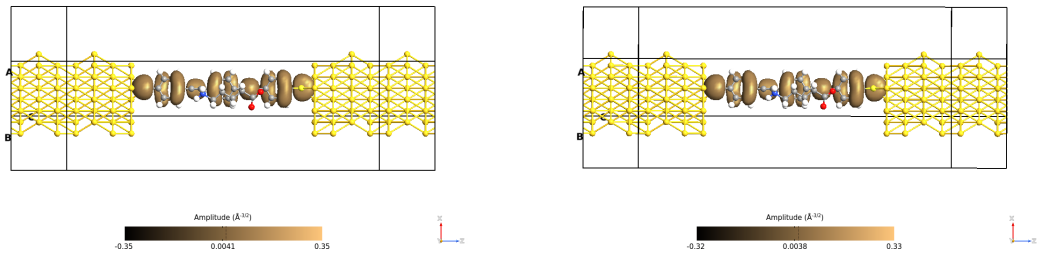

(a) Distance 11 Å. (b) Distance 14.5 Å.

Figure 6.432: Picture of the orbitals corresponding to the HOMO level for the OPE3 molecule with the small driver at different distances, logic '1' configuration, on the xz plane with the driver. The orbitals are taken with an isosurface value equal to 0.015.

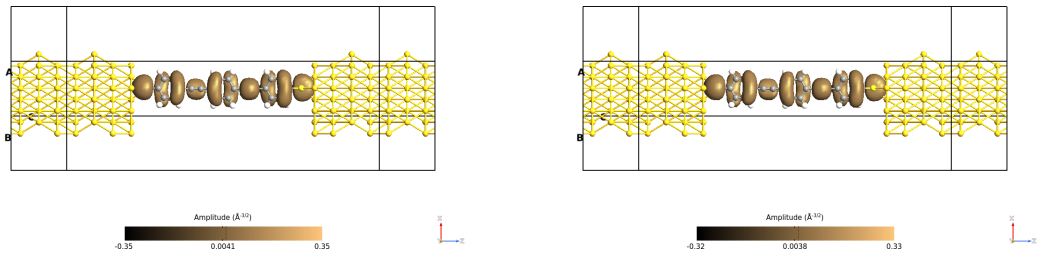

(a) Distance 11 Å. (b) Distance 14.5 Å.

Figure 6.433: Picture of the orbitals corresponding to the HOMO level for the OPE3 molecule with the small driver at different distances, logic '1' configuration, on the xz plane without the driver. The orbitals are taken with an isosurface value equal to 0.015.

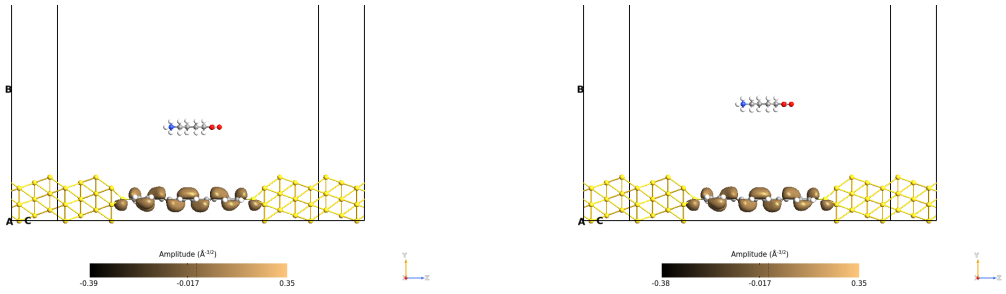

(a) Distance 11 Å. (b) Distance 14.5 Å.

Figure 6.434: Picture of the orbitals corresponding to the LUMO level for the OPE3 molecule with the small driver at different distances, logic '1' configuration, on the yz plane. The orbitals are taken with an isosurface value equal to 0.015.

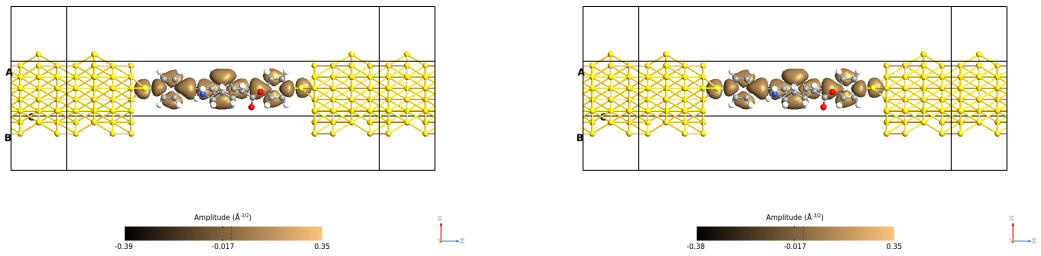

(a) Distance 11 Å. (b) Distance 14.5 Å.

Figure 6.435: Picture of the orbitals corresponding to the LUMO level for the OPE3 molecule with the small driver at different distances, logic '1' configuration, on the xz plane with the driver. The orbitals are taken with an isosurface value equal to 0.015.

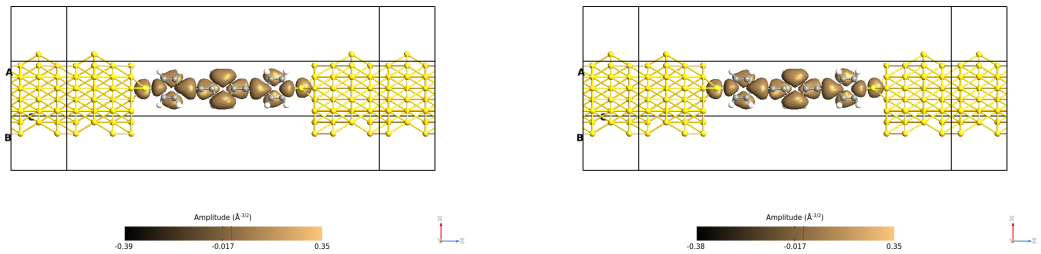

(a) Distance 11 Å. (b) Distance 14.5 Å.

Figure 6.436: Picture of the orbitals corresponding to the LUMO level for the OPE3 molecule with the small driver at different distances, logic '1' configuration, on the xz plane without the driver. The orbitals are taken with an isosurface value equal to 0.015.

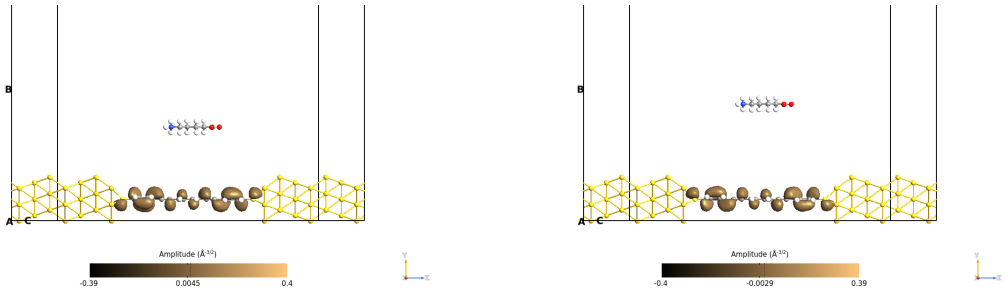

(a) Distance 11 Å. (b) Distance 14.5 Å.

Figure 6.437: Picture of the orbitals corresponding to the LUMO+1 level for the OPE3 molecule with the small driver at different distances, logic '1' configuration, on the yz plane. The orbitals are taken with an isosurface value equal to 0.015.

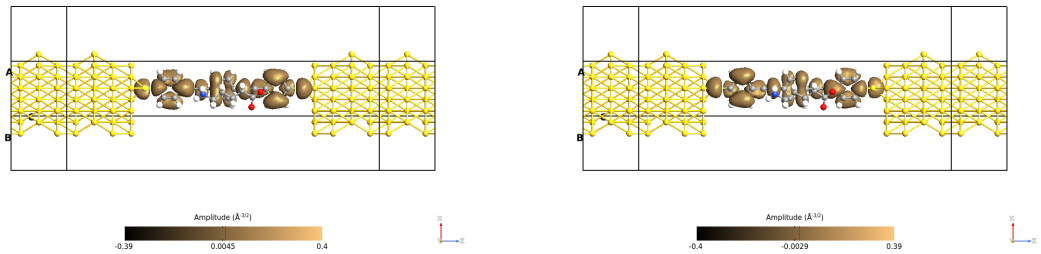

(a) Distance 11 Å. (b) Distance 14.5 Å.

Figure 6.438: Picture of the orbitals corresponding to the LUMO+1 level for the OPE3 molecule with the small driver at different distances, logic '1' configuration, on the xz plane with the driver. The orbitals are taken with an isosurface value equal to 0.015.

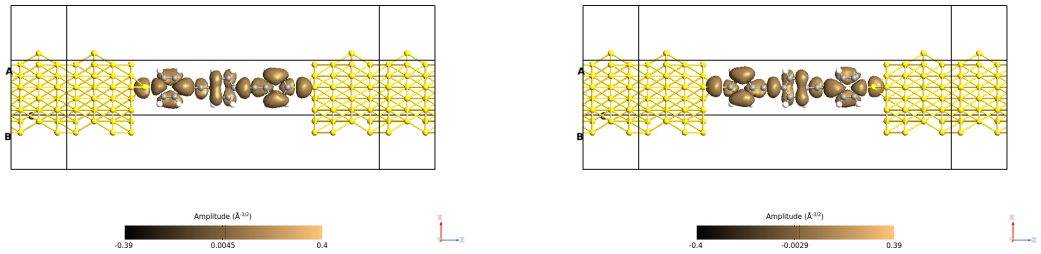

(a) Distance 11 Å. (b) Distance 14.5 Å.

Figure 6.439: Picture of the orbitals corresponding to the LUMO+1 level for the OPE3 molecule with the small driver at different distances, logic '1' configuration, on the xz plane without the driver. The orbitals are taken with an isosurface value equal to 0.015.

The transmission pathways don't reveal surprises, they confirm the previous trend. The figures from 6.440 to 6.445 refer to the logic '0' configuration, while from 6.446 to 6.451 to the logic '1' one.

For the plots concerning the angle, as expected, the higher the energy, the higher the amount of electrons that flow in the opposite direction with respect to the conduction direction.

The weight graphs show the same trend that the TS (figure 6.53a) tells us. Higher is the magnitude value according to the amplitude of the peak in the TS.

The small driver analysis with 14.5 Å of distance between the junction molecule and the driver plays a relevant role because it modelizes the not-perfect charge localization in the molFCN molecule (small driver) and the fabrication tolerances (accuracy in the deposition).

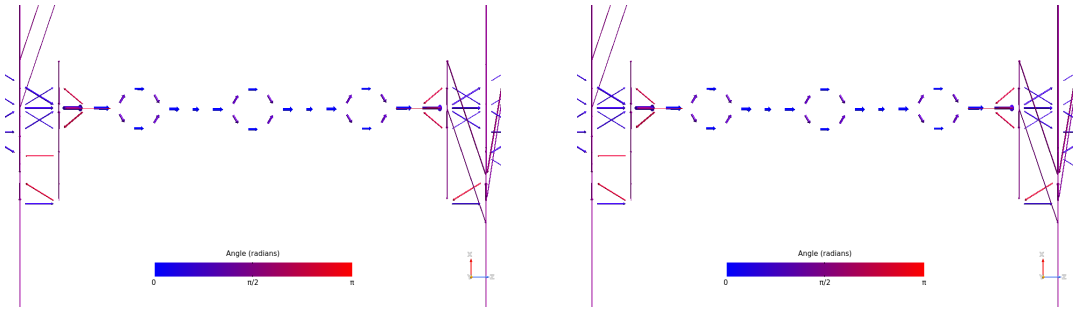

(a) Distance 11 Å. (b) Distance 14.5 Å.

Figure 6.440: Picture of the pathways corresponding to the energy 0.2 eV for the OPE3 molecule with the small driver at different distances, logic '0' configuration, on the xz plane. The blue arrows are in the same direction as the z-axis, while the red ones are in the opposite direction.

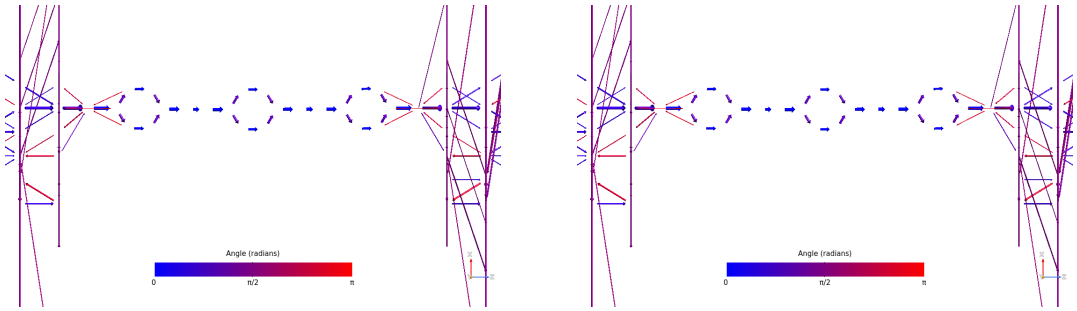

(a) Distance 11 Å. (b) Distance 14.5 Å.

Figure 6.441: Picture of the pathways corresponding to the energy 0.28 eV for the OPE3 molecule with the small driver at different distances, logic '0' configuration, on the xz plane. The blue arrows are in the same direction as the z-axis, while the red ones are in the opposite direction.

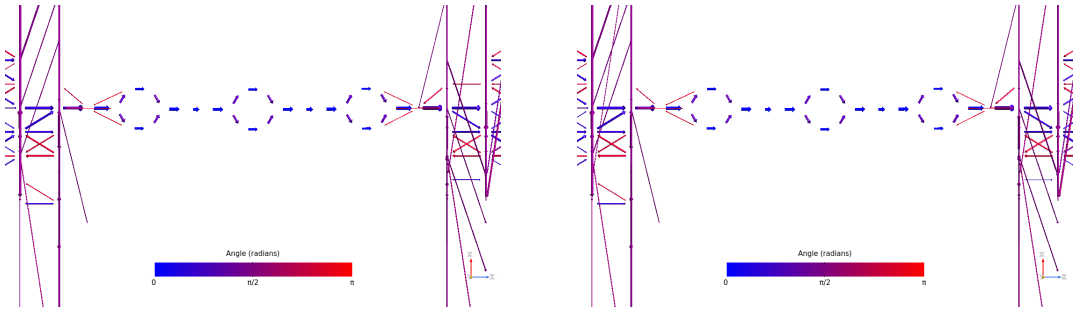

(a) Distance 11 Å. (b) Distance 14.5 Å.

Figure 6.442: Picture of the pathways corresponding to the energy 0.44 eV for the OPE3 molecule with the small driver at different distances, logic '0' configuration, on the xz plane. The blue arrows are in the same direction as the z-axis, while the red ones are in the opposite direction.

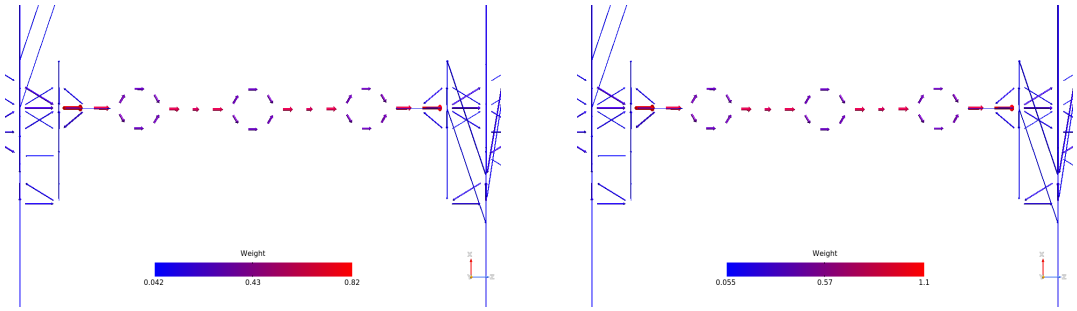

(a) Distance 11 Å. (b) Distance 14.5 Å.

Figure 6.443: Picture of the pathways corresponding to the energy 0.2 eV for the OPE3 molecule with the small driver at different distances, logic '0' configuration, on the xz plane. The plots show the arrows' magnitude.

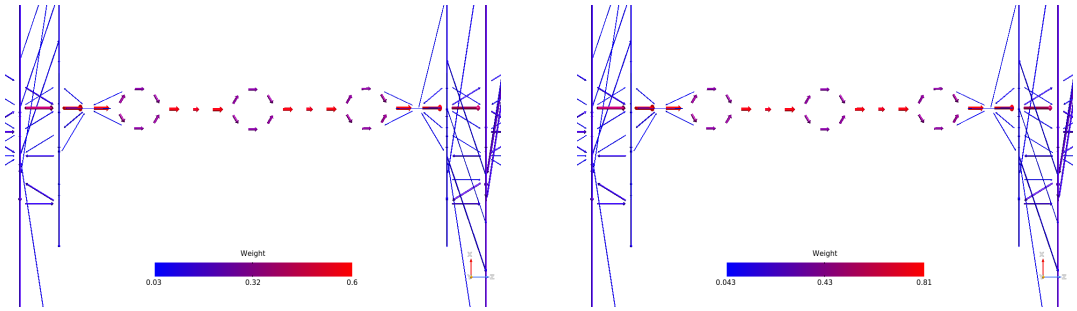

(a) Distance 11 Å. (b) Distance 14.5 Å.

Figure 6.444: Picture of the pathways corresponding to the energy 0.28 eV for the OPE3 molecule with the small driver at different distances, logic '0' configuration, on the xz plane. The plots show the arrows' magnitude.

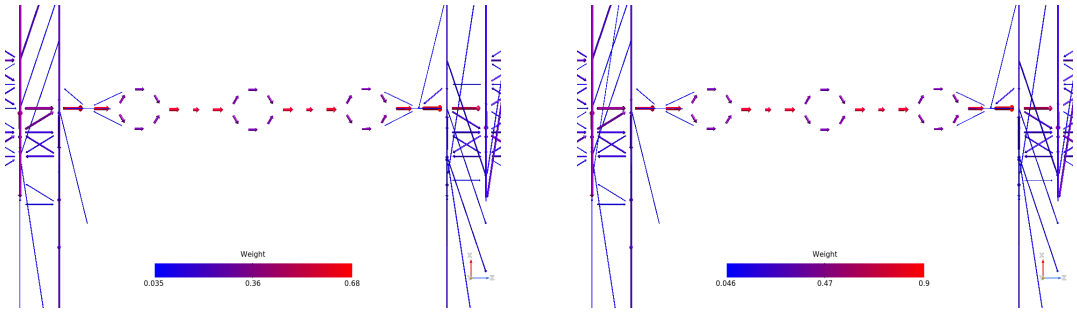

(a) Distance 11 Å. (b) Distance 14.5 Å.

Figure 6.445: Picture of the pathways corresponding to the energy 0.44 eV for the OPE3 molecule with the small driver at different distances, logic '0' configuration, on the xz plane. The plots show the arrows' magnitude.

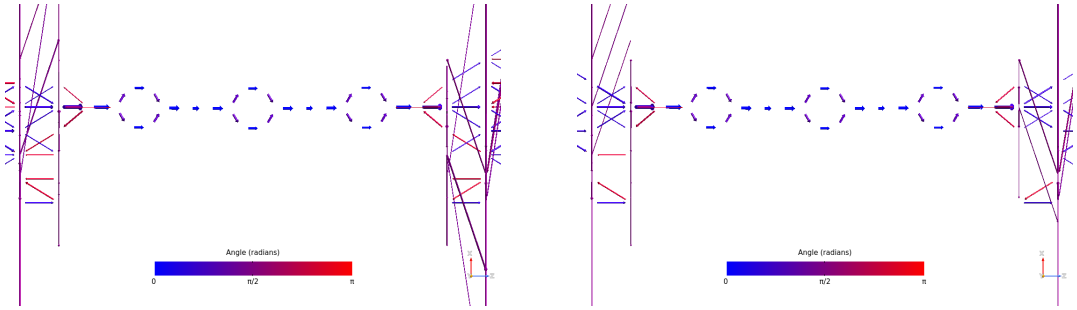

(a) Distance 11 Å, energy 0.16 eV. (b) Distance 14.5 Å, energy 0.2 eV.

Figure 6.446: Picture of the pathways for the OPE3 molecule with the small driver at different distances, logic '1' configuration, on the xz plane. The blue arrows are in the same direction as the z-axis, while the red ones are in the opposite direction.

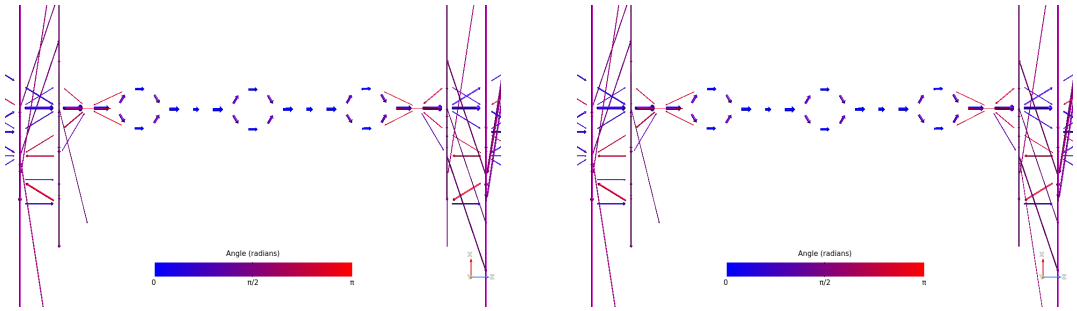

(a) Distance 11 Å. (b) Distance 14.5 Å.

Figure 6.447: Picture of the pathways corresponding to the energy 0.28 eV for the OPE3 molecule with the small driver at different distances, logic '1' configuration, on the xz plane. The blue arrows are in the same direction as the z-axis, while the red ones are in the opposite direction.

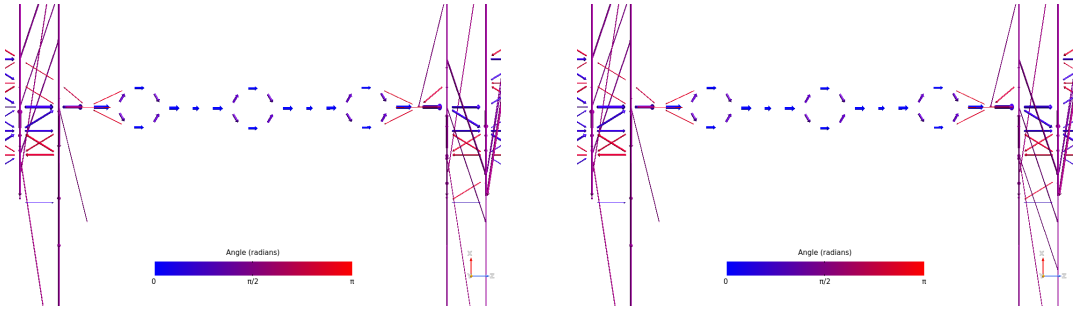

(a) Distance 11 Å. (b) Distance 14.5 Å.

Figure 6.448: Picture of the pathways corresponding to the energy 0.44 eV for the OPE3 molecule with the small driver at different distances, logic '1' configuration, on the xz plane. The blue arrows are in the same direction as the z-axis, while the red ones are in the opposite direction.

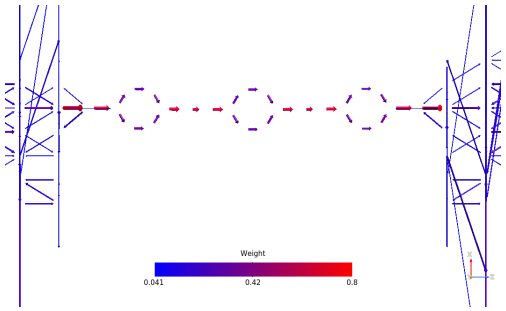

(a) Distance 11 Å, energy 0.16 eV.

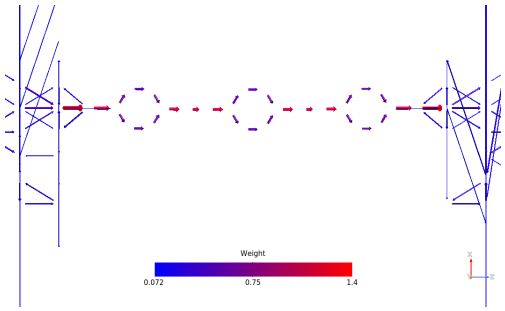

(b) Distance 14.5 Å, energy 0.2 eV.

Figure 6.449: Picture of the pathways for the OPE3 molecule with the small driver at different distances, logic '1' configuration, on the xz plane. The plots show the arrows' magnitude.

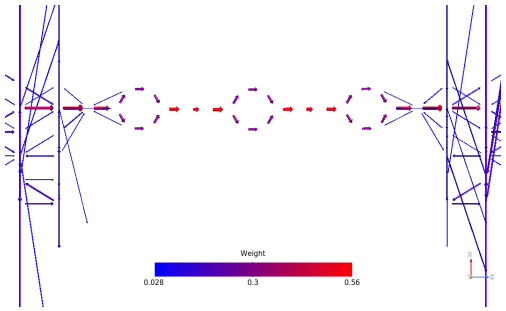

(a) Distance 11 Å.

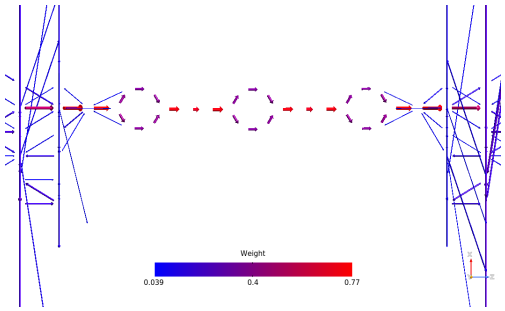

(b) Distance 14.5 Å.

Figure 6.450: Picture of the pathways corresponding to the energy 0.28 eV for the OPE3 molecule with the small driver at different distances, logic '1' configuration, on the xz plane. The plots show the arrows' magnitude.

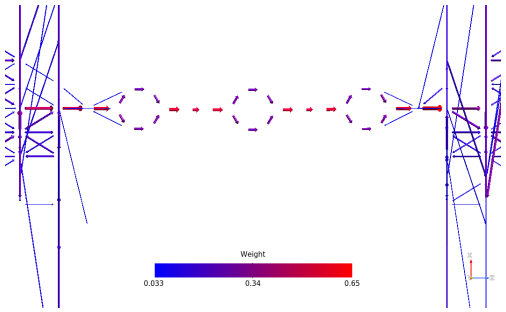

(a) Distance 11 Å.

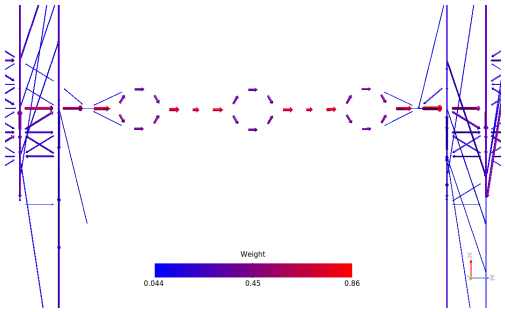

(b) Distance 14.5 Å.

Figure 6.451: Picture of the pathways corresponding to the energy 0.44 eV for the OPE3 molecule with the small driver at different distances, logic '1' configuration, on the xz plane. The plots show the arrows' magnitude.

6.14 Transmission eigenstate

The transmission eigenstate plots reveal the direct influence of the driver on the junction molecule's orbitals. These simulations have been performed only for the OPV3 and OPE3 molecules at a distance of about 7 Å between the junction and the driver. The transmission eigenstates are calculated starting from a specific energy value (of the TS) and an eigenvalue. The eigenstates and eigenvalues come from the solution of the Schrödinger's equation. The eigenvalues represent the probability of the transmission operator, while the eigenstates are the space where the transmission happens.

6.14.1 OPV3

The OPV3 results reveal different phases for the two different configurations (different colors in the plots). An interesting fact can be observed by looking at the eigenvalue parameters, for each energy considered there is always a more probable eigenvalue, which the corresponding transmission eigenstate effectively shows an interaction with the junction molecules. The other eigenvalues refer to the electrodes only, their probabilities are very low compared to the previously cited ones.

Another important behavior can be noticed by the yz plots (figures 6.452, 6.454, 6.457 and 6.459), in which no direct interaction between driver and molecule has been highlighted, this means that no van der Waals forces are relevant at those distances, the interaction is purely electrostatic.

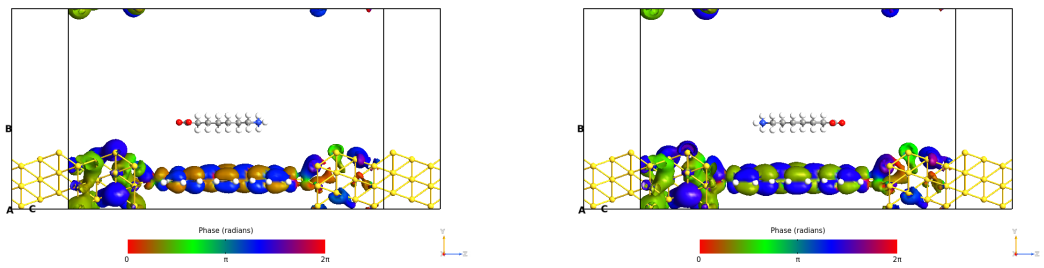

(a) Logic '0', eigenvalue equal to 0.291296.

(b) Logic '1', eigenvalue equal to 0.354054.

Figure 6.452: Picture of the transmission eigenstate corresponding to the energy 0.08 eV for the OPV3 molecule with the long driver, yz plane.

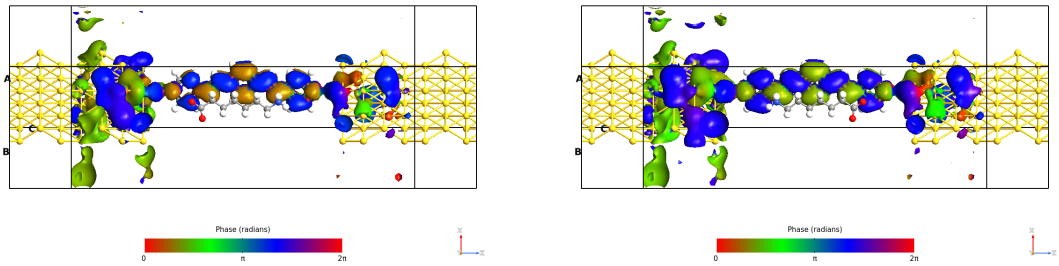

(a) Logic '0', eigenvalue equal to 0.291296. (b) Logic '1', eigenvalue equal to 0.354054.

Figure 6.453: Picture of the transmission eigenstate corresponding to the energy 0.08 eV for the OPV3 molecule with the long driver, xz plane.

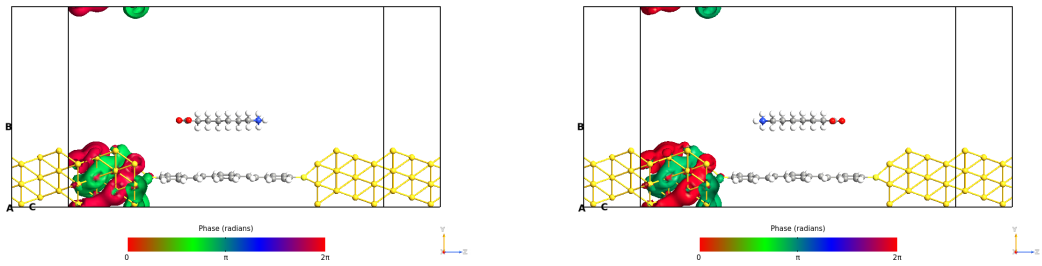

(a) Logic '0', eigenvalue equal to 3.34247 e-14. (b) Logic '1', eigenvalue equal to 2.42861 e-14.

Figure 6.454: Picture of the transmission eigenstate corresponding to the energy 0.08 eV for the OPV3 molecule with the long driver, yz plane.

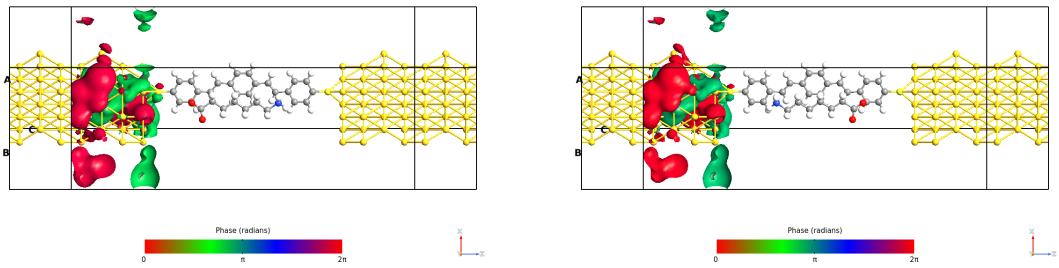

(a) Logic '0', eigenvalue equal to 3.34247 e-14. (b) Logic '1', eigenvalue equal to 2.42861 e-14.

Figure 6.455: Picture of the transmission eigenstate corresponding to the energy 0.08 eV for the OPV3 molecule with the long driver, xz plane.

6.14.2 OPE3

For the OPE3 molecule can be derived with the same considerations as the OPV3 one. In this case, the eigenvalues are more than the OPV3, but their probability is very low

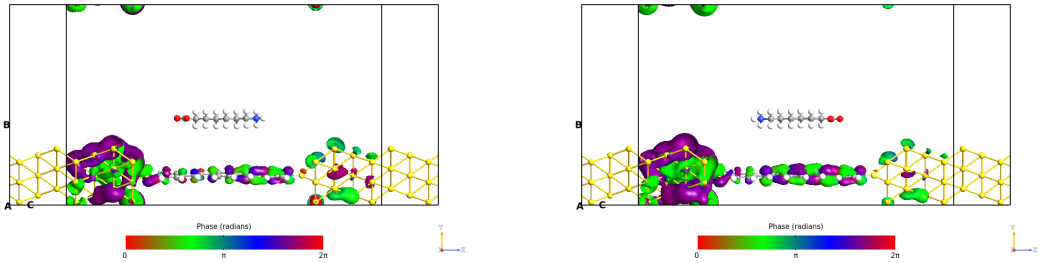

(a) Logic '0', eigenvalue equal to 0.208151.

(b) Logic '1', eigenvalue equal to 0.213047.

Figure 6.456: Picture of the transmission eigenstate corresponding to the energy 0.28 eV for the OPV3 molecule with the long driver, yz plane.

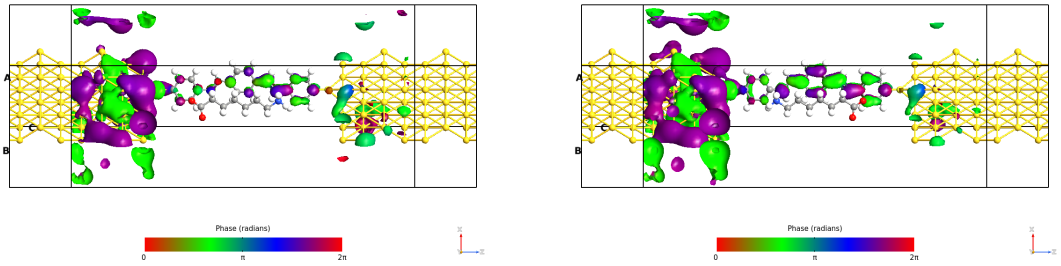

(a) Logic '0', eigenvalue equal to 0.208151.

(b) Logic '1', eigenvalue equal to 0.213047.

Figure 6.457: Picture of the transmission eigenstate corresponding to the energy 0.28 eV for the OPV3 molecule with the long driver, xz plane.

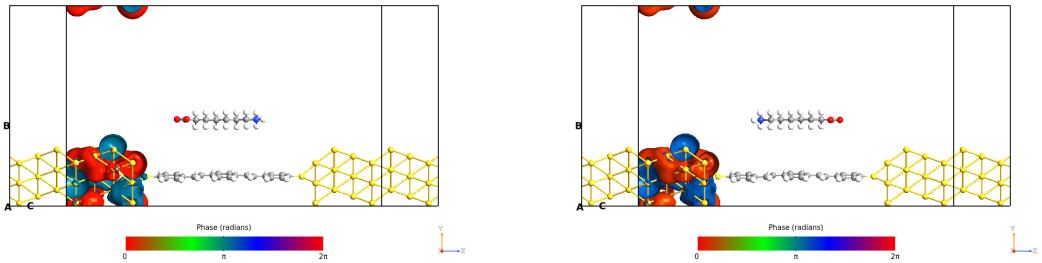

(a) Logic '0', eigenvalue equal to 9.53473 e-14.

(b) Logic '1', eigenvalue equal to 9.95870 e-14.

Figure 6.458: Picture of the transmission eigenstate corresponding to the energy 0.28 eV for the OPV3 molecule with the long driver, yz plane.

(e-18).

For the logic '1' configuration, there is an extra eigenvalue with respect to the logic '0' one, it is reported in figure 6.466. It is not so relevant because its value is equal to 2.46834 e-18, which is a very low value considering the fact that it is a probability.

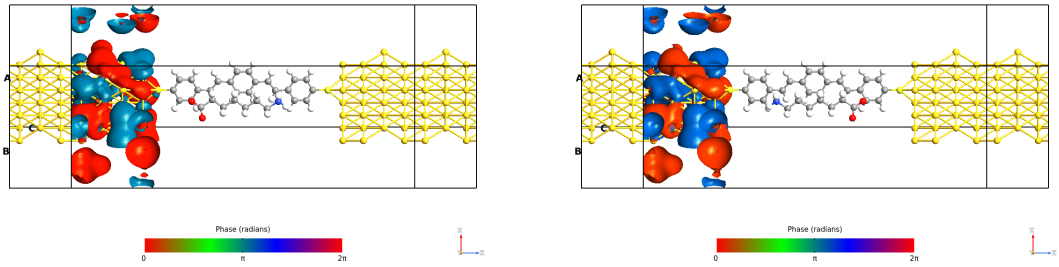

(a) Logic '0', eigenvalue equal to 9.53473 e-14. (b) Logic '1', eigenvalue equal to 9.95870 e-14.

Figure 6.459: Picture of the transmission eigenstate corresponding to the energy 0.28 eV for the OPV3 molecule with the long driver, xz plane.

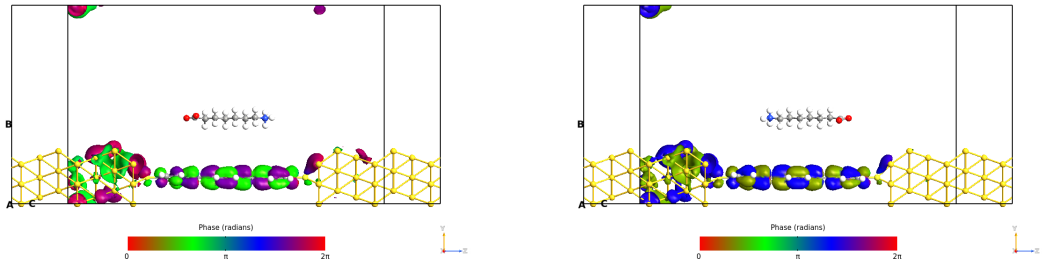

(a) Logic '0', eigenvalue equal to 0.198450. (b) Logic '1', eigenvalue equal to 0.092798.

Figure 6.460: Picture of the transmission eigenstate corresponding to the energy 0.12 eV for the OPE3 molecule with the long driver, yz plane.

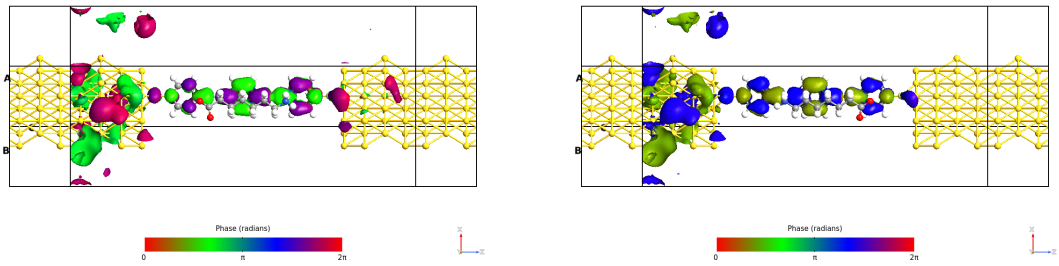

(a) Logic '0', eigenvalue equal to 0.291296. (b) Logic '1', eigenvalue equal to 0.354054.

Figure 6.461: Picture of the transmission eigenstate corresponding to the energy 0.12 eV for the OPE3 molecule with the long driver, xz plane.

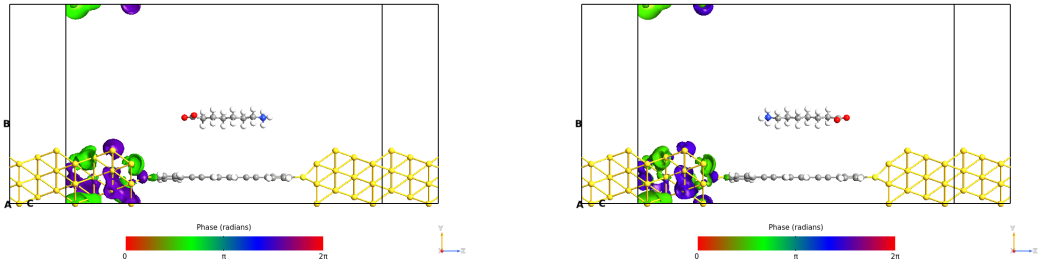

(a) Logic '0', eigenvalue equal to 5.78868 e-12. (b) Logic '1', eigenvalue equal to 4.85139 e-12.

Figure 6.462: Picture of the transmission eigenstate corresponding to the energy 0.12 eV for the OPE3 molecule with the long driver, yz plane.

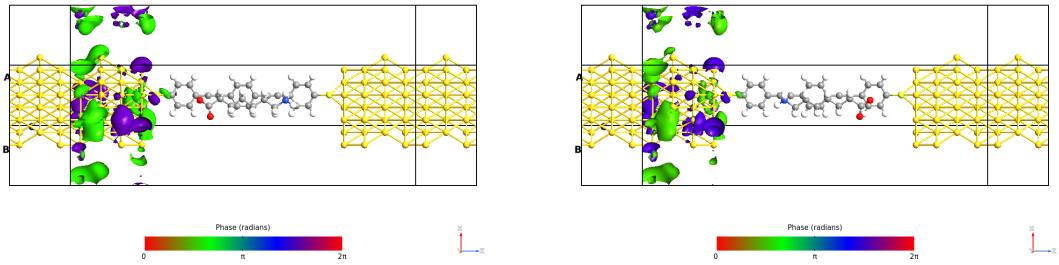

(a) Logic '0', eigenvalue equal to 5.78868 e-12. (b) Logic '1', eigenvalue equal to 4.85139 e-12.

Figure 6.463: Picture of the transmission eigenstate corresponding to the energy 0.12 eV for the OPE3 molecule with the long driver, xz plane.

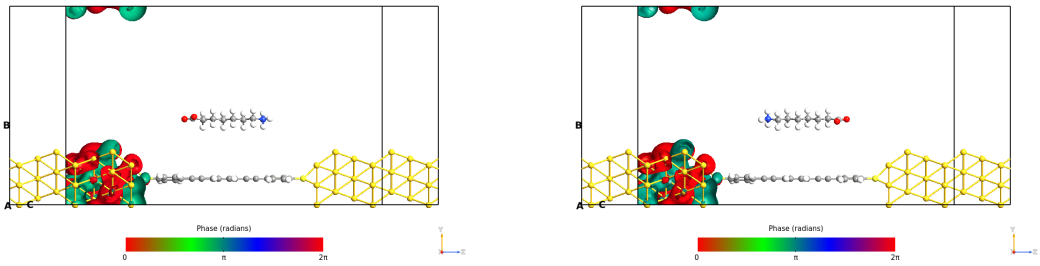

(a) Logic '0', eigenvalue equal to 7.00131 e-16. (b) Logic '1', eigenvalue equal to 8.02548 e-16.

Figure 6.464: Picture of the transmission eigenstate corresponding to the energy 0.12 eV for the OPE3 molecule with the long driver, yz plane.

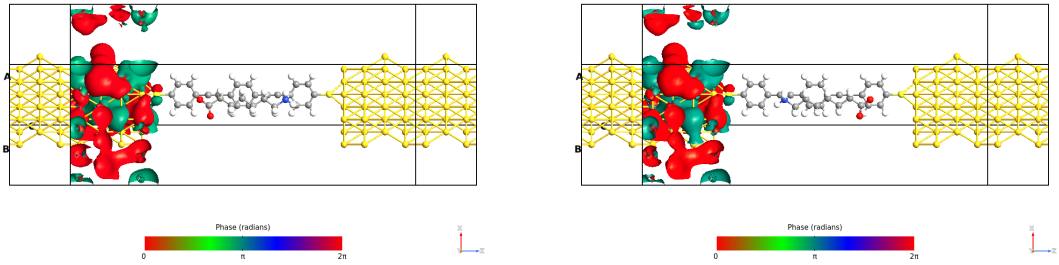

(a) Logic '0', eigenvalue equal to 7.00131 e-16. (b) Logic '1', eigenvalue equal to 8.02548 e-16.

Figure 6.465: Picture of the transmission eigenstate corresponding to the energy 0.12 eV for the OPE3 molecule with the long driver, xz plane.

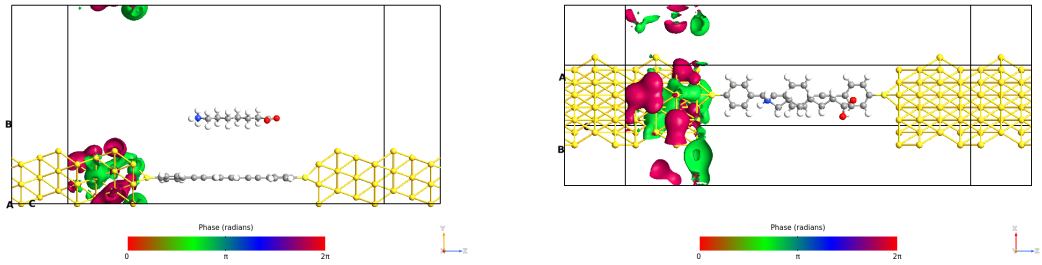

(a) Eigenvalue equal to 2.46834 e-18, yz plane. (b) Eigenvalue equal to 2.46834 e-18, xz plane..

Figure 6.466: Picture of the transmission eigenstate corresponding to the energy 0.12 eV for the OPE3 molecule with the long driver, logic '1' configuration.

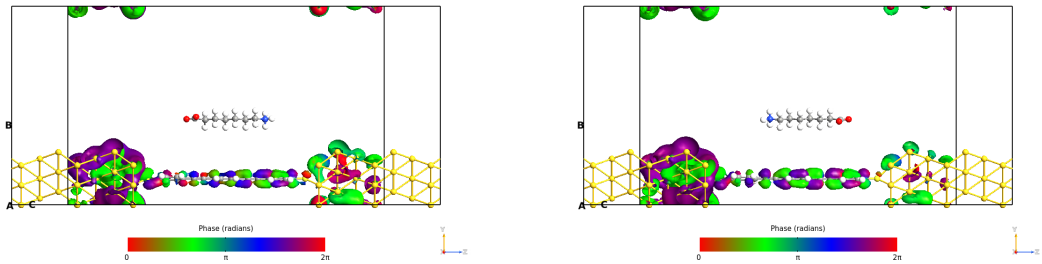

(a) Logic '0', eigenvalue equal to 0.309318. (b) Logic '1', eigenvalue equal to 0.279186.

Figure 6.467: Picture of the transmission eigenstate corresponding to the energy 0.28 eV for the OPE3 molecule with the long driver, yz plane.

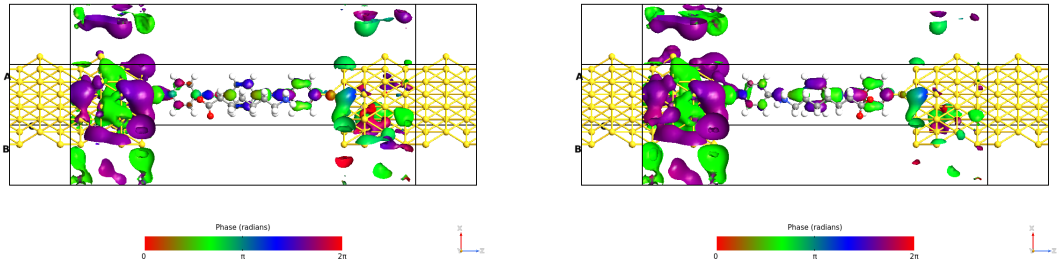

(a) Logic '0', eigenvalue equal to 0.309318. (b) Logic '1', eigenvalue equal to 0.279186.

Figure 6.468: Picture of the transmission eigenstate corresponding to the energy 0.28 eV for the OPE3 molecule with the long driver, xz plane.

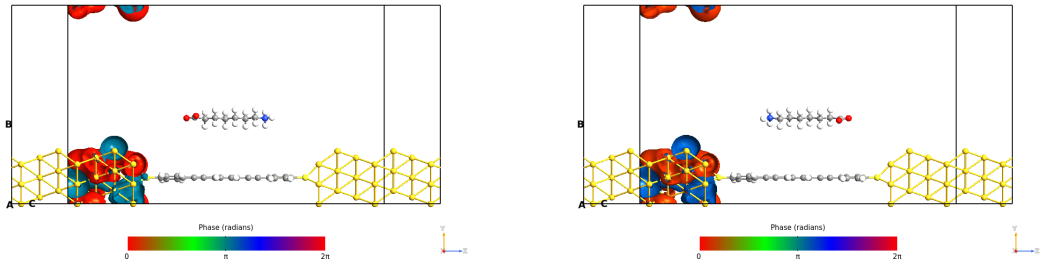

(a) Logic '0', eigenvalue equal to 1.11050 e-13. (b) Logic '1', eigenvalue equal to 8.86652 e-14.

Figure 6.469: Picture of the transmission eigenstate corresponding to the energy 0.28 eV for the OPE3 molecule with the long driver, yz plane.

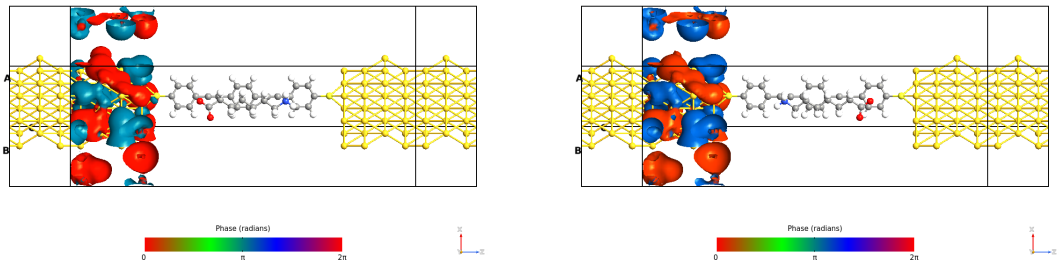

(a) Logic '0', eigenvalue equal to 1.11050 e-13. (b) Logic '1', eigenvalue equal to 8.86652 e-14.

Figure 6.470: Picture of the transmission eigenstate corresponding to the energy 0.28 eV for the OPE3 molecule with the long driver, xz plane.

Chapter 7

Conclusion and future perspectives

7.1 Feasibility of the readout system

Considering the results presented in the chapters before, it is possible to affirm that the readout system for molFCN could be done through a molecular junction. The driver's influence through the electric field provides a significant change in the molecular junction's current, which is detectable from today's measurement systems. A picture of the readout system is shown in figure 7.1.

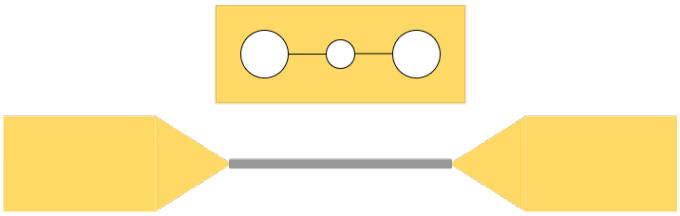

Figure 7.1: Picture of the readout system based on a molecular junction. the white figure represents the molFCN (the 3 dots), while the grey rectangle is the junction molecule.

The OPV3, OPE3, ZnPc, polar molecule 2 and polar molecule 7 work better than the other molecules. They present a current difference higher than 2.5 μA in at least one voltage point in the range from -0.5 V to 0.5 V as the applied voltage. They are the molecules that exhibit the best conduction properties, therefore a molecule that can drive a high current seems to fit well for this purpose.

The ZnPc with thiol chains and the ethyl4-(benzyl-methylamino) benzoate molecules show the worst behavior. Their current difference is still measurable but it is more difficult to sense with respect to the other selected molecules. The common feature is the low conduction properties, this means that the difference between the two logic configurations is small, and more difficulties arise for the detection.

Another important parameter is the wideness of the range in which a current of a logic value prevails on the other logic configuration's current. This allows the correct

function of the readout system even if the conditions are real and not ideal.

Looking at the table 7.1 is possible to notice that the OPV3 presents the highest current difference with respect to all the other selected molecules. Its value is higher than 4 μA, which is a big current. The OPE3, instead, reveals a wide interval in which the logic '1' configuration is higher than the logic '0' one. Its current difference is also important (higher than 3 muA). For these reasons and because they have current applications in MT, the two molecules have been simulated with the small driver and at different distances, in order to observe their response to the non-idealities.

Table 7.1: The table shows the current difference for the different molecules in a specific voltage point and the interval in which a current corresponding to a logic value is higher than the other.

Molecule	V_{point} **[V]**	$I_1 - I_0$ **[nA]**	**Positive range [V]**
OPV3	0.35	4042.3	from 0.3 to 0.5
OPE3	0.35	3352.93	from 0 to 0.7
Pc	0.9	2212.29	from 0.1 to 0.95
ZnPc	0.35	3300.11	from 0.3 to 0.4
ZnPc thiol chains	-0.95	21.9809	from -0.9 to -1
4Aminobenzoic acid	0.35	1306.56	from 0.2 to 0.4
Ethyl4-(benzyl-methylamino) benzoate	-1	0.246315	from -0.85 to -1
Polar molecule 2	-0.35	2661.71	from -0.05 to -0.7
Polar molecule 7	-0.6	2859.23	from 0 to -0.9

7.2 Robustness

As highlighted before, OPV3 and OPE3 are two of the best simulated molecules to fulfill the readout system based on a molecular junction, they are also currently employed in MT. For these reasons, the simulations at different distances have been performed. The results reveal the feasibility of the readout system because also in the worst case, the molecular junction exhibits different behavior between the two configurations, therefore the current difference is large enough to correctly distinguish the two logic values.

In the table 7.2 are reported the current difference values for the OPV3 molecule at different distances and considering the two drivers. As expected the best result is reached for the long driver at 7 Å as distance, in which the current difference is equal to 4.04 μA. The goodness of the readout system must be searched in the worst case because it tells us if the system is robust enough to the non-idealities. The worst case is the small driver at the longest distance between the junction and the driver because the small driver presents the lowest dipole moment and the electric field decreases with the distance increase. It is possible to notice that the current difference is 1.66 μA in the worst case, this result confirms that the OPV3 is a strong candidate for our purpose.

The table 7.3 reveals the possible implementation of the readout system through an OPE3 molecular junction. The current difference is in each case lower than the OPV3

Table 7.2: The table shows the current difference for the OPV3 molecule at different distances in a specific voltage point.

Distance [Å]	**Driver**	V_{point} **[V]**	$I_1 - I_0$ **[nA]**
7	long	0.35	4042.3
10.5	long	0.35	2836.9
14	long	0.35	2248.98
7	small	0.35	3558.41
10.5	small	0.35	2527.55
14	small	0.35	1662.1

one, but it is clearly measurable by today's technologies. The best and worst cases present an easily distinguished current difference, which is 3.35 μA and 780 nA respectively. The OPE3 molecule, instead, shows a wider interval in which the logic '1' current prevails on the logic '0' one with respect to the OPV3 molecule. This can be important if the electric parameters are not well controlled.

Table 7.3: The table shows the current difference for the OPE3 molecule at different distances in a specific voltage point.

Distance [Å]	**Driver**	V_{point} **[V]**	$I_1 - I_0$ **[nA]**
7.5	long	0.35	3352.93
11	long	0.35	1728
14.5	long	0.35	1188.71
7.5	small	0.35	3009.34
11	small	0.35	1184.89
14.5	small	0.35	780.985

7.3 How the dream molecule should be

At the end of my simulations, an identikit of the junction molecule can be derived in order to provide new data for future research in this field.

The considerations can be subdivided into two main categories:

- Symmetric molecules;
- Asymmetric molecules.

They react in different ways to the electric field's influence generated by the driver.

The symmetric molecules are usually distinct by a high polarizability value, which provides a significant interaction between the driver and the junction molecule. The main feature that the molecule should have is *conductivity*, good conduction properties amplify the current difference generated by the orientation of the electric field.

Concerning the asymmetric molecule, *the more the asymmetry, the more probable the ON/OFF TS*. This behavior is highlighted by the Ethyl4-(benzyl-methylamino) benzoate in which the asymmetry is relevant, in fact, its TS is ON/OFF type, while the polar molecule 7 presents a higher value of dipole moment, but its asymmetry is not emphasized as the ethyl4-(benzyl-methylamino)benzoate one, therefore it shows no ON/OFF TS.

The channel length is one of the parameters that is relevant in both cases. It influences not only the conduction properties of the molecule but indicates also the amount of junction molecule's surface directly exposed to the electric field generated by the driver. The OPE5 simulations with different alignments reveal that the best channel length should be slightly larger than the molFCN molecule length. This condition allows us to limit the not-perfect alignment, which could be relevant for high polarizability molecules. The polar molecules, thanks to their asymmetry, should be less subjected to the not-perfect alignment.

The conduction properties are not important only in the case of symmetric molecules, they are also a key feature for the asymmetric molecules but in the first case, they are more relevant than the second one.

7.4 From the molecular junction to the CMOS world

A possible solution for taking the output current of the molecular junctions to the CMOS standard voltage is shown in figure 7.2.

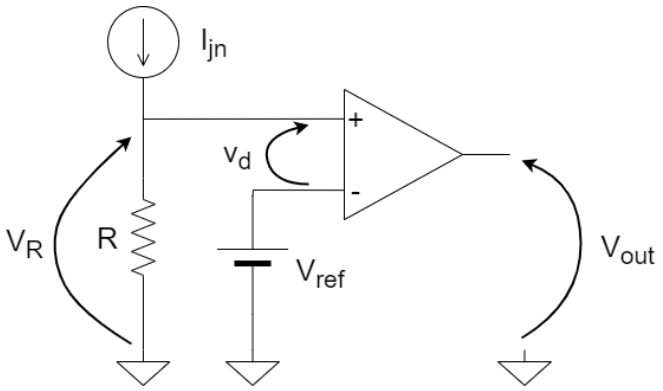

Figure 7.2: Picture of one of the possible circuits for adapting the current of the molecular junction at the CMOS devices.

The voltage at the non-inverting input can be evaluated as in the equation 7.1, while the inverting input voltage (V^-) is equal to the reference voltage (V_{ref}).

$$V^+ = V_R = R * I_{jn} \tag{7.1}$$

The differential voltage v_d can be easily found as in the equation 7.2.

$$v_d = V^+ - V^- = R * I_{jn} - V_{ref} \tag{7.2}$$

The constrain relations are reported in the equation 7.3:

$$\begin{cases} v_d^0 < 0 \\ v_d^1 > 0 \end{cases} \tag{7.3}$$

where v_d^0 is the differential voltage for the '0' logic value, while v_d^1 is the one for the '1' logic value. If the system is respected the operational amplifier works as a differential amplifier, for low values of v_d the OPAMP output voltage saturates. In these conditions the V_{out} should assume only two values that can be easily read by a digital device.

Considering the equations 7.2 and 7.3 it is possible to obtain the relation in the equation 7.4.

$$\begin{cases} R * I_{jn}^0 - V_{ref} < 0 \\ R * I_{jn}^1 - V_{ref} > 0 \end{cases} \tag{7.4}$$

where I_{jn}^0 is the current of the molecular junction for the '0' logic value, while I_{jn}^1 is the one for the '1' logic value. After some mathematical passages, it is possible to find the design constraints related to V_{ref} and R, the final result is written in the equation 7.5.

$$I_{jn}^0 < \frac{V_{ref}}{R} < I_{jn}^1 \tag{7.5}$$

Probably an OPAMP for each readout system is too much, therefore a multiplexer solution can be exploited. The sharing of resources is well known in digital electronics, for example in analog to digital converters and vice-versa. In figure 7.3 is drowned the solution considering a 4-bit multiplexer, the selection signal (SEL) is formed by two bits because it is the minimum number of bits for addressing 4 configurations.

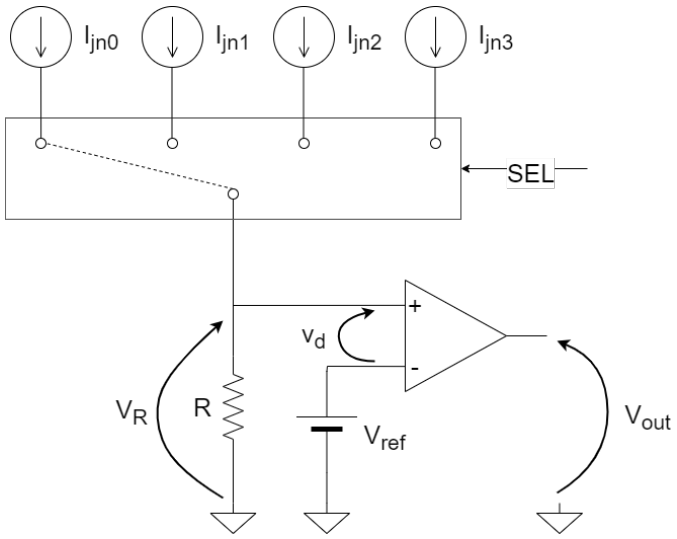

Figure 7.3: Picture of the possible circuit for adapting the current of the molecular junction at the CMOS devices, considering the multiplexer solution.

7.5 Future analyisis

There are several factors that we can modify to obtain significant data. In particular, the anchoring group offers an important change in the molecular junction current. In all the analyzed cases the anchoring group considered was a sulfur atom, it is interesting to see the result if we change it. Indium, Fluorine, Chlorine, and other atoms or molecules can be used as anchoring groups. It is more intriguing for the asymmetric molecules to consider different anchoring groups for the two electrodes, in this way, the asymmetry is enhanced with respect to the same anchoring group situation.

The electrodes' impact could be understood by changing them. In the simulations, gold (1,1,1) was used as the electrode. It is possbile to investigate other metals or carbon-based materials, such as graphene. The two electrodes could be made of different materials to increase the asymmetry.

One of the future aims could be to make the molecular junction condition closer to the real ones, in particular, it will be interesting to see the response of some not neglectable physical aspects. I try to summarize some relevant non-idealities:

- molecular torsion, it affects the conduction and the surface exposed to the electric field;
- not perfect anchoring of the molecule at the electrodes, low current is expected;
- more than one molecule anchored at the same electrodes.

At the moment no polar molecules are employed in molecular junctions, the research of a synthesizable polar molecule between two electrodes could raise interest in the gate contact due to the ON/OFF TS of the molecule.

A more suitable driver can be designed for the simulation. The driver used is a polar molecule that mimics the dipole moment of the driver. If a molecule for the molFCN is selected, it is possible to design it in a more realistic way to obtain more accurate results. Another effect related to the driver could be the not perfect alignment, the driver could be not parallel to the junction molecule but it could be rotated by an angle.

Bibliography

[1] G.E.Moore, “Cramming more components onto integrated circuits,” Electronics, 1965.

[2] J. Wu, J. Min and Y. Taur, "Short-Channel Effects in Tunnel FETs," in IEEE Transactions on Electron Devices, vol. 62, no. 9, pp. 3019-3024, Sept. 2015, doi: 10.1109/TED.2015.2458977.

[3] Q. Xie, C. -J. Lee, J. Xu, C. Wann, J. Y. . -C. Sun and Y. Taur, "Comprehensive Analysis of Short-Channel Effects in Ultrathin SOI MOSFETs," in IEEE Transactions on Electron Devices, vol. 60, no. 6, pp. 1814-1819, June 2013, doi: 10.1109/TED.2013.2255878.

[4] ITRS experts, "International Technology Roadmap for Semiconductors", 2015 report, 2015.

[5] A. B. Kahng, "Scaling: More than Moore's law," in IEEE Design & Test of Computers, vol. 27, no. 3, pp. 86-87, May-June 2010, doi: 10.1109/MDT.2010.71.

[6] Purkayastha, Tamoghna, Chattopadhyay, Tanay and De, Debashis. "Design of reversible logic circuits using quantum dot cellular automata-based system" Nanotechnology Reviews, vol. 4, no. 5, 2015, pp. 375-392. https://doi.org/10.1515/ntrev-2015-0033.

[7] Liu, M., Lent, C.S. "Reliability and Defect Tolerance in Metallic Quantum-dot Cellular Automata". J Electron Test 23, 211–218 (2007). https://doi.org/10.1007/s10836-006-0627-8.

[8] C.G Smith, S Gardelis, A.W Rushforth, R Crook, J Cooper, D.A Ritchie, E.H Linfield, Y Jin, M Pepper, "Realization of quantum-dot cellular automata using semiconductor quantum dots", Superlattices and Microstructures, Volume 34, Issues 3–6, 2003, Pages 195-203, ISSN 0749-6036.

[9] S. Bhanja and J. Pulecio, "A review of magnetic cellular automata systems," 2011 IEEE International Symposium of Circuits and Systems (ISCAS), Rio de Janeiro, Brazil, 2011, pp. 2373-2376, doi: 10.1109/ISCAS.2011.5938080.

[10] J. F. Pulecio, P. K. Pendru, A. Kumari and S. Bhanja, "Magnetic Cellular Automata Wire Architectures," in IEEE Transactions on Nanotechnology, vol. 10, no. 6, pp. 1243-1248, Nov. 2011, doi: 10.1109/TNANO.2011.2109393.

[11] F. M. Spedalieri, A. P. Jacob, D. E. Nikonov and V. P. Roychowdhury, "Performance of Magnetic Quantum Cellular Automata and Limitations Due to Thermal Noise," in IEEE Transactions on Nanotechnology, vol. 10,

no. 3, pp. 537-546, May 2011, doi: 10.1109/TNANO.2010.2050597.

[12] A. Pulimeno, M. Graziano, A. Sanginario, V. Cauda, D. Demarchi and G. Piccinini, "Bis-Ferrocene Molecular QCA Wire: Ab Initio Simulations of Fabrication Driven Fault Tolerance," in IEEE Transactions on Nanotechnology, vol. 12, no. 4, pp. 498-507, July 2013, doi: 10.1109/TNANO.2013.2261824.

[13] M. Momenzadeh, Jing Huang, M. B. Tahoori and F. Lombardi, "Characterization, test, and logic synthesis of and-or-inverter (AOI) gate design for QCA implementation," in IEEE Transactions on Computer-Aided Design of Integrated Circuits and Systems, vol. 24, no. 12, pp. 1881-1893, Dec. 2005, doi: 10.1109/TCAD.2005.852667.

[14] S. S. Kavitha and N. Kaulgud, "Quantum dot cellular automata (QCA) design for the realization of basic logic gates," 2017 International Conference on Electrical, Electronics, Communication, Computer, and Optimization Techniques (ICEECCOT), Mysuru, India, 2017, pp. 314-317, doi: 10.1109/ICEECCOT.2017.8284519.

[15] Y. Ardesi, G. Turvani, M. Graziano and G. Piccinini, "SCERPA Simulation of Clocked Molecular Field-Coupling Nanocomputing," in IEEE Transactions on Very Large Scale Integration (VLSI) Systems, vol. 29, no. 3, pp. 558-567, March 2021, doi: 10.1109/TVLSI.2020.3045198.

[16] C. S. Lent and B. Isaksen, "Clocked molecular quantum-dot cellular automata," in IEEE Transactions on Electron Devices, vol. 50, no. 9, pp. 1890-1896, Sept. 2003, doi: 10.1109/TED.2003.815857.

[17] R. Wang, A. Pulimeno, M. R. Roch, G. Turvani, G. Piccinini and M. Graziano, "Effect of a Clock System on Bis-Ferrocene Molecular QCA," in IEEE Transactions on Nanotechnology, vol. 15, no. 4, pp. 574-582, July 2016, doi: 10.1109/TNANO.2016.2555931.

[18] Graziano, Mariagrazia & Wang, Ruiyu & Ruo Roch, Massimo & Ardesi, Yuri & Riente, Fabrizio & Piccinini, Gianluca. (2019). "Characterisation of a bis-ferrocene molecular QCA wire on a non-ideal gold surface". Micro & Nano Letters. 14. 22-27. 10.1049/mnl.2018.5201.

[19] Monika Gupta, "A Study of Single Electron Transistor (SET)", International Journal of Science and Research (IJSR), Volume 5 Issue 1, January 2016, pp. 474-479.

[20] Rai C, Khursheed A and Haque FZ, "Review on Single Electron Transistor (SET): Emerging Device in Nanotechnology", Austin Journal of Nanomedicine & Nanotechnology, October 2019.

[21] Maddalena Francesco, "Single-electron Transistor As Fast and Ultra-Sensitive Electrometer".

[22] Aassime, Abdelhanin & Johansson, G & Wendin, G. & Schoelkopf, R & Delsing, P. (2001). "Radio-Frequency Single-Electron Transistor as Readout Device for Qubits: Charge Sensitivity and Backaction". Physical review letters. 86. 3376-9. 10.1103/PhysRevLett.86.3376.

[23] Anil Kumar and Dharmender Dubey, "Single Electron Transistor: Applications and Limitations", Advance in Electronic and Electric Engineering ISSN 2231-1297, Volume 3, Number 1 (2013), pp. 57-62.

[24] Om Kumar and Manjit Kaur, "Single electron transistor: applications and problems", International journal of VLSI design & Communication Systems (VLSICS) Vol.1, No.4, December 2010

[25] Lin-Jun Wang; Gang Cao; Tao Tu; Hai-Ou Li; Cheng Zhou; Xiao-Jie Hao; Zhan Su; Guang-Can Guo; Hong-Wen Jiang; Guo-Ping Guo; "A graphene quantum dot with a single electron transistor as an integrated charge sensor", Applied Physics Letters 97, 262113 2010.

[26] Wesley R. Browne, John J. McGarvey, "The Raman effect and its application to electronic spectroscopies in metal-centered species: Techniques and investigations in ground and excited states", Coordination Chemistry Reviews, Volume 251, Issues 3–4, 2007, Pages 454-473, ISSN 0010-8545.

[27] Vaskova, Hana. (2011). "A powerful tool for material identification: Raman spectroscopy". International Journal of Mathematical Models and Methods in Applied Sciences. 5. 1205-1212.

[28] Rostron, P., Gaber, S., & Gaber, D. (2016). Raman spectroscopy, review. laser, 21, 24.

[29] Yi Cao, Mengtao Sun, "Tip-enhanced Raman spectroscopy", Reviews in Physics, Volume 8, 2022, 100067, ISSN 2405-4283.

[30] Zhenglong Zhang, Shaoxiang Sheng, Rongming Wang, and Mengtao Sun, "Tip-Enhanced Raman Spectroscopy", Analytical Chemistry 2016 88 (19), 9328-9346.

[31] Liza N, Murphey D, Cong P, Beggs DW, Lu Y, Blair EP. "Asymmetric, mixed-valence molecules for spectroscopic readout of quantum-dot cellular automata". Nanotechnology. 2021 Dec 21;33(11). doi: 10.1088/1361-6528/ac40c0. PMID: 34875643.

[32] O. Schmidt, M. Rekas, C. Wirth, J. Rothhardt, S. Rhein, A. Kliner, M. Strecker, T. Schreiber, J. Limpert, R. Eberhardt, and A. Tünnermann, "High power narrow-band fiber-based ASE source," Opt. Express 19, 4421-4427 (2011).

[33] S. Sugavanam, N. Tarasov, X. Shu, and D. Churkin, "Narrow-band generation in random distributed feedback fiber laser," Opt. Express 21, 16466-16472 (2013).

[34] Czuchnowski, J., Prevedel, R., "Improving the Sensitivity of Planar Fabry–Pérot Cavities via Adaptive Optics and Mode Filtering". Adv. Optical Mater. 2021, 9, 2001337.

[35] Pfeifer, H., Ratschbacher, L., Gallego, J. et al. Achievements and perspectives of optical fiber Fabry–Perot cavities. Appl. Phys. B 128, 29 (2022).

[36] Lapierre, Ray & Robson, Mitchell & Khalifa, Azizur-Rahman & Kuyanov, Paul. (2017). "A Review of III-V Nanowire Infrared photodetectors and Sensors". Journal of Physics D: Applied Physics. 50. 10.1088/1361-6463/aa5ab3.

[37] Gallo, Eric & Chen, Guannan & Currie, Marc & Mcguckin, Terrence & Prete, Paola & Lovergine, Nico & Nabet, Bahram & Spanier, Jonathan. (2011). "Picosecond response times in GaAs/AlGaAs core/shell nanowire-based photodetectors". Applied Physics Letters. 98. 241113-241113. 10.1063/1.3600061.

[38] Hui Xia, Zhen-Yu Lu, Tian-Xin Li, Patrick Parkinson, Zhi-Ming Liao, Fu-Hao Liu, Wei Lu, Wei-Da Hu, Ping-Ping Chen, Hong-Yi Xu, Jin Zou, and Chennupati Jagadish, "Distinct Photocurrent Response of Individual GaAs Nanowires Induced by n-Type Doping", ACS Nano 2012 6 (7), 6005-6013, DOI: 10.1021/nn300962z.

[39] Gao, Jianbo & Nguyen, Son & Bronstein, Noah & Alivisatos, A.. (2016). "Solution-Processed, High-Speed, and High-Quantum-Efficiency Quantum Dot Infrared Photodetectors". ACS Photonics. 3. 10.1021/acsphotonics.6b00211.

[40] Xia, Fengnian & Mueller, Thomas & Lin, Yu-Ming & Valdes, Alberto & Avouris, Phaedon. "Ultrafast Graphene Photodetector". IBM Thomas J. Watson Research Centre, Yorktown Heights, NY 10598.

[41] Cui, Ajuan, Huanli Dong, and Wenping Hu. "Nanogap electrodes towards solid state single-molecule transistors." Small 11.46 (2015): 6115-6141.

[42] Ma, Buyong & Lii, Jenn-Huei & Allinger, Norman. (2000)." Molecular Polarizabilities and Induced Dipole Moments in Molecular Mechanics". Journal of Computational Chemistry. 21. 813-825. 10.1002/1096-987X(20000730)21:103.0.CO;2-T.

[43] Kenneth J. Miller, "Calculation of the molecular polarizability tensor", Journal of the American Chemical Society 1990 112 (23), 8543-8551, DOI: 10.1021/ja00179a045.

[44] M. Fjeld, D. Hobi, L. Winterthaler, B. Voegtli and P. Juchli, "Teaching electronegativity and dipole moment in a TUI," IEEE International Conference on Advanced Learning Technologies, 2004. Proceedings., Joensuu, Finland, 2004, pp. 792-794, doi: 10.1109/ICALT.2004.1357659.

[45] Batsanov, Stepan S. 2022. "Energy Electronegativity and Chemical Bonding" Molecules 27, no. 23: 8215. https://doi.org/10.3390/molecules27238215.

[46] "ORCA - An ab initio, DFT and semiempirical SCF-MO package - ", Version 4.2.1, Design and Scientific Directorship: Frank Neese, Technical Directorship: Frank Wennmohs, Max-Planck-Institut f¨ur Kohlenforschung, Kaiser-Wilhelm-Platz 1, 45470 M¨ulheim a. d. Ruhr, Germany.

[47] Arroyo, C.R., Frisenda, R., Moth-Poulsen, K. et al. "Quantum interference effects at room temperature in OPV-based single-molecule junctions". Nanoscale Res Lett 8, 234 (2013). https://doi.org/10.1186/1556-276X-8-234.

[48] Liao, Jianhui, et al. "Reversible formation of molecular junctions in 2D nanoparticle arrays." Advanced Materials 18.18 (2006): 2444-2447.

[49] Guo, X., Zhu, Q., Zhou, L. et al. "Evolution and universality of two-stage

Kondo effect in single manganese phthalocyanine molecule transistors". Nat Commun 12, 1566 (2021). https://doi.org/10.1038/s41467-021-21492-x.

[50] Bo Fu, Martín A. Mosquera, George C. Schatz, Mark A. Ratner, and Liang-Yan Hsu, "Photoinduced Anomalous Coulomb Blockade and the Role of Triplet States in Electron Transport through an Irradiated Molecular Transistor", Nano Letters 2018 18 (8), 5015-5023, DOI: 10.1021/acs.nanolett.8b01838.

[51] A. Zahir, S. A. A. Zaidi, A. Pulimeno, M. Graziano, D. Demarchi, G. Masera, and G. Piccinini. 2014. "Molecular transistor circuits: from device model to circuit simulation". In Proceedings of the 2014 IEEE/ACM International Symposium on Nanoscale Architectures (NANOARCH '14). Association for Computing Machinery, New York, NY, USA, 129–134. https://doi.org/10.1145/2770287.2770318.